Utjecaj veličine, oblika i površinske strukture nanočestica srebra na njihovu interakciju s modelnim proteinima

Capjak, Ivona

Sveučilište u Zagrebu

Farmaceutsko-biokemijski fakultet

Ivona Capjak

UTJECAJ VELIČINE, OBLIKA I POVRŠINSKE STRUKTURE NANOČESTICA SREBRA NA NJIHOVU INTERAKCIJU S MODELNIM PROTEINIMA

DOKTORSKI RAD

Zagreb, 2019.

Sveučilište u Zagrebu

Farmaceutsko-biokemijski fakultet

Ivona Capjak

UTJECAJ VELIČINE, OBLIKA I POVRŠINSKE STRUKTURE NANOČESTICA SREBRA NA NJIHOVU INTERAKCIJU S MODELNIM PROTEINIMA

DOKTORSKI RAD

Mentori: dr.sc. Ivana Vinković Vrček
doc.dr.sc. Sandra Šupraha Goreta

Zagreb, 2019.

University of Zagreb

Faculty of Pharmacy and Biochemistry

Ivona Capjak

EFFECT OF SIZE, SHAPE AND SURFACE STRUCTURE OF SILVER NANOPARTICLES ON THEIR INTERACTION WITH MODEL PROTEINS

DOCTORAL DISSERTATION

Supervisors: dr.sc. Ivana Vinković Vrček

doc.dr.sc. Sandra Šupraha Goreta

Zagreb, 2019.

Rad je predan na ocjenu Fakultetskom vijeću Farmaceutsko-biokemijskog fakulteta Sveučilišta u Zagrebu radi stjecanja akademskog stupnja doktora znanosti iz područja biomedicine i zdravstva, polje farmacija, smjer farmaceutske znanosti.

Rad je izrađen pod mentorstvom dr. sc. Ivane Vinković Vrček na Institutu za medicinska istraživanja i medicinu rada, i komentorstvom doc. dr. sc. Sandre Šupraha Goreta, u sklopu doktorskog studija „Farmaceutske znanosti“ Farmaceutsko-biokemijskog fakulteta Sveučilišta u Zagrebu.

“Želiš li postići nešto veliko, počni s malim.”
Tomislav Ivančić

ZAHVALA

Moje najveće hvala želim izreći dragom Bogu koji je u svakom koraku uz mene!

Zahvaljujem se dr.sc. Ivani Vinković Vrček na mentorstvu i stručnom vodstvu te nesebičnoj pomoći tijekom izrade doktorske disertacije. Zahvaljujem se na pružanju povjerenja i prilike za rad, stvaranju poticajne radne sredine i prenošenju znanja i iskustava. Zahvaljujem se što je od trenutka prihvaćanja mentorstva pokazivala veliku vjeru i pouzdanje u mene.

Veliko hvala Prim.dr.sc. Ireni Jukić što je prepoznala dobrobit ovog rada te što je u svakoj dilemi bila glas podrške.

Zahvaljujem se doc.dr.sc. Sandri Šupraha Gorete na komentorstvu, savjetima i podršci.

Zahvaljujem se dr. sc. Maji Dotour Sikirić i dr. sc. Darji Domazet Jurašin koje su svojim savjetima, znanjem i iskustvom doprinijele koncepciji i izradi ovog rada.

Zahvalu upućujem Tei Crnković na pomoći u praktičnom radu.

Hvala dr.sc. Mariu Gabričević i dr.sc. Tinu Weitner sa Zavoda za Opću i anorgansku kemiju, Farmaceutsko-biokemijskog fakulteta na pomoći u praktičnom radu.

Posebnu zahvalnost dugujem svome suprugu, djeci i mojoj majci koji su mi životna podrška.

SAŽETAK

Zbog svojstava na nano razini, primjena nanočestica srebra (AgNP) u potrošačkim i medicinskim proizvodima sve je veća što nužno zahtijeva stalnu procjenu njihovih učinaka na ljudsko zdravlje. Iako se sigurnost primjene AgNP intenzivno istražuje, raspoloživa znanja nisu dostatna za konačni regulatorni okvir primjene i upotrebe nanosrebra u različitim proizvodima.

Cilj ovog doktorskog rada bio je utvrditi kako različita fizikalno-kemijska svojstva AgNP određuju njihovo ponašanje, stabilnost i interakcije u različitim biološkim medijima. U tu svrhu je sintetizirano šesnaest vrsta AgNP različitih oblika i površinske stabilizacije, veličina od 10 nm i 50 nm. Sve vrste AgNP su detaljno karakterizirane obzirom na raspodjelu veličine, zeta potencijal, topljivost, oblik i stabilnost u vodi. Ispitan je utjecaj različitih pH medija, prisustva elektrolita i površinski aktivnih tvari na stabilnost AgNP u slijedećim modelnim biološkim medijima: ultra čistoj vodi, fiziološkoj otopini, fosfatnom puferu i fosfatnom puferu uz dodataka 0.9% NaCl. Nano-bio interakcije istražene se koristeći dva modelna proteina: albumin i α-1-kiseli glikoprotein. U tu je svrhu istraženo kako različita fizikalno-kemijska svojstva utječu na konstante vezanja ta dva proteina na površinu AgNP, te utjecaj na sekundarnu strukturu proteina uslijed vezanja na AgNP. Antibakterijski učinak AgNP određen je na sojevima E. coli i S. aureus.

Utvrđeno je da osim naboja površinskog stabilizatora, značajnu ulogu u nano-bio interakcijama ima nominalni promjer AgNP. S porastom ionske jakosti ili pH medija mijenja se zeta potencijal, a AgNP se destabiliziraju. Ukoliko u mediju nema biomolekula kao što su proteini, AgNP su nestabilne i podložne aglomeraciji. Proteini se vežu na AgNP površinu čim se AgNP izlože mediju koji sadrže proteine, a konstante vezanja proteina na površinu AgNP slične su vezanju nekih lijekova na istraživane proteine. Promjena sastava medija ne uzrokuje značajne promjenom u tim interakcijama. Vezanje albumina s AgNP rezultira većom i raznolikijom promjene sekundarne/tercijarne strukture u odnosu na onu koja se događa s α-1-kiselim glikoproteinom.

Ključne riječi: *nanočestice srebra, proteini, interakcije, albumin*, *α-1-kiseli glikoprotein, stabilnost, antibakterijska aktivnost, nano-bio međuprostor.*

SUMMARY

Due to properties of silver at nano scale, silver nanoparticles (AgNP) are currently being used in an increasing number of consumer and medical products. However, exisiting knowledge on their activity and effects on human as well as environmental health is still lacking reliable data. Because of their small size, nanoparticles (NPs) can enter almost all parts of body, including tissues, organs and organelles (mitochondria, lysosomes, and endosomes) by different routes (e.g., inhalation, ingestion, injection or physical contact with cuts or wounds). In spite of a increasing number of scientific papers on interaction of AgNPs with biological systems, detailed mechanistic principles of the biological interfaces encountered by NPs after their suspension in different biological medium, and after their interaction with cell components, should be gathered and analysed from the perspective of colloidal chemistry. Behaviour of NPs in vivo may be quite complex leaving many challenges to study the NPs distribution, excretion, metabolism, and pharmacokinetics. This knowledge is, in turn, needed for development of safe and effective nano-based biomedical agents.

Therefore, the aim of this doctoral thesis was to systematically investigate effects of different physicochemical characteristics of AgNPs, as the most commercialized metallic NPs, on their stability, behaviour and fate in biological media, as well as the mechanism of their interaction with model proteins. For this purpose, sixteen types of AgNP, differing in shape and surface stabilization, with sizes of 10 nm and 50 nm, were synthesized by validated protocol using eight surface coating agents. Evaluation of stability and possible transformation of different AgNP were performed in model systems with and without the presence of proteins.

For the synthesis of various types of AgNP, a reduction method was used. The ability to control nucleation and growth of NP was investigated by varying the various experimental reaction conditions such as temperature and reaction time. Various reducing agents such as hydrogen peroxide, sodium citrate, sodium borohydride and ascorbic acid were used. Functionalization of AgNPs' surface was carried out using different stabilizing agents providing stericall or electro-static stabilization: neutral (polyvinylpyrrolidone (PVP) of different molecular weight, polysorbate (Tween 80), polyoxyethylene glycol-alkyl ether (Brij 35)), positively charged (poly-L-lysine (PLL), cetyltrimethylammonium bromide (CTA)) and negatively charged (citrate (CIT), sodium sulfosuccinate (AOT)). The full characterization and stability evaluation of AgNP included determination of the size distribution, shape, zeta

potential, chemical composition and also physical and optical properties using transmition electron microscopy (TEM), dynamic light scattering (DLS), electrophoretic light scattering (ELS), inductively coupled plasma mass spectrometry (ICP-MS), UV-VIS and fluorescence spectroscopy. Selected AgNps were exposed to various biological-physico-chemical conditions, with purpose to determine behavior and stability in model media. The influence of pH media, concentrations and tipe of electrolytes, presence of surface active agents or proteins on the stability of AgNP was analyzed by determining in size distribution and zeta potenctial, agglomeration and dissolution behaviour. The following model systems were tested: ultrapure water, ultrapure water with the addition of different amounts of electrolytes and/or surfactants, media of different pH and ionic strength: phosphate buffer, saline media, as well as different media with the added proteins; albumin and α-1-acid glycoprotein using above mentioned methods. Determination of possible AgNP dissolution or the release of free silver ions under specific conditions was determined by applying a combination of ultrafiltration and centrifugation procedures with atomic absorption spectroscopy for quantification. The binding mechanism of albumin and alpha-acid glycoprotein to different AgNP in model systems was determinated using UV-VIS and fluorescence spectroscopy, circular dichroism (CD), TEM, ELS and DLS.

The first part of the work undertaken within this doctoral thesis aimed to setup a validated protocol and scientific methodology for what the model system consisting of AgNP stabilized by citrate (CITAgNP) was used as the system well described in the scientific literature. Physico-chemical properties, stability and behaviour of CITAgNP were analysed in systems with different pH, ionic strenght, electrolyte type and concentration, with/without addition of surfactants. During this work, whole methodology for the doctoral work was defined as well as parameters that will be evaluated. Obtained results demonstrated that change in pH value of the medium reduced the absolute value of the ζ potential of AgNP leading to their instability and agglomeration as well as dissolution. Effect of mono- and bivalent cations, as well as mono- and bivalent anions, was consistent with the DLVO theory. At higher electrolyte concentrations, the absolute value of zeta potential of CITAgNP decreased, resulting in a reduction of electrostatic repulsion forces between the AgNP and their subsequent agglomeration. The AgNP behaviour in the presence of surfactant was rather complicated depending on the type of surfactant.

Next phase of doctoral work was dedicated to the preparation of AgNP of different sizes (10 nm (AgNP10) and 50 nm (AgNP50)), shapes (spherecial (sph), triangular plates (tri) and cubes (cub)) and surface structure. All AgNP were characterized immediately after

synthesis and purification using DLS, ELS, UV-VIS and TEM techniques. Since the main application of AgNP in different products is their antibacterial activity, antibacterial efficacy of selected AgNP was tested by minimal bactericidal concentration (MBC) spot test using two clinically relevant and pathogen bacterial strains: *E. coli* and *S. aureus*. The role of possible dissolution of AgNP on their biocidal effects was also estimated by measuring the release of Ag^+ ions under the given experimental conditions. Also, the antimicrobial activity of the AgNP species was compared with the antimicrobial activity of the Ag^+ ions themselves applied as $AgNO_3$. Significantly stronger antibacterial effect after prolonged incubation in *E. coli* culture was recorded only for PVP10sph, CTA50sph and AOT50sph. AgNP10sph were significantly more toxic for the tested bacteria compared to AgNP50sph, irrespective of the type of surface stabilizer. However, the most important role in AgNP toxicity effects can be attribute to the bioavailable Ag^+ ions. Indeed, greater antibacterial efficacy of AgNP10sph corresponds to a higher percentage of free Ag^+ ions in AgNP10sph suspension compared to AgNP50sph. Another important factor for the antibacterial effects of AgNP is their zeta potential. In established experimental conditions, the role of the surface stabilizer in modulating the release of Ag^+ ions was more important than the effects of directing the interaction of AgNP bacteria with the zeta potential.

Further more, stability of each AgNP type was evalauted in biological media including ultrapure water (UW), physiological saline (FP), phosphate buffer (FB) and phosphate buffer saline (FBNaCl). Changing the media from UW to FPNaCl followed the increase in diameter of AgNP and decrease in the absolute value of zeta potential indicating their instability in biological fluids. The most significant changes were recorded for CTA-coated AgNP, while TweenAgNP10sph and BrijAgNP10sph were quite stable. However, addition of proteins in tested media completely changed AgNP behaviour leading to their stabilization. Proteins attached to the AgNP surface immidiately upon their interaction.

Evaluation of mechanism of AgNP interaction with proteins demonstrated that binding of proteins was not depend on the type of media and AgNP surface structure. Because AgNP10 had larger unit surface area compared to the AgNP50, the protein binding was stronger than for the other AgNPs they bound proteins more strongly. Furthermore, AgNP with the negatively zeta potential bounded poorly AGP, which is at thep H 7.4 highly negatively charged, while this was not the case for BSA, which is at a pH 7.4 poorly charged. Given the ability of the protein structure to adjust, BSA binding with AgNP resulted in greater and more varied changes in the secondary/tertiary structure relative to the AGP.

Information and scientific dana gathered through this doctoral work can be used to design AgNP which will create a corona with a desired medical performance and a minimum risks to human health. Knowledge on the fate and stability of AgNP in biological systems is also of utmost importance to understand the distribution, excretion, metabolism, and pharmacokinetics of NPs, which is needed for development of safe and effective nano-based biomedical agents.

Key words: *silver nanoparticles, protein interaction, albumin, a-1-acid glycoprotein, stability, antibacterial efficacy, nano-bio interface*

SADRŽAJ

POPIS SLIKA

POPIS TABLICA

1. UVOD

1.1. Nanomaterijali

Pojam „nano“ dolazi od grčke riječi *nanos*, što znači patuljak, a po prvi put se u literaturi pojavljuje 1980. godine za definiciju malih čestica (Bennemann i Koutecky, 1984). Za izražavanje vrijednosti fizikalnih veličina prefiks *nano* na metričkoj skali označava vrijednost od 10^{-9}. Metrička nanoskala je izuzetno zanimljiva u tehnologiji materijala, te je omogućila razvoj jedne od ključnih tehnoloških grana – nanotehnologije koja se bavi razvojem i primjenom nanomaterijala (NM). Prema definiciji Europske komisije NM su “prirodni, slučajni ili proizvedeni materijali koji sadrže čestice, u nevezanom, agregiranom ili aglomeriranom stanju, a 50% ili više tih čestica ima jednu ili više dimenzija u rasponu od 1-100 nm“ (European Commission, 2011; Cushing i dr., 2004; Goesmann i Feldmann, 2010; European Commission, 2013; European Commission, 2014). Ukoliko su sve tri dimenzije materijala na nanoskali govorimo o nanočesticama (NP, od eng. nanoparticles). Postoje i NM koji mogu imati samo jednu dimenziju na nanoskali kao što su nanofilmovi i nanostrukturirane površine ili materijali s dvije dimenzije na nanoskali kao što su nanožice, nanovlakna ili nanocjevčice (Rosei, 2004; Chaturvedi i dr., 2012). Jedna od najvažnijih značajki NM koja određuje sva ostala njihova fizikalno-kemijska, pa i biološka svojstva jest velik omjer površine i volumena. Kako se veličina NP smanjuje, povećava se broj atoma na njihovoj površini u odnosu na broj atoma unutar čestica, odnosno dolazi do povećanja specifične površine NP temeljem čega one dobivaju sasvim nova svojstva u odnosu na tvari na atomskoj odnosno molekularnoj razini ili u odnosu na „bulk“ materijale. Tako se zbog velikog omjera površina / volumen mijenjaju optička, elektronska, magnetska, katalitička i druga svojstva (Paresh-Chira, 2011; Chaturvedi i dr., 2012; Barbero i dr., 2017; Conde i dr., 2014). Ovisno o kemijskom sastavu, NP pod utjecajem vanjskog magnetskog polja ili instrumentalnom obradom mogu pokazati jaku stabilnu fluorescenciju, Ramanovu optičku aktivnost ili druga jedinstvena svojstva koja omogućuju njihove različite primjene (Aguilar, 2014). Također, odlikuju se pojavom površinske plazmonske rezonancije (SPR od eng. Surface Plasmon Resonance) koja je posljedica kolektivnih oscilacija ili fluktuacija u elektronskoj gustoći s interaktivnim elektromagnetskim poljem. Upravo ta svojstva omogućavaju ogromnu fleksibilnost dizajna i primjenu NP u različitim područjima. Potpuno iskorištenje prednosti NP za stvaranje novih proizvoda, uređaja i tehnologija ili poboljšanje postojećih postiže se manipulacijom veličine, ali i njihovog oblika i površinske funkcionalizacije (Aguilar, 2014).

Nanotehnologija tako bilježi eksponencijalan napredak poslijednjih nekoliko desetljeća. Primjerice, javna ulaganja u nanotehnologiju u Europi povećana su šest puta u razdoblju od 1998. do 2003., a u Americi i Japanu osam puta za isto razdoblje. Svjetsko tržište nanotehnologije u 2009. godini iznosilo je 11,7 milijardi dolara, a do 2016. godine naraslo je na 39,2 milijarde dolara. Zabilježena je godišnja stopa rasta od 18,2% temeljem koje je procijenjeno da će u 2021. svjetsko tržište nanotehnologije dostići iznos od 90,5 milijardi dolara (BCC, 2016).

Obzirom da su NP veličinom usporedive s komponentama bioloških sustava, primjerice s proteinima (5-50 nm), genima (širina 2-nm i duljina 10-100 nm) i virusima (20-450 nm), nanotehnologija je duboko prodrla i u područje medicine te omogućila eksponencijalni razvoj multidisciplinarnog područja medicine – nanomedicine. Upotreba NP u medicini temelji se na fenomenima koji su karakteristični za nanoskalu, kao što su mehanizmi enzimskih reakcija, stanični ciklus, signalizacija stanica ili popravak staničnih oštećenja (Aguilar, 2014). Danas se tako dizajniraju NP za analizu strukture stanica i tkiva, dijagnostiku, proizvodnju biokompatibilnih NM u regenerativnoj medicini, dizajn nanonosača koji precizno lociraju i vežu se na specifične proteine i nukleinske kiseline povezane s bolestima i/ili poremećajima. Mnogi se nanomedicinski proizvodi već nalaze na tržištu, a još je veći broj nanomedicinskih sustava koji se razvijaju u svrhu rješavanja mnogih gorućih medicinskih problema, ali i u svrhu napretka precizne i personalizirane medicine (Aguilar, 2014).

1.2. Priprava nanočestica

Sintetski postupci NP razvijeni su do razine na kojoj je moguće odabirom reaktanata, stabilizatora i drugih uvjeta priprave moguće kontrolirati veličinu, oblik, zeta potencijal i površinsku strukturu samih NP. U literaturi je opisan veliki broj različitih postupaka koji se mogu klasificirati prema pristupu, a razlike se svode na reaktante i reakcijske uvjete (El-Badawy i dr., 2010). Općenito, sinteze su kategorizirane u kategorije kao što su „top down“ i „bottom up“, „green“ i na „non-green“ te konvencionalne i nekonvencionalne. Konvencionalne metode sinteze uključuju upotrebu citrata, borovog hidrida, dvostrukih sustava (voda i organska otapala), organskih reducensa ili primjene inverznih micela u procesu sinteze. Nekonvencionalne metode uključuju lasersku ablaciju, radiokatalizu, vakuum uparavanje metala i Svedbergovu metodu elektro kondenzacije (El-Badawy i dr., 2010).

„Top down“ odnosno pristup „od vrha prema dolje“ pristup (Slika 1) temelji se na smanjenju veličine početnih „bulk“ materijala do NM koristeći fizikalne, kemijske i mehaničke metode. Najzastupljenije fizikalne tehnike su lasersko rezanje, metoda usitnjavanja, elektro evaporacija i litiografija (Pacioni i dr., 2015). Metode usitnjavanja uključuju proces smanjenja veličine čestica do nano veličine izdvajanjem atoma iz početnih reaktanata korištenjem primjerice tehnika poput mehaničkog ili laserskog usitnjavanja (El-Badawy i dr., 2010; Guzmán i dr., 2009). Najznačajnija prednost takve sinteze je kemijska čistoća NP, a nedostaci uključuju veliki stupanj aglomeracije NP, površinski defekti te mali udio čestica manjih od 50 nm (Goesmann i Feldmann, 2010; Korbekandi, 2012). „Bottom up“ odnosno pristup „od dna prema vrhu“ (Slika 1) temelji se na sintezi u kojoj atomi ili molekule kroz niz reakcija prelaze u NP.

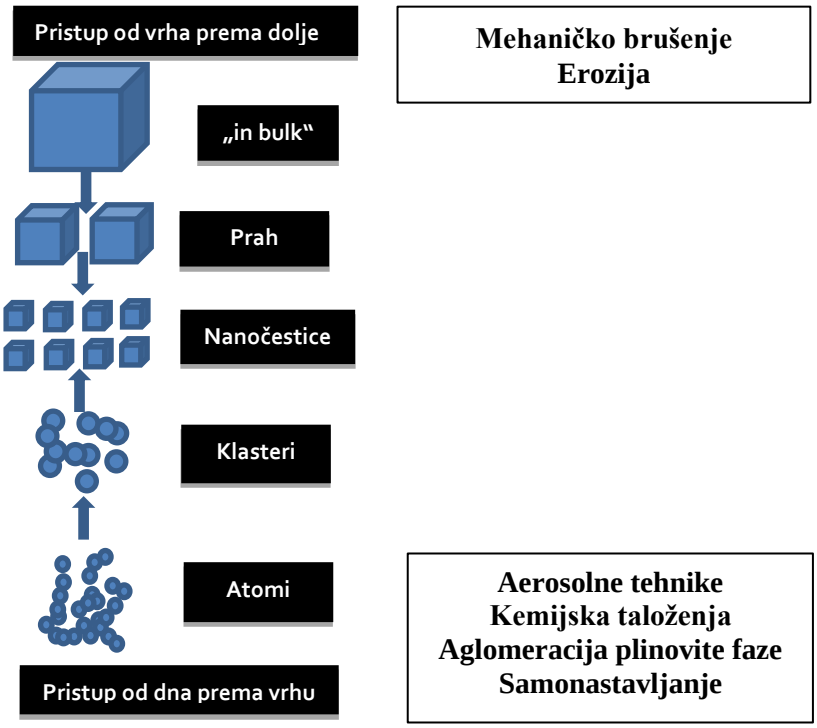

Slika 1. Sintetske metode „top down“ i „bottom up“.

Osnovne metode „bottom up“ pristupa su (a) metode s plinovitom fazom gdje se koriste visoke temperature (500 °C) pri čemu nastaju veliki aglomerati koji se teško uklanjaju procesima pročišćavanja, (b) metode s tekućom fazom koje obično započinju s prekursorom koji se izlaže redukcijskim uvjetima u kemijskoj reakciji, (c) metode s čvrstom fazom koje primjenjuju mehaničku silu koja djeluje na čvrstu fazu definiranom brzinom, uz djelovanje sile okretanja kugli odgovarajućeg materijala spremnika (čelik) pri čemu dolazi do sinteze NP u količini i od nekoliko tona na sat, te (d) biološke metode ili „biosinteze“ ili „zelene sinteze“

koje su sve zastupljenije zadnjih godina, a primarni cilj im je razvoj biokompatibilnih NM (Goesmann i Feldmann, 2010; Sakthivel i Prasanna, 2012; Pacioni i dr., 2015).

Za „bottom up“ pristup je najvažniji je proces nukleacije i rasta NP. Tijekom postupka priprave osigurava se polagano povećanje koncentracije atoma, pri čemu u točki prezasićenja procesom autonukleacije nastaju jezgre koje vrlo brzo kontroliranim rastom sazrijevaju u termodinamički stabilne klice (Simo i dr., 2012). U trenutku kad nakupina jezgri postigne kritičnu veličinu, strukturne fluktuacije postaju energetski nepovoljne i nakupina ostaje u dobro definiranoj strukturi. Trenutak sazrijevanja jezgri u klice (Slika 2) je ključni korak u kontroliranoj sintezi nanočestica koji se odvija vrlo brzo, dok se faze rasta i sazrijevanja NP odvijaju nešto sporije (Pacioni i dr.; Cushing i dr., 2004; El-Badawy i dr., 2010; Cushing i dr., 2004).

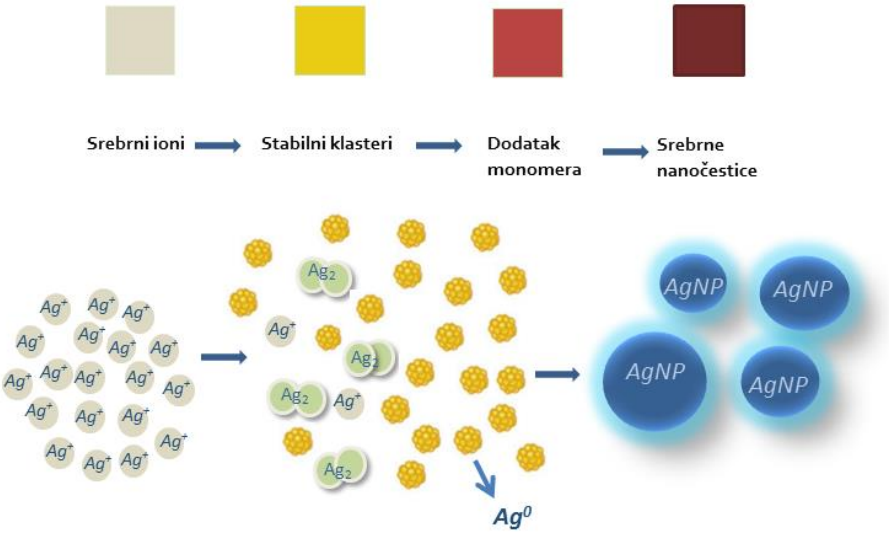

Slika 2. Sazrijevanje jezgri u klice na primjeru srebrnih nanočestica (AgNP).

Klice ubrzano rastu uz posljedični pad koncentracije slobodnih atoma u otopini pri čemu nastaju nanokristali. Proces rasta može biti kontroliran brzinom difuzije ili brzinom kemijske reakcije. Smatra se da je brzina difuzije kritični parametar koji je određen koncentracijskim gradijentom i temperaturom. U toj fazi koncentracija slobodnih atoma u otopini određuje daljnji tijek reakcije. Ako je koncentracija ispod točke prezasićenja daljnji rast se neće nastaviti. Ako je u reakcijskoj smjesi još uvijek prisutna dovoljna koncentracija slobodnih atoma ili se potrebna koncentracija održava daljnjim dodavanjem reaktanata, nastali nanokristali prolaze kroz fazu zrenja do postizanja ravnotežnog stanja između slobodnih atoma u otopini i atoma na površini nanokristala. Osim rasta klica u nanokristale, moguća je i aglomeracija atoma i nanokristala (Slika 3).

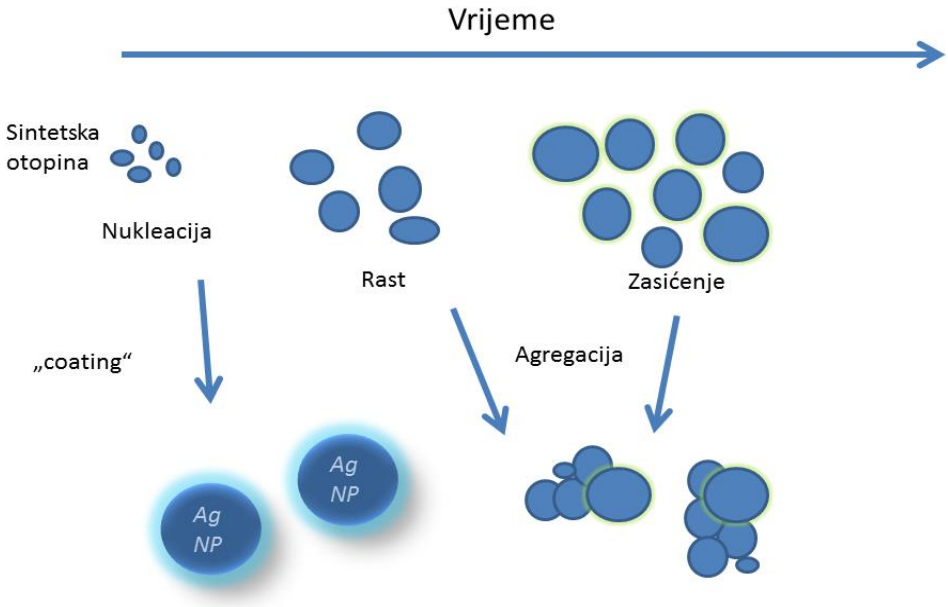

Slika 3. Rast i stabilizacija nanočestica**.**

Nastajanje aglomerata je nepoželjno jer su aglomerati nakupine nekontroliranih svojstva koje se procesima pročišćavanja trebaju ukloniti s ciljem dobivanja NP kontroliranih i definiranih svojstava. S obzirom na reaktivnost površine NP, aglomeracija malih čestica je neizbježna ako se ne koriste stabilizatori. Dva su osnovna mehanizma stabilizacije NP: (a) sterička stabilizacija u kojoj se NP međusobno odbijaju zbog prisustva molekula stabilizatora (npr. površinski aktivnih tvari ili polimera) i (b) elektrostatska stabilizacija pri kojoj do odbijanja NP dolazi zbog prisustva nabijenih grupa na površini NP, odnosno njihove površinske skupine se disociraju pri čemu nastaje dovoljno veliki zeta potencijal da se odbijaju (Cushing i dr., 2004).

Strogo definiranim uvjetima sinteze i uporabom stabilizatora specifičnih karakteristika moguće je upravljati procesom sinteze te postići pripravu NP definiranog oblika, veličine i strukture (Agnihotria, i dr., 2014).

1.3. Ponašanje nanočestica u biološkim medijima

Istraživanje ponašanja i interakcija NP u biološkim sustavima - nano-bio interakcija - od presudne je važnosti za razvoj učinkovitih i sigurnih NM za medicinsku primjenu (Corbo i dr., 2016). Naime, neposredno nakon kontakta NP s biološkim medijem, a ovisno o svojstvima biološkog okoliša (pH, sastav, puferski sistem…), o svojstvima samih NP te vremenu njihove izloženosti, NP podliježu različitim procesima transformacije od kojih je

najdominantniji proces stvaranja prostora između površine NP i bioloških komponenti poput proteina, nukleinskih kiselina, lipida i bioloških metabolita. Novonastali prostor naziva se nano-bio međuprostor (od *eng. nano-bio interface*). Svojstva i sudbina nano-bio međuprostora određena su dinamičkim i fizikalno-kemijskim interakcijama, te kinetikom i termodinamikom vezanja bioloških molekula na površinu NP (Duran i dr., 2015; Pisani i dr. 2017). U tom se međuprostoru stvara kruna ili tzv. korona (od eng. corona) građena je od biomolekula koje se vežu na površinu NP (Pisani i dr., 2017). Svojstva NP, poput oblika, veličine, naboja, kemijskog sastava, hidrofobnosti, hidrofilnosti, vrste kemijskog omotača, prisustvo specifičnih grupa na površini NP određuju svojstva i sastav korone (Tablica 1), odnosno koje biomolekule će stupiti u interakciju s NP (Saptarshi i dr., 2013; Klein, 2007). Formiranje korone je multifaktorijalni proces koji ne ovisi samo o svojstvima NP nego i o svojstvima biomolekula i biološkog medija (Saptarshi, i dr., 2013), a određen je nizom fizikalno-kemijskih interakcija koje se odvijaju u nano-bio međuprostoru kako je prikazano u Tablici 2 (Nel i dr., 2009; Treuel i Nienhaus, 2012).

Tablica 1. Utjecaj fizikalno-kemijskih svojstava NP na biomolekularnu koronu.

Čimbenik	Učinak
Veća gustoća naboja na površini NP	povećana gustoća i debljina korone, NP imaju veću brzinu opsonizacije, povećane konformacijske promjene proteina
Veća hidrofobnost NP	povećana debljina korone, NP imaju veću brzinu opsonizacije, povećane konformacijske promjene proteina
Veća zakrivljenost NP	povećana debljina korone, smanjene konformacijske promjene proteina, nema konformacijskih promjena adsorbiranih proteina
Viša koncentracija biomolekula	povećana debljina korone, konformacijske promjene adsorbiranih proteina

Primjerice, funkcionalne skupine na površini NP mogu kontrolirati vrstu biomolekula koji će se vezati na NP. Hidrofobnost NP utječe na udio i sastav adsorbiranih biomolekula (Aggarwal i dr., 2009). Tako je adsorpcija proteina povećana na hidrofobnim NP za razliku od hidrofilnih iako je afinitet proteina za obje vrste NP jednak, što povećava brzinu opsonizacije NP (Rahman i dr., 2013; Lindman i dr., 2007). Razlika u sastavu i organizaciji biomolekularne korone je jako značajna kada se veličina NP približi veličini proteina (Lynch i Dawson, 2008). Jako zakrivljene površine NM smanjuju interakcije između proteina i proteini adsorbirani na jako zakrivljenim NP prolaze kroz manje promjena u svojoj konformaciji.

Tablica 2. Kemijske interakcije u „nano-bio“ međuprostoru.

Vrsta interakcije	Svojstva i kemijska priroda interakcija	Domet (nm)
Hidrodinamičke	interakcij izazvane kretanjem čestica u tekućini, transportom, smicanjem i Brownovom difuzijom. Povećavaju jačinu i frekvenciju sudara između NP-a i drugih površina u sustavu	10^2–10^6
Elektrostatske	Coulombove interakcije, nabijene površine privlače suprotno nabijene ione i odbijaju ione istoimenog naboja što dovodi do stvaranja električkog međupovršinskog sloja (electrical interfacial layer, EIL)	1–100
Elektrodinamičke	van der Waalsove interakcije opisuju interakcije između slučajno orijentiranih dipola, između dipola i induciranog dipola, te fluktuacijskog dipola i induciranog dipola	1–100
Interakcije s otapalom	Reakcije između liofilnih i liofobnih molekula i molekula otapala	1–10
Steričke	Polimerne vrste adsorbirane na NP-e dovode do odbojnih interakcija s molekulama iz neposrednog okoliša	1–100
Interakcije premošćivanja polimerima	Jedna te ista molekula može se adsorbirati na dvije NP i tako ih premostiti, povezati.	1–100

Prva istraživanja o nano-bio međuprostoru i stvaranju biomolekularne korone na površini NP provedena su prije dva desetljeća na NP i proteinima humane plazme (Diederichs, 1996; Lück, 1998), a najveći broj istraživanja nano-bio međuprostora se upravo odnosi na istraživanje interakcije između proteina i NP, te stvaranje proteinske korone (PK). Poznavanje nastajanja PK na površini NP od izuzetne je važnosti za sve biomedicinske primjene NP, jer svojstva PK-NP kompleksa određuje bioaktivnost i biološki identitet NP, te posljedično način unosa, rapodjelu, aktivnost i eliminaciju NP u biološkom sustavu, jednako kao i moguće štetne učinke NP (Monopoli i dr., 2011; Lynch i Dawson, 2008; Shannahan i dr., 2013; Park i dr.. 2011; El-Badawy i dr., 2010). Osim svojstava NP i vrste fizikalno-kemijskih interakcija u nano-bio međuprostoru, na formiranje PK-NP kompleksa utječe i vrijeme inkubacije te fiziološko stanje biološkog medija koje može biti promijenjeno zbog bolest i drugih medicinskih stanja (npr. prisustvo ksenobiotika) (Corbo i dr., 2016).

Studije utjecaja vremena izloženosti na svojstva PK pokazale su da je proces stvaranja PK-NP kompleksa kontinuiran i dinamični proces (Huang i dr., 2013; Casals i dr., 2010). Adsorpcija proteina na površini NP uglavnom je regulirana afinitetom proteina prema površini NP i afinitetom jednog proteina prema drugom. Ulaskom NP u biološki medij započinje kompeticija prisutnih biomolekula za adsorpciju i vezanje na površinu NP. Korona je građena od dvije zone koje su u svrhu lakšeg razumijevanja predstavljene u formi prstena, što je odraz specifičanog biološkog odgovora na unos NP. U takvom obliku, sekundarno vezane biomolekule maskiraju primarno vezane i tako onemogućuju primarno vezanim biomolekulama interakciju sa staničnim medijem (Duran i dr., 2015; Fleischert i Payne, 2014; Ding i dr., 2013; Tavanti i dr., 2015; Koshkina i dr., 2015; Yallapu i dr., 2013; Cedervall i dr., 2007). Brzina asocijacije i disocijacije u PK-NP kompleksu ovisi o vrsti i stabilnosti i proteina i NP (Chanana i dr., 2013; Zook i dr., 2011). Istraživanja kinetike nastajanja PK-NP kompleksa pokazala su da je vremenska skala izmjene adsorbiranih proteina u intervalu između 100 sekundi i nekoliko sati (Duran i dr., 2015; Cedervall i dr., 2007). U nastalom PK-NP kompleksu proteini su u dinamičkoj ravnoteži koja se temelji na kompetitivnoj adsorpciji/desorpciji proteina na površini NP, ovisno o uvjetima reakcije. Inicijalno, PK je građena od proteina koji su prvi dostupni, a tijekom vremena dolazi do izmjene prvotno vezanih proteina s proteinima višeg afiniteta (Duran i dr., 2015; Fleischert i Payne, 2014; Tavanti i dr., 2015; Koshkina i dr., 2015). Dok svojstva NP utječu na profil vezujućih proteina i kinetiku vezanja, profil vezanih proteina utječe na dinamičnost nano-bio međuprostora i na biološku sudbinu NP. Korona daje NP novi identitet koji je odgovoran za odgovor biološkog sustava na prisustvo NP (Lynch i Dawson, 2008; Duran i dr., 2015; Ding i dr., 2013; Tavanti i dr., 2015). Nastajanjem korone mijenjaju se svojstva i funkcionalnost NP-a, ali i vezanih proteina (Slika 4 i Slika 5). Tako se u PK-NP kompleksu, uslijed njegove dinamične prirode, odvijaju promjene koje određuju adsorpciju, distribuciju, nakupljanje, razgradnju i/ili aglomeraciju, te eliminaciju NP. Procesi na NP uključuju fazne transformacije površine NP, aglomeraciju NP, rekonstrukciju njihove površine, otapanje NP, formiranje različitih tipova korona (Slika 4) (Pisani i dr., 2017; Corbo i dr., 2016; Walkey i dr., 2012; Huang i dr., 2013). S druge strane, moguće su promjene adsorbiranih proteina, primjerice konformacijske promjene, gubitak funkcionalnih svojstava, oksidativne reakcije (Lynch i Dawson, 2008; Nel i dr., 2009).

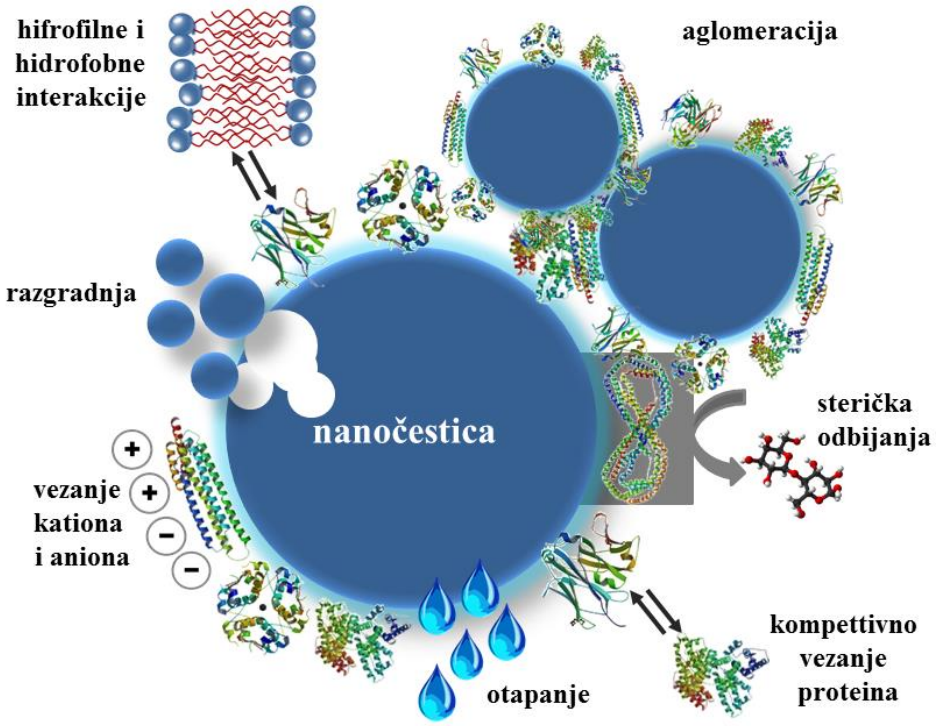

Slika 4. Nano-bio međuprostor definiran je svojstvima nanočestica, biomolekularne korone i okolišnog medija (Capjak i dr., 2017).

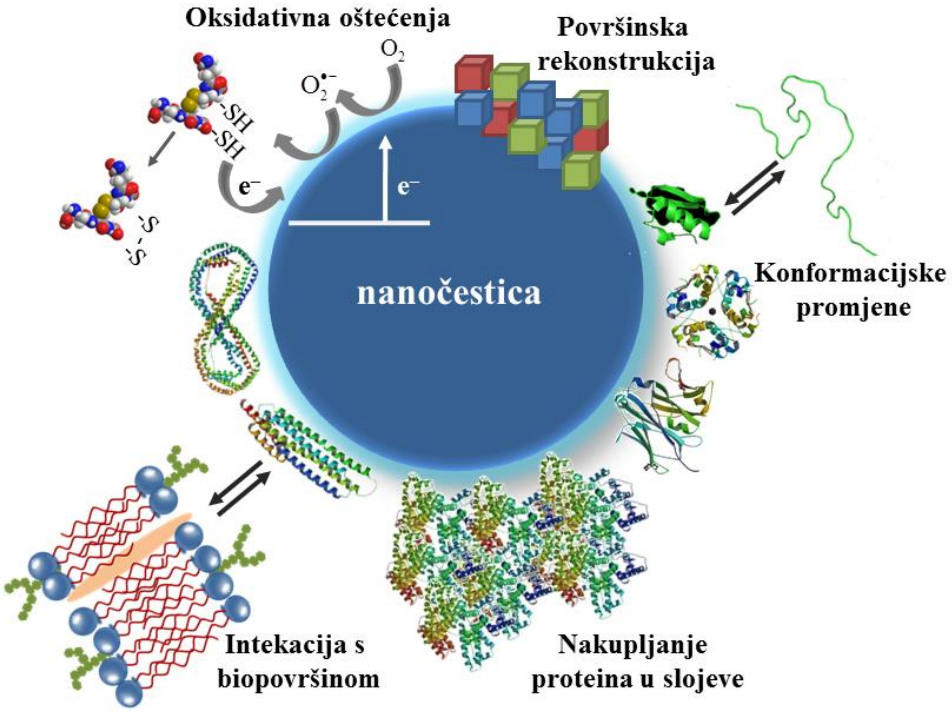

Slika 5. Promjene na nanočesticama i proteinima koje se događaju u nano-bio međuprostoru (Capjak i dr., 2017).

Vezani proteini koji mijenjaju veličinu, oblik i zeta potencijal NP direktno utječu na procese ulaska NP u makrofage što izravno mijenja raspodjelu NP u organizmu, njihov stanični unos, vrijeme zadržavanja u cirkulaciji, transport, kinetiku vezanja, signalizaciju, nakupljanje i/ili toksičnost (Rahman i dr., 2013). Konformacijske promjene proteina koje su uzrokovane interakcijom s NP, mogu utjecati na kaskadu protein–protein interakcija, staničnu signalizaciju i transkripciju DNA što se direktno odražava na enzimsku aktivnost (Lynch i Dawson, 2008). Važno je istaknuti da korona posljedično omogućuje prelazak NP preko membrana, ulazak NP u biološke elemente koji su inače zaštićeni neprolaznim barijerama. Stabilnost PK određena je njenom debljinom i postotkom pokrivenosti površine NP (El-Badawy i dr., 2010). Svojstva i sastav PK značajniji su u određivanju biološkog odgovora na NP nego karakteristike samih NP jer je upravo PK u direktnom kontaktu s biološkim medijem te je time od presudne važnost za biokompatibilnost NP (Sahoo i dr., 2007; Lynch i Dawson, 2008). Kao i ostala svojstva PK, tako i njen sastav ovisi o fizikalno-kemijskim svojstvima NP (veličina, oblik, sastav, površinska struktura i zeta potencijal), svojstvima biološkog medija (krv, stanice, citoplazma) i vremenu inkubacije (Tavanti i dr., 2015). Primjerice, u humanoj plazmi sastav PK razlikuje se ovisno o tipu NP kako je prikazano u Tablici 3.

Tablica 3. Sastav proteinske korone različitih nanočestica (NP) u humanoj plazmi (Aggarwal i dr., 2009; Saptarshi i dr.,2013, Monopoli i dr., 2011, Cedervall i dr., 2007)

Vrsta nanočestica	Proteini korone
Polistirenske NP	Faktori koagulacije, imunoglobulini, lipoproteini, proteini akutne faze, komplementni proteini, plazminogen, anti-CD4, c4a, albumin
Latex NP	albumin, apolipoproteini, immunoglobulini, hemoglobin, haptoglobini
Kopolimerne NP	albumin, apolipoproteini, fibrinogen, immunoglobulini, c4bp lanac
MWCNT	plazminogen, čimbenici komplementa, čimbenici koagulacije
SPION	Albumin, α-1-antitripsin, fibrinogenski lanci, imunoglobulinski lanci, transferin, transtiretin
Zlatne	Albumin, Fibrinogen lanci, Apolipoprotein A1, čimbenici koagulacije,
kvarcne i ugljične nanocjevčice	Fibrinogenski lanci, imunoglobulin lagani lanci, fibrin, albumin, ApoA1, komplement, proteini komplementa, fibronektin,
SiO_2 NP	Imunoglobulini, lipoproteini, proteini komplementa, koagulacijski proteini, proteini akutne faze, stanični proteini, serumski proteini
TiO_2 NP, ZnO NP	Albumin, imunoglobulini, fibrinogen, transferin, apolipoprotein A1, komplementni proteini
cit – AgNP	Serumski albumin, α-1-antiproteinaza, α-2-HS-glikoprotein, Apolipoprotein AI, Serotransferin, α-2-makroglobulin, α-fetoprotein, Apolipoprotein B-100, α-2 antiplazmin, komplement C3, 1, Fetuin-B, teški lanac H1 hemoglobinskih fetusa, inhibitor inter α-tripsina, hemoglobin, komplementarni faktor B, hemopeksin, serpin A3-6
PVP – AgNP	Serumski albumin, α-2-HS-glikoprotein, α-1 antiproteinaza, Apolipoprotein AI, Serotransferin, α-2 makroglobulin, α-fetoprotein, Apolipoprotein B-100, Complement C3, α-2-antiplazmin, Fetuin-B, β-2-glikoprotein 1, hemoglobina fetalna podjedinica α, inhibitor Inter- α-tripsina, protein za vezanje vitamina D, Transtyretin, hemoglobin
Polistiren s poloksamerom	Faktor B, transferin, albumin, fibrinogen, IgG, apolipoproteini
Liposomi	Albumin, fibrinogen, apolipoproteini, IgG, α1-antitripsin, α2, IgM
Čvrste lipidne NP	Fibrinogen, IgG, IgM, apolipoproteini (osim ApoE), transtiretin
NP Fe oksida	Albumin, IgG, IgM, fibrinogen, C3b
Polistirenske NP	Albumin, IgG, fibrinogen, apolipoproteini, PLS:6

1.4.Modelni sustav nanočestica srebra i transportnih proteina

Istraživanje interakcija bioloških sustava i NP te razumijevanje mehanizma interakcija NP i proteina od posebnog je značaja za određivanje učinkovitosti, kvalitete i sigurnosti biomedicinskih NP, te predstavlja prvi korak u sigurnoj primjeni nanotehnologije u medicini. To je i bio cilj ove doktorske radnje za čiju se izradu odabrao modelni nano-bio sustav koji se sastojao od AgNP kao najzastupljenijih metalnih NM u medicinskim proizvodima i proizvodima opće uporabe, te albumina i α1-kiselog glikoproteina, kao važnih transportnih proteina krvne plazme.

1.4.1. Primjena i važnost nanočestica srebra

Srebro se zbog svojih izraženih antibakterijskih, antifungalnih i antivirusnih svojstava koristi oko 7000 godina. Još u doba Heroda spominje se antibakterijsko djelovanje srebra (Alexander, 2009), a od 19. stoljeća ta se svojstva pripisuju ionima srebra koji se otpuštaju u medij (Lansdown, 2006; Lansdown, 2010). Koloidno srebro poznato je oko 120 godina (Nowack i dr., 2011), a danas je njegova primjena u sve većem porastu o čemu govore i brojna znanstvena istraživanja. Pretraživanje baze podataka ISI Web of Science uz upotrebu ključnog izraza "antimicrobial coating" dobiveno je 3455 publikacija, od kojih se 1031 publikacija odnosi na srebro, 463 za titan, 184 za bakar, 133 za cink i 107 za zlato (Slika 6).

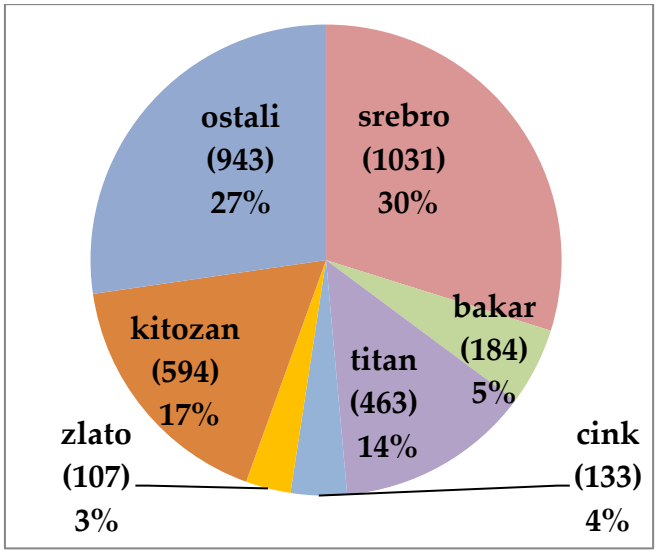

Slika 6. Broj i udio radova dostupnih u ISI Web of Science bazi podataka za različite materijale s antimikrobnim svojstvima. Pretraga je izvršena 14.03.2017.

U usporednoj procjeni učinaka komercijalno dostupnih antimikrobnih materijala, pokazano je da su srebrne NP trenutno najrašireniji i najučinkovitiji nanomaterijal u antimikrobnim premazima (Kubo i dr., 2018).

Sinteza AgNP uglavnom se temelji na „bottom up“ pristupu u tekućoj fazi koji se temelji na redukciji topivih srebrnih soli pomoću redukcijskih sredstava u vodi ili organskim otapalima. Dodatak stabilizirajućih spojeva spriječava aglomeraciju sintetiziranih AgNP. Reaktanti u toj metodi su otopljene soli srebra (Ag^+) koje se reduciraju (Ag^0) pri čemu procesom nukleacije i rasta nastaju AgNP (El-Badawy i dr., 2010; Korbekandi, 2012). Kemijska redukcija je vjerojatno najčešće korištena kemijska reakcija u sintezi NP metodom tekućih faza. Relativno veliki elektropozitivni redukcijski potencijal $Ag^+ \rightarrow Ag^0$ u vodi (E^Θ = + 0,799 V) omogućuje upotrebu većeg broja reducensa: natrijev citrat ($E\Theta$ = - 0,180 V), natrijev bor hidirid (E^Θ = - 0,481 V), hidrazin (E^Θ = - 0,23 V) (Cushing i dr., 2004; Pacioni i dr., 2015; Yonezawa i dr., 2000).

Redukcija srebrnih kationa uz bor hidrid prikazana je sljedećom jednadžbom:

$$AgNO_3 + NaBH_4 \rightarrow Ag + H_2 + B_2H_6 + NaNO_3 \quad (1)$$

Nedostaci ove metode sinteze su kemijske nečistoće u suspenzijama, najčešće neizreagirano ionsko srebro koje je zaostalo nakon redukcije (El-Badawy i dr., 2010). U praksi se pokazalo da je reproducibilna sinteza AgNP u laboratoriju teža od očekivanog pri čemu je najvjerojatniji uzrok nastajanje jezgre metalnog srebra koja se razvija u strukture različite morfologije i veličine kristala prilikom promjene reakcijskih uvjeta (koncentracije, redukcijskog agensa, temperatura, prisutnost stabilizatora) (Chernousova i Epple, 2013). Odabirom površinski aktivnih tvari, polimera i uvjeta reakcije (pH, temperatura) moguće je postići stabilizaciju sintetiziranih AgNP te posljedično kontrolu veličine, oblika i zeta potencijala (Goesmann i Feldmann, 2010; Korbekandi, 2012). Zbog lakoće i prilagodljivosti sintetskih postupaka u pripravi AgNP željenih svojstava, primjena i upotreba AgNP eksponencijalno raste u mnogim gospodarskim granama (Slika 7).

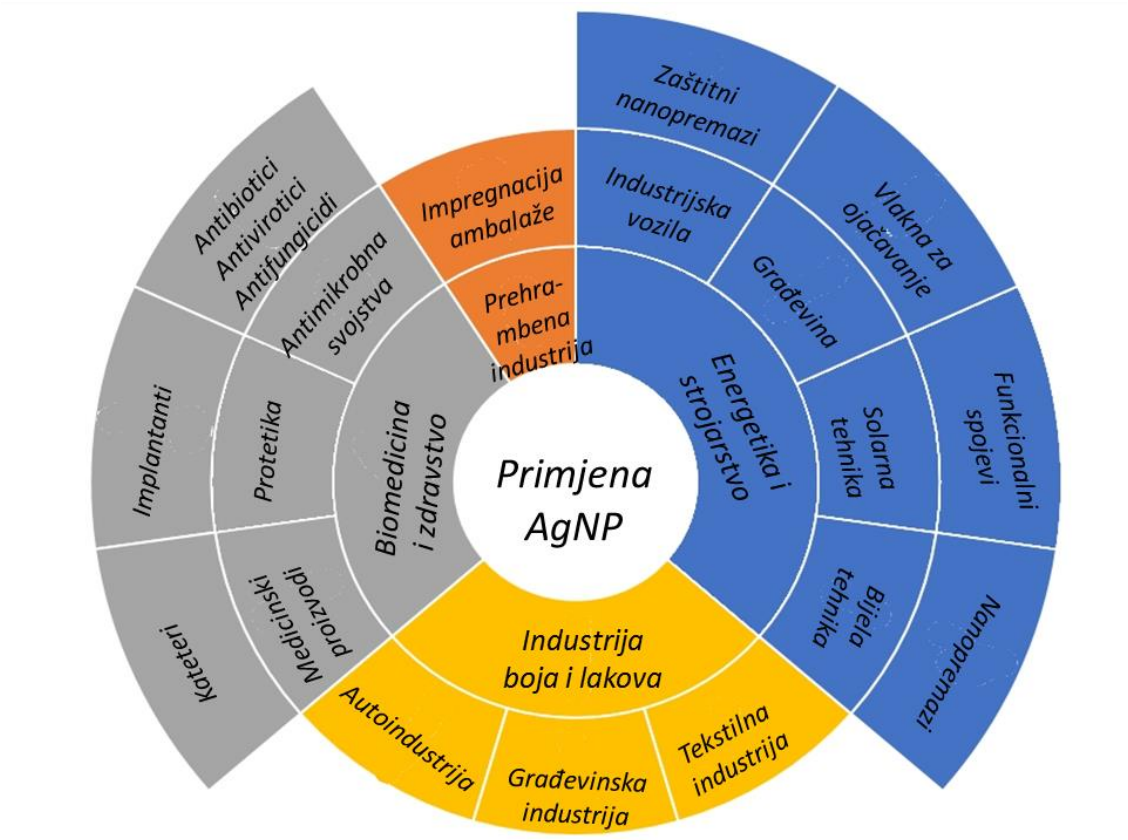

Slika 7. Primjena nanočestica srebra (AgNP).

AgNP su danas zastupljene u svim proizvodnim industrijama (Tablica 4).

Tablica 4. Primjena nanočestica srebra (AgNP).

Primjena AgNP	Funkcionalnost	Reference
Tekstilna industrija	Osigurava nove funkcionalnosti: vodootpornost, čistljivost, prozračnost, UV zaštita, vodljiva i antistatička svojstva, otpornost na mrlje, bakterije ili gljivice, otpornost na mehanička oštećenja	(Walser i dr., 2011; Byko 2005; Som i dr., 2011; EMPA i Schweiz, 2011)
Prehrambena industrija, u proizvodnji kontaktne ambalaže naprednih funkcionalnih svojstava	*Poboljšana ambalaža* - poboljšanja svojstva plinske barijere i otpornost na temperaturu i vlažnost, *"Aktivna" ambalaža* - omogućuje bolja zaštita proizvoda. Npr. AgNP premazi mogu osigurati antimikrobna svojstva, *"Inteligentna / pametna" ambalaža* - namijenjena za otkrivanje biokemijskih ili mikrobioloških promjena u hrani.	(Reidy i dr., 2013; Duncan, 2011; Silvestre, 2011)
Procesi obrada vode	Filteri s površinskim AgNP premazima koriste se za obradu pitke vode i vode visokih performansi.	(Spring, 2014)
Elektrotehnika i strojarstvo	Proizvodnja vodljivih folija, elektroda za fleksibilne uređaje, fleksibilne tanke solarne ćelije, u proizvodnji biosenzora i bioslika. Svojstva AgNP koja se koriste u elektroindustriji su vodljivost i električna svojstva, pri čemu je izlaganje takvim uređajima tijekom uporabe minimalne nanotoksičnosti dok je velike nanotoksičnosti prilikom odlaganja i skladištenja.	(Zeng i dr., 2010; Georgios i dr., 2011)
Industrija boja i lakova	Primjena AgNP-a u bojama i lakovima povećava otpornost od oštećenja, olakšava čišćenje, povećava trajnost i postojanost boja.	(Som i dr., 2013)
Biomedicina i zdravstvo	Zbog svojih antimikrobnih svojstava velika je upotreba AgNP u krirurškim, oftalmološkim i stomatološkim sredstvima, zatim u izradi implatanata, proteza i katetera.	(Reidy i dr., 2013)

Koriste se u tekstilu s antibakterijskim svojstvima, sportskoj opremi, dodacima prehrani, sredstvima za čišćenje, baterijama, filterima za zrak, premazima za hladnjake, magnetima, perilicama za rublje, spremnicima za hranu itd. U industriji se koriste kao katalizatori,

nanoelektrode za elektroničke uređaje, u detekciji DNA sljedova, kolorimetrijskom određivanju herbicida, te za mnoge druge istraživačke svrhe. Očekuje se da će globalno tržište AgNP do 2022. dosegnuti 2,45 milijardi dolara, s povećanom potražnjom za antimikrobnim materijalima u medicinskom sektoru (Grand View Research, Report, 2015).

Medicinsko područje donosi preko 30% ukupnih prihoda na tržištu AgNP, te gotovo sve medicinske grane koriste proizvode koji su impregnirani ili sadrže AgNP (Tablica 5). Jedan od najvažnijih razloga jest stalna borba protiv rezistentnih bakterija i pronalaženje rješenja da se spriječi povećanje njihovog broja, posebice bolničkih patogena (European Commission, 2014; Duran i dr., 2015).

Tablica 5. Primjeri primjene nanočestica srebra u medicini *(*El-Badawy i dr., 2010).

Područje	**Primjeri**
Anesteziologija	Maske za disanje i endotrahealne cijevi za mehaničku ventilacijsku pomoć
Kardiologija	Kateteri za dijagnostičko praćenje
Stomatologija	Aditivi u dentalnim materijalima, srebrom punjene nanokompozitne smole
Dijagnostika	Dijagnostički teskovi infarkta miokarda, fluorescentno opažanje RNA
Dostava lijeka	Mikrokapsule koje se induciraju udaljenom laserskom zrakom
Optika	Kontaktne leće
Vizualizacija	Nanokompoziti za stanično obilježavanje i vizualiziranje
Neurokirurgija	Kateteri za drenažu cerebrospinalne tekućine
Ortopedija	Aditivi u cementima za kost, implantati za zamjenu zglobova, čarape
Palijativa	Superapsorbirajući hidrogel za materijale za inkontinenciju
Farmaceutici	Tretmani za dermatitis, ulcerozni kolitis i akne, inhibicija HIV-1, čarape
Kirurgija	Bolnički tekstil (kirurške odore, maske...), dijagnostički kateteri
Urologija	Kirurške mreže za zdjeličnu rekonstrukciju
Liječenje rana	Hidrogel za rane, zavoji za opekline

Biološki učinak nanoformulacija srebra nije konačno objašnjen i dokazan, ali rezultati podupiru teoriju da su citotoksični učinci AgNP posljedica otpuštanja srebrnih iona koji u biološkim medijima stvaraju srebrne komplekse i organske srebrne spojeve, a djeluju na stanične membrane, te inhibiriaju disanje i reprodukciju stanica (Kaiseri dr., 2017; Duran i dr., 2016). Veličina AgNP, njihova slobodna površina, oblik i naboj su ključni parametri koji određuju biodostupnost srebrnih iona u smislu otapanja, transporta i interakcije s biološkim

molekulama (El Badawy i dr., 2011). Ako je ciljani učinak dezinficirati ili sterilizirati, a ciljni organizam patogeni mikroorganizam, toksično djelovanje AgNP se može tumačiti kao pozitivan ishod. Međutim, ako isti materijal ima nepoželjne utjecaje na druge organizme, a posebno na ljudski, takva toksičnost predstavlja ozbiljnu opasnost koju treba pažljivo utvrditi (Marambio-Jones i Hoek, 2010). Idealne AgNP za antimikrobno djelovanje, prema tome, moraju biti selektivno toksične, tj. antibakterijske u određenoj koncentraciji, ali ne i toksičan za ljudski organizam i okoliš. Stoga je za sve NM, pa tako i za AgNP, nužna realna procjena omjera koristi u odnosu na rizike njihove primjene i upotrebe.

Zabrinutosti zbog potencijalne toksičnosti AgNP danas je stalna tema u svim relevantnim regulatornim tijelima Europske Unije. Primjerice, Znanstveni odbor za nastajuće i novo identificirane zdravstvene rizike (akronim SCHEER od *eng.* Scientific committee on health, environmental and emerging risks) istaknuo je u svom zaključnom mišljenju o zdravstvenim učincima nanometrijala važnost istraživanja rizika u odnosu na koristi različitih oblika srebra koji se koriste u potrošačkim i medicinskim proizvodima, jer AgNP podliježu različitim transformacija (aglomeracija, otapanje, nastajanje novih vrsta) tijekom svog životnog ciklusa (European Commission, 2015). Smjernica "Guidance on the Determination of Potential Health Effects of Nanomaterials Used in Medical Devices" daje analizu specifičnih čimbenika koji se moraju razmotriti u procjeni sigurnosti nano-materijala koji se upotrebljavaju u medicini, a posebno ističe potrebu za proučavanjem učinka različitih fizikalno-kemijskih svojstava na interakcije i učinke NM u biološkim sustavima (Rosslein i dr., 2017). Veliki izazov u daljnjim istraživanjima predstavlja razlučiti toksični utjecaj AgNP uvjetovan svojstvima nanočestica (veličina, oblik, vrsta stabilizirajućeg omotača) od toksičnog utjecaja Ag^+ iona koji nastaju otapanjem AgNP-a (Slika 8). Prema dostupnim literaturnim podacima, neosporno je da AgNP izazivaju citotoksičnost (Toduka i dr., 2012; Sabella i dr., 2014; Vinković Vrček i dr., 2016; Milić i dr., 2015; Vinković Vrček i dr., 2014; Pongrac i dr., 2016). Citotoksični učinci AgNP dokazani su in vitro za širok raspon staničnih kultura pri čemu su povećan oksidacijski stres, apoptoza i DNA oštećenja definirani kao glavni stanični ishodi uslijed izloženosti staničnih kultura s AgNP (Toduka i dr., 2012; Sabella i dr., 2014; Vinković Vrček i dr., 2016; Milić i dr., 2015; Vinković Vrček i dr., 2014). Također je poznato da AgNP različite površinske funkcionalizacije pokazuje i različitu razinu toksičnosti. To se potvrdilo i u našem laboratoriju na primjeru neuralnih matičnih stanica (Pongrac i dr. 2018) i humanih hepatoma stanica (Brkić Ahmed i dr., 2017). Procjena citotoksičnosti i genotoksičnosti AgNP ukazuje da razina oksidativnog stresa i primarno oštećenje DNA ovisi o dozi i vrsti AgNP (Pongrac i dr. 2018; Brkić Ahmed i dr., 2017).

Citotoksičnost AgNP direktna je posljedica njihovog staničnog unosa koji se, ovisno o fizikalno-kemijskim svojstvima i primijenjenim stabilizatorima, odvija različitim mehanizmima, kao što su kao fagocitoza, makropinocitoza, pinocitoza, klatrinom ili kaveolinom posredovana endocitoza (Brkić Ahmed i dr., 2017; Vinković i dr., 2017; Milić i dr., 2014; Asharani i dr., 2009a; Dziendzikowska i dr., 2012; Wang i dr., 2012).

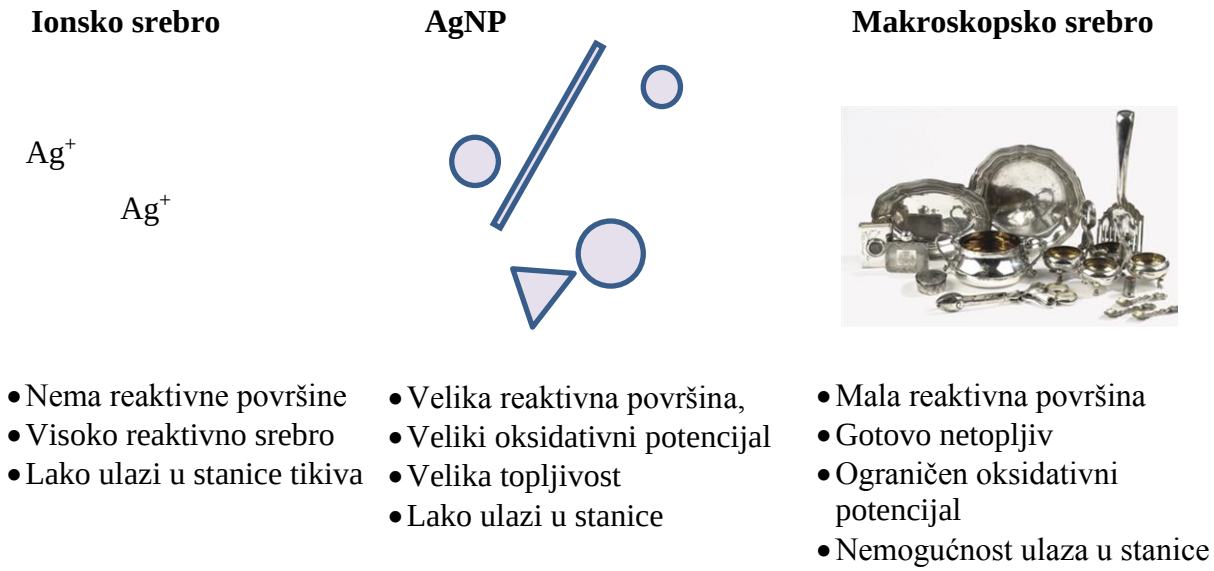

Slika 8. Osnovne razlike ionskog srebra, AgNP i makroskopskog srebra.

Međutim, osim osnovnih karakteristika AgNP, svojstva biološkog medija te formiranje PK također značajno utječu na učinke AgNP na žive stanice, te mogu dovesti ili do smanjenja ili do pojačavanja njihovog toksičnog učinka.

1.4.2. Albumin

Albumin je najzastupljeniji protein krvne plazme s koncentracijom od 35-50 mg/mL što odgovara udjelu od oko 60% ukupnih proteina plazme. Veličinom je oko 69 KDa, a sadrži 585 aminokiselina, 17 disulfidnih veza i jednu slobodnu sulfhidrilnu grupu (Cys 34) (Curry i dr., 1999). Albumin (Slika 9) je monomerni protein srcolika oblika s ukupnom molekularnom masom od 66 400 Da i dimenzijama 80x80x80x30 Å (Curry i dr., 1999; Curry, 2009). Konformacijska struktura karakterizirana je sa 67% udjela α-heliksa, bez prisustva β-ploča (Brown i Shockley, 1982). Jedinstvenu strukturu albumina (Slika 9) određuje triptofan na aminokiselinskom položaju 214, a smješten je u središtu poddomene 2A. Zbog te lokacije triptofana, albumin posjeduje i specifična fluorescencijska svojstava koja su vrijedan alat

prilikom istraživanja njegove stabilnosti i interakcije s ligandima. Albumin ima izoelektričnu točku 4.7, pa je pri pH 7.4 negativno nabijen pri čemu sadrži 60 pozitivno nabijenih lizinskih grupa. To mu omogućuje stupanje u interakciju s pozitivnim i negativnim ligandima. Slobodna tiolna skupina cisteina ima važnu ulogu u transportu i pohranjivanju dušičnog oksida, ali i vezanje mnogih malih metalnih iona (Cu^{2+}, Cd^{2+}, Hg^{2+}, Ag^{+}, Au^{3+}) (Carter i Ho, 1994). Serumski albumin organiziran je u tri homologne domene povezane disulfidnim vezama (domena I, II i III), a svaka se domena sastoji od 2 poddomene: IA i IB, IIA i IIB, IIIA i IIIB (Kragh-Hansen i dr., 2002; Curry i dr., 1999; Zemek i dr., 2013). Egzogene tvari, prvenstveno lijekovi, najveći afinitet za vezanje pokazuju za domenu I i domenu II. Detaljna analiza aminokiselinskih ostataka pokazuje da pojedini aminokiselinski ostaci (npr. Trp-214 i Arg-218) pospješuju vezanje liganada dok npr Lys-199 i His-242 sabotiraju vezanje (Zemek i dr., 2013).

Slika 9. Kristalna struktura albumina (PDB ID 3BXK).

Albumin se sintetizira u jetri u obliku prekursora prealbumina u količini od 12 g dnevno nakon čega posttranslacijskom modifikacijom sazrijeva u albumin (Peters, 1996, Zemek i dr., 2013; Peters i Anfinsen, 1950). Oko 40% ukupno sintetiziranog proteina zastupljeno je u krvnoj plazmi dok je ostatak pohranjen u ekstracelularnim tkivima (Zemek i dr., 2013). Razina albumina u plazmi održava se uravnoteženom sintezom i razgradnjom, reguliranom genskom ekspresijom i prehrambenim faktorima (Kirsch i dr., 1968). Budući da je održavanje osmotskog tlaka u krvi jedna od glavnih funkcija albumina u ljudskoj plazmi, njegova sinteza je dodatno njime strogo regulirana (Brown i Shockley, 1982). Biološka uloga albumina najvećim je dijelom transport endogenih i egzogenih liganada (masne kiseline, hormoni, toksični metaboliti) s umjerenim afinitetom vezanja (Ka = 104 do 106) (Steiner i dr.,

1966; Petitpas i dr., 2001). Albumin posjeduje i enzimatsku aktivnost djelujući kao esteraza p-nitrofenil acetata (Watanabe i dr., 2000; Means i Bender, 1975; Means i Wu, 1979).

Poznato je da se albumin veže na metalne NP (Usawadee i dr., 2014; Zhang i dr., 2015; Mariam i dr., 2011; Ravindran i dr., 2010) pri čemu je od velike važnosti istražiti mehanizam reakcije, odrediti konstante vezanja i promjenu biološkog učinka kako proteina tako i NP nakon stvaranja kompleksa. Primjerice, pokazalo se da albumin tvori jednostruki prsten na površini NP pri pH 7.4 pri čemu sekundarna struktura proteina ostaje nepromijenjena (Huang i dr., 2013; Gebauer i dr., 2012). Smanjenjem pH vrijednosti, na oko pH 4.0 formiraju se aglomerati i narušava se sekundarna struktura proteina. Neovisno o naboju, pozitivne i negativno nabijene NP u interakciji s albuminom stvarat će negativno nabijenu proteinsku koronu odnosno negativno nabijen PK-NP kompleks (Fleischert i Payne, 2014; Zemek i dr., 2013). Međutim, površinski naboj samih NP može utjecati na promjene u sekundarnoj strukturi proteina. Tako su rezultati dobiveni primjenom spektroskopije cirkularnog dikroizma (CD) pokazali da kationske NP uzrokuju promjenu zastupljenosti α–heliksa u strukturi albumina što dovodi do promjene afiniteta PK za albuminske stanične receptore. Anionske NP pak vežu veći broj molekula albumina na svojoj površini u usporedbi s kationskim NP (Fleischert i Payne, 2014). To jasno upućuje na iznimnu važnost dobivanja sustavnih podataka o mehanizmu vezanja albumina na AgNP ovisno o fizikalno-kemijskim svojstvima samih nanočestica, ali i o svojstvima medija u kojem se te interakcije odvijaju.

1.4.3. α-1-kiseli glikoprotein

α1-kiseli glikoprotein (AGP), pod nazivom orozomukoid, je protein akutne faze, koji ima malu molekularnu masu od 41-43 kDa, a u svojoj strukturi ima pet ugljikohidratnih lanaca koji čine oko 40% - 45% ukupne mase tog glikoproteina (Dorian i dr., 2008; Israili i Dayton, 2001; Schmid i dr., 1977). Proteinski dio sastoji od jednog proteinskog lanca koji se sastoji od 183 aminokiseline, dok je glikanski dio nositelj funkcionalnosti AGP (Fournier i dr., 2000; Zemek i dr., 2013).

Biointeza AGP-a odvija se jetri, uglavnom u hepatocitima, a koncentracija u cirkulaciji je od 0,6 do 1,2 mg/mL (udio od 1% - 3% ukupnih proteina u krvnoj plazmi) (Allen i dr., 1977). Novija istraživanja pokazuju da sinteza AGP nije ograničena samo na hepatocite nego se on sintetizira i u mijelocitima nakon čega se pohranjuje u sekundarnim granulama te otpušta iz aktiviranih neutrofila kao odgovor na upalu pri čemu djeluje lokalno s imunomodulirajućim učinkom (Theilgaard-Mönch i dr., 2005). Obzirom da mu se

koncentracija poveća između 2 i 4 puta (Gornik i Lauc, 2008) kao odgovor na upalni proces, trudnoću, unos lijekova u organizam, svrstava se u proteine akutne faze (Theilgaard-Mönch i dr., 2005; Kremer i dr., 1988). Osim imunomodulatornog djelovanja, dokazano je da sudjeluje u agregaciji trombocita, modulaciji proliferacije limfocita, u transportu lijekova i endogenih tvari, poput steroidnih hormona i ksenobiotika (Zemek i dr., 2013; Taguchi i dr., 2013). Slično kao i kod albumina, vezanje i transport niza endogenih i egzogenih spojeva su jedna od glavnih fizioloških funkcija AGP (Otagiri, 2005).

N-glikozilacijska mjesta AGP (Asn-15, -38, -54, -75, -85) mogu vezati glikane različitih stupnjeva razgrananja (bi-, tri- i tetraantenski glikani) (Fournier i dr., 2000). Ti glikani su strukturno heterogeni zbog velike raznolikosti terminalnih ugljikohidrata. Kao što je prikazano na Slici 10, sialinska kiselina je uobičajen završetak glikanskih lanaca te se veže na ostatke galaktoze a moguće je i vezanje na ostatke fukoze (Taguchi i dr., 2013). Upravo zbog sijalinske kiseline je AGP negativno nabijen pri fiziološkom pH zbog čega je pogodan za vezanje bazičnih i neutralnih lipofilnih lijekova te steroidnih hormona u krvi. Glikozilacija AGP varira u raznim fiziološkim i patološkim stanjima što u kombinaciji s različitim stupnjevi razgranatosti i vrstama ugljikohidrata dovodi do heterogenosti AGP, pri čemu je poznati najmanje 20 vrsta glikanskih struktura u AGP-u (Taguchi i dr., 2013; Ceciliani i Pocacqua, 2007). Na primjer, utvrđeno je da AGP ima povećan stupanj sialilacije i fukozilacije, te različite relativne omjere bi-, tri- i tetraantenarnih sekvencija u bolesnika s karcinomima (limfom, tumor jajnika itd.) (Duche i dr., 2000; Hashimoto i dr., 2004). Nadalje, stanja poput kroničnih upala, trudnoća, reumatoidnog artritisa, alkoholne ciroze jetre, također uzrokuje promjene u AGP glikozilaciji (Biou i dr, 1991; Biou i dr., 1989; Jezequel i dr., 1988).

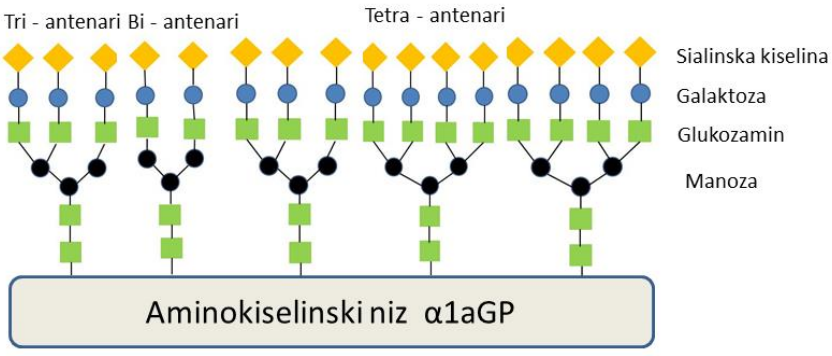

Slika 10. Shematski prikaz strukture α1-kiselog glikoproteina.

Zbog svega navedenog, AGP je zanimljiv kao model u proučavanju nano-bio interakcija.

2. OBRAZLOŽENJE TEME

Poznavanje mehanizma i prirode nano-bio interakcija od izuzetne je važnosti za razvoj učinkovitih i sigurnih nanomaterijala u biomedicini, ali i za sigurnu uporabu nanomaterijala općenito. Unatoč brojnim provedenim istraživanjima i velikoj količini objavljenih podataka, još uvijek je pristup takvim istraživanjima nesustavan i manjkav. Poznati su samo detalji interakcija između specifičnih NP i pojedinih proteina, a nedostaje detaljna analiza prirode i mehanizma vezanja medicinski relevantnih proteina na nanočestice u ovisnosti o njihovim različitim fizikalno-kemijskim svojstavima, te o svojstvima biološkog sustava koji je izložen djelovanju tih nanočestica.

Cilj ove doktorske disertacije je upravo sustavno istraživanje na modelnom sustavu koji je prikazan Slikom 11. Osnovna hipoteza istraživanja koje je obuhvaćeno ovom doktorskom disertacijom jest da veličina, oblik te površinska struktura nanočestica određuju prirodu i mehanizam njihove interakcije s proteinima krvne plazme. U svrhu provođenja sustavnog istraživanja nano-bio međuprostora izabran je modelni sustav koji obuhvaća:

1) set od šesnaest vrsta AgNP različitih veličina, oblika i površinske stabilizacije. AgNP su izabrane zbog važnosti i sve veće primjene u biomedicini kako je opisano u uvodnim poglavljima. Ispitane su AgNP veličina 10 nm i 50 nm, sferičnog, triangularnog i kubičnog oblika, te stabilizirane neutralnim, pozitivno i negativno nabijenim površinskim omotačima.
2) dva modelna plazmatska proteina: albumin i α1-kiseli glikoprotein, koji su važni transporteri egzogenih tvari u ljudskom organizmu.
3) četiri fiziološki relevantna medija: ultra čista voda, fiziološka otopina, fosfatni pufer pH 7.4 i fosfatni pufer pH 7.4 u 0,9% NaCl.

Za dokazivanje glavne hipoteze ovog istraživanja postavljeni su slijedeći specifični ciljevi:

a) optimizacija i validacija protokola za sintezu AgNP različitih veličina, oblika te površinskih struktura;
b) određivanje antibakterijskog učinka različitih AgNP kako bi se ispitala njihova relevantnost za primjenu u biomedicini;
c) procjena stabilnosti i mogućih tranformacija različitih AgNP u različitim fiziološki relevantnim uvjetima uz i bez prisustva modelnog proteina;
d) određivanje mehanizma vezanja albumina i α1-kiselog glikoproteina na različite AgNP u simuliranim fiziološkim uvjetima;

e) određivanje konformacijskih promjena modelnih proteina nakon interakcije s različitim AgNP.

Dobiveni rezultati unaprijedit će postojeće znanje o nano-bio interakcijama, olakšati dizajn učinkovitih i sigurnih nanomaterijala, te olakšati regulatornim tijelima donošenje smjernica nužno potrebnih za odobravanje primjene inovativnih nanosustava u biomedicini.

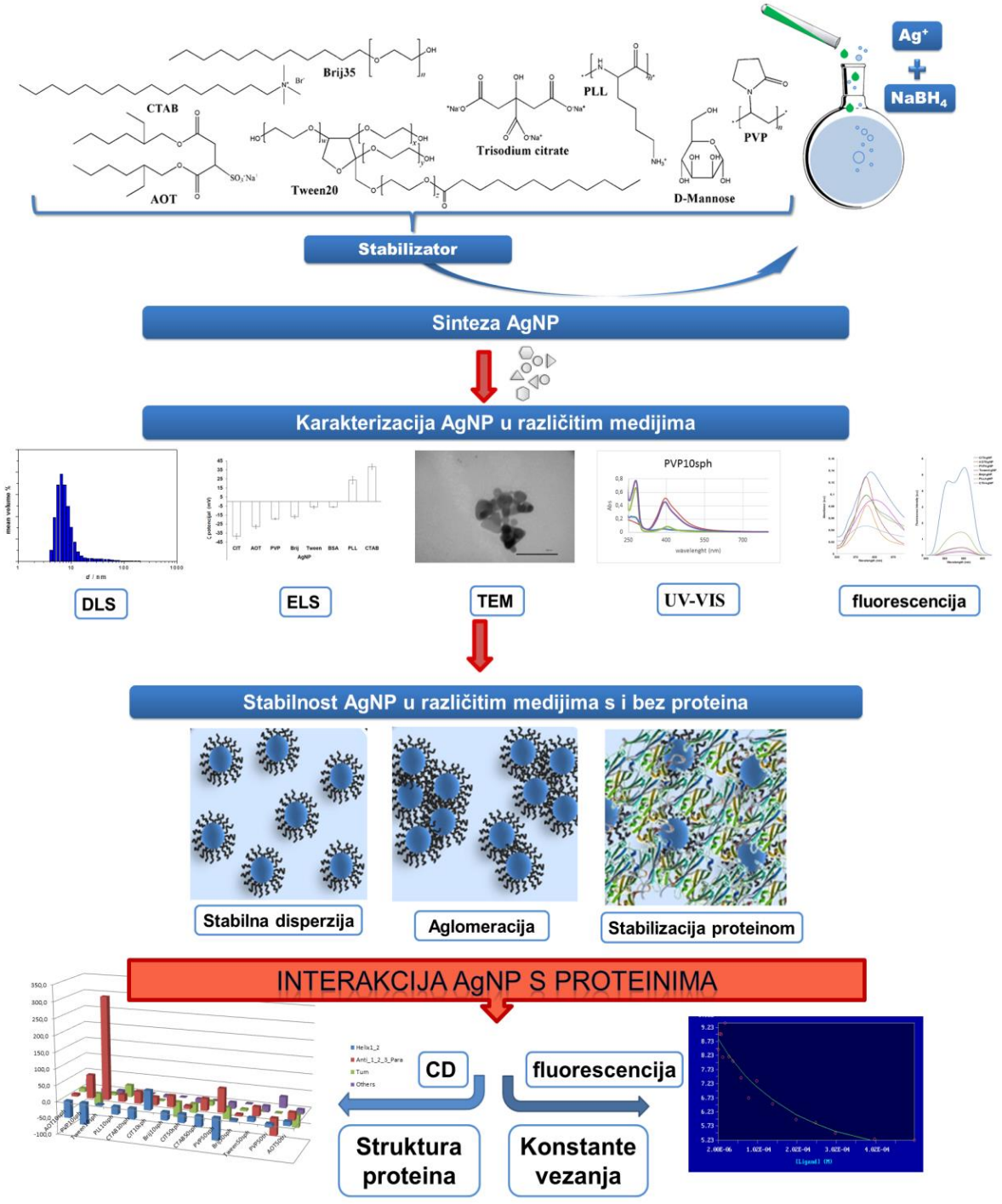

Slika 11. Koncept doktorskog rada.

3. MATERIJALI I METODE

3.1. Materijali

Analitički čiste kemikalije; srebrov nitrat ($AgNO_3$, Mr 169,87), natrijev citrat ($Na_3C_6H_5O_7$, Mr 258,06), natrijev borhidrid ($NaBH_4$, Mr 37,83), natrijev hidroksid (NaOH, Mr 39,997) i nitratna kiselina (HNO_3, Mr 36,01) nabavljeni su od tvrtke Merck (Darmstadt, Njemačka), dok su askorbinska kiselina ($C_6H_8O_6$, Mr 176,2), natrijev bis (2-etilheksil) sulfosukcinat ($C_{20}H_{37}NaO_7S$, Mr 444,56), cetiltrimetilamonijev bromid ($C_{19}H_{42}BrN$, Mr 364,45), poli(vinilpirolidon) [$(CH_9NO)_n$, Mr 40000] ε-poli-L-lizin [(C6H12N2O)n, Mr 4700], Tween 80 ($C_{64}H_{124}O_{26}$, Mr 1310), i Brij 35 ($C_{12}H_{25}O(CH_2CH_2O)_{23}H$, Mr 1225) su kupljene od tvrtke Sigma Chemical Co. (Taufkirchen, Njemačka).

Od proteina korišteni su komercijalno dostupni nativni α1-kiseli glikoprotein (AGP) (Sigma, G3643-25mg, 99%, CAS:66455-27-4, Lot#111M7401V PCode: 1002054631) i goveđi serumski albumin (BSA; *eng. bovine serum albumin*) (Sigma-Aldrich Chemie GmbH, Steinheim, Germany, A2153-50g Lot #SLBS1213V PCode: 1002530279).

Plastični pribor nabavljen je od tvrtke Sarstedt (Belgija), a stakleni od tvrtke Schott (Njemačka). Za sva razrjeđenja korištena je ultračista voda (UV) dobivena kao deionizirana voda električne vodljivosti od 18,2 MΩ/cm pomoću GenPure UltraPure vodenog sustava (TKA Wasseraufbereitungssysteme GmbH, Niederelbert, Njemačka).

3.2. Sinteza srebrnih nanočestica

Sintetske metoda AgNP korištene u ovom radu temelje se na „bottom up“ načelu. To su koprecipitacijske metode kojima se nanočestice dobivaju redukcijom ionskog oblika srebra uz prisutnost različitih stabilizatora. Promjenom uvjeta sinteze, kao što su koncentracija reaktanata, koncentracija stabilizatora, temperatura, brzina, te redoslijed dodavanja reaktanata, moguće je varirati veličinu, oblik, ζ potencijal i površinsku strukturu AgNP.

Glavni prekursor AgNP bio je s*rebrov nitrat* koji je za razliku od ostalih srebrovih soli, kemijski stabilan.

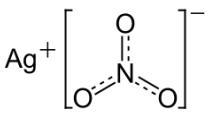

Kao reducensi u sintezama korišteni su *natrijev borhidrid*, brzo i jako anorgansko redukcijsko sredstvo koje uzrokuje formiranje brojnih srebrovih jezgri na početku sinteze i time smanjuje vrijeme rasta te time sprječava stvaranje većih nanočestica;

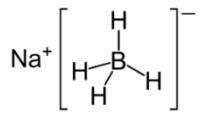

askorbinska kiselina (C6H8O6, Mr 176.12), poznatija kao vitamin C, koja ima antioksidativni i blagi redukcijski potencijal;

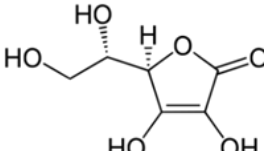

i *natrijev citrat*

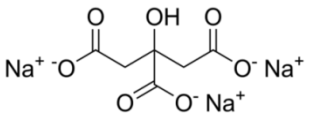

Za pripravljanje stabilnih AgNP nužno je korištenje stabilizatora koji po svojoj strukturi mogu biti polielektroliti, polimeri ili surfaktanti. U ovom istraživanju korišteni su stabilizatori prikazani u Tablici 6.

Tablica 6. Stabilizatori korišteni za pripravu AgNP.

Naziv / skraćeni naziv	**Molekularna formula i struktura**	**Molekularna masa, g/mol**	**Tip stabilizatora**
Natrijev citrat / CIT	$Na_3C_6H_5O_7$ 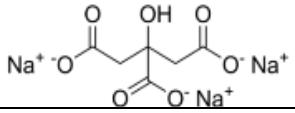	294,10 (dihidrat)	Anionski stabilizator
Natrijev bis (2-etilheksil) - sulfosukcinat / AOT	$C_{20}H_{37}NaO_7S$ 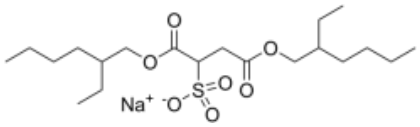	444,56 (natrijeva sol)	Anionski surfaktant
Cetiltrimetilamonijev bromid / CTA	$C_{19}H_{42}BrN$ 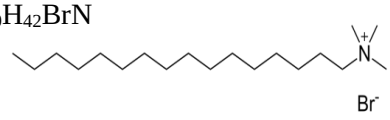	364,45	Kationski polimerni surfaktant
Poli(vinilpirolidon) / PVP	$(CH_9NO)_n$ 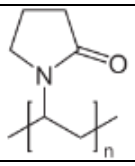	40000	Neionski polimer
ε-poli-L-lizin / PLL	$(C_6H_{12}N_2O)_n$ 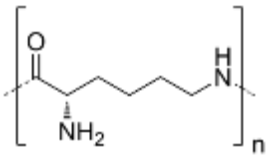	4700	Pozitivno nabijeni polimer
Tween 80 / Tween	$C_{64}H_{124}O_{26}$ 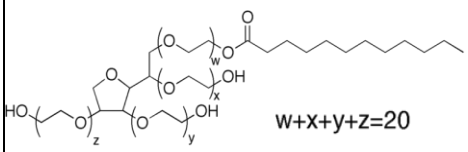	1310	Neionski surfaktant
Brij 35 / Brij	$(C_{12}H_{25}O(CH_2CH_2O)_{23}H$ 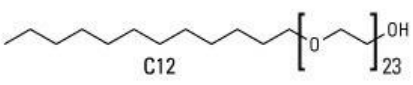	1225	Neionski surfaktant

3.2.1. Postupci priprave sferičnih AgNP veličine 10 nm

Sinteze AgNP primjenom AOT, PVP, Tween 80, PLL i CTA stabilizatora provedene su redukcijom $AgNO_3$ s $NaBH_4$ tako da je 5 mL 90 mM otopine $AgNO_3$ dokapavano u pripremljenu otopinu stabilizatora uz energično miješanje na IKA RCT magnetskoj miješalici (IKA Werke, Germany). Nakon toga je u tu mješavinu dokapano 5 mL 160 mM $NaBH_4$ (približno 1 kap/sec.). Dodatkom reducensa smjesa poprimi žutu boju koja tijekom 45 minuta miješanja prelazi u tamno-smeđu boju. Ukupni volumen reakcijske smjese bio je 200 mL, a konačne koncentracije reaktanata u reakcijskoj smjesi: 4,5 mM $AgNO_3$, 8 mM $NaBH_4$, te 0,5 mM AOT, 0,5 mM CTA, 0,3 % (v/v) PVP, 0,05 % (v/v) PLL, i 0,5 mM Tween 80.

Postupak priprave AgNP stabiliziranih natrijevim citratom započinje dodatkom otopine $NaBH_4$ (47,5 mL 52,6 mM) u 200 mL ledeno ohlađene otopine natrijevog citrata (3,75 mM). Zatim se dodaje 2,5 mL 10 mM $AgNO_3$ uz miješanje na ledenoj kupki. Boja otopine iz bezbojne prelazi u žutu. Konačni molarni omjer reaktanata u reakcijskoj smjesi je 0,1 mM $AgNO_3$: 10 mM $NaBH_4$: 3 mM Na-citrat.

Sinteza srebrnih nanočestica obloženih sa BSA započinje dokapavanjem otopine $AgNO_3$ (7,6 mL, 50 mM) u 33 mL čiste vode u kojoj je prethodno otopljeno 90 mg BSA, uz energično miješanje. Zatim se dokapava otopina $NaBH_4$ (1 mL, 0,397 M) uz konstantno miješanje otopine. Ukupni volumen reakcijske smjese je 40 mL, a sadrži 13,50 μmol BSA. Molarni odnos reaktanata u reakcijskoj smjesi je Ag^+ : BSA : BH_4^- je 28:1:1. Vrijeme trajanja reakcije je 1 sat, nakon čega je produkt pročišćen.

3.2.2. Postupci priprave sferičnih AgNP veličine 50 nm

AgNP stabilizirane s AOT, PVP, Tween 80, CTA i Brij35 su sintetizirane kemijskom redukcijom kationskog kompleksa $[Ag(NH_3)_2]^+$ s D-glukozom. Početne koncentracije reaktanata su: $AgNO_3$ 1 mM; amonijak i D-glukoza (reducirajuća sredstva) 10 mM. Stabilizatori (0,5 mM AOT, 0,5 mM CTA, 0,3% (v/v) PVP, 0,5 mM Brij 35 i 0,5 mM Tween 80) pomiješani su s $AgNO_3$ neposredno prije dodatka reducensa. Otopine stabilizatora pripremljene su otapanjem odgovarajuće količine stabilizirajućeg sredstva u UW u koje se dokapava otopina $AgNO_3$ (2,22 mL 90 mM) uz konstantno miješanje na magnetskoj mješalici. Zatim se dodaje otopina NH_3 (0,133 mL, 15 M) odjednom, u mlazu, potom kap po kap 4 mL, 0,5 M otopine glukoze (otprilike 1 kap/sec.). Na kraju se pH reakcijske smjese podesi na pH 11,5 dodatkom 0,6 mL 1M NaOH jer je brzina reakcije pod snažnim utjecajem

pH. Sve reakcije su izvedene na sobnoj temperaturi pri čemu je reakcijska smjesa cijelo vrijeme zaštićena od svjetlosti i energično miješana 45 min.

Nanočestice srebra stabilizirane citratom sintetizirane su primjenom metode opisane u literaturi (Li i dr., 2013). 200 μL 0,1 μM vodene otopine askorbinske kiseline dodaje se u 194 mL kipuće UW. Paralelno se pripremi smjesa naizmjeničnim dodavanjem 0,538 mL vodene otopine natrijevog citrata (250 mM) i 0,667 mL vodene otopine $AgNO_3$ (90 mM), koja se nakon 5 min inkubacije na sobnoj temperaturi doda u kipuću vodenu otopinu askorbinske kiseline tako da je ukupni volumen reakcijske smjese 200 mL a konačne koncentracije reaktanata: 0,1 μM askorbinska kiselina, 0,673 mM citrat i 0,3 mM $AgNO_3$. Boja reakcijske otopine brzo prelazi iz bezbojne u žutu. Otopina se dalje zagrijava 1 sat uz stalno miješanje.

3.2.3. Postupci priprave triangularnih AgNP

Triangularne pločice AgNP veličine 10 nm pripremljene uz korištenje PVP i AOT stabilizatora. Postupak sinteze započinje miješanjem otopine $AgNO_3$, natrijevog citrata, PVP ili AOT i H_2O_2 u UW uz energično miješanje na sobnoj temperaturi. U tako pripremljenu otopinu jednokratno se ubrizga otopina $NaBH_4$ (0,5 mL, 200 mM) pri čemu nastaje otopina svjetlo žute boje koja nakon 30 minuta miješanja prelazi u tamno žutu boju što označava nastajanja AgNP. Tijekom nekoliko sljedećih sekundi boja otopine prelazi u crvenkastu boju. Konačne koncentracije reaktanata u reakcijskoj smjesi su 0,3 % PVP, 0,1 mM $AgNO_3$, 3 mM natrijev citrat, 0,5 mM $NaBH_4$, odnosno 0,5 mM AOT, 0,1 mM $AgNO_3$, 3,15 mM natrijevog citrata, 0,75 mM $NaBH_4$. Konačni volumen reakcijske smjese je 200 mL. Dodatkom reducensa nastaje najprije otopina svijetlo žute boje koja nakon 30 minuta miješanja prelazi u tamno žutu boju, a tijekom nekoliko sljedećih sekundi boja otopine prelazi u crvenu, zatim ljubičastu i na kraju stabilnu ljubičasto-plavu boju koja ukazuje na sintezu triangularnih AgNP.

3.2.4. Postupci priprave kubičnih AgNP

Kubične AgNP sintetiziraju se otapanjem 0,586 g PVP (M_w= 40,000) u 18,4 mL etilenglikola nakon čega se dodaje 1 mL $AgNO_3$ otopine (0,93 M u etilenglikolu). U tako pripremljenu otopinu dodaje se 0,6 mL otopine NaCl (0,01 M u etilenglikolu). Konačne koncentracije $AgNO_3$, NaCl, i PVP su 46,5 mM, 0,3 mM, i 264 mM. Otopina se zagrijava na temperaturu vrenja etilenglikola (198 °C) u uljnoj kupelji, a nakon provedbe redukcije otopina se hladi sobnu temperaturu.

3.2.5. Pročišćavanje sintetiziranih nanočestica

Posljednji korak u pripremi AgNP je pročišćavanje koje se provodi nakon kemijske sinteze pri čemu se uklanjaju neiskorišteni reaktanati u smjesi. Pročišćavanje se provodi ultracentrifugiranjem na 12 000 okr/min (15 000 × g) 30 min u RC5C Sorvall ultracentrifugi (DuPont, SAD). Nakon pažljivog izdvajanja supernatanta automatskom pipetom, talog AgNP s dna epruvete suspendira se u UW. Postupak se provodi 3 puta. Pročišćene AgNP se čuvaju na 4 °C u tamnim staklenim bočicama, zaštićene od svjetlosti do daljnje upotrebe.

3.3. Karakterizacija nanočestica srebra

Oblik, veličina, kemijski sastav i zeta potencijal sintetiziranih AgNP određeni su transmisijskom elektronskom mikroskopijom (TEM), dinamičkim raspršenjem svjetlosti (DLS, od eng. Dynamic Light Scattering), elektroforetskim raspršenjem svjetlosti (ELS, od eng. Electrophoretic Light Scattering), UV-VIS i fluorescentnom spektroskopijom, te AAS-om (Tablica 7).

Tablica 7. Instrumentalne metode karakterizacije AgNP.

NP svojstva	Analitičke tehnike	Kratki analitički opis
Veličina	DLS	Određivanje promjene hidrodinamičkog promjera NP, raspodjela d_H
	TEM	Određivanje promjera NP
Naboj	ELS	Određivanje ζ potencijala
Plazmonska svojstva	UV-VIS spektrofotometrija	Određivanje površinske plazmonske rezonancije
Fluorescentna svojstva	Spektrofluorimetrija	Određivanje fluorescencije
Oblik i struktura	TEM	Vizualizacija strukture nanočestica
Sastav	AAS	Određivanje elementarnog sastava AgNP
Topljivost	AAS	Određivanje koncentracije Ag^+ iona otpuštenih s površine AgNP tj. određivanje topljivosti AgNP

Stupanj iskorištenja sintetskih reakcija i temeljitost pročišćavanja produkata utječu na konačne koncentracije sintetiziranih AgNP. U pročišćenim pripravcima određene su koncentracije srebra pomoću AAS.

3.3.1. Atomska apsorpcijska spektroskopija

Princip rada AAS temelji se na činjenici da atomi različitih elemenata izloženi svjetlosti apsorbiraju svjetlost samo određene valne duljine. Obasjavajući uzorak svjetlošću koja sadrži element od interesa, dolazi do apsorbcije svjetlosti od strane elementa u uzorku (Slika 12). Uzorak se atomizira - tj. pretvara u slobodne atome osnovne energetske razine u stanju pare pri čemu zraka emitiranog elektromagnetnog zračenja koju emitiraju pobuđeni atomi prolazi kroz uzorak. Što je veći broj atoma u pari, to će više zračenja biti apsorbirano. Količina apsorbirane svjetlosti proporcionalna je koncentraciji atoma u uzorku.

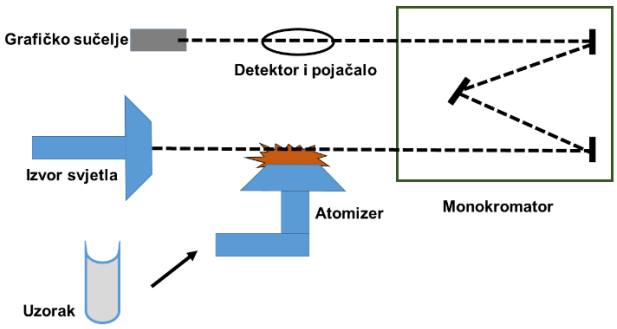

Slika 12. Princip rada atomskog apsorpcijskog spektrometra.

Ukupna koncentracija Ag u pripravljenim uzorcima AgNP određena je AAS-om pomoću uređaja Analyst 600 (Perkin Elmer, SAD) korištena je za određivanje ukupne koncentracije srebra u pripravljenim AgNP, te za određivanje njihova otapanja u različitim medijima. U tu su se svrhu uzorci razrjeđivali s 5% (w/v) HNO_3. Korištena je valna duljina apsorbirane svjetlosti 328 nm, a kalibracija se provodila uporabom standardnih otopina Ag u koncentracijskom rasponu između 0,5 i 20 µg/L. Koncentracija analita se očita iz kalibracijske krivulje (Slika 13).

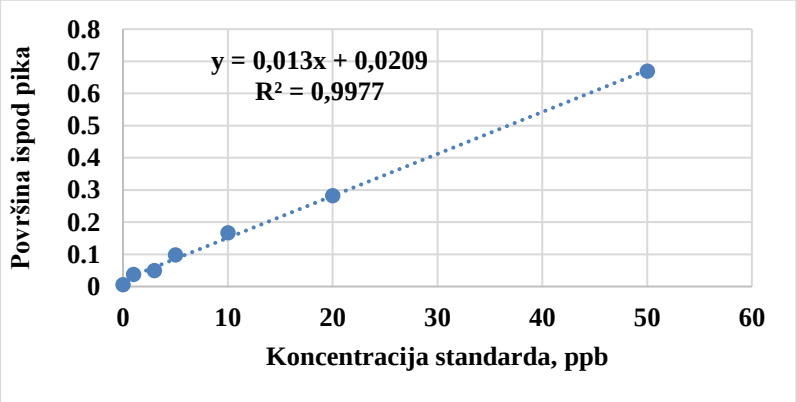

Slika 13. Kalibracijska krivulja korištena tijekom AAS mjerenja.

3.3.2. Metoda dinamičkog i elektroforetskog raspršenja svjetlosti

Metode dinamičkog raspršenja svjetlosti (DLS, od eng. *dynamic light scattering*) i elektroforetskog raspršenja svjetlosti (ELS, od eng. *electrophoretic light scattering*) korištene su kao neinvazivne fizikalne metode za određivanje raspodjele veličine i zeta potencijala AgNP.

DLS metoda se koristi za određivanje raspodjele veličina nanočestica u uzorku temeljem promjene intenziteta raspršene svjetlosti (Kato, 2012). Osnovno načelo je osvjetljenje uzorka laserskom zrakom odnosno elektromagnetnim zračenjem, pri čemu čestice raspršuju svjetlost i time daju informacije o njihovom kretanju, a analiza fluktuacije intenziteta raspršene svjetlosti daje informacije o veličini čestica. Čestice suspendirane u mediju se neprestano gibaju tzv. Brownovim gibanjem koje je definirano kao nasumično gibanje čestica do kojeg dolazi zbog sudaranja s molekulama otapala. Brownovo gibanje čestica ili molekula u suspenziji uzrokuje raspršenje laserskog svjetla različitim intenzitetom. Čestica u otopini će raspršiti svjetlost ako se njezina polarizabilnost razlikuje od polarizabilnosti okoline. Pri tome, intenzitet raspršene svjetlosti ovisi o smjeru polarizacije upadne zrake, kutu raspršenja i svojstvima otopine (Puthussericka l, i dr., 2015). Što je čestica veća, to je njeno gibanje sporije, suprotno, manje čestice su ubrzane molekulama otapala te se kreću brže u odnosu na čestice većih veličina. Analizom fluktuacije intenziteta raspršene svjetlosti računa se brzina Brownovog gibanja (Slika 14), a izmjerenu brzinu preračunava u veličinu čestica koristeći translacijski difuzijski koeficijent pomoću Stokes-Einsteinove jednadžbe (Kato, 2012).

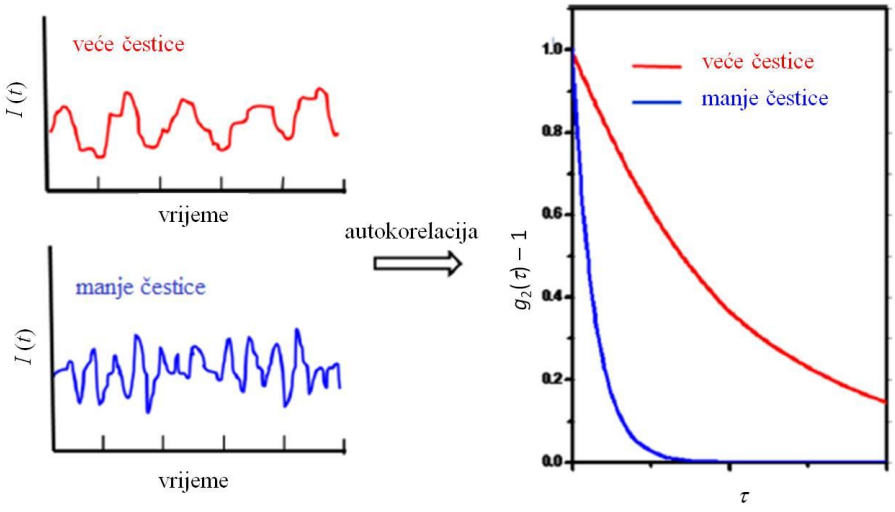

Slika 14. Shematski prikaz fluktuacija intenziteta raspršene svjetlosti.

Promjer koji je dobiven ovim postupkom je promjer sfere, a odnosi se na to kako čestica difundira unutar tekućine te se stoga naziva i hidrodinamičkim promjerom (d_H) kojim se mjeri veličina čestica i slovatacijska ovojnica koja se s njom giba. Vrijednost difuzijskog koeficijenta ovisi o veličini čestice bez solvatacijske ovojnice, ionskoj jakosti medija, vrsti prisutnih iona, strukturi površine i obliku čestice (Hassan i dr., 2015). Hidrodinamički promjer čestice koja nema oblik sfere promjeru sferične čestice koja ima jednak translacijski koeficijent. Obzirom da je sfera jedini oblik čija se dimenzija može opisati samo jednom veličinom, metode koje mjere veličinu čestica imaju problem s određivanjem veličine čestica koje nisu sferičnog oblika. Suvremena DLS tehnika automatski obavlja kumulativnu analizu koja određuje i indeks polidisperznosti (PDI od eng. *polidispersity index*) uzorka. PDI je bezdimenzijska veličina koja se nalazi između 0 i 1. Kolodina suspenzija NP je monodisperzna ako je vrijednost PDI ispod 0,05 (Zetasizer, 2013). Za bi- i polimodalne raspodjele veličina potrebne su složenije metode analize. Podaci dobiveni DLS-om mogu biti izraženi kao raspodjela veličine čestica u uzorku po intenzitetu, volumenu ili broju. Ako je raspodjela veličine po intenzitetu karakterizirana većim brojem pikova ili je asimetrična, pomoću Mieove teorije pretvara se u raspodjelu po volumenu ili broju, pri čemu se dobiva bolji uvid u važnost drugog pika i asimetrije. Općenito vrijedi: *d*(intenzitet) > *d*(volumen) > *d*(broj). Razlika je posljedica toga što npr. dvije čestica različitih veličina jednako doprinose ukupnom broju čestica, ali različito volumenu čestica ili dinamičkom raspršenju. Primjerice, ukoliko se u sustavu nalazi jednaki broj čestica veličina 5 i 50 nm, raspodjela veličine po broju dati će dva pika omjera 1:1, za raspodjelu po volumenu dobit će se omjer 1:1000 jer je volumen sfere proporcionalan d^3, dok će omjer pikova biti 1:1000000 za raspodjelu po intenzitetu, jer je intenzitet proporcionalan d^6 kako je prikazano na Slici 15 (Zetasizer, 2013).

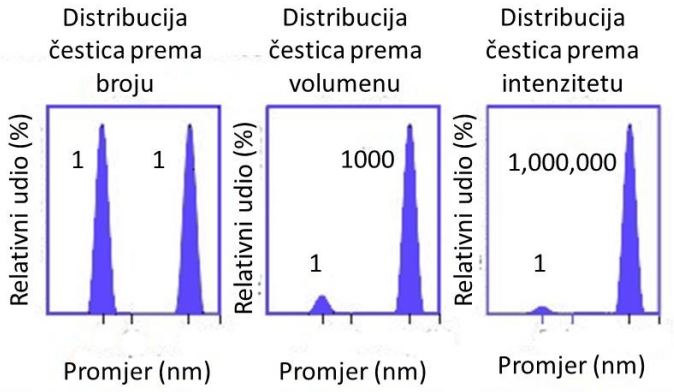

Slika 15. Shematski prikaz raspodjele veličine prema broju, volumenu i intenzitetu za bimodalni koloidni sustav.

ELS je tehnika koja se koristi za mjerenje elektroforetske pokretljivosti čestica u disperziji ili molekula u otopini. Zeta potencijal se određuje iz izmjerene elektroforetske mobilnosti i brzine gibanja čestica u električnom polju, poznatom kao mobilnost, iz koje se računa ζ potencijal.

U ovom je istraživanju za DLS i ELS mjerenja korišten je Zetasizer Nano ZS instrument (Malvern, UK) opremljen zelenim laserom (532 nm). Pripremljene su otopine AgNP u koncentracijama 1 i 10 mg/L. Intenzitet raspršenog svjetla detektiran je pod kutem od 173°. Hidrodinamički promjer (d_H) i raspodjela veličina AgNP dobivene su iz raspodjele po volumenu, broju i intenzitetu u svrhu usporedbe prosječnih vrijednosti dobivenih iz 10 mjerenja. Površinski naboj AgNP određen je mjerenjem ζ potencijala koji je izračunat iz izmjerene elektroforetske pokretljivosti prema Henryjevoj jednadžbi koristeći Smoluchowskijevu aproksimaciju (f(Ka) = 1,5). Rezultati ζ potencijala su prikazani kao prosječna vrijednost 6 mjerenja. Mjerenja su provedena na 25 °C i podaci su obrađeni u Zetasizer 6,32 programskom paketu (Malvern Instruments Ltd., 1997).

3.3.3. UV-VIS spektrofotometrija

Spektroskopske metode koriste se za proučavanje atomske i molekulske strukture spojeva, a baziraju se na interakciji elektromagnetskog zračenja s uzorkom, pri čemu analit emitira ili apsorbira određenu količinu zračenja koja se mjeri. Elektromagnetsko zračenje karakterizirano je valnom duljinom (λ/nm) i frekvencijom (ν/Hz). Valna duljina je udaljenost između susjednih vrhova (ili korita), a izražava se u nanometrima (10^{-9} metara). Frekvencija je broj valnih ciklusa koji prolaze kroz fiksnu točku po jedinici vremena, a mjerna jedinica je hertz (Hz). Kada bijela svjetlost prođe kroz obojenu tvar ili se od nje reflektira od, apsorbira se karakteristični dio valnih duljina. Preostala svjetlost će tada preuzeti boju koja se nalazi na apsorbiranoj valnoj duljini (Slika 16).

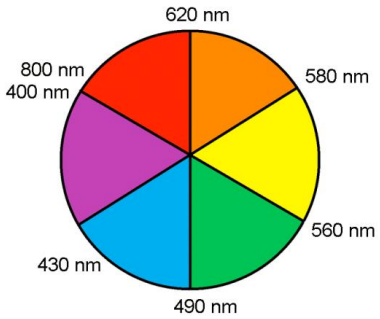

Slika 16. Preuzimanje boje na apsorbiranoj valnoj duljini.

Slika 17 prikazuje regije elektromagnetskog zračenja uz prikaz recipročnog odnosa između valne duljine i frekvencije.

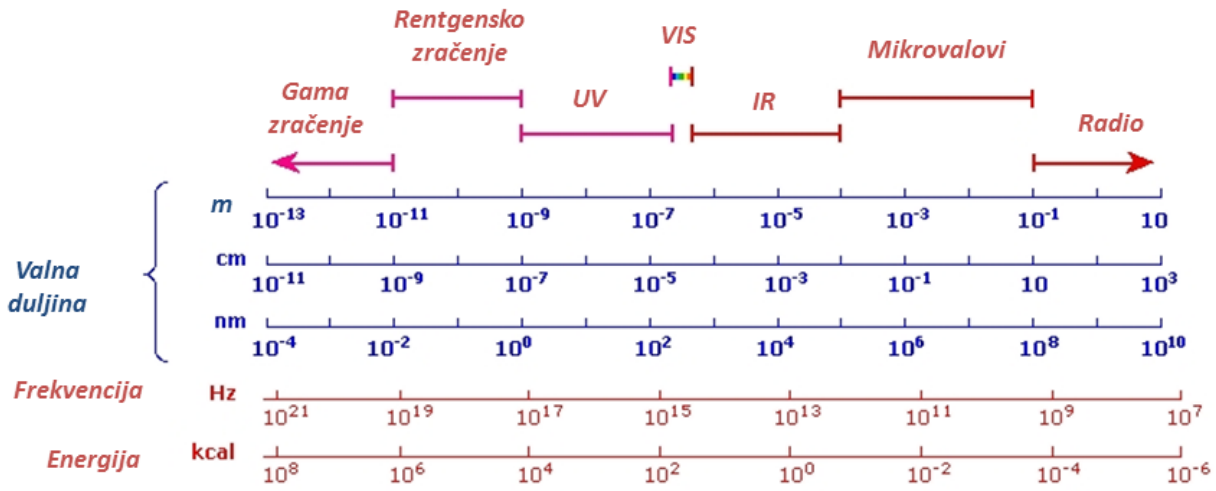

Slika 17. Područje elektromagnetnog zračenja.

Zajednička značajka obojenih spojeva je kemijska struktura karakterizirana velikim brojem konjugiranih π-elektrona. UV-VIS zračenje u molekuli uzrokuje prijelaz valentnih elektrona u više nepopunjene elektronske orbitale. Dio molekule koji apsorbira zračenje naziva se kromofor. Budući da je apsorbancija uzorka proporcionalna broju apsorbirajućih molekula u svjetlosnoj zraci spektrometra, potrebno je ispraviti vrijednost apsorpcije. Ispravljena apsorpcijska vrijednost naziva se "molarnom apsorpcijom" i izražava se Beer-Lambertovim zakonom a osobito je korisna kada se uspoređuju spektri različitih spojeva i određuje relativna snaga apsorpcije svjetlosti. Molarna apsorpcija (ε) definirana je kao:

$$A = \log (I_0/I) = \varepsilon * c * l \qquad (2)$$

gdje I_0 intenzitet ulazne zrake, I intenzitet zrake nakon prolaska kroz uzorak, A apsorbancija, c koncentracija uzorka izražena u molovima / litri i l duljina svjetlosnog puta kroz uzorak u cm. Uzorak je apsorbirao zračenje kad je intenzitet ulazne zrake veći od intenziteta izlazne zrake, odnosno omjer I_0/I je veći od 1. UV-VIS spektar je grafički prikaz apsorbancije uzorka (A) u ovisnosti o valnoj duljini (λ). Spektralni podaci karakteristični za analit su valna duljina pri apsorpciji (λ_{max}) te vrijednost molarnog apsorpcijskog koeficijenta ε pri maksimalnoj apsorbanciji. Molarni apsorpcijski koeficijent (ε) je mjera za intenzitet, odnosno, daje podatak koliko je jako molekula apsorbirala zračenje pri određenoj λ.

Apsorpcijski spektar se mjeri spektrofotometrom (Slika 18). Osnovno načelo UV-VIS spektroskopije je da analit apsorbira dio elektromagnetnog zračenja prilikom prolaska zračenja kroz otopinu uzorka. Elektromagnetsko zračenje, tj. izvor svjetlosti se dobiva iz

volfram-halogene (290-900 nm) i Deuterijeve lampe (210-370 nm). Takva svjetlost sadrži zračenje različitih valnih duljina tako da je potreban monokromator koji će razložiti svjetlost na pojedine valne duljine. Monokromatska svjetlost prolazi kroz uzorak i detektira se fotodetektorom (fotomultiplikatorske cijevi ili fotodioda). Dio zračenja koji se apsorbira izražava se apsorbancijom (A) a dio koji prolazi kroz uzorak označava se transmisijom (T). U kratkom vremenu, spektrofotometar skenira UV-VIS spektar i na detektoru registrira valnu duljinu pri kojoj dolaui do apsorpcije. Otapalo koje se koristi ne smije apsorbirati UV-VIS zračenje, a kivete su izrađene od kvarcnog stakla koje propušta UV-VIS zračenje (Sheehan, 2009).

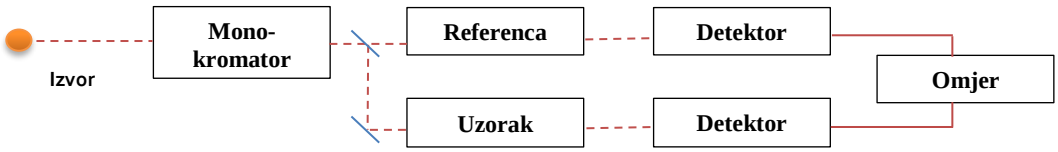

Slika 18. Pojednostavljena shema dvosnopnog spektrometra.

Mjerenje UV-VIS spektara otopina nanočestica srebra u različitim medijima provodila se na spektrofotometru Cary 50 UV-VIS (Varian, Agilent Technologies) u rasponu valnih duljina od 240 do 800 nm.

3.3.4. Elektronska mikroskopija

Vizualizacija AgNP u ovom istraživanju provedene je pomoću TEM mikroskopa (Zeiss 902A, Jena, Njemačka) u svjetlom polju pri naponu ubrzanja od 80 kV. Slike su snimljene Canon PowerShot S50 kamerom spojenom na mikroskop. TEM uzorci pripremljeni su stavljanjem kapi suspenzije uzorka na bakrenu rešetku obloženu Formavar membranom. Uzorak je osušen na zraku na sobnoj temperaturi.

U elektronskom mikroskopu elektromagnetne zavojnice savijaju snopove elektrona čime se dobiva veliko povećanje slike. Mala valna duljina elektrona omogućuje elektronskim mikroskopima veću razlučenje i optičko povećanje u odnosu na svjetlosni (Slika 19).

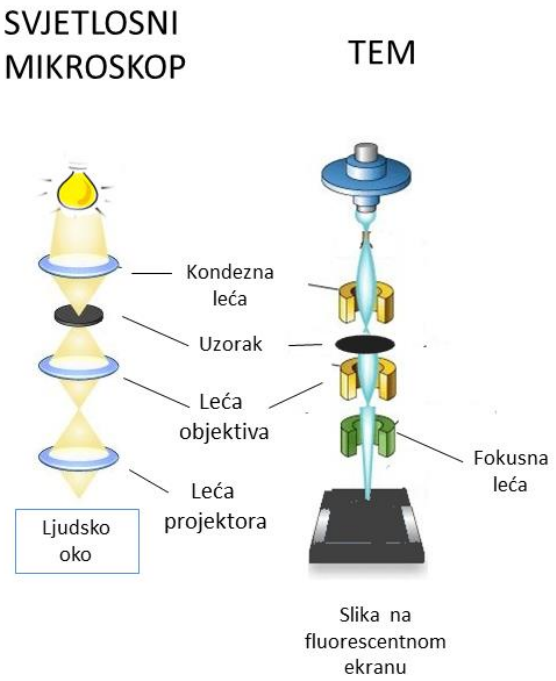

Slika 19. Shematski prikaz TEM mikroskopa i usporedba sa svjetlosnim

3.4. Ispitivanje ponašanja nanočestica srebra u biološkim medijima s i bez proteina

Ispitivanje stabilnosti, ponašanja i interakcije različitih AgNP u modelnim biološkim medijima s i bez proteina (BSA i AGP) provedeno je korištenjem tehnika navedenih u Tablici 8. U tu svrhu korištena su 4 modelna biološka medija: ultračista voda (UW), fosfatni pufer pH 7,4 (FP), fiziološka otopina (FO) i FP uz dodatak 0,9% NaCl (FPNaCl). Stabilnost i ponašanje različitih AgNP u navedenim medijima praćeni su tijekom 1 sata. Vezanje albumina na različite AgNP određeno je u svim navedenim medijima, dok je vezanje AGP na različite AgNP određeno u UW i FP. Sva mjerenja provedena su najmanje tri puta.

Za pripremu 0,5 L 50 mM fosfatnog pufera pH 7,4 (FP) izvagano je 0,8807 g natrijevog dihidrogenfosfatdihidrata ($NaH_2PO_4x2H_2O$, Mr 156,01) i 6,9318 g dinatrijevog hidrogenfosfatdodekahidrata ($Na_2HPO_4x12H_2O$, Mr 358,14) otopljenih u UW tako da su im konačne koncentracije u FB redom 11,29 mM i 38,71 mM. Za pripremu fiziološke otopine (FO) otopljeno je 9 g NaCl u 1 L UW, a za pripremu FPNaCl 4,5 g NaCl je u 0,5 L FP.

Tablica 8. Metode korištene za ispitivanje nano-bio interakcija.

NP svojstva	Analitičke tehnike	Kratki analitički opis
Afinitet vezanja proteina	Fluorescentna spektroskopija	Mjeri promjene u fluorescenciji proteina
	UV-VIS spektrofotometrija	Mjeri promjenu apsorpcijskih spektara
Promjene AgNP svojstava uslijed vezanja s proteinima	DLS	Promjene u distribuciji veličina
	ELS	Promjene zeta potencijala
	TEM	Strukturne promjene
Strukturne promjene proteina nakon vezivanja	Spektroskopija cirkularnog dikroizma	Mjeri promjene u sekundarnoj strukturi proteina ovisno o kiralnim svojstvima proteina

3.4.1. Promjene svojstava nanočestica nakon interakcije s proteinima

Za određivanje promjena u distribuciji veličina, zeta potencijala i topljivosti različitih vrsta AgNP u različitim medijima (UW, FP, FO i FPNaCl), te uslijed i nakon interakcije s albuminom i AGP, korištene su DLS, ELS, TEM, UV-VIS i AAS metode kako je opisano u prethodnom poglavlju. Aglomeracijsko ponašanje u navedenim medijima tijekom 1 sata istraženo je određivanjem promjena u distribuciji veličina DLS metodom, a vizualizirano TEM tehnikom. ELS tehnika je korištena za praćenje promjena u zeta potencijalu AgNP nakon njihovog izlaganja određenom biološkom mediju. Otapanje AgNP u modelnim biološkim medijima određeno je AAS mjerenjem količine ukupnog Ag u filtratima dobivenim ultracentrifugiranjem smjesa AgNP i modelnih medija nakon inkubacije od 1 sata. UV-VIS spektroskopskim mjerenjima određene su promjene u SPR signalu istraživanih AgNP nakon njihovog izlaganja modelnom biološkom mediju.

3.4.2. Određivanje konstante vezanja proteina na nanočestice

Interakcije NP i proteina mogu se opisati protein – ligand interakcijama u kojima je koncentracija produkata ovisna o koncentraciji reaktanata i uvjetima reakcije. Vezanje NP na protein, intenzitet fluorescenicje proteina se smanjuje što omogućuje određivanje konstante vezanja ispitivane NP. Titracijom stalne koncentracije proteina [P] ligandom NP povećava se

koncentracija produkta P-NP do ravnotežnog stanja. Načelo vezanja proteina i NP može se prikazati bimolekularnom reakcijom:

$$[P] + [NP] \underset{}{\overset{K_a}{\rightleftharpoons}} [P\text{-}NP] \quad (3)$$

U stanju ravnoteže izjednačuju brzine nastanka i raspadanja kompleksa [P-NP]

$$k_1 \cdot [P] \cdot [NP] = k_{-1} \cdot [P - NP] \quad (4)$$

$$K_a = \frac{k_1}{k_{-1}} = \frac{[P-NP]}{[P]\cdot[NP]} \quad (5)$$

pri čemu je K_a konstanta asocijacije. Za bimolekularne reakcije, mjerna jedinica za K_a je koncentracija^{-1} (M^{-1}). Iz niže navedenog odnosa vidljivo je da će se promjenom konstante kemijske ravnoteže K promijeniti omjer između kompleksa NP-P i slobodnih frakcija NP, odnosno proteina, što može rezultirati promjenom kliničkog učinka bilo proteina bilo NP.

Prvi korak u određivanu konstante ravnoteže je izrada titracijske krivulje pri čemu je koncentracija P stalna, koncentracija NP titracijski se povećava a koncentracija kompleksa se povećava do ravnotežnog stanja (Slika 19).

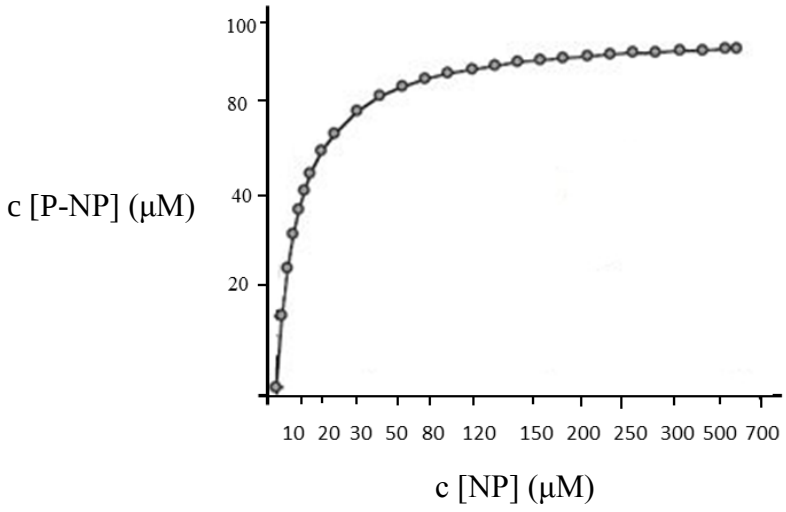

Slika 20. Titracijska krivulja

Matematički odnos između udjela vezanog reaktanta P i koncentracije slobodnog rekatanta NP je:

$$P\ vezana\ frakcija = \frac{[P-NP]}{[P]+[P-NP]} = \frac{1}{\frac{[P]}{[P-NP]}+1} = \frac{1}{\frac{K_d}{[NP]}+1} = \frac{[NP]}{K_d+[NP]} \quad (6)$$

Pri čemu je K_d konstanta disocijacije ($1/K_a$). Udio vezanog reaktanta P (Θ_b) izražen je izrazom:

$$\theta_b = \frac{[NP]}{K_d + [NP]} \quad (7)$$

Ako je [NP] = K_d, onda Θb = 0,5. Odnosno, ako je koncentracija slobodnog reaktanta NP jednaka konstanti disocijacije, tada je udio vezanog P jednak polovici maksimalno moguće vezanog reaktanta što omogućuje određivanje konstante disocijacije iz titracijske krivulje (Slika 20).

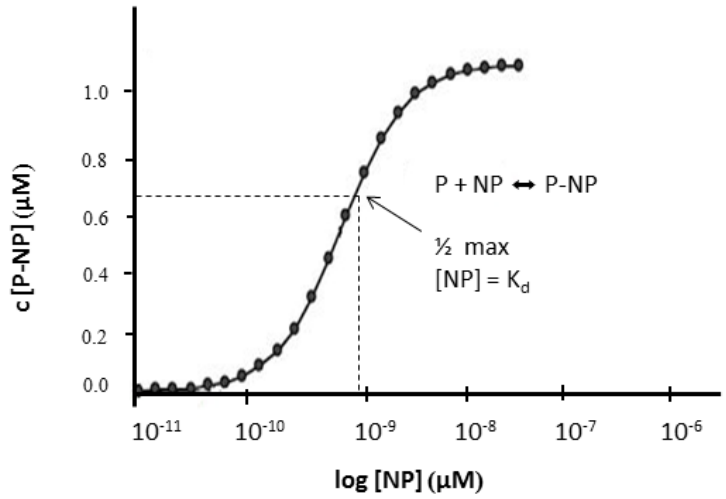

Slika 21. Određivanje konstante disocijacije iz titracijske krivulje

Općenito, za bimolekularne reakcije vrijedi da je 10% rekatanta P vezano kad je [NP] = K_d/9 i 90% reaktanta P bit će vezano kad je [NP] = 9K_d.

Prijenosom podataka vezanja bimolekularne reakcije u lineranu funkciju dobiva se jednadžba pravca i dijagram koji jasno pokazuju odnos koncentracija i ravnotežnih konstanti. Linerarni prikaz naziva se Scatchardov dijagram (Slika 21), a koristi za izračun ravnotežnih konstanti.

$$\theta_b = \frac{[NP]}{K_d + [NP]} \quad \text{preoblikuje se u:} \quad (8)$$

$$\theta_P K_d + \theta_P [NP] = [NP] \quad (9)$$

$$\theta_P K_d / [NP] + \theta_P = 1 \quad (10)$$

$$\theta_P K_d / [NP] = 1 - \theta_P \quad (11)$$

$$\frac{\theta_P}{[NP]} = -\frac{\theta_P}{K_d} + \frac{1}{K_d} \quad (12)$$

Dakle, korelacijom omjera θ_P/[NP] kao funkcije θp dobiva se pravac nagiba -1 / K_d. odnosno Scatchardov grafički prikaz. Zbog dostupnih računalnih programa uz koje se

jednostavno računaju ravnotežne konstante bez linearizacije, Scatchardov dijagram se u praksi više ne koristi (Hegyi i dr., 2013).

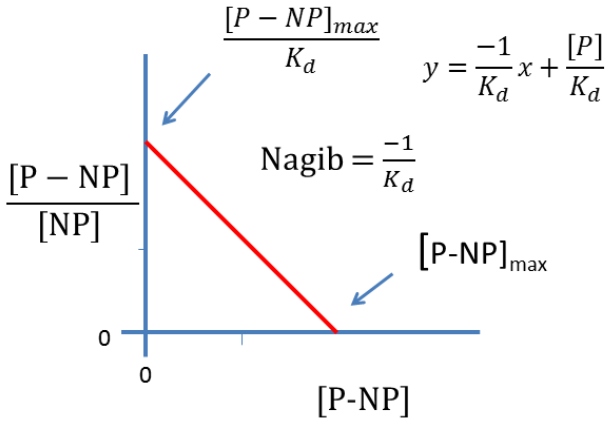

Slika 22. Scatchardov dijagram određivanja konstante disocijacije

U ovom se istraživanju za određivanje konstanti vezanja proteina na AgNP koristila metoda fluorescencijske spektroskopije temeljem fizikalnog svojstva gašenja fluorescencije proteina uslijed njegovog vezanja na površinu NP. Naime, albumin i AGP imaju svojstvo fluorescencije zbog prisutnosti triptofanskog aminokiselinskog ostatka u albuminu, te triptofanskih i tirozinskih aminokiselinskih ostatka u AGP. Obje aminokiseline daju fluorescentni signal koji omogućuje praćenje vezanje proteina i promjene u njihovoj strukturi, jer se uslijed tih promjena mijenja intenzitet signala (Eskiari i dr., 2013). Kad se ligand veže u njihovoj blizini, intenzitet njihove fluorescencije se smanjuje.

Vezanjem proteina na NP nastaje početni monosloj pri čemu vezujuća interakcija između molekula proteina može biti važna u nastajanju proteinske korone. Sam protein fluorescira, dok vezanjem na NP dolazi do gašenja fluorescencije proteina koje se može izrazite preko Stern-Volmer jednadžbe:

$$F_0 / F = K_{sv}[Q] + 1 \quad (13)$$

gdje je F_0 ukupna fluorescencija proteina (u odsutnosti NP), F je fluorescencija proteina pri danoj koncentraciji NP, K_{sv} je Stern-Volmerova konstanta a Q je koncentracija inhibitora, odnosno NP. Koncentracija NP u otopini povećava se do točke zasićenja, pri čemu će fluorescencija proteina biti minimalna. Ako pretpostavimo gašenje fluorescencije pri čemu protein i NP formiraju stabilan kompleks, K_{sv} postaje K_a (konstanta asocijacije). Hillova jednadžba može se upotrijebiti za kvantifikaciju odnosa između intenziteta fluorescencije i koncentracije NP:

$$\log (F_0 - F) / (F - F_{sat}) = \log K_a + n \log [NP] \quad (14)$$

gdje se F_{sat} odnosi na fluorescenciju proteina kod zasićenja NP. Hillov koeficijent, n, opisuje stupanj kooperativnosti vezanja proteina (liganda) na površinu. Ako je n > 1, vezanje liganda se pojačava ako već postoje drugi ligandi adsorbirani na površinu. Ako je n < 1, vezanje liganda se smanjuje ako već postoje drugi ligandi adsorbirani na površinu. U slučajevima gdje je n = 1, vezanje liganda je neovisno od drugih liganada koji su već vezani na površini (Eskiari, i dr., 2013; Cui i dr., 2013; Boulos i dr., 2013).

Ioni i molekule prisutne u uzorku mogu utjecati na fluorescenciju analita inhibitorski ili aktivatorski proporcionalnio koncentraciji aktivatora odnosno inhibitora (Luterotti i Bicanic; 2013). Inhibitorski djeluju mnogi metalni i drugi ioni (npr. Mn, Ni, Co, I^-, Br^-, NO_2^-, $-COO^-$) što znači da smanjuju kvantni prinos, odnosno fluorescencija spojeva pod UV svjetlom slabi. Inhibitorsko djelovanje se tumači:

1. apsorpcijom primarnog zračenja; to je tzv. efekt "unutarnjeg filtra". Inibitor (Q) oduzima apsorpcijom dio primarnog zračenja tvari koja fluorescira. Time joj ustvari smanjuje mogućnost apsorpcije i emisije.

2. fizikalno-kemijskom interakcijom između fluorescentne tvari i inhibitora tzv. reakcije gašenja fluorescencije koje mogu biti dinamičke ili statičke a pojavljuju se kao posljedica međumolekulskih interakcija unutar fluorescirajuće molekule (Luterotti i Bicanic, 2013).

U svrhu procjene utjecaja AgNP na fluorescenciju proteina snimljeni su UV-VIS i fluorescencijski spektri AgNP bez prisutnosti proteina. U ultračistoj vodi, u kojoj ne dolazi do aglomeracije AgNP vrsta, su snimljeni UV-VIS spektri iz kojih je vidljivo da niti jedna AgNP vrsta ne apsorbira značajno u valnom području koje je korišteno za računanje konstanti vezanja proteina na AgNP. Uz to, iz ekscitacijskih i emisijskih spektara AgNP vrsta koji su izmjereni u koncentracijskom rasponu korištenom za određivanje konstanti vezanja proteina (Slika 52) vidljivo je da AgNP vrste ne interferiraju s ekscitacijskim i emisijskim spektrima samih proteina (poglavlje 7, Slika 51). Postoji li učinak unutarnjeg filtra ispitano je provođenjem eksperimenata u kojima su izmjereni fluorescencijski i UV-VIS spektri svih AgNP vrsta pri različitim koncentracijama (u rasponu od 10 do 1000 μM), te fluorescencijski i UV-VIS spektri oba proteina (u rasponu od 0.1 do 100 μM). Naime, ukoliko je opažena vrijednost intenziteta fluorescencije linearno ovisna o absorbanciji uzorka na valnim duljinama excitacije i emisije, tada treba uzeti u obzir učinak unutarnjeg filtera i uvesti korekcijski faktor (Kubista i dr., 1994; Lutz i Luisi, 1983). Obzirom da su oba proteina pokazala učinak unutarnjeg filtera, a opažena vrijednost intenziteta fluorescencije za AgNP vrste je bila proporcionalna njihovoj koncentraciji, te se linearno odnosila prema njihovoj

absorbanciji na valnim duljinama ekscitacije i emisije (poglavlje 7, Slika 62), sve titracije su provedene na način da je koncentracija proteina držana konstantnom, dok su se varirale koncentracije AgNP suspenzija. Vrijednosti fluorescencije AgNP suspenzija u danom mediju su korištene kao bazna linija (Slika 22).

Titriranjem otopine proteina s AgNP mjeren je pad intenziteta fluorescencije proteina (F.U. = fluorescence units = omjer signala mjerne i referentne fotomultiplikacijske cijevi). U tu je svrhu korišten spektrofluorimetar RSM 1000F (Olis, SAD). Korištena je kiveta za fluorescencijska mjerenja Helma Analytics 105.253-QS s putem svjetlosti od 10 × 2 mm (ekscitacija × emisija). Valna duljina ekscitacije je bila 280 nm, a emisijski spektar je sniman u rasponu 310–370 nm. Sva mjerenja su provedena u triplikatu koristeći širine proreza pri ekscitaciji i emisiji od 1,24 mm. Sve otopine su bile mjerene nakon inkubacijskog razdoblja od 10 minuta kako bi se uspostavila ravnoteža. Preliminarnim mjerenjima definirane su optimalne eksperimentalne koncentracije i određeni su fluorescencijski spektri proteina (poglavlje 7, Slika 51). U Eppendorf epruvetama su pripremljene reakcijske smjese dodavanjem određenih volumena reagenasa kako je opisano u Tablici 9.

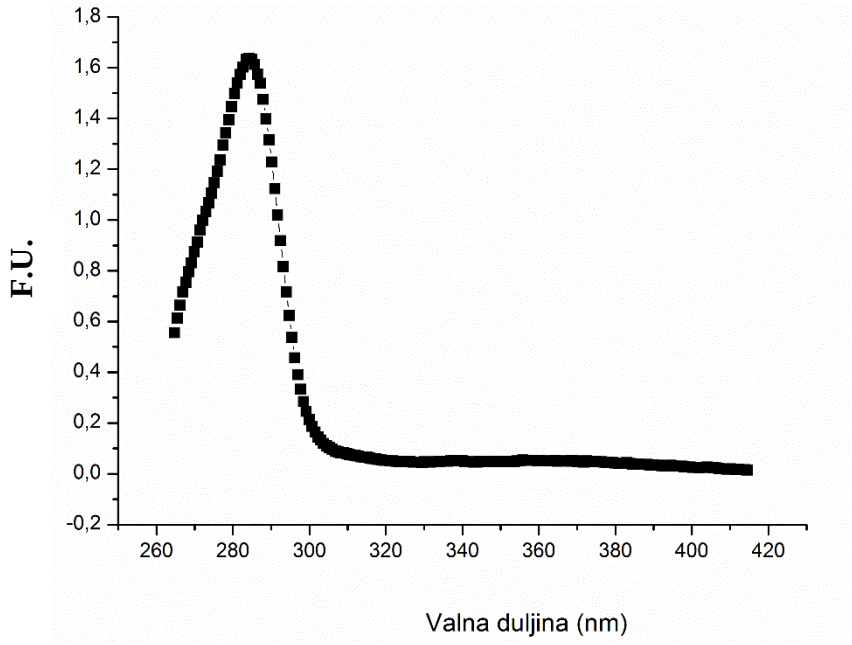

Slika 23. Fluorescencijski spektar AOT10sph

Redoslijed pripreme otopina je sljedeći: medij (UW, FP, FO, FPNaCl), zatim matična otopina proteina te na kraju matična otopina AgNP. Otopina je lagano promiješana nakon dodavanja svih reagensa kako ne bi nastali mjehurići koji smetaju fluorescencijskim mjerenjima. Posebno je važno da se protein dodaje u medij prije dodatka AgNP u svrhu

sprječavanja aglomeracije nanočestica koja je osobito izražena u FO i FPNaCl zbog veće ionske jakosti koja dovodi do smanjenja stabilnosti AgNP. Koncentracija proteina je održavana stalnom (0,15, 0,2 ili 0,3 μM), tako da su se reakcijske smjese pripremale uz omjer koncentracija protein: AgNP od 1:10 do 1:3000. Matična otopina albumina pripremljena je otapanjem 65 μg albumina u 10 mL UW tako da je konačna koncentracija proteina 100 μM. Također, pripremljena je vodena otopina AGP volumena 2 mL, koncentracije c = 100 μM. Korištena je odvaga od 0,0086 g AGP u UW volumena 2 mL. Tako pripremljene otopine proteina razrijeđene su 10 puta. Uvijek svježe pripremljene otopine korištene su kao matična otopina kod priprema svih reakcijskih smjesa.

Tablica 9. Protokol pripreme reakcijskih smjesa za mjerenje smanjenja fluorescencije proteina nakon interakcije s AgNP u različitim medijima.

	Matična otopina AgNP, μmol/L	Konačna koncentracija AgNP, μmol/L	Volumen dodane matične otopine AgNP, mL	Volumen dodanog proteina (10 μM), mL	Volumen dodanog medija, mL	Ukupni volumen, mL
1.	100	2	0,01	0,0075	0,4825	0,5
2.	100	6	0,03	0,0075	0,4625	0,5
3.	100	10	0,05	0,0075	0,4425	0,5
4.	3000	14	0,0023	0,0075	0,4902	0,5
5.	3000	20	0,0033	0,0075	0,4892	0,5
6.	3000	30	0,005	0,0075	0,4875	0,5
7.	3000	40	0,0067	0,0075	0,4858	0,5
8.	3000	60	0,01	0,0075	0,4825	0,5
9.	3000	80	0,0133	0,0075	0,4792	0,5
10.	3000	100	0,0167	0,0075	0,4758	0,5
11.	3000	140	0,0233	0,0075	0,4692	0,5
12.	3000	200	0,0333	0,0075	0,4592	0,5
13.	3000	250	0,0417	0,0075	0,4508	0,5
14.	3000	300	0,05	0,0075	0,4425	0,5
15.	3000	400	0,0667	0,0075	0,4258	0,5
16.	3000	500	0,0833	0,0075	0,4092	0,5

Svaki spektar dobiven tijekom titracije je prosjek 10000 fluorescencijskih spektara izmjerenih kroz 10 sekundi. Izmjereni spektri obrađeni su u programu *SPECFIT Global Analysis System* za prilagođavanje ravnotežnih i kinetičkih sustava koji koristi analizu faktora i Marquardtovu minimizaciju.

3.4.3. Određivanje specifične površine AgNP

Da bi se mogla odrediti specifična površina potrebno je znati koji broj AgNP čestica ima u gramu uzorka. Za čestice koje imaju monomodalnu raspodjelu račun je jednostavan i ima više mogućnosti. U ovom je radu korištena metoda prema Schmidtu i Stoegeru (Schmidt i Stoeger, 2016) prema kojoj se broj AgNP (N) određuje iz mase uzorka (m) i gustoće materijala (ρ) stavljajući u omjer volumen uzorka (m/ρ) i volumen čestice promjera d:

$$N = \frac{6m}{\rho \Pi d^3} \tag{15}$$

U svrhu određivanja broja AgNP različitih veličine potrebna su dva podatka: broj atoma srebra koji grade česticu određene veličine i broj atoma srebra u uzorku. Broj atoma srebra koji grade pojedinu česticu izračunat je temeljem činjenice da AgNP imaju fcc strukturu te da je postotak popunjenosti volumena (f) 0,74 (volume filling percentage). U omjer se uzima volumen AgNP i volumen atoma srebra, vodeći računa o f:

$$N_{\text{atoma Ag u NP}} = \frac{f V_{NP}}{V_{Ag}} = \frac{f d_{NP}^3}{d_{Ag}} \tag{16}$$

Treba uzeti u obzir da je $d_{Ag} = 290$ pm. Također, uzevši u obzir udio AgNP pojedinih veličina (oznake w_1 i w_2, bimodalna raspodjela) određen u 1. koraku i broj atoma Ag u AgNP određene veličine (N_1 i N_2) izračunat u prethodnom koraku, broj pojedine vrste čestica (x i y) dobiva se kao rješenje sustava dviju jednadžbi:

$$xN_1 + yN_2 = \text{ukupan broj atoma} \tag{17}$$

$$x/y = w_1 / w_2 \tag{18}$$

Specifična površina AgNP izračunata je iz promjera dobivenih iz TEM mjerenja i izračunatog broja AgNP. Kod monomodalnih raspodjela veličina, specifična površina se računa prema jednadžbi 17 (ako je broj čestica računat na 1 g, ako nije treba ga preračunati):

$$A = Nd^2\Pi \tag{19}$$

Dok se u slučaju bimodalne raspodjele postupa prema jednadžbi 18:

$$A = N_1 d_1^2 \Pi + N_2 d_2^2 \Pi \quad (20)$$

Na taj način se u odnos stavlja izračunata specifična površina pojedine vrste AgNP, njihov ζ potencijal i log K_a vrijednosti.

3.4.4. Analiza strukturnih promjena proteina primjenom cirkularnog dikroizma

Cirkularni dikroizam (CD) je metoda određivanja razlika u apsorpciji lijevo (L-CPL; od eng. l*eft-hied circularly polarised light*) i desno (R-CPL; od eng. *right-hied circularly polarised light*) kružno polarizirane svjetlosti optički aktivnih tvari a pojavljuje se kada molekula sadrži jedan ili više kiralnih kromofora (Kelly i dr., 2005; Greenfield, 2006). CD spektroskopija se koristi u analizi sekundarne strukture i konformacije makromolekula, za praćenje stabilnosti proteina uslijed promjene uvjeta (toplina, pH, ionska jakost ili svojstva otapala), za evaluaciju konformacijskih razlika proteina iz raznih ekspresijskih sustava ili vrsta, promatranje promjene u strukturi proteina uslijed interakcije protein-protein ili protein-ligand te za kontrolu kvalitete postupaka pročišćavanja (Pokutta i dr., 1994; Sasahara i dr., 2002; Litovchick i Rio, 2003).

Za razumijevanje CD spektra potrebno je razumjeti osnove polarizacije. Linearno polarizirana svjetlost je svjetlost čije su oscilacije ograničene na jednu ravninu. Sva stanja polarizirane svjetlosti mogu se opisati kao zbroj dvaju linearno polariziranih stanja pod pravim kutovima svakog od njih, a obično se iz pozicije gledatelja promatra kao okomito i vodoravno polarizirano svjetlo. Ako su vodoravno i okomito polarizirana svjetlost valova jednake amplitude međusobno u interakciji, rezultantni val je linearno polarizirana svjetlost na 45º stupnjeva izvan faze. Međutim, kada se susretnu dva vala ravnine polarizirane svjetlosti jednake amplitude i valne duljine međusobno okomiti, 90 ° ili -90 ° izvan faze, rezultat je kružno polariziran val.

Kad molekula kromofora stupa u interakciju s cirkularno polariziranim svjetlom, može apsorbirati lijevo ili desno polarizirane valove što rezultira prijenosom svjetlosti koja je eliptički polarizirana (Kelly i dr., 2005). Spektropolarimetar, ili CD instrument, mjeri razliku u apsorbanciji, ΔA, između lijevo (A_{LCP}) i desno (A_{RCP}) kružno polarizirane svjetlosti (Sreerama i Woody, 2004). CD signal ovisi o koncentraciji analita, broju aminokiselina i duljini optičkog puta kivete (Kelly i dr., 2005; Greenfield, 2006; Sreerama i Woody, 2004).

Izračunava se preko koncentracije i broja ponavljajućih jedinica koji pridonose promatranom CD signalu.

CD spektroskopija bilježi signal kromofora koji su kiralni bilo zbog svoje intrinzične strukture, kovalentnog vezanja na kiralne centre ili asimetričnosti strukture u određenim uvjetima, a temeljem 3-dimenzionalne strukture kao što su proteini i oligonukleotidi (Kelly i dr., 2005; Sreerama i Woody, 2004). Na primjer, proteini apsorbiraju UV svjetlost temeljem n $\rightarrow \pi^*$ i $\pi \rightarrow \pi^*$ elektronskih prijelaza koji su povezani s peptidnim vezama i aromatskim ostacima u molekuli proteina (Kelly i dr., 2005; Sreerama i Woody, 2004). α heliks i β ploče proteina mogu se identificirati karakterističnim apsorpcijskim svojstvima (Sreerama i Woody, 2004). U spektralnoj regiji iznad 240 nm kromofori poput aromatskih ostataka mogu pridonijeti promatranoj eliptičnosti pri čemu se informacije o tercijarnoj strukturi mogu se odrediti iz intenziteta ovih spektralnih vrpci (Kelly i dr., 2005).

Mjerenja cirkularnog dikroizma proteinskog spektra izvedena su na Jasco J-810 CD spektrofotometru (Jasco Corp., Japan) u kvarcnoj kiveti veličine od 0,1 cm na 25 ° C. Spektri svakog uzorka zabilježeni su u rasponu valnih duljina 190 - 250 nm u triplikatu s brzinom skeniranja od 100 nm / min i veličinom skeniranja veličine 0.2 nm. Koncentracija proteina (albumin ili AGP) tijekom mjerenja bila je 2 μM a koncentracija AgNP bila je 10-500 μM. Nakon miješanja sve otopine ostavljene su na sobnoj temperaturi tijekom 10 minuta. Također, snimljeni su spektri čistih AgNP, albumina i AGP. Spektar AgNP u odsutnosti proteina oduzet je od spektra kompleksa protein-AgNP za svaku primijenjenu koncentraciju AgNP i proteina.

4. REZULTATI I RASPRAVA

Istraživanje provedeno tijekom izrade ove doktorske disertacije podijeljeno je u pet cjelina:

(1) Razvoj protokola za sintezu, karakterizaciju i određivanje stabilnosti nanočestica srebra u različitim medijima na modelu citratom stabiliziranih AgNP (poglavlje 4.1.)
(2) Sinteza, karakterizacija i procjena stabilnosti AgNP različitih veličine, oblika i površinske strukture (poglavlje 4.2)
(3) Antibakterijsko djelovanje pripravljenih AgNP (poglavlje 4.3.)
(4) Ponašanje sintetiziranih AgNP u različitim biološkim medijima u prisustvu albumina (poglavlje 4.4.)
(5) Mehanizam interakcije različitih AgNP s albuminom i α-1-kiselim glikoproteinom (poglavlje 4.5.).

Zaključci ovog istraživanja dani su u poglavlju 5., a literatura korištena tijekom istraživanja u poglavlju 6. Eksperimentalni podaci nastali tijekom izrade ove doktorske disertacije, a koji, radi jasnoće prikaza rezultata i rasprave, nisu dani u poglavlju 4. prikazani su u Poglavlju 7.

4.1. Razvoj protokola za sintezu, karakterizaciju i određivanje stabilnosti nanočestica srebra u različitim medijima

Razvoj protokola za sintezu, karakterizaciju i procjenu stabilnosti AgNP u različitim medijima proveden je na modelnom sustavu citratom stabiliziranih AgNP (CITAgNP). Ispitani su različiti parametri sintetskog postupka priprave stabilnih AgNP uključujući omjere reaktanata, brzinu i vrijeme miješanja, temperaturu reakcijske smjese, redoslijed dodavanja reaktanata. Najoptimalniji uvjeti za pripravu AgNP željenih svojstava detaljno su prikazani u poglavlju 3.2.

Za razvoj protokola za ispitivanje stabilnost i ponašanja (aglomeracija, otapanje, kompleksiranje, adsorpcija ili desorpcija) AgNP u različitim medijima primijenjeni su slijedeći modelni mediji: (i) mediji različite pH vrijednosti (pH 3 - pH 9); (ii) mediji koji sadrže različite monovalentne i dvovalentne elektrolite; (iii) mediji s neionskim, anionskim i kationskim površinski aktivnim tvarima (PAT); (iv) mješoviti sustavi koji sadrže različite PAT i različite elektrolite otopljene u ultračistoj vodi (Capjak i dr; 2018).

4.1.1. Svojstva modelnih nanočestica srebra stabiliziranih citratnim ionima

Svježe pripravljene modelne CITAgNP vizualizirane su primjenom TEM tehnike (Slika 24a), a stabilnost u UW određena je mjerenjem hidrodinamičkog promjera DLS tehnikom i zet potencijal ELS tehnikom tijekom 24 h (Slika 24b).

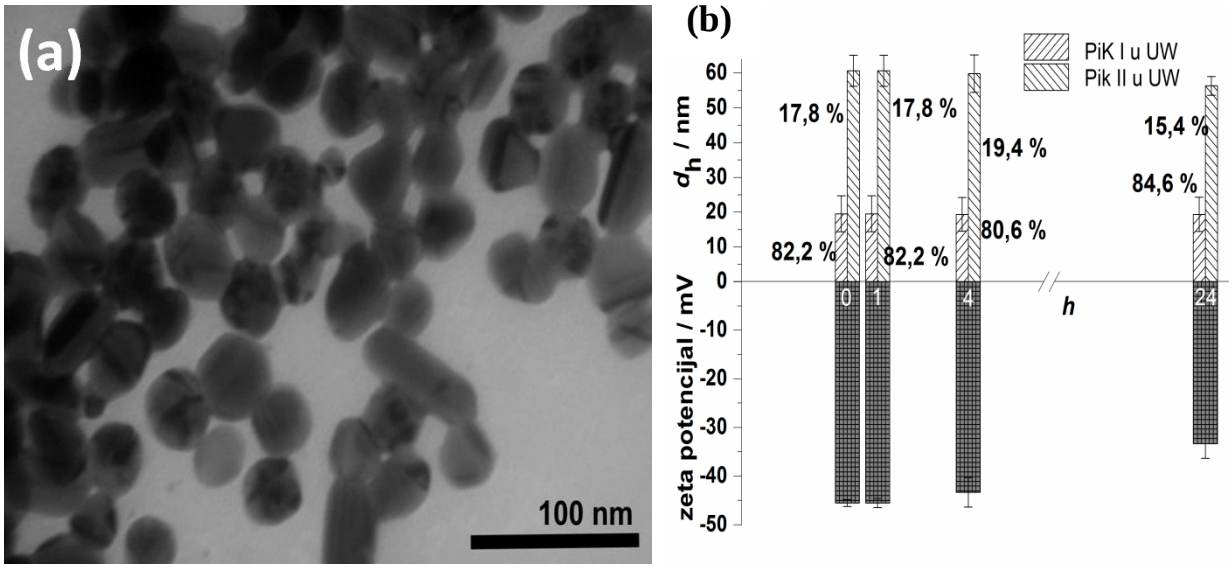

Slika 24. a) TEM slika CITAgNP b) Promjena d_H i zeta potencijala CITAgNP u UW tijekom 24 h.

Pripremljene CITAgNP imaju SPR signal na valnoj duljini od 433 nm karakterističan za AgNP, što je u skladu s klasičnom Mieovom teorijom (Capjak i dr., 2018). Položaj i širina SPR signala u apsorpcijskom spektru suspenzije AgNP ovise o raspodjeli veličine, obliku, kao i o prisutnosti adsorbiranih tvari ili oksidacijskog sloja na površini AgNP. Zbog vrlo velike stabilnosti pripremljenih CITAgNP, položaj i visina SPR pika nisu se mijenjali tijekom 24 sata (Tablice 10 - 12). TEM slike pokazale su da su CITAgNP nanočestice različitih veličina i oblika: sferičnog, štapičastog i trokutastog (Slika 24a), što je u skladu s rezultatima DLS mjerenja koja su pokazala bimodalnu raspodjelu veličine. Iz raspodjele veličine prema volumenu dominantna populacija (82,2%) ima d_H 19,54±5,17 nm, dok su čestice veličine 60,70±4,49 nm prisutne u znatno manjem postotku (17,8% ukupnog volumena) (Slika 24).

Citratne AgNP bile su stabilne ne samo tijekom 24 h, što se može vidjeti iz rezultata prikazanih na Slici 24b, nego i nekoliko mjeseci. Naime, svježe pripremljene CITAgNP čuvane su u tamnim bočicama u hladnjaku tijekom više od 6 mjeseci, te su periodično karakterizirane DLS i ELS tehnikama, koje su potvrdile da se tijekom tog perioda vrijednosti d_H i ζ potencijala ne mijenjaju više od 10% u odnosu na početno izmjerene vrijednosti. To je

bilo i očekivano obzirom na veliku negative vrijednost ζ potencijala od -45,5 ± 0,7 mV (Slika 24) koja sprječava aglomeraciju i osigurava dugoročnu stabilnost CITAgNP. Obzirom da je ζ potencijal vezan uz električni potencijal u međuprostoru između difuznog ionskog sloja na površini NP i okolnog medija, velika aposlutna vrijednost ζ potencijala ukazuju na djelovanje odbojnih sila koje stabilizairaju nanočestice jednu od drugih (Fornes 1985). Općenito se smatra da stabilne one NP koje su karakterizirane ζ potencijalom <- 30 mV ili > 30 mV.

4.1.2. Učinak pH na stabilnost nanočestica srebra

U svrhu razvoja metodologije za ispitivanje stabilnosti i ponašanja AgNP u različitim biološkim sustavima, najprije je primijenjena kombinacija tehnika iz Tablice 7 za ispitivanje svojstava modelnih CITAgNP u medijima različitih pH vrijednosti. U tu svrhu su se CITAgNP dispergirale u UW koja je prethodno zakiseljena na pH 3 dodatkom HNO_3 ili zalužena na pH 9 dodatkom NaOH. Ponašanje CITAgNP u tim medijima praćeno je tijekom 24 sata (Slika 25), te su rezultati uspoređeni s onima dobivenim u UW (Slika 24b).

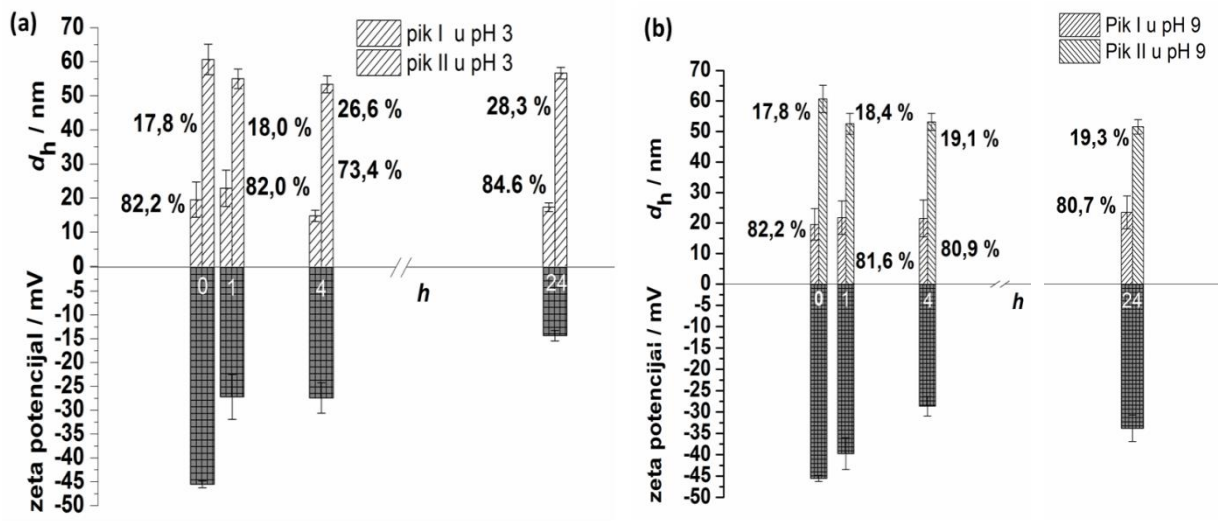

Slika 25. Raspodjela veličina i zeta potencijala CITAgNP pri pH 3 i pH 9.

Značajno povećanje ili smanjenje pH vrijednosti medija smanjilo je apsolutnu vrijednost ζ potencijala AgNP. Nakon 24 sata, izmjereni ζ potencijal promijenjen je iz početnih vrijednosti od -45,5 ± 0,7 mV pri pH 6,8 u UW (Slika 24b) na -14,3 ± 1,1 mV u mediju s pH 3 (Slika 25), odnosno na -33,8 ± 3,1 mV u mediju s pH 9 (Slika 25). Jedino je pH 3 značajnije utjecao na aglomeraciju CITAgNP, što se može objasniti protoniranjem citratnih iona pri nižem pH što uzrokuje smanjenje odbojnih elektrostatskih sila (El-Badawy i dr.,

2010; Pfeiffer i dr., 2014; Alvarez-Puebla i dr., 2005; Elzey i Grassian, 2010; Hedberg i dr., 2012). Tako je suspendiranje CITAgNP u mediju s pH 3 rezultiralo povećanjem udjela populacije većih čestica (Slika 25), što ukazuje na njihovu aglomeraciju u skladu sa smanjenjem apsolutne vrijednosti ζ potencijala. Naime, CITAgNP su stabilizirane negativno nabijenim citratnim ionima. Povećanje pH disperzijskog medija dovelo je do povećanja negativnog zeta potencijala CITAgNP, a uslijed toga i povećavanja jačine odbojnih sila. Tako je na pH 9 dobivena gotovo jednaka raspodjela veličine kao u UW, koja se nije mijenjala tijekom 24 sata.

Praćenje otapanja CITAgNP u medijima s različitim pH vrijednostima (Tablica 10) potvrdilo je da su CITAgNP stabilnije pri pH 9 nego pri pH 3. Naime, pri pH 9 zabilježen je umjeren učinak otapanja AgNP, dok je pri pH 3 zabilježeno značajno povećanje brzine oslobađanja Ag^+ iona s površine CITAgNP. Vjerojatno je to posljedica protoniranja pri pH 3 koje osim protoniranja površine CITAgNP, dovodi i do otpuštanja srebrnih kationa.

Tablica 10. Utjecaj pH medija na otapanje i SPR signal AgNP-a. Postotak slobodnog Ag^+ i SPR signali određeni su u 10 mg/L AgNP-a suspendiranih u UW, u mediju s pH 3 i 9, nakon 1 h, 4 h i 24 h.

Medij	**Otpuštanje Ag^+ (%)**			**SPR, nm**			**Apsorbancija**		
	1 h	4 h	24 h	1 h	4 h	24	1 h	4 h	24 h
UW	0,45	0,48	0,74	431	430	430	0,81	0,82	0,81
pH 3	0,62	0,65	0,87	433	429	430	0,82	0,54	0,19
pH 9	0,73	0,73	0,74	435	423	433	0,73	0,62	0,63

Dobiveni rezultati su dodatno potvrđeni UV-VIS spektroskopijom (Tablica 10). Nije bilo značajnijih promjena tijekom 24 sata u SPR signalu između UW i pH 9, dok je na pH 3 uočeno izrazito smanjenje visine SPR signala što jasno upućuje na otapanje. Otapanje AgNP u prisustvu HNO_3 već je i ranije opisano u literaturi (Ozmetin i dr.; 2000).

4.1.3. Učinak različitih elektrolita na stabilnost nanočestica srebra

Učinak elektrolita na stabilnost CITAgNP procijenjen je dodavanjem NaCl, $MgCl_2$, Na_2SO_4 i $MgSO_4$ u UW u dvije različite koncentracije (0,01 i 0,1 M). Na taj način istražen je utjecaj i mono- i dvovalentnih kationa, kao i mono- i dvovalentnih aniona. DLS i ELS metode korištene su za ispitivanje vremenski ovisne aglomeracije AgNP tijekom 24 sata.

Reprezentativni aglomeracijski profili AgNP-a u različitim otopinama elektrolita prikazani su na Slici 26. Ponašanje CITAgNP u prisutnosti elektrolita bilo je u skladu s DLVO teorijom koja objašnjava mehanizme stabilnosti nabijenih molekula elektrostatskim interakcijama i van der Waalsovim silama a naziv je dobila po Boris Derjaguin, Lev Landau, Evert Verwey i Theodor Overbeek-u. Kod viših koncentracija svih elektrolita, smanjila se apsolutna vrijednost ζ potencijala CITAgNP, što je za posljedicu imalo i smanjenje elektrostatskih odbojnih sila među NP, a time dovelo do destabilizacije i aglomeracije CITAgNP. Što je smanjenje apsolutne vrijednosti ζ potencijala bilo veće to je i aglomeracija bila izraženija (Slika 26).

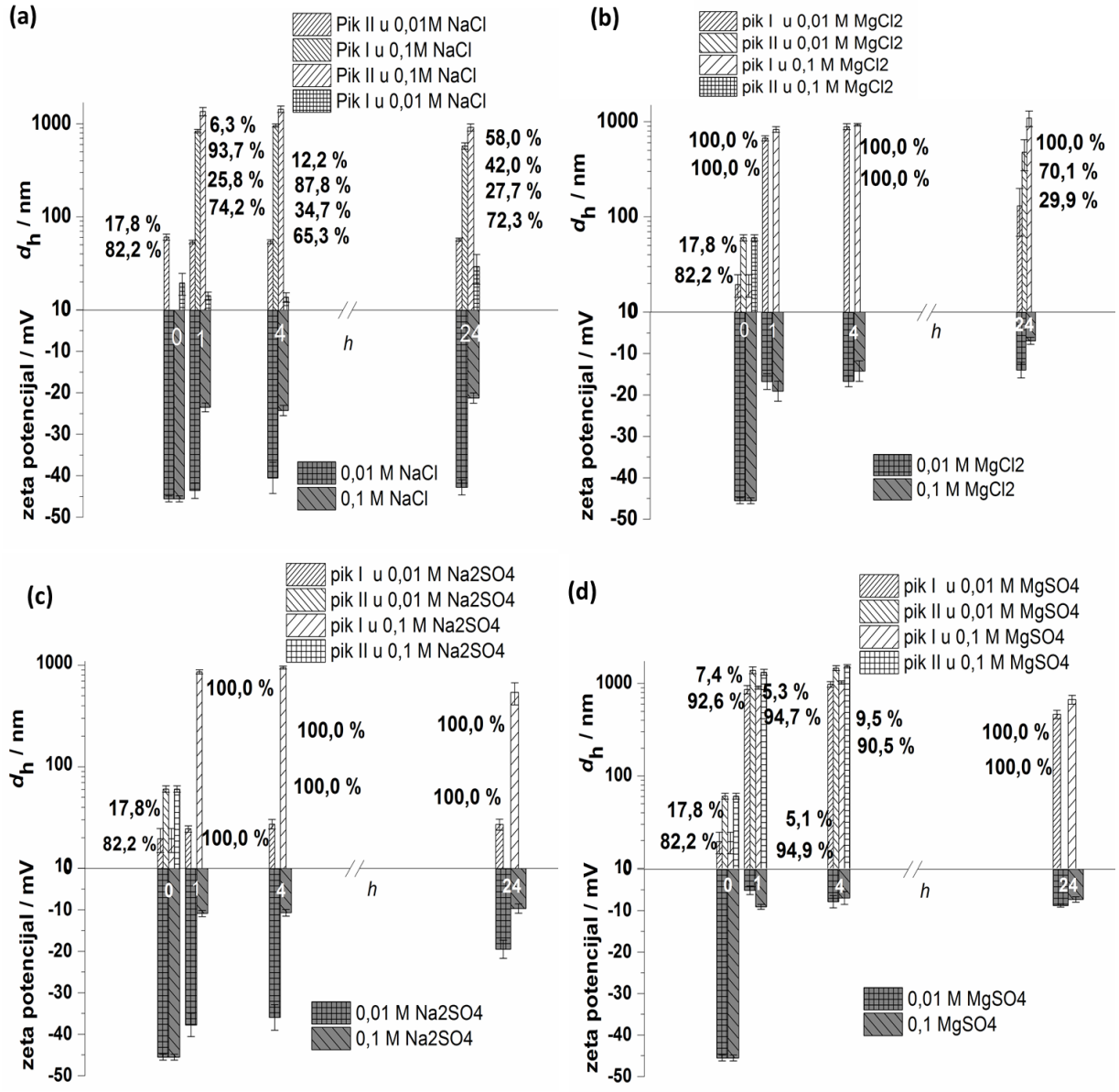

Slika 26. Aglomeracijski profil CITAgNP u otopinama različitih elektrolita pri koncentracijama 0,01 i 0,1 M.

Zanimljivo je da je u mediju koji je sadržavao 0,01 M NaCl stabilnost CITAgNP bila očuvana zbog prisustva dovoljnog broja Cl^- iona koji su održali elektrostatska odbijanja među NP. Kod većih koncentracija NaCl, a posebno kod povećanja naboja kationske komponente (Mg^{2+} vs. Na^+) pri istoj koncentraciji, došlo je do značajne destabilizacije i aglomeracije CITAgNP, jer veći pozitivni naboj (veća koncentracija Na^+ ili veći pozitivni naboj u slučaju Mg^{2+}) maskiraju negativni površinski naboj koji potječe od citratnih iona na površini CITAgNP. To je jasno vidljivo iz izmjerenih vrijednosti ζ potencijala. Takvo ponašanje je izraženije kod natrijevog i magnezijevog sulfata što navodi na zaključak da prisutnost dvovalentnih kationa ima veći učinak na ζ potencijal CITAgNP od anionskih komponenti pozadinskog elektrolita (Cl^- i SO_4^{2-}). Uvođenje dvovalentnih kationa (Mg^{2+}) u medije umjesto monovalentnih kationa (Na^+), znatno destabilizira AgNP zbog smanjenja vrijednosti ζ potencijala već na nižoj koncentraciji elektrolita od 0,01 M (Slika 26). Pri višoj koncentraciji elektrolita, prisutnost SO_4^{2-} aniona povećala je ζ potencijal u mediju s Na^+, ali nedovoljno za održavanje stabilnosti. Zanimljivo je da su *ζ* potencijali bili negativniji u prisutnosti Cl^- u usporedbi s medijem koji sadrži SO_4^{2-}, što se može objasniti formiranjem $AgCl_x^{(x-1)}$ čestica. Dakle, CITAgNP bile su destabilizirane zbog povećanja ionske jakosti, kada je kompleksiranje Na^+ s citratnim karboksilnim skupinama na AgNP površini dovelo do aglomeracije. UV-VIS analiza pokazala je u otopinama elektrolita značajan crveni pomak samo u prisutnosti magnezijevih soli (Tablica 11). Tipični SPR signal AgNP aglomerata koji se može naći u rasponu između 600-800 nm, a detektirani su DLS-om, nije uočen tijekom UV-VIS analize. Međutim, aglomeracija AgNP može se dokazati bilo prisutnošću dodatnih SPR signala ili smanjenjem intenziteta SPR signala (Capjak i dr, 2018). Doista, u slučaju 0,1 M Na_2S0_4, $MgSO_4$ i $MgCl_2$, pojavili su se dvostruki SPR signali, dok je visina SPR signala neznatno smanjena u 0,01 M NaCl ili Na_2SO_4, ali je signal gotovo nestao u prisutnosti magnezijevih soli, ili pri višim koncentracijama natrijevih soli što upućuje na aglomeraciju CITAgNP koja je pokazana i DLS mjerenjima. Međutim, nedostatak SPR maksimumima nije jednoznačan dokaz da AgNP aglomeriraju, nego može upućivati i na njihovo otapanje. Tako je značajno povećanje postotka slobodnog Ag^+ uočeno u svim otopinama elektrolita. U jednostavnim modelnim sustavima koji su korišteni u ovom istraživanju, najizraženije otapanje CITAgNP zabilježeno je u mediju koji je sadržavao 0,1 M $MgCl_2$ nakon 4 h (Tablica 11). Zanimljivo je da je postotak slobodnog Ag^+ u svim otopinama elektrolita smanjen nakon 24 sata u usporedbi s rezultatima dobivenim nakon 4 h. Razlog može biti vezanje slobodnog Ag^+ na površinu AgNP aglomerata koji su se istaložili. Dakle, povećanje ionske jakosti destabiliziralo je CITAgNP ne samo u smjeru njihove aglomeracije nego i otapanja.

Tablica 11. Utjecaj elektrolita na otapanja i SPR signal AgNP. Postotak slobodnog Ag^+ i SPR signali određeni su u 10 mg/L AgNP suspendiranim u ultra čistoj vodi (UW), u mediju s pH 3 i 9, nakon 1 h, 4 h i 24 h

Medij	Otpuštanje Ag^+ (%)			SPR, nm			Apsorbancija		
	1 h	4 h	24 h	1 h	4 h	24	1 h	4 h	24 h
UW	0,45	0,48	0,74	431	430	430	0,81	0,82	0,81
0,01 M NaCl	2,50	2,00	0,50	428	427	431	0,71	0,63	0,52
0,1 M NaCl	2,58	2,43	0,61	427	428	428	0,18	0,11	0,002
0,01 M Na_2SO_4	2,00	1,59	1,11	433	433	433	0,56	0,31	0,14
0,1 M Na_2SO_4	0,87	1,00	1,14	433	433	433	0,21	0,13	0,006
0,01 M $MgCl_2$	1,77	2,67	0,75	414	415	418	0,26	0,13	0,006
0,1 M $MgCl_2$	0,25	4,38	9,05	468	468	468	0,19	0,12	0,01
0,01 M $MgSO_4$	1,03	0,80	1,23	441	441	441	0,26	0,2	0,01
0,1 M $MgSO_4$	1,44	0,80	0,96	441	441	441	0,27	0,16	0,02

4.1.4. Učinak površinski aktivnih tvari na stabilnost nanočestica srebra

AgNP su prisutne u potrošačkim proizvodima, pa se otpuštaju u okoliš uslijed proizvodnje i uporabe. Obzirom da je stabilnost nanosustava određena hidrodinamičkim, elektrostatskim, elektrodinamičkim i steričkim interakcijama s komponentama okolišnog sustava, moguće su raznovrsne transformacije AgNP ovisno o sastavu okolišnog sustava. Stoga je kao nastavak ispitivanja stabilnosti i transformacija AgNP u modelnim sustavima, izabran je medij u kojem su dodane površinski aktivne tvari, odnosno surfaktanti (Capjak i dr., 2018). Biološke makromolekule se ponašaju kao surfktanti te se koriste kao modeli proteina i membrana (Ramanathan i dr., 2013). Izabrani su oni surfaktanti koji su relevenatni u proizvodnji detergenata, kako bi modelni sustav bio sličan sastavu otpadnih voda, a u svrhu prikupljanja informacija nužnih za procjenu rizika od upotrebe i primjene AgNP. Istraživana je interakcija između CITAgNP i tri surfaktanta različitog naboja u koncentracijama ispod i iznad njihovih kritičnih micelarnih koncentracija (cmc, od eng. *critical micelar concentration*). Pri koncentracijama većim od cmc vrijednosti, surfaktanti formiraju micele, dok se pri koncentracijama manjim od cmc vrijednosti surfaktanti nalaze u obliku solvatiranih monomera (Jurašin i dr., 2014). Tako su primijenjeni slijedeći modelni mediji: 0,1, 0,6 i 1 mM neionski Triton X-100, 5 i 30 mM kationski DDACl, te 15 mM anionski SDS. Ispitani su i mješoviti sustavi koji su sadržavali medij visoke ionske jakosti (0,1 M NaCl) uz dodatak PAT u koncentracijama iznad CMC. Rezultati raspodjele veličina i zeta potencijala CITAgNP u tim medijima dobiveni DLS i ELS mjerenjima prikazani su na Slici 27.

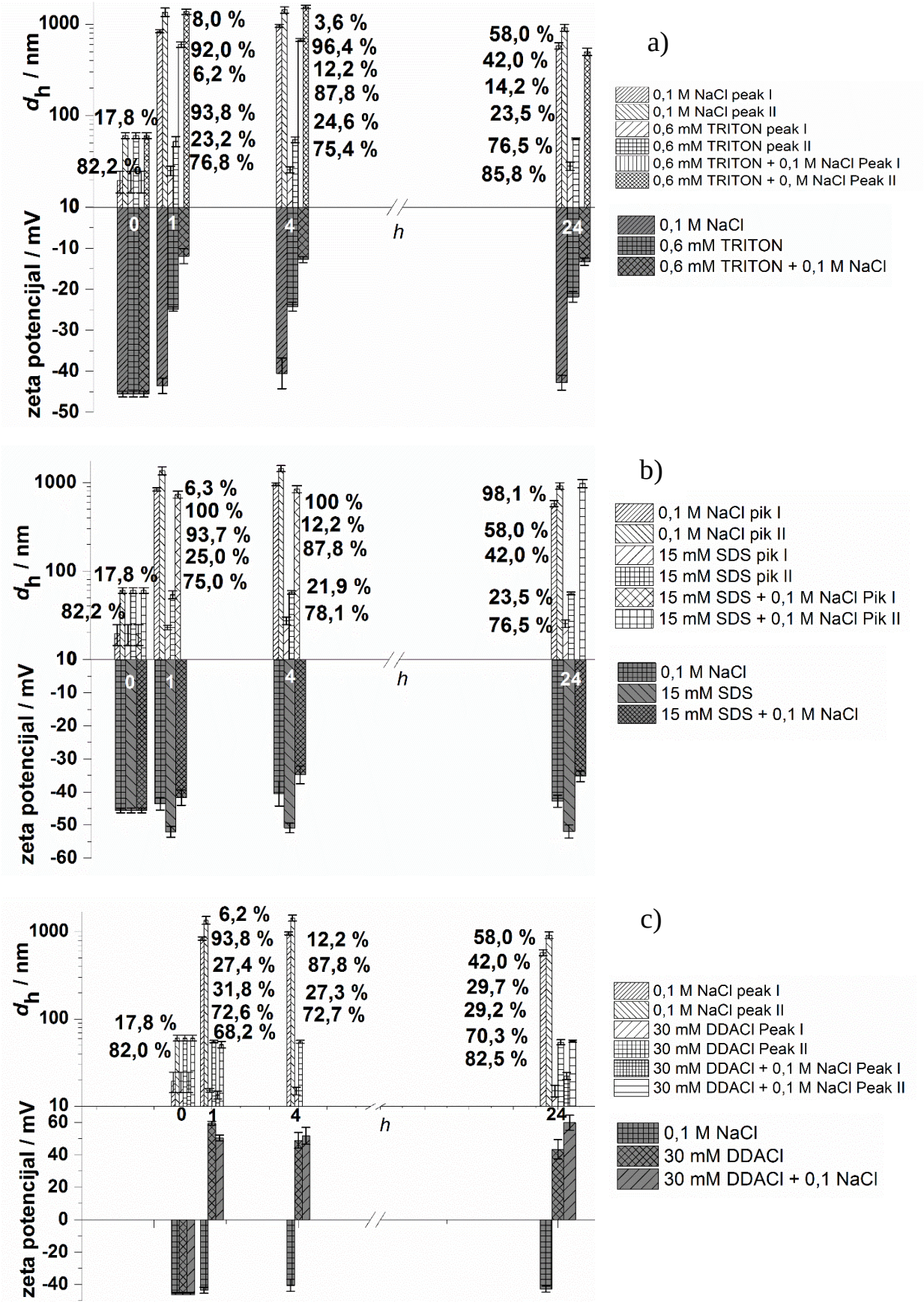

Slika 27. Aglomeracijski profil CIT AgNP u sustavima sa surfaktantima Triton, SDS i DDACl.

Nijedan od surfaktanata nije značajnije utjecao na stabilnost CITAgNP (Slika 27). Prisustvo surfaktanata u mediju samo je promijenilo ζ potencijala CITAgNP. Tako je prisustvo Tritona X-100 prisutnog u monomernim i micelarnim koncentracijama smanjilo apsolutnu vrijednost ζ potencijala CITAgNP u medijima (Slika 27a) iako je ranije opisano da neionski surfaktanti ne mijenjaju značajno zeta potencijal nabijenih NP (Hedberg i dr., 2012). Razlog može biti zasjenjivanje negativnih citratnih iona na površini CITAgNP pomoću molekula i/ili micela Tritona X-100. Prisustvo SDS nije značajnije utjecalo na ζ potencijal CITAgNP. Prisustvo DDACl dovelo je pak do inverzije ζ potencijala jer su se molekule DDACl lako vezale na negativno nabijenu površinu CITAgNP, te time osigurale ζ potencijal CITAgNP koji je bio iznad 40 mV. Na taj način su CITAgNP u svim medijima sa surfaktantima ostale stabilne tijekom 24 sata. Dodatna potvrda stabilnosti CITAgNP su SPR signali, te rezultati određivanja topljive forme CITAgNP u medijima sa surfaktantima (Tablica 12).

Prisustvo surfaktanata nije dovelo niti do smanjenja SPR signala niti do otpuštanja slobodnih Ag^+ iona s površine CITAgNP. Negativno nabijeni i neionski surfaktanti se upotrebljavaju u detergentima za pranje rublja, dok se pozitivno nabijeni surfaktanti koriste u omekšivačima. Nakon upotrebe oni neminovno završavaju u sustavima otpadnih voda, te na taj način mogu djelovati na transformacijske procese AgNP koji se u tim otpadnim vodama mogu istovremeno naći (Smulders i dr., 2007).

Rezultati jasno ukazuju da prisutnost surfaktanata u bilo kojem sustavu gdje se AgNP mogu osloboditi sprječava njihovu aglomeraciju, sedimentaciju i otapanje pri neutralnom pH i niskoj ionskoj jakosti. Međutim, različiti sustavi okoliša su puno složeniji i obično karakterizirani s većom ionskom jakosti. Stoga su ispitani kombinirani efekti surfaktanata (Triton X-100, SDS i DDACl) i elektrolita (0,1 M NaCl) na ponašanje CITAgNP. Kao što je već opisano u prethodnom odjeljku, CITAgNP se značajno aglomeriraju u prisutnosti 0.1 M NaCl (Slika 26a i Tablica 12). Zanimljivo je da je samo DDACl značajnije inhibirao aglomeraciju CITAgNP u otopini koja sadrži 0,1 M NaCl (Slika 27), dok niti Triton X-100 ni SDS nisu spriječili aglomeraciju (Slika 27). To je prilično iznenađujuće za SDS obzirom na izrazito negativnu vrijednost ζ potencijala u takvom mješovitom sustavu. Ta vrijednost vjerojatno nije bila samo rezultat zeta potencijala CITAgNP nego i prisutnih micela i drugih ionskih kompleksa. Doista, zabilježena vrijednost ζ potencijala za čisti sustav 15 mM SDS u 0,1 M NaCl bila je -23,9 ± 2,6 mV. Samo je DDACl osigurao elektrostatske sile koje su držale CITAgNP stabilnima.

Tablica 12. Utjecaj površinski aktivnih tvari na otapanje i SPR signal AgNP. Postotak slobodnog Ag^+ i SPR signali određeni su u 10 mg/L AgNP suspendiranim u ultra čistoj vodi (UW), u mediju s pH 3 i 9, nakon 1 h, 4 h i 24 h.

Medij	**Otpuštanje Ag^+ (%)**			**SPR, nm**			**Apsorbancija**		
	1 h	4 h	24 h	1 h	4 h	24	1 h	4 h	24 h
UW	0,45	0,48	0,74	431	430	430	0,8	0,8	0,81
5 mM DDACl	0,43	0,08	0,38	438	438	441	0,7	0,7	0,68
5 mM DDACl + 0,1 M NaCl	8,75	9,40	17,7	436	436	436	0,3	0,2	0,12
5 mM SDS	0,14	0,22	0,49	433	433	433	0,7	0,7	0,75
15 mM SDS	0,48	0,42	0,53	433	433	433	0,7	0,7	0,71
15 mM SDS + 0,1 M NaCl	3,75	5,57	13,4	433	433	433	0,2	0,1	0,13
0,1 mM Triton X-100	0,63	0,70	0,53	423	423	423	0,7	0,7	0,69
1 mM Triton X-100	0,86	0,86	1,04	423	423	423	0,7	0,7	0,72
0,1 mM Triton X-100 + 0,1 M NaCl	1,24	1,24	1,36	423	423	423	0,1	0,1	0,05
1 mM Triton X-100 + 0,1 M NaCl	1,48	1,69	2,27	423	423	423	0,2	0,1	0,03

Nažalost, detaljan mehanistički opis učinka takvog miješanog sustava na elektrostatske ili steričke odbojne sile između NP nije jednostavan zbog niza mogućih interakcija i nastajanja kompleksnih specija između iona, surfaktanata i NP (Capjak i dr, 2018). Međutim, dobiveni rezultati jasno pokazuju da prisutnost surfaktanta u sustavima s AgNP može spriječiti njihovu aglomeraciju, sedimentaciju i otapanje, što može omogućiti dugotrajnu prisustnost AgNP u okolišu, a time i mogućnost njihovog štetnog djelovanja na zdravlje ljudi i okoliš.

Rezultati dobiveni u modelnim sustavima, prikazani u Slikama 25-27 i Tablicama 10-12, jasno pokazuju da je stabilnost i sudbina AgNP u nekom mediju kontrolirana ne samo fizikalno-kemijskim svojstvima samih AgNP, nego i svojstvima medija kao što su pH, ionska jakost i sadržaj organskih tvari u skladu s dosadašnjim opažanjima (Jurašin i dr., 2016.). Kombinacija eksperimentalnih tehnika navedenih u Tablici 7 i primjenjenih u ovom istraživanju omogućuje detalajn opis opisuje svojstva, stabilnost i ponašanje AgNP u nekom mediju te je stoga takav pristup korišten za istraživanje ponašanja drugih vrsta AgNP.

4.2. Sinteza, karakterizacija i procjena stabilnosti AgNP različitih veličina, oblika i površinske strukture

Protokoli za sintezu, karakterizaciju i procjenu stabilnosti AgNP prikazani u poglavlju 4.1. primijenjeni su na sustavu AgNP različitih veličina, oblika i površinske strukture u svrhu istraživanja učinka različitih fizičko-kemijskih svojstava AgNP na njihovu interakcija s albuminom i α-1-kiselim glikoproteinom. U tu svrhu sintetizirano je 16 vrsta AgNP različitih veličina, oblika i površinskih struktura navedenih u Tablici 13.

Tablica 13. Sustav AgNP primijenjen u istraživanju interakcija s proteinima.

AgNP oblik	AgNP veličina	Površinski stabilizator	Naziv AgNP
Sferične	~ 10 nm	AOT	AOT10sph
		PVP	PVP10sph
		Tween 80	TW10sph
		PLL	PLL10sph
		CTA	CTA10sph
		Citrat	CIT10sph
		BSA	BSA10sph
Sferične	~ 50 nm	AOT	AOT50sph
		Citrat	CIT50sph
		CTA	CTA50sph
		PVP	PVP50sph
		Brij 35	BRIJ50sph
		Tween 80	TW50sph
Triangularne		AOT	AOT50tri
		PVP	PVP50tri
Kubične		PVP	PVP50cube

Kako bi se ispitao utjecaj veličine na interakcije pripremljene su AgNP dviju ciljanih veličina: ~ 10 nm i ~ 50 nm. Za površinsku stabilizaciju primijenjeni su negativno nabijeni AOT i CIT, pozitivno nabijeni PLL i CTA, te neutralni stabilizatori PVP, Tween 80 i Brij35. Dodatno su pripremljene i karakterizirane AgNP stabilizirane s BSA. Uz sferične AgNP veličine ~ 10 nm i ~ 50 nm, pripremljene su i triangularne pločice stabilizirane s PVP i AOT,

te kubične, stabilizirane s PVP, veličine ~ 50 nm. Sve AgNP su karakterizirane neposredno nakon sinteze i pročišćavanja korištenjem DLS, ELS, UV-VIS i TEM tehnika

4.2.1. Sinteza i karakterizacija nanočestica srebra različitih veličina, oblika i površinske strukture

Sferične AgNP u veličini od 10 nm sintetizirane su prema postupcima opisanim u odjeljku 3.2.1. ovog rada koristeći CIT, AOT, CTA, PVP, PLL, BSA, Brij 35 i Tween 80 površinske stabilizatore. Makroskopski izgled otopina sintetiziranih AgNP u koncentraciji od 10 mg/L prikazan je na Slici 28 i TEM slika na slici 29.

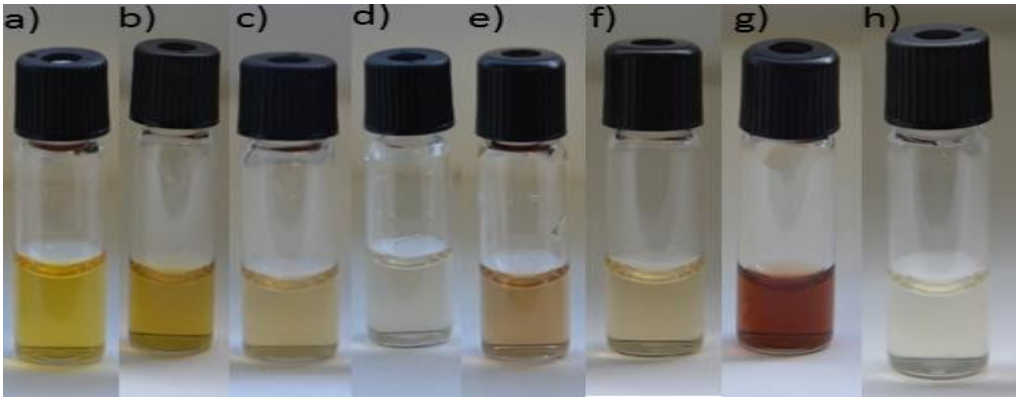

Slika 28. Otopine sintetiziranih AgNP10: a) CIT10sph, b) AOT10sph, c) PVP10sph, d) Brij10sph, e) Tween10sph, f) BSA10sph, g) PLL10sp, h) CTA10sph.

Boja otopina varira ovisno o primijenjenom stabilizatoru, obliku i sintetskom postupku. Dobivene AgNP vizualizirane su TEM tehnikom koja je pokazala da su neke AgNP polidisperzne (Slika 28), što je potvrđeno i DLS mjerenjima. Izmjerene su vrijednosti hidrodinamičkog promjera (d_H) prema intenzitetu, volumenu i broju čestica dane u Tablici 14. Iako je uobičajeno analizirati raspodjelu veličina NP prema intenzitetu, takva obrada DLS mjerenja može davati krivu informaciju o onim NP sustavima u kojima je prisutno više od jedne populacije čestica ili je ta raspodjela asimetrična. U tim je slučajevima potrebno analizirati i raspodjelu d_H prema volumenu ili broju, a poželjno je takve DLS podatke dodatno potvrditi TEM mjerenjima iz kojih se dobivaju i vrijednosti primarnih veličina NP.

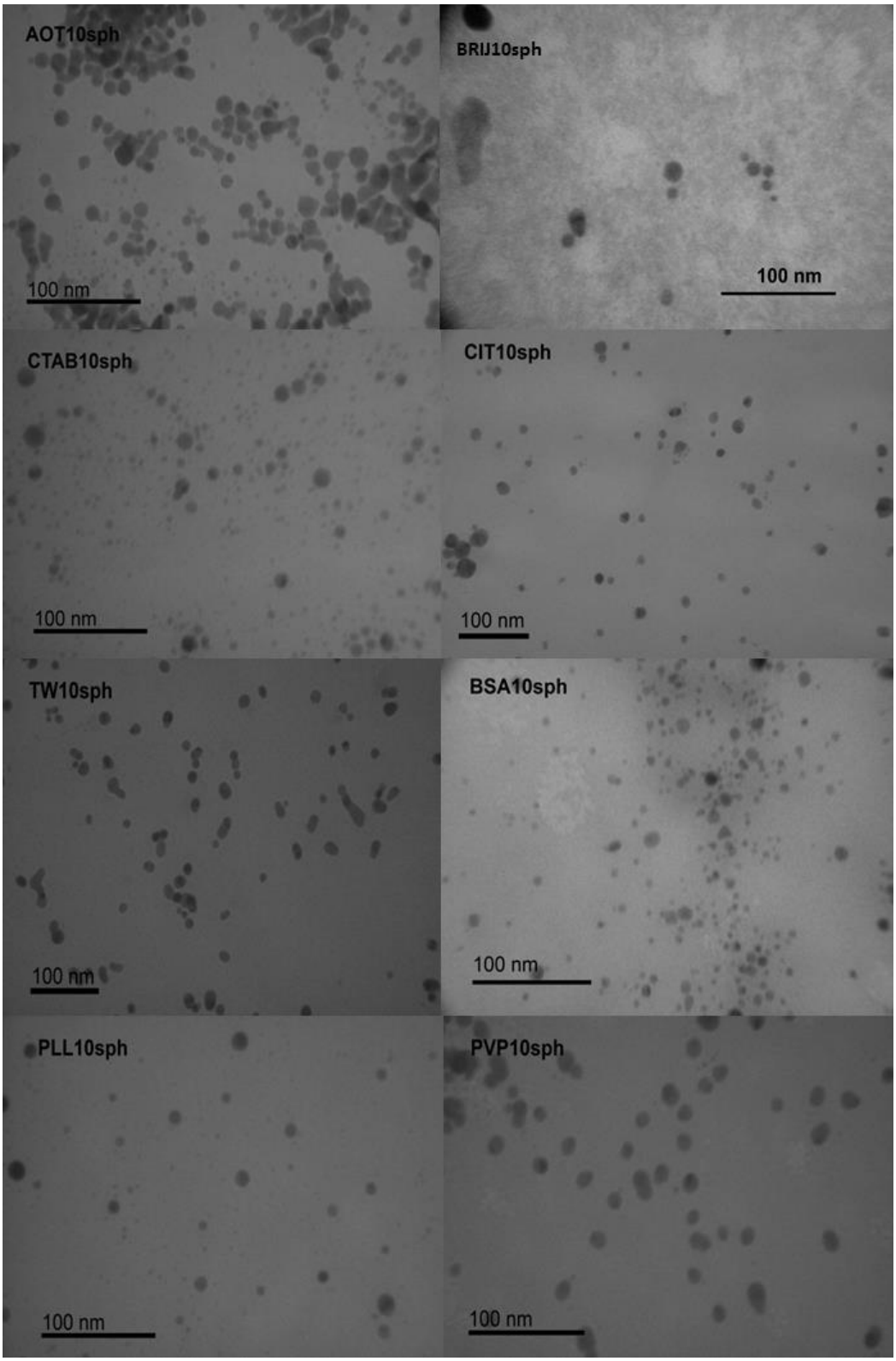

Slika 29. TEM slika AgNP10 u ultračistoj vodi.

Rezultati dobiveni za AgNP10sph (Tablica 14) jasno pokazuju da se kod polidisperznih koloidnih sustava analizi treba pristupiti krajnje pažljivo. Prema podacima za d_H po volumenu vidi se da AgNP10sph stabilizirane s PVP, Tween 80, CTA i Brij 35 imaju

monomodalnu raspodjelu, a veličine tih AgNP kreću se od 3,3 do 11,7 nm. AgNP10sph stabilizirane s AOT, PLL, CIT i BSA imaju bimodalnu raspodjelu veličina ako se analiziraju samo podaci za d_H po volumenu, te im se veličina manje populacije kreće od 4,9 do 18,2 nm, a veća populacija sadržava čestice u rasponu veličina od 18,9 do 43,9. Populacija čestica manjih veličina ujedno je i dominantnija, te je kod svih vrsta prisutna u više od 90% volumena, osim kod BSA10sph. Jedino su BSA stabilizirane AgNP izrazito polidisperzne. Slični podaci dobivaju se i za d_H po broju. Međutim, d_H po intenzitetu daje sasvim drugačiju sliku. To je zbog toga što veće NP daju i veći intenzitet raspršenja laserske zrake, pa se se iz d_H po intenzitetu krivo može zaključiti da je prosječna veličina AgNP10sph puno veća od stvarno dobivene.

Tablica 14. Hidrodinamički promjeri (d_H) prema intenzitetu, volumenu i broju za AgNP10sph u ultra čistoj vodi dobiveni DLS mjerenjima, te primarni promjer AgNP dobiven iz TEM slika (d_{TEM}). U zagradama su dani odgovarajući % pojedine populacije u ukupnom uzorku AgNP.

AgNP	Intenzitet	Broj	Volumen	TEM
	d_H (nm) (%)	d_H (nm) (%)	d_H (nm) (%)	d_{TEM} (nm) (%)
AOT10sph	3,4 ± 1,0 (7,7) 51,9 ± 7,7 (92,3)	2,6 ± 0,9 (96,6) 15,2 ± 5,3 (3,4)	5,9 ± 3,5 (97,1) 18,9 ± 2,1 (2,9)	3,3 ± 1,3 (39,0) 7,4 ± 1,6 (46,7) 12,3 ± 1,9 (14,3)
PVP10sph	6,3 ± 0,6 (16,5) 61,0 ± 1,6 (83,5)	5,0 ± 0,6 (98,8) 33,2 ± 2,6 (1,2)	9,3 ± 2,4 (100,0)	9,8 ± 2,7 (100,0)
TW10sph	7,9 ± 1,0 (16,4) 66,2 ± 3,0 (83,6)	3,8 ± 0,2 (99,5) 28,3 ± 0,3 (0,5)	5,8 ± 0,4 (100,0)	10,2 ± 2,9 (100,0)
PLL10sph	8,9 ± 1,7 (12,0) 85,6 ± 3,9 (88,0)	3,8 ± 0,4 (100,0)	4,1 ± 0,4 (99,0) 43,9 ± 0,7 (1,0)	6,3 ± 1,9 (91,1) 11,9 ± 1,3 (8,9)
CTA10sph	14,6 ± 1,6 (17,1) 77,2 ± 9,1 (82,9)	8,0 ± 1,5 (100,0)	11,7 ± 3,2 (100,0)	5,15 ± 3,1 (100,0)
CIT10sph	8,4 ± 0,7 (12,5) 69,6 ± 5,2 (87,5)	4,8 ± 0,9 (100,0)	6,8 ± 1,2 (92,8) 40,5 ± 3,1 (7,2)	7,9 ± 1,3 (53,6) 13,9 ± 3,7 (42,0) 31,7 ± 5,1 (3,6)
BSA10sph	23,8 ± 0,0 (2,5) 154,3 ± 7,3 (97,5)	21,3 ± 0,4 (44,1) 110,8 ± 31,1 (43,7) 228,4 ± 0,9 (12,2)	18,2 ± 5,9 (57,1) 70,8 ± 6,4 (43,0)	3,0 ± 1,1 (54,9) 6,4 ± 1,3 (35,3) 12,5 ± 1,3 (9,8)
Brij10sph	4,9 ± 0,3 (25,6) 55,7 ± 0,8 (74,4)	2,4 ± 0,4 (100,0)	3,3 ± 0,3 (100,0)	13,5 ± 4,6 (100,0)

Obzirom da su vrijednosti d_H po volumenu najtočnije opisivale pripremljene AgNP10sph dalje su se tijekom istraživanja uglavnom koristile te vrijednosti u svrhu tumačenja stabilnosti, ponašanja i transformacija AgNP. Izmjereni ζ potencijal AgNP10sph prikazan je na Slici 30. Očekivano, stabilizacija s PLL i CTA rezultirala je pozitivno

nabijenim AgNP koje su karakterizirane ζ potencijalom od 23,6 ± 4,0 i 38,5 ± 2,9 mV, budući da su oba navedena stabilizatora pozitivno nabijena pri pH 6–7. Također, BSA10sphAgNP su imale blago negativni ζ potencijal kojim se BSA molekula odlikuje pri neutralnom pH u ultračistoj vodi. Negativno nabijeni stabilizatori CIT i AOT dali su negativno nabijene AgNP kojima je vrijednost ζ potencijala bila negativnija od -30 mV. Međutim, stabilizacija s neutralnim PVP, Tween 80 i Brij 35 rezultirala je negativno nabijenim AgNP uz izmjereni ζ potencijal u rasponu od −6 do −19 mV. To je lako objasniti obzirom je u sintezi korišten borhidrid kao reducens $AgNO_3$. Ioni BH_4^- su se tijekom postupka sinteze čvrsto vezali za površinu PVP10sph, Tween10sph i Brij10sph, te ih nije bilo moguće ukloniti tijekom pročišćavanja. Oni su doprinijeli ukupnom zeta potencijalu tih AgNP.

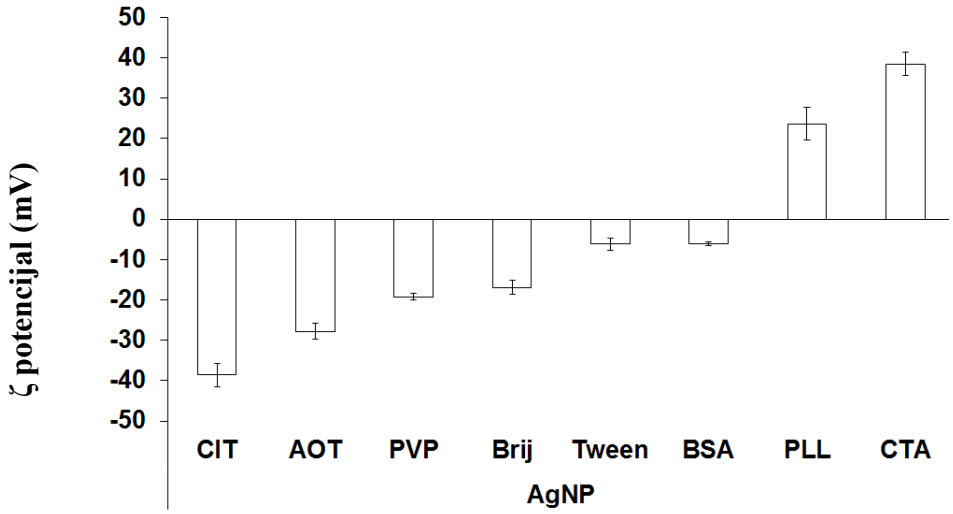

Slika 30. ζ potencijal pripremljenih AgNP10sph.

Sferične AgNP prosječne veličine 50 nm sintetizirane su prema postupcima opisanim u odjeljku 3.2.2. koristeći CIT, AOT, CTA, PVP, Brij 35 i Tween 80 površinske stabilizatore. Osim sferičnih, sintetizirane su i triangularne pločice stabilizirane s AOT i PVP prema postupcima opisanim u odjeljku 3.2.4, te kubične stabilizirane s PVP prema postupku iz odjeljka 3.2.5. AgNP50 stabilizirane s PLL nije bilo moguće sintetizirati. Svi primijenjeni postupci rezultirali su ili dobivanjem PLL10sph ili izrazito polidsiperznih AgNP. Na Slici 31 prikazan je makroskopski izgled otopina AgNP u koncentraciji od 10 mg/L.

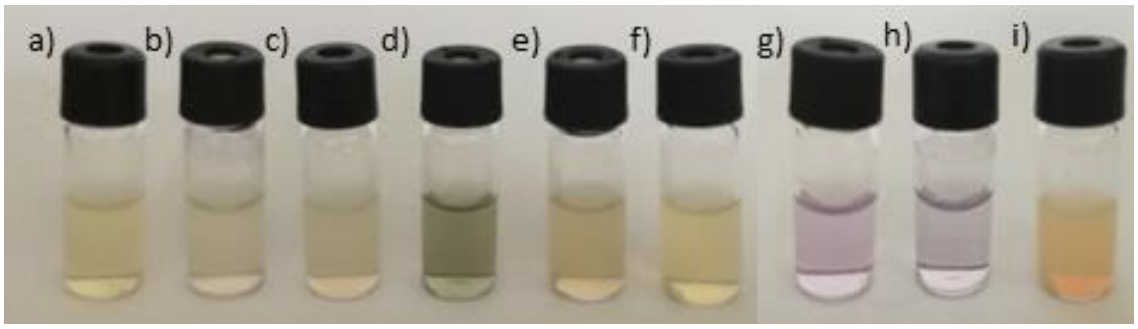

Slika 31. Sintetizirane AgNP veličine ~ 50 nm sferičnog, triangularnog i kubičnog oblika stabiliziranih različitim stabilizatorima: a) AOT50sph, b) BRIJ50sph, c) CIT50sph, d), CTA50sph e) PVP50sph f) TW50sph, g)PVP50tri h)AOT50tri i)PVP50cube.

Raspodjela veličina tako pripremljenih AgNP određena je iz DLS i TEM mjerenja (Tablica 15), dok su TEM slike potvrdile nastanak AgNP željenog oblika (Slika 32).

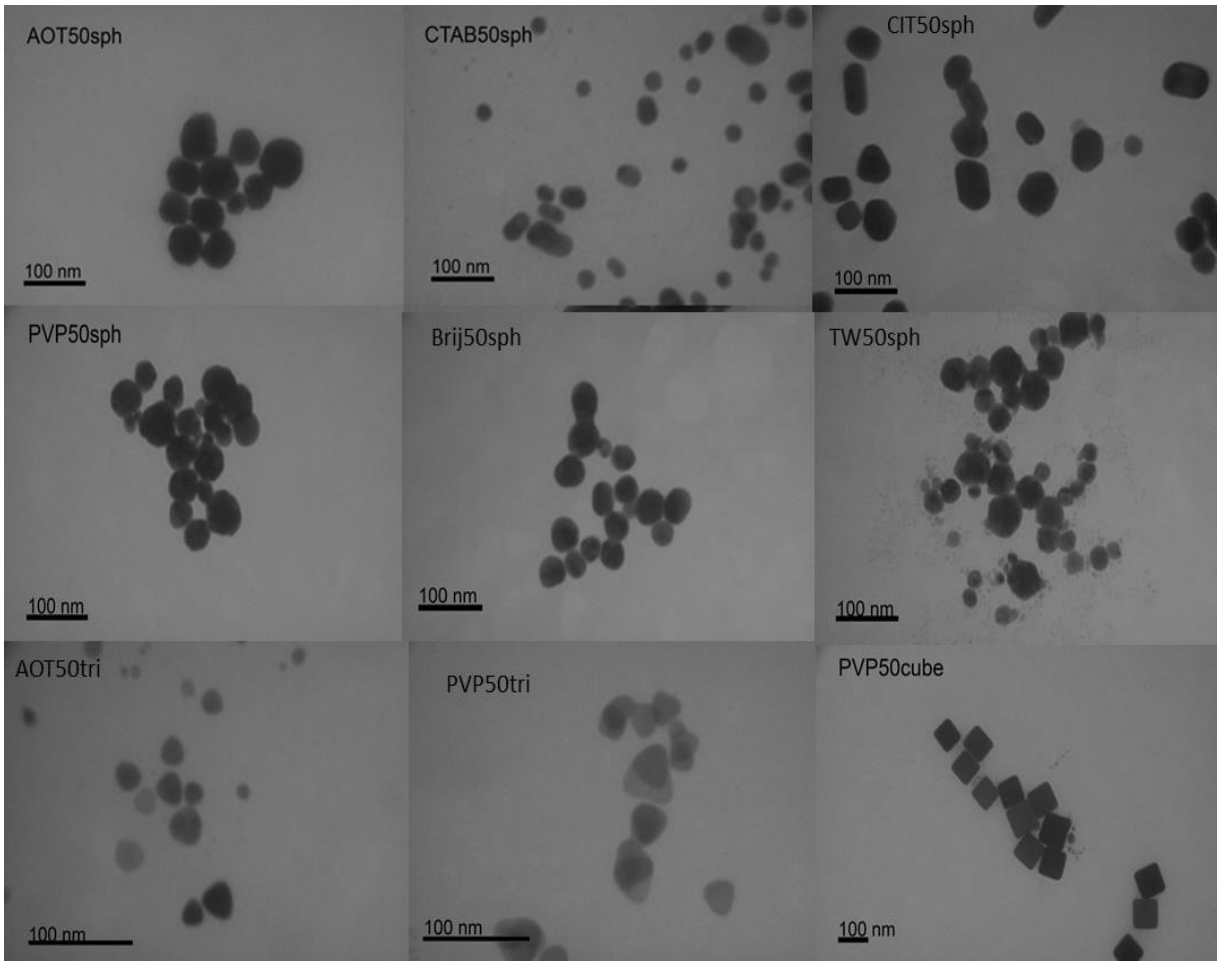

Slika 32. TEM slike AgNP50 različitih oblika i površinskih struktura u ultračistoj vodi.

Tablica 15. Hidrodinamički promjeri (d_H) prema intenzitetu, volumenu i broju za različite AgNP50 u ultračistoj vodi dobiveni DLS mjerenjima, te primarni promjer AgNP dobiven iz TEM slika (d_{TEM}).

AgNP	Intenzitet d_H (nm) (%)	Broj d_H (nm) (%)	Volumen d_H (nm) (%)	TEM d_{TEM} (nm) (%)
AOT50sph	10,2 ± 1,5 (5,1) 70,5 ± 3,9 (94,9)	8,5 ± 1,2 (60,0) 37,5 ± 2,6 (40,0)	9,3 ± 1,3 (14,6) 50,1 ± 3,1 (85,4)	12,4 ± 2,6 (35,7%) 24,2 ± 5,2 (64,3%)
CIT50sph	29,7 ± 10,6 (12,3) 151,5 ± 9,7 (87,8)	35,6 ± 3,2 (91,9) 248,1 ± 28,8 (8,2)	42,0 ± 16,4 (84,2) 248,1 ± 26,2 (15,8)	4,3 ± 2,7 (12,0%) 23,2 ± 5,4 (36,0%) 41,9 ± 6,9 (52,0%)
CTA50sph	54,6 ± 17,9 (12,2) 118,5 ± 18,9 (50,2) 406,2 ± 117,1 (37,6)	65,3 ± 22,7 (32,6) 113,5 ± 14,0 (38,5)	64,9 ± 17,6 (76,1) 178,2 ± 76,7 (23,9)	15,2 ± 2,6 (17,9%) 38,9 ± 9,8 (82,1%)
PVP50sph	40,7 ± 11,6 (13,0) 338,7 ± 66,5 (87,0)	7,8 ± 2,1 (68,5) 30,2 ± 8,2 (31,5)	35,2 ± 12,6 (86,3) 376,1 ± 53,4 (13,7)	15,2 ± 2,6 (17,9%) 38,9 ± 9,8 (82,1%)
BRIJ50sph	10,0 ± 1,1 (4,5) 68,4 ± 0,9 (95,5)	8,6 ± 1,3 (84,8) 39,6 ± 3,5 (15,2)	43,6 ± 7,5 (100,0)	7,9 ± 1,9 (9,34%) 15,2 ± 3,3 (30,8%) 30,6 ± 7,0 (59,8%)
TW50sph	109,5 ± 1,1 (100,0)	90,2 ± 1,3 (100,0)	64,6 ± 2,7 (100,0)	15,3 ± 3,9 (11,3%) 36,8 ± 10,9 (79,4%) 61,8 ± 8,3 (9,3%)
PVP50tri	2,8 ± 0,3 (14,1) 41,2 ± 1,0 (85,9)	32,3 ± 7,3 (100,0)	12,4 ± 2,5 (12,4) 29,3 ± 7,2 (87,6)	35,1 ± 10,1 (100,0%)
AOT50tri	3,7 ± 0,8 (17,3) 35,3 ± 2,5 (82,8)	1,2 ± 0,3 (100,0)	33,4 ± 6,1 (78,6) 5,3 ± 2,3 (21,4)	33,1 ± 10,1 (100,0%)
PVP50cube	123,7 ± 2,2 (100,0)	115,3 ± 1,5 (100,0)	92,0 ± 2,5 (100,0)	69,6 ± 7,5 (100,0%)

Rezultati DLS mjerenja AgNP50 suspendiranih u UW pokazuju da je veličina čestica prema volumenu monomodalna samo za Tween50sph, Brij50sph i PVP50cube. Samo AgNP50 stabilizirane s AOT i PVP imale su osim željene populacije veličine ~50 nm, i populaciju koja je bila znatno manja, dok su ostale bimodalne vrste imale aglomerate veće od 100 nm (Tablica 16). ELS podaci (Slika 32) pokazuju da su sve AgNP50, osim CTA50sphAgNP, imale negativan ζ potencijal u UW. Za AgNP stabilizirane neutralnim stabilizatorima (PVP, Tween i Brij 35), te su vrijednosti bile u rasponu od -10 do -20 mV, dok su one stabilizirane CIT i AOT imale ζ potencijal negativniji od -30 mV. Usporedbom ζ potencijala AgNP veličina 10 nm i 50 nm (Slike 30 i 33), vidljivo je da su AOT, PVP i CIT AgNP srodnog zeta potencijal bez obzira na njihovu veličinu. Međutim, zabilježena je značajna razlika između CTA10sph i CTA50sph, pri čemu su CTA10sph karakterizirane pozitivnim ζ-potencijalom od 28,17 ± 1,54 mV, a CTA50sph ζ potencijalom od 5,5 ± 1,1 mV koji je blizu nulte vrijednosti.

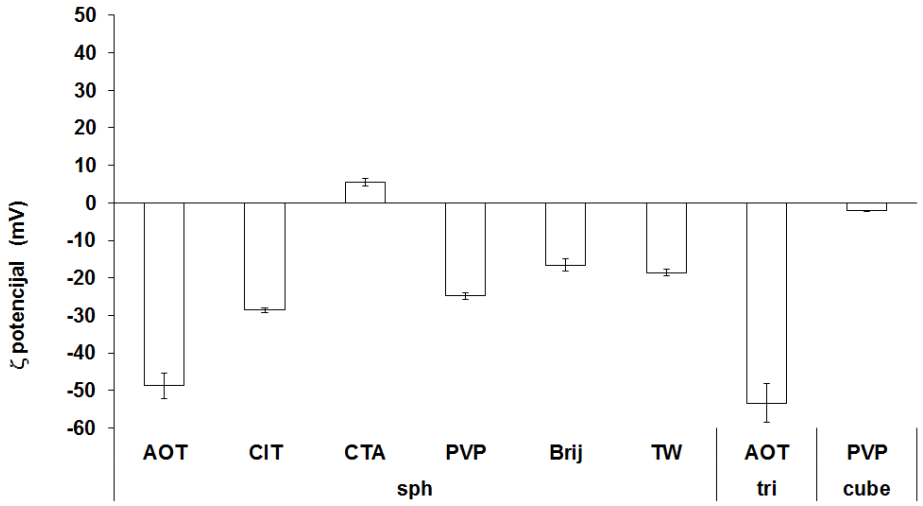

Slika 33. ζ potencijal pripremljenih AgNP50.

Stabilnost pripremljenih AgNP ispitana je i s obzirom na njihovu topljivost, odnosno otpuštanje slobodnih Ag^+ iona (Tablica 16). Pri tome je mjeren udio slobodnih Ag^+ neposredno nakon sinteze i pročišćavanja AgNP, 4 sata nakon inkubacije u UW u zatvorenim bočicama, 4 sata nakon inkubacije u UW u mikrotitarskim pločicama s 12 jažica, te 30 dana nakon sinteze. Podaci iz Tablice 16 jasno pokazuju da niti jedna AgNP vrsta nije otpustila više od 5% slobodnih Ag^+ iona, a vremenski ovisna mjerenja su dokazala dugotrajnu stabilnost svih AgNP vrsta obzirom na oslobađanje slobodnih iona.

Tablica 16. Udio slobodnih Ag^+ iona u pripremljenim AgNP vrstama neposredno nakon sinteze i pročišćavanja (t=0 h), 4 sata nakon inkubacije u zatvorenim bočicama ($t_{zatvoreno}$ =4 h), 4 sata nakon inkubacije u mikrotitarskim pločicama ($t_{pločice}$ =4 h), te 30 dana nakon sinteze (t=30 dana) pri koncentraciji AgNP otopina od 10 ppm, dobiveni AAS-om.

AgNP	**t=0h**	**$t_{zatvoreno}$= 4h**	**$t_{pločice}$=4 h**	**t=30dana**
	% Ag^+ (SD%)	**% Ag^+ (SD%)**	**% Ag^+ (SD%)**	**% Ag^+ (SD%)**
CIT10sph	0,2 ± 0,08	0,76 ± 0,04	1,1 ± 0,06	0,2 ± 0,03
AOT10sph	2,5 ± 0,16	2,9 ± 0,17	4,1 ± 0,34	1,4 ± 0,13
PVP10sph	2,8 ± 0,12	1,8 ± 0,21	2,1 ± 0,31	3,0 ± 0,32
TW10sph	0,3 ± 0,04	1,1 ± 0,08	1,2 ± 0,23	0,5 ± 0,12
CTA10sph	0,6 ± 0,07	0,2 ± 0,03	0,4 ± 0,05	0,5 ± 0,21
PLL10sph	0,8 ± 0,04	0,5 ± 0,06	1,4 ± 0,18	2,1 ± 0,54
CIT50sph	0,1 ± 0,01	2,8 ± 0,29	3,6 ± 0,43	0,1 ± 0,03
AOT50sph	1,7 ± 0,09	2,8 ± 0,34	3,3 ± 0,45	0,1 ± 0,04
PVP50sph	1,2 ± 0,11	0,6 ± 0,08	1,1 ± 0,07	0,7 ± 0,11
TW50sph	0,8 ± 0,12	0,7 ± 0,06	0,7 ± 0,03	0,6 ± 0,13
CTA50sph	0,2 ± 0,03	1,0 ± 0,14	1,7 ± 0,11	0,4 ± 0,02
PVP50tri	0,9 ± 0,11	1,0 ± 0,21	0,8 ± 0,15	0,9 ± 0,18
AOT50tri	1,2 ± 0,07	1,4 ± 0,16	1,6 ± 0,24	1,1 ± 0,23
PVP50cube	0,9 ± 0,18	1,9 ± 0,12	2,8 ± 0,25	1,0 ± 0,18

S ciljem optimizacije postupka, sinteze su ponovljene u različitim vremenima starenja suspenzija nakon sinteza, a prije pročišćavanja. U prvom nizu sinteza, postupak pročišćavanja je proveden neposredno nakon sinteza dok je u postupku optimizacije, proveden nakon stajanja suspenzija od 24 sata do tjedan dana. Uočeno je da je postupak pročišćavanja nužno provesti odmah nakon završetka sinteze, a najkasnije u roku od 6 sati od završetka sinteze jer u suprotnom reaktanti ili nusprodukti dalje ragiraju s nastalim AgNP i dolazi do destabilizacije AgNP. Također je zaključeno da samo mala izmjena u brzini dodavanja pojedinog reagensa, vremenu i brzini miješanja značajno utječe na konačan ishod sinteze te mijenja raspodjelu veličina i oblik AgNP. Stoga je za svaki tip AgNP pažljivo razrađen postupak sinteze uz definiciju svih parametara.

4.2.2. Antibakterijska učinkovitost odabranih nanočestica srebra

Obzirom da je osnovna funkcija AgNP u različitim proizvodima upravo njihovo antibakterijsko djelovanje, ispitali smo antibakterijsku učinkovitost odabranih AgNP. Kako bi se istražio utjecaj veličine, zeta potencijala i primijenjenog stabilizatora na antibakterijsku aktivnost AgNP odabrane su sferične nanočestice u dvije veličine (10 i 50 nm), stabilizirane slijedećim površinskim omotačima: CIT, AOT, PVP, Tween 80, CTA, i PLL. Ispitivanja su provedena na dva klinički relevantna patogena: gram-negativna vrsta *Escherichia coli* i gram-pozitivna vrsta *Staphylococcus aureus*. Uloga mogućeg otapanja AgNP na njihove biocidne učinke procijenjena je mjerenjem oslobođenih Ag^+ iona u danim eksperimentalnim uvjetima. Također, antimikrobno djelovanje različitih AgNP uspoređeno je s antimikrobnim djelovanjem samih Ag^+ iona primijenjenim u testiranjima u obliku $AgNO_3$. Antimikrobna učinkovitost AgNP određena je pomoću MBC (od eng. *minimal bactericidal concentration*) spot testa (Kubo i dr., 2018) (poglavlje 7, Tablica 33.). Vrijednosti MBC za odabrane AgNP dobivene nakon 4 i 24 sata prikazane su na Slikama 34 i 35. Usporedba antibakterijske učinkovitosti AgNP pokazuje je da su AgNP10 snažniji antibakterijski agensi od AgNP50 za oba bakterijska soja (Slika 34). Međutim, u slučaju AgNP obloženih CIT i PVP, razlike u toksičnim učincima ovisno o veličini nisu značajne, s izuzetkom 4-satnog učinka na *S. aureus* (Slika 34). Antibakterijska djelotvornost svih proučavanih AgNP prema *S. aureusu* značajno se povećava s produljenjem vremena tretmana osim za TW50sph (Slika 34). Povećanje toksičnog učinka s vremenom za *S. aureus* opažena je za $AgNO_3$, što upućuje na važnu ulogu oslobođenih Ag^+ iona u toksičnosti AgNP. Značajno jači antibakterijski učinak nakon produžene inkubacije u *E. coli* zabilježen je samo za PVP10sph, CTA50sph i AOT50sph (Slika 35).

Usporedba osjetljivosti dvaju različitih bakterijskih sojeva pokazala je značajno veću osjetljivost gram-negativne *E. coli* od gram-pozitivnog *S. aureus* na ispitivane AgNP i na ionski oblik srebra. Očekivano, Ag^+ ioni su znatno toksičniji za navedene bakterijske sojeve od AgNP. MBC nakon 4 sata izlaganja za Ag^+ ione u *E. coli* je 0,02 mg Ag/L, te 0,16 mg Ag/L za *S. aureus*. To je oko 12 puta više od MBC vrijednosti dobivenih za AgNP tretman u *E. coli*, odnosno 8 puta više nego AgNP tretman u *S. aureus*.

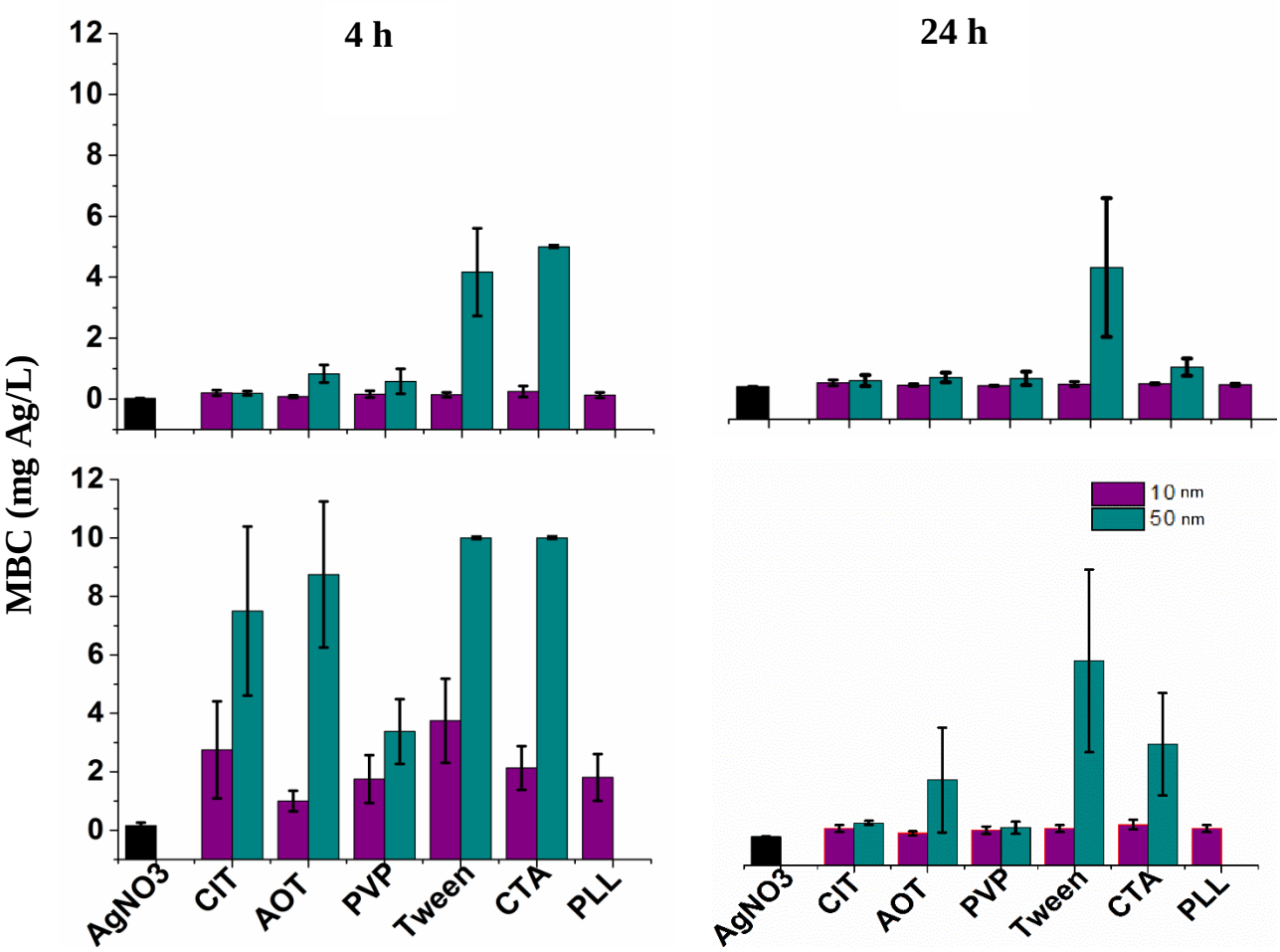

Slika 34. Utjecaj veličine AgNP na MBC kod *Escherichie coli* (gornji prikazi) i *Staphylococcus aureusa* (donji prikazi). Ljubičasti stupci označavaju rezultate za AgNP10, a zeleni za AgNP50. Podaci predstavljaju srednje vrijednosti dobivene iz 3 - 5 eksperimenta, a standardne devijacije su prikazane barovima.

Nadalje je ispitan biocidni učinak mogućeg oslobađanja Ag^+ iona s površine AgNP kvantifikacijom intracelularnog srebra prema ranije opisanoj metodi (Bondarenko i dr., 2013), korištenjem rekombinantne luminescentne sensorske bakterije *E. coli* MC1061 (pSLcueR/pDNPcopAlux) u Laboratoriju za toksikologiju okoliša u Tallinu. Podaci o topljivosti AgNP u UW, dobiveni pomoću AAS, uspoređeni su s podacima dobivenim korištenjem biosenzora (Slika 36). Rezultati su pokazali da je biodostupnost srebra najveća za PLL10sph i najniža za CTA50sph (Slika 36). Iako je biodostupna frakcija Ag na prvi pogled usporediva s njegovom topljivom frakcijom, podaci o topljivosti dobiveni korištenjem biosenzora bili su značajno različiti za slijedeće AgNP vrste: CIT10sph, CIT50sph, CTA10sph, CTA50sph, TW10sph, TW50sph i PLL10sph. Kod citratom stabiliziranih AgNP pretpostavlja se da površinski stabilizator CIT formira komplekse s Ag^+ ionima koji nisu

biološki raspoloživi za Ag-senzorne bakterije. U slučaju PLL10sph, bioraspoloživost otopljenih Ag^+ iona je otprilike 3 puta viša od njihove topljivosti mjerene s AAS, što ukazuje da biološki čimbenici (npr. interakcije stanica-AgNP) mogu doprinijeti njihovoj bioraspoloživosti.

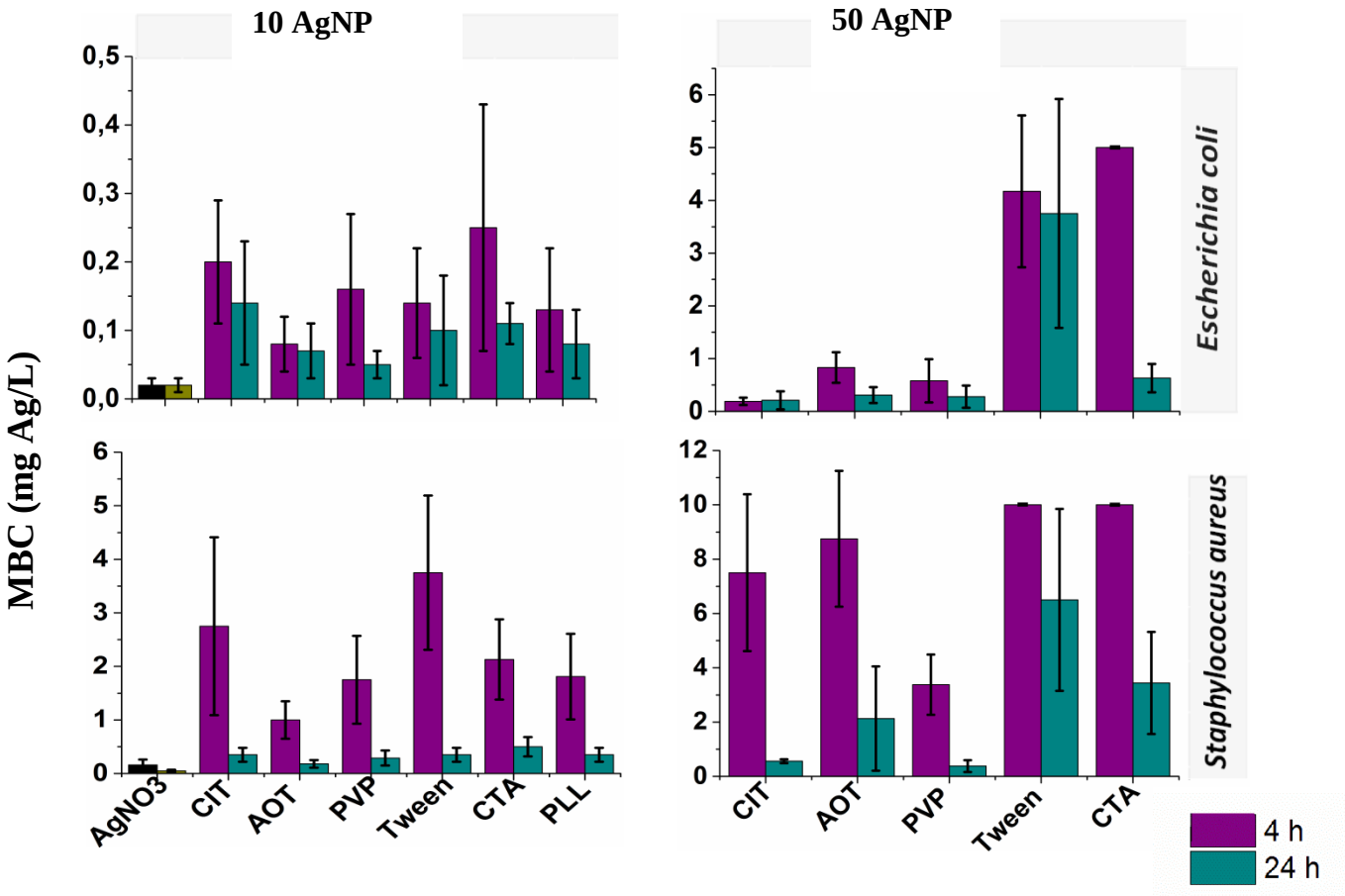

Slika 35. Učinak vremena inkubacije na MBC vrijednosti (A) ispitivanih AgNP i (B) $AgNO_3$ na sojeve *Escherichia coli* (gornji grafovi) i *Staphylococcus aureus* (donji grafovi). MBC vrijednosti dobivene nakon 4 sata inkubacije dane su u ljubičastim, a nakon 24 sata zelenim kolonama. Podaci predstavljaju srednje vrijednosti dobivene iz 3 - 5 eksperimenta, a standardne devijacije su prikazane barovima.

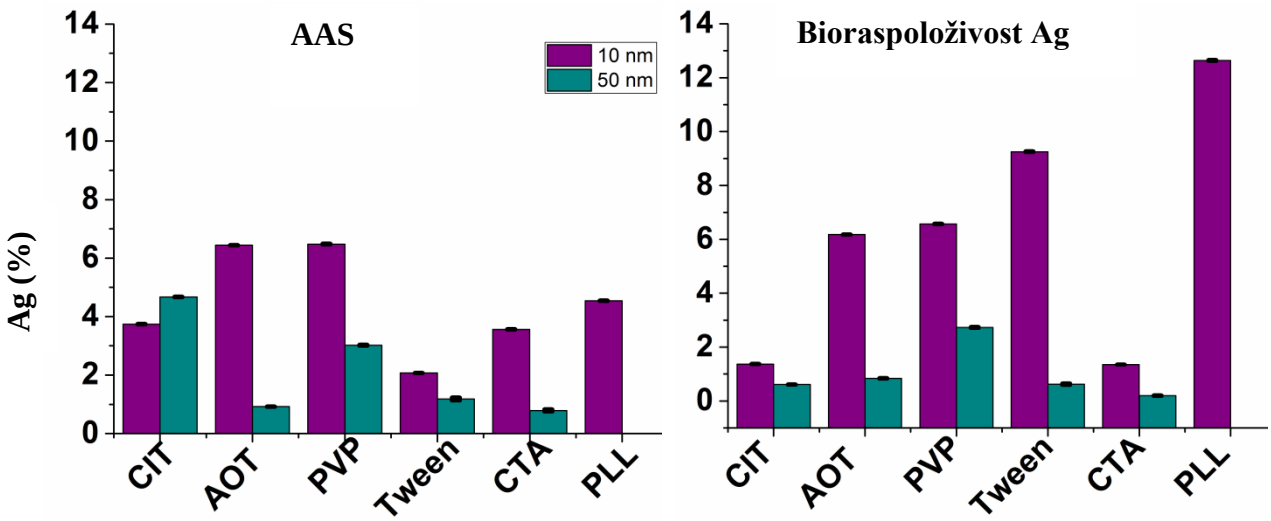

Slika 36. Topljivost (mjerena AAS-om) i biološka raspoloživost (određena Ag-biosenzorskim bakterijama) različitih AgNP izražena kao % početnog sadržaja Ag u AgNP. Analiza topljivosti provedena je pri AgNP koncentraciji od 1 mg AgNP/L. Ljubičasti stupci označavaju rezultate za AgNP10, a zeleni za AgNP50. Podaci predstavljaju srednje vrijednosti dobivene iz 3 - 5 eksperimenta, a standardne devijacije su prikazane barovima.

Istraživanje antibakterijskog djelovanja AgNP potvrdilo je glavnu paradigmu nanotehnologije, tj. mala veličina čestica ima veći utjecaj. AgNP10sph bili su značajno toksičniji za testirane bakterije u odnosu na AgNP50sph, neovisno o tipu površinskog stabilizatora. Međutim, najveću ulogu u toksičnosti AgNP imali su zapravo bioraspoloživi Ag^+ ioni. Razlika u toksikološkim profilima AgNP i Ag^+ iona za gram-negativne i gram-pozitive bakterije najvjerojatnije je posljedica činjenice da je sloj peptidoglikana u staničnoj zoni gram-pozitivnih bakterija debljine 30 nm, dok je isti sloj kod gram-negativnom debljine 2-3 nm. Deblji sloj peptidoglikana može djelovati kao barijera koja štiti stanicu od prodiranja AgNP i/ili Ag^+ iona u citoplazmu, čime se osigurava niža osjetljivost gram-pozitivnih u usporedbi s gram-negativnim bakterijama (López-Heras i dr., 2015.; Kim i dr., 2007.). Razlika u debljini tog sloja može također objasniti duže vrijeme potrebno za postizanje jednake antibakterijske učinkovitosti AgNP/Ag^+ iona protiv *S. aureus* i *E. coli* (Slike 34 i 35).

Antibakterijski učinci AgNP su u korelaciji s otpuštanjem Ag^+ iona s površine AgNP (Slika 36). Štoviše, veća antibakterijska učinkovitost AgNP10sph odgovara većem postotku slobodnih Ag^+ iona u AgNP10sph suspenzijama u usporedbi sa suspenzijama AgNP50sph (Slika 36). Oslobođeni Ag^+ ioni mogu dodatno destabilizirati AgNP i oštetiti bakterijske stanične membrane (McShan i dr., 2014.; Duran i dr., 2016.; Gurunathan i dr., 2014.)

Drugi važan faktor za dobivene antibakterijske učinke AgNP je njihov zeta. Negativni zeta potencijal bakterijskih stanica dokazan je u ranijim istraživanjima (Stoimenov i dr., 2002.), a potvrđen je i ovom studijom (ζ potencijal za *S. aureus* bio je -42 mV, a za *E. coli* -52 mV). U ovom je istraživanju postavljena pretpostavka da pozitivno nabijene AgNP (CTA i PLL) imaju veću antibakterijsku učinkovitost od negativno nabijenih AgNP zbog većeg potencijala za vezanje pozitivnih AgNP na negativno nabijene bakterijske stanice. Neki od površinskih stabilizatora, kao što su kationski polimer PLL i kationski surfaktant CTA mogu biti inherentno toksični za različite tipove stanica (Kubo et. al., 2018). Tako je pokazana toksičnost stabilizatora i prema *S. aureusu* i prema *E. coli* (poglavlje 7, Tablica 24,) (Kubo et. al., 2018). Kontakt bakterija i AgNP ostvaruje se preko površinskih stabilizatora pri čemu brzina otapanja, biodostupnost i stanje aglomeracije AgNPs *in vitro* i *in vivo* (López-Heras i dr., 2015) ovisi upravo o vrsti površinskog stabilizatora. Primjerice, neobložene AgNP imaju visoku tendenciju aglomeraciji i pokazuju nižu antibakterijsku aktivnost (Kubo i dr., 2018). Dakle, stabilizacija AgNP je vrlo važno svojstvo koje modulira fizikalno-kemijsko ponašanje AgNP i interakcije AgNP-stanica. Za usporedbu toksičnosti stabilizatora, provedeno je ispitivanje inhibicije rasta bakterija prema standardu ISO 20776-1 (Kubo et. al., 2018). Rezultati toksičnosti stabilizatora prema tom testu bili su jednaki kao i u spot testu: PVP, AOP, CIT i Tween nisu bili toksični (MBC> 100 mg / L), dok su PLL i CTA pokazali toksičnost (MBC = 75 i 36,5 mg / L, za E. coli i MBC = 30 i 1,8 mg / L za S. aureus) (Kubo i dr., 2018). Iako su CTA i PLL bili najtoksičniji stabilizatori kao čiste kemikalije, AgNPs obloženi tim stabilizatorima nisu pokazali veću antibakterijsku aktivnost u usporedbi s ostalim AgNP u 4-h i 24-h testu.

Konačno, rezultati nisu u potpunosti potvrdili postavljenu pretpostavku da je zeta potencijal AgNP odlučujući za njihovo antibakterijsko djelovanje. Iako su pozitivno nabijene AgNP bile učinkovitije u oštećivanju bakterijskih membrana nakon kratkih izlaganja i viših koncentracija (Slika 34), što pokazuje da je pozitivan nabojzeta potencijal važan, to nije bio odlučujući faktor za stvarni baktericidni učinak. Izravni učinak ove interakcije bio je zanemariv, u usporedbi s toksičnim učincima uzrokovanima Ag^+ ionima oslobođenim s površine AgNP. U danim eksperimentalnim uvjetima, uloga površinskog stabilizatora u modulaciji oslobađanja Ag^+ iona bila je važnija od učinaka usmjeravanja interakcija AgNP-bakterija postojećim zeta potencijalom (Kubo i dr., 2018.) Kada je topljivost i biološka raspoloživost AgNP prikazana u odnosu na odgovarajuću minimalnu baktericidnu koncentraciju (MBC), očigledno je da je toksičnost AgNP u korelaciji s njihovim brzinama otapanja (Kubo i dr., 2018).

Zaključno, ispitivane AgNP imaju učinkovito antimikrobno djelovanje, a mehanizmi toksičnosti se temelje na njihovoj topivosti, zeta potencijalu i veličini.

4.2.3. Stabilnost nanočestica srebra u biološkim medijima

Slijedeći korak ovog doktorskog istraživanja bio je odrediti stabilnost i ponašanje AgNP opisanih u prethodnim poglavljima u 3 modelna biološka medija: fosfatnom puferu pH 7.4 (FP), fiziološkoj otopini (FO) i FP uz dodatak 0.9% NaCl (FPNaCl) korištenjem tehnika navedenih u Tablicama 7 i 8 i opisanima u Poglavljima 3.3 i 3.4. Rezultati dobiveni za UW daju osnovne karakteristike i ukazuju na dugotrajnu stabilnost ispitivanih AgNP obzirom da je cilj sinteza bio pripremiti AgNP kao suspenzije u UW kao otapalu. Sve ispitivane AgNP su bile stabilne i nisu mijenjale svoja fizikalno-kemijska svojstva u UW tijekom najmanje 3 mjeseca (poglavlje 4.2.1.). Ti podaci su služili kao referentni podaci za dani AgNP sustav.

Raspodjela veličina prema volumenu ispitivanih AgNP nakon 1-satnog izlaganja modelnim medijima prikazana je u Tablici 17, dok su promjene u ζ potencijalu prikazane Slikom 37. Otprilike pola od ukupnog broja ispitivanih AgNP pokazao je tendenciju aglomeraciji nakon izlaganja FO, dok je većina AgNP bila nestabilna u FP i FPNaCl. Zanimljivo je da, unatoč visokoj ionskoj jakosti, u FO nije došlo do značajnije aglomeracije PVP10sph, Tween10sph, PLL10sph, Brij10sph, AOT50sph, CIT50sph, PVP50sph i PVPcube. U FP i FPNaCl medijima, jedino su Tween10sph, Brij10sph, PVP50sph i PVPcube ostale stabilne obzirom na aglomeraciju. Takvu stabilnost objašnjavaju rezultati ζ potencijala čija se vrijednost nije značajno promijenila za PVP10sph, Brij10sph, AOT50sph, CIT50sph, PVP50sph i PVPcube, dok se svim ostalim AgNP vrstama ζ potencijal značajno promijenio u modelnim medijima. Zanimljivo je da su i AOT10sph i BSA10sph značajno aglomerirale u FO, FP i FPNaCl unatoč nepromijenjenim vrijednostima ζ potencijala u tim medijima. Vrijednost ζ potencijala u FO i FP približavala se 0 mV za sve AgNP vjerojatno zbog djelomičnog vezanja ionskih komponentni tih medija za negativno nabijene komponente na površini AgNP.

Tablica 17. Hidrodinamički promjeri (d_h) u nm dobiveni iz distribucije veličina prema volumena ispitivanih AgNP u modelnim biološkim medijima: ultračistoj vodi (UW), fosfatnom puferu pH 7.4 (FP), fiziološkoj otopini (FO) i FP uz dodatak 0.9% NaCl (FPNaCl) nakon 1 sata izlaganja. U zagradama su dani % pojedine populacije u ukupnom volumenu AgNP.

AgNP vrsta	**UW**	**FO**	**FP**	**FPNaCl**
	d_h (nm) *(%)*	d_h (nm) *(%)*	d_h (nm) *(%)*	d_h (nm) *(%)*
AOT10sph	5,9 ± 3,5 (97) 18,9±2,1 (3)	38,0 ± 10,5 (76) 182,9±41,2 (24)	4,7 ± 1,4 (78) 118,3± 86,1(22)	27,2 ± 5,1 (96) 699,3± 78,4 (4)
PVP10sph	9,3± 2,4 (100)	8,6 ± 2,1 (100)	26,7 ± 4,3 (100)	3,4 ± 0,6 (86) 30,5 ± 2,9 (14)
Tween10sph	5,8 ± 0,4 (100)	6,0 ± 2,7 (100)	5,0 ± 1,0 (98) 30,2 ± 2,9 (2)	7,9 ± 0,7 (98) 21,4 ± 5,5 (2)
PLL10sph	4,1 ± 0,4 (99) 43,9 ± 0,7 (1)	9,9 ± 3,2 (93) 46,0 ± 1,5 (7)	39,9 ± 13,8 (55) 655,0±55,5 (45)	192,1 ± 34,7 (2) 1051,7± 48,6 (98)
CTA10sph	11,7 ± 3,2 (100)	371,1±69,2 (100)	54,1±14,8 (80) 393,1±57,8 (2)	263,3 ± 21,2 (100)
CIT10sph	6,8 ± 1,2 (93) 40,5 ± 3,1 (7)	3,5 ± 1,1 (31) 45,6 ± 4,2 (69)	16,7 ± 6,7 (97) 788,8±121,5 (3)	36,7 ± 10,6 (35) 366,3 ± 56,7 (65)
BSA10sph	18,2 ± 5,9 (57) 70,8 ± 6,4 (43)	47,9 ± 5,8 (85) 411,9 ± 249,2 (15)	40,8 ± 2,0 (97) 577,7±190,2 (3)	54,0 ± 5,0 (61) 12,4 ± 1,1 (39)
Brij10sph	3,3±0,80 (100)	5,1 ± 1,1 (98) 56,7 ± 0,5 (2)	12,9 ± 1,3 (62) 78,5 ± 6,5 (38)	10,3 ± 3,3 (77) 73,5 ± 3,4 (23)
AOT50sph	9,3 ± 1,3 *(14)* 50,1 ± 3,1 *(86)*	20,2 ± 9,0 (51) 68,6 ± 13,2 (49)	64,1 ± 11,9 (52) 168,1 ± 85,7 (48)	12,4 ± 5,1 (39) 131,2 ± 66,2 (61)
CIT50sph	42,0± 16,4 *(84)* 248,1±26,2 *(16)*	51,1 ± 14,9 (100)	31,1 ± 8,1 (62) 359,0 ± 119,3 (38)	37,1 ± 0,8 (21) 398,9 ± 68,5 (79)
CTA50sph	64,9 ± 17,6 (76) 178,2 ± 76,7 (24)	465,6 ± 72,5 (100)	38,0 ± 8,7 (19) 352,0 ± 34,6 (81)	535,4 ± 144,9 (100)
PVP50sph	35,2 ± 12,6 (86) 376,1 ± 53,4 (14)	20,9 ± 9,9 (73) 90,6 ± 16,7 (27)	65,2 ± 8,0 (100)	47,5 ± 8,8 (51) 191,7 ± 16,7 (49)
Brij50sph	43,6 ± 7,5 (100)	121,9 ± 10,7 (100)	49,5 ± 16,4 (20) 121,8 ± 22,1 (80)	173,1 ± 100,4 (4) 1031,6 ± 135,7 (96)
Tween50sph	64,6 ± 2,7 (100)	99,9 ± 1,5 (100)	90,2 ± 1,3 (100)	58,7 ± 18,2 (58) 394,8 ± 119,1 (42)
PVP50tri	2,4 ± 0,5 (12) 29,3 ± 11,2 (88)	8,4 ± 1,7 (4) 62,5 ± 11,6 (96)	40,1 ± 13,4 (49) 300,0 ± 33,6 (51)	39,8 ± 2,3 (62) 510,3 ± 99,4 (38)
AOT50tri	5,3 ± 2,3 (21) 33,4 ± 6,1 (79)	11,1 ± 2,6 (8) 115,3 ± 2,4 (92)	36,3 ± 4,1 (69) 540,9 ± 105,1 (31)	35,3 ± 7,3 (68) 354,9 ± 82,6 (32)
PVP50cube	92,0 ± 12,5 (100)	125,8 ± 2,4 (100)	131,7 ± 11,7 (100)	114,7 ± 1,3 (100)

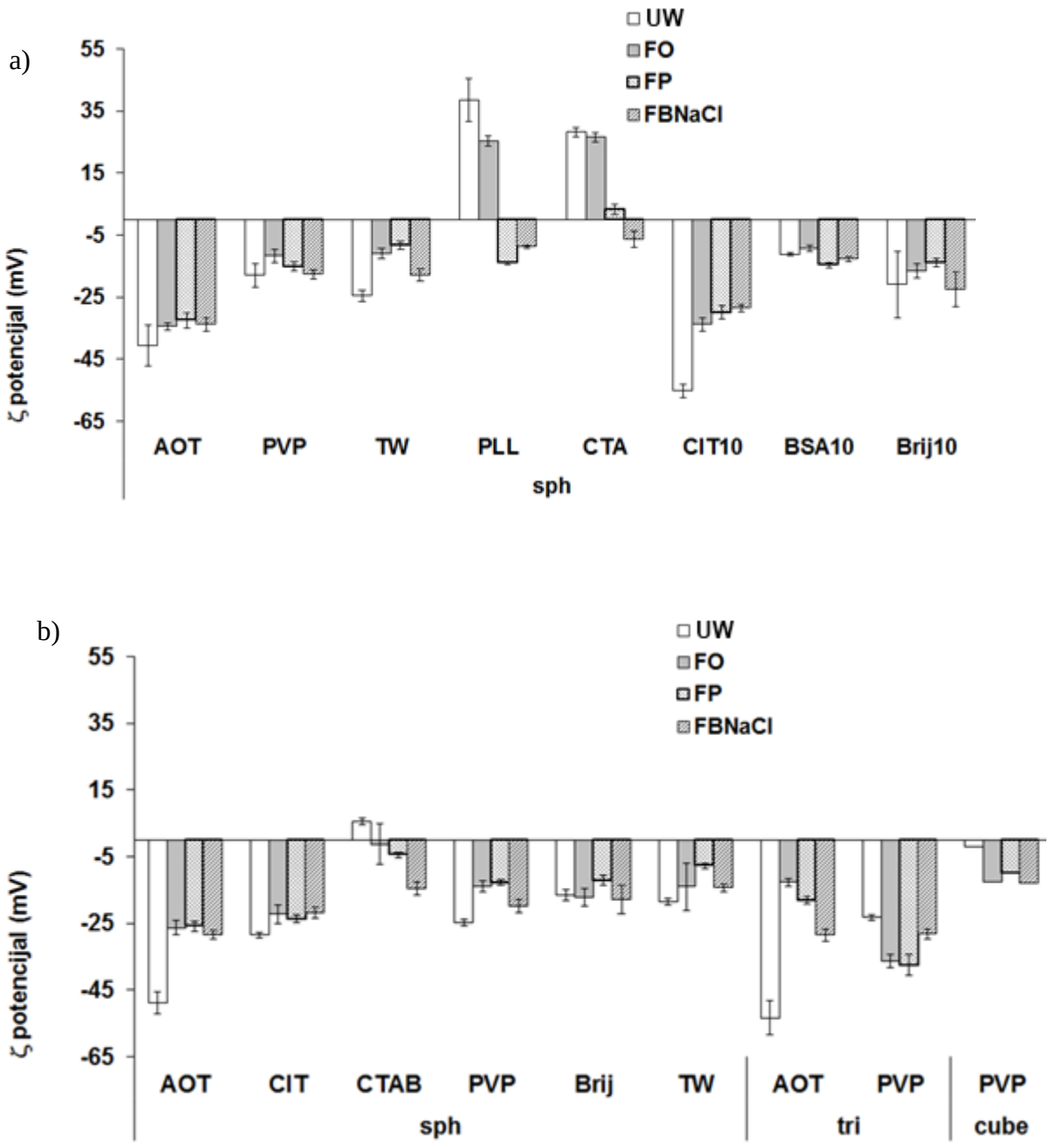

Slika 37. ζ-potencijal a) AgNP u veličini od 10 nm i b) AgNP u veličini od 50 nm.

S porastom ionske jakosti FP, FO i FPNaCl modelnih medija u odnosu na UW apsolutna vrijednost ζ potencijala se približava nuli. Kod pozitivno nabijenih AgNP njihov ζ potencijal postaje blago negativan u puferskom sustavu, te im vrijednost ζ potencijala postaje slična vrijednosti negativno nabijenih AgNP u tim istim medijima. Hidrodinamički promjer dominantno zastupljenih AgNP je najmanji u vodenom mediju bez pufera dok FP, a osobito FPNaCl dovode do značajnog povećanja tog promjera. Najveće promjere imaju AgNP stabilizirane CTA-om, a najmanje promjere imaju AgNP stabilizirane s Tween-om i Brij-om.

Osim promjene ζ potencijal koji ima učinak povećanja promjera AgNP u modelnim biološkim medijima u odnosu na UW i nominalni promjer čestica ima značajnu ulogu: nominalni promjer od 50 nm doista rezultira većim mjerenim promjerom AgNP u FP, FO i FPNaCl. Vidljivo je da promjer nekih AgNP u tim medijima raste značajno iznad 100 nm te se više i ne može govoriti o nanočesticama, nego o aglomeratima. Čini se da bi za primjenu u biološkim tekućinama od svih ispitanih nanočestica najpogodniji kandidati trebale biti AgNP stabilizirane s AOT u obje veličine i oba oblika koje, osim što ne aglomeriraju, ne otpuštaju niti ionsko srebro u otopinu. Na aglomeracijsko ponašanje AgNP u ispitivanim biološkim medijima ukazali su i podaci dobiveni za SPR signale (Tablica 18).

Tablica 18. Optički parametri za ispitivane AgNP (10 μM) nakon 1-satnog izlaganja UW, FO, FP i FPNaCl medijima.

AgNP tip	λ_{max} **nm**	$\Delta\lambda_{max}$			A_{max}			
	UW	**FO**	**FP**	**FPNaCl**	**UW**	**FO**	**FP**	**FPNaCl**
AOT10sph	395	0	0	-5	0,076	0,033	0,042	0,016
PVP10sph	385	5	5	5	0,054	0,111	0,07	0,11
TW10sph	440	-45	-40	-55	0,078	0,041	0,031	0,011
PLL10sph	400	5	50	30	0,065	0,037	0,025	0,014
CTA10sph	530	-105	-120	-110	0,023	0,025	0,022	0,029
CIT10sph	395	5	0	-5	0,122	0,17	0,049	0,031
BSA10sph	210	205	270	205	0,067	0,05	0,002	0,037
Brij10sph	340	55	65	55	0,003	0,043	0,057	0,022
AOT50sph	425	-5	0	-30	0,089	0,053	0,064	0,144
CIT50sph	420	0	25	-20	0,189	0,066	0,012	0,19
CTA50sph	400	20	10	-5	0,053	0,046	0,028	0,016
PVP50sph	465	-55	-60	-55	0,06	0,096	0,038	0,087
BRIJ50sph	435	-10	-5	-5	0,049	0,114	0,03	0,025
TW50sph	395	40	50	25	0,07	0,062	0,074	0,015
AOT50tri	580	-75	-30	-185	0,05	0,57	0,031	0,0131
PVP50tri	410	75	125	65	0,039	0,083	0,016	0,072
PVP50cube	395	80	75	85	0,035	0,088	0,053	0,038

Za sve AgNP u UW, pozicija signala površinske plazmonske rezonancije (SPR) zabilježena je u području od 385 i 580 nm. Iz dobivenih rezultata može se zaključiti da i oblik i vrsta stabilizatora i veličina AgNP imaju značajan utjecaj na optička svojstva AgNP. Usporedba optičkih svojstava AgNP10 i AgNP50 (Tablica 18) jasno pokazuje da se SPR signal većih AgNP pomiče prema višim valnim duljinama, što je u skladu s Mie-ovom teorijom (Mie, 1908; van de Hulst, 1957.). To se također događa sa SPR signalom triangularnih pločica i kocaka u odnosu na sferične oblike. Kod onih AgNP koje su izlaganjem FO, FP i FPNaCl medijima bile destabilizirane aglomeracijom evidentno je da su svi SPR signali bili prošireni, pomaknuti prema višim ili nižim valnim duljinama, a intenzitet im je bio smanjen u odnosu na UW (poglavlje 7, Slika 53,). Pojavljivanje dodatnih apsorpcijski maksimuma u području iznad 600 nm (poglavlje 7, Slika 53,) ukazalo je na nastanak aglomeriranih AgNP što je u skladu s opisanim DLS rezultatima (Tablica 18).

Navedeni rezultati dodatno su potkrijepljeni TEM slikama odabranih AgNP nakon 1-satnog izlaganja FP mediju (Slika 38) koje su također u skladu s DLS rezultatima. Vidljivi su aglomerati onih vrsta AgNP za koje su i DLS mjerenja upućivala na nestabilnost u FP mediju.

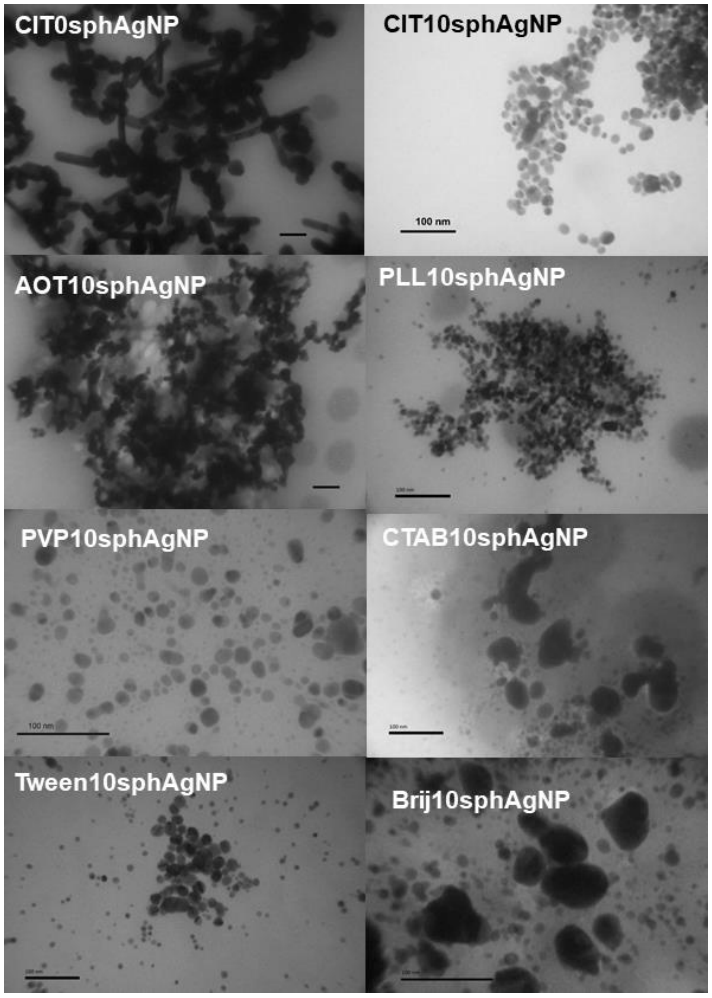

Slika 38. TEM slike AgNP nakon 1 satnog izlaganja FP mediju.

4.2.4. Učinak prisustva albumina na stabilnost srebrnih nanočestica u biološkim medijima

Istraživanje ove doktorske radnje na interakcijama AgNP s modelnim proteinima započela je ispitivanjem stabilnosti i mogućih transformacija AgNP10sph u modelnom biološkom mediju (FP) u koji je dodan BSA. Dobiveni rezultati uspoređeni su s onima opisanim u prethodnom poglavlju 4.2.3. Promjene u veličini, izražene kao d_H u nm, i ζ potencijalu, ispitivanih AgNP nakon izlaganja FP uz dodatak 0,1% BSA prikazani su Tablici 19.

Tablica 19. Hidrodinamički promjer (d_H u nm) i ζ potencijal (u mV) različitih AgNP10sph u FP uz dodatak 0,1% BSA.

Vrsta AgNP	d_H (nm)	Prosječni volumen %	ζ potencijal, mV
AOT10sph	47,8 ± 8,9	91,2	-9,9 ± 1,0
	671,0 ± 140,4	7,6	
PVP10sph	59,6 ± 11,4	100	-10,1 ± 0,7
Tween10sph	55,2 ± 6,8	100	-11,5 ± 0,8
PLL10sph	85,6 ± 17,6	41,2	-12,3 ± 1,2
	208,4 ± 14,8	56,7	
CTA10sph	71,8 ± 6,4	100	-12,4 ± 1,8
CIT10sph	114,2 ± 12,9	83,8	-11,8 ± 0,5
	22,4 ± 2,9	17,7	
BSA10sph	86,5 ± 17,5	100	-12,0 ± 1,5
Brij10sph	59,2 ± 9,4	94,2	-11,6 ± 1,3
	848,3 ± 9,6	5,1	

Dobiveni podaci ukazuju da je prisustvo BSA spriječilo aglomeraciju AgNP, što je već i ranije opisano u literaturi za slične vrste NP (Dominguez-Medina i dr., 2013; Kittler i dr., 2010, Gebauer i dr., 2012; Ravindran i dr., 2010). Međutim, do tog zaključka nije bilo moguće doći samo na temelju DLS i ELS podataka. Naime, ako se usporede rezultati iz Tablice 19 s rezultatima iz Tablice 17 i Slike 38, prvi dojam je da je BSA uzrokovao smanjenje apsolutne vrijednosti ζ potencijala što može utjcati na stabilnost AgNP u FP. ELS podaci pokazuju kako AgNP neovisno o stabilizatoru imaju gotovo jednak ζ potencijal u FP

uz dodatak BSA, koji se kreće se od -10,0 do -12,5 mV (Tablica 19). Izmjereni ζ potencijali su blizu vrijednosti određene za čisti BSA (-7,5 ± 0,04 mV) što nije iznenađujuće uzimajući u obzir relativno visoku koncentraciju proteina primijenjenu u modelnom mediju. Dobivene vrijednosti ζ potencijala za AgNP10sph pokazuje da je BSA vezan na njihovu površinu i određuje njihova površinska svojstva. Uz to, sve AgNP vrste su nakon 1-satnog izlaganja imale 2 ili više puta veći d_H po volumenu u odnosu na vrijednosti dobivene u UW (Tablica 17). Razlog tome je globularna priroda BSA koji se odmah nakon kontakta s AgNP veže na njihovu površinu te je neuniformno prekriva. BSA može biti vezan na površinu AgNP relativno jakim elektrostatskim vezama putem cisteinskih ostataka, ali je važno napomenuti i postojanje protein-protein elektrostatskih i deplecijskih interakcija. Ukoliko se obje vrste interakcija odvijaju istovremeno, debljina proteinske korone će se razlikovati ovisno o vrsti AgNP. Tako se BSA molekule na površini različitih AgNP mogu različito klasterirati, pokrivati te površine ne samo u monosloju nego i višeslojno. Obzirom da se molekule BSA različito vežu i adsorbiraju na površini različitih AgNP, konačni rezultat jesu varijacije u vrijednosti hidrodinamičkog promjera, odnosno veličine čestica. Dobivene razlike u raspodjeli veličina za različite AgNP ukazuju na njihovu neujednačenu površinsku pokrivenost s BSA ovisno o površinskom stabilizatoru. Za PVP10sphAgNP, Tween10sphAgNP i BSA10sphAgNP, koje su karakterizirane bimodalnom raspodjelom veličine u UW, interakcija s BSA rezultira monomodalnom raspodjelom veličina. Važno je napomenuti da je za sve AgNP koji su aglomerirale u FP, dodavanje BSA potpuno inhibiralo ili značajno smanjilo proces aglomeriranja. Usporedbom Tablica 17 i 19 vidi se da su se d_H vrijednosti za AOT10sphAgNP, Bri10sphAgNP, PLL10sphAgNP i CTA10sphAgNP značajno smanjile u FP nakon dodatka 0,1% BSA. Te su tvrdnje potkrijepljene TEM vizaulizacijom (Slika 39) koja je jasno pokazala neaglomerirane i dobro raspršene AgNP10sph u fosfatnom puferu u prisustvu BSA. TEM vizualizacija je također olakšala tumačenje DLS i ELS rezultata jer se na TEM slikama jasno vidi da se primarna veličina AgNP10sph nije promijenila nakon izlaganja FP uz dodatak BSA, te se promjene u d_H i ζ potencijalu mogu tumačiti jedino vezanjem BSA na površinu AgNP.

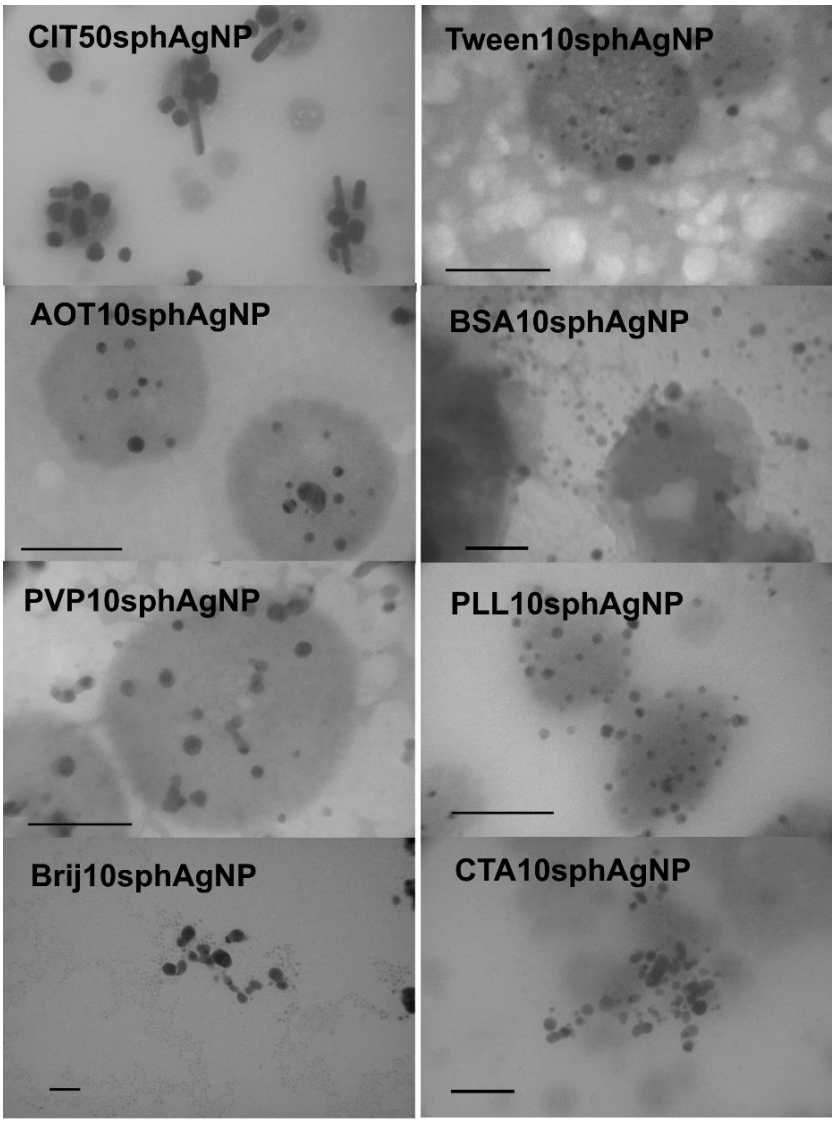

Slika 39. TEM slike različitih AgNP10sph nakon 1-satnog izlaganja FP u prisustvu 0.1% BSA.

Najvažnije opažanje ovog istraživanja je da BSA omogućuje stabilizaciju NP u modelnim biološkim tekućinama bez obzira na kemijski sastav i površinsku strukturu AgNP. Navedeni rezultati su u skladu s objavljenim podacima za stabilizaciju različitih metalnih NP u medijima koji sadrže proteine (Dominguez-Medina i dr., 2013; Kittler i dr., 2010, Gebauer i dr., 2012; Ravindran i dr., 2010). Mehanizmi adsorpcije na NP površinu i stvaranje proteinske korone ključni su za razumijevanja biološke reaktivnosti NP (Jurašin i dr., 2016). Proteinska stabilizacija NP u biološkim medijima može se koristiti u različitim nanomedicinskim primjenama.

4.3. Interakcija albumina i α-1-kiselog glikoproteina sa srebrnim nanočesticama

Nakon dobivenih podataka o stabilnosti i transformacijama AgNP različitog oblika, veličine i površinske strukture u modelnim biološkim medijima, detaljnije su ispitane interakcije tih AgNP s dva važna plazmatska proteina koji imaju transportnu ulogu u ljudskom krvotoku: albuminom i α-1-kiselim glikoproteinom. Ta su dva proteina odabrana kao modelni sustav, zbog svoje važne biološke uloge kako je opisano u uvodnom dijelu ovog rada.

Obzirom da su prethodno dobiveni rezultati ponašanja AgNP u prisustvu proteina (opisani u poglavlju 4.2.4) jasno pokazali da proteini stupaju u interakciju s AgNP formirajući protein koronu na njihovoj površini, pristupilo se određivanju jačine vezanja proteina na površinu AgNP ovisno o fizikalno-kemijskim svojstvima tih NP. Također su istražene i moguće promjene u strukturi tih proteina nakon njihovog vezanja na AgNP površinu.

4.3.1. Konstante vezanja albumina i α-1-kiselog glikoproteina na površinu različitih srebrnih nanočestica

Konstante vezanja albumina i AGP određene su primjenom metode opisane u poglavlju 3.4.2. Na Slici 40 prikazani su reprezentativni fluorescencijski spektri BSA tijekom interkacije s PLL10sphAgNP. Evidentno je da se povećavanjem koncentracije AgNP pri stalnoj koncentraciji BSA, intenzitet emisije BSA postupno smanjuje s pomakom od 7 nm iz maksimuma emisije na nižu valnu duljinu. Također, povećanjem koncentracije AgNP gasi se fluorescencija BSA na 360 nm. Fenomen pomaka maksimuma emisije u lijevo prema manjoj valnoj duljini prisutan je u spektrima svih korištenih AgNP što je u skladu s ranije dobivenim rezultatima za interakciju NP s BSA. Taj pomak je zapravo posljedica činjenice da je SPR signal inherentno svojstvo AgNP (Mariam i dr., 2011; Jhonsi i dr., 2009).

Konstante vezanja proteina na AgNP izračunate su pomoću računalnog programa *SPECFIT* kako je opisano u Materijalima i metodama (poglavlje 3.4.2). Taj program metodom rastava singularnih vrijednosti (SVD, od eng. Singular Value Decomposition), a primjenom metode najmanjih kvadrata, predviđa logaritamsku krivulju čiji je primjer prikazan na Slici 41. To je zapravo titracijska krivulja dobivena titracijom 0,2 μM BSA s AgNP u koncentracijama od 2, 6, 10, 14, 20, 30, 40, 60, 80, 100, 140, 200, 250, 300, 400 i 500 μM.

Vrijednosti fluorescencije BSA dobivene na 380 nm nalaze se na ordinati, a na apscisi je gradijent koncentracija AgNP od niže prema višoj (Slika 41).

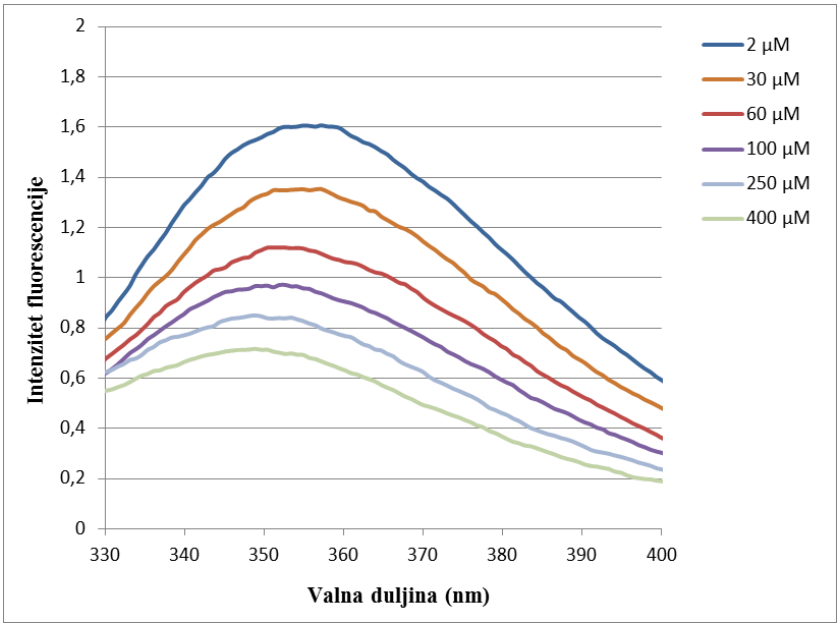

Slika 40. Promjene emisijskog fluorescencijskog spektra 0,2 µM BSA uz dodatak različitih koncentracija PLL10sphAgNP.

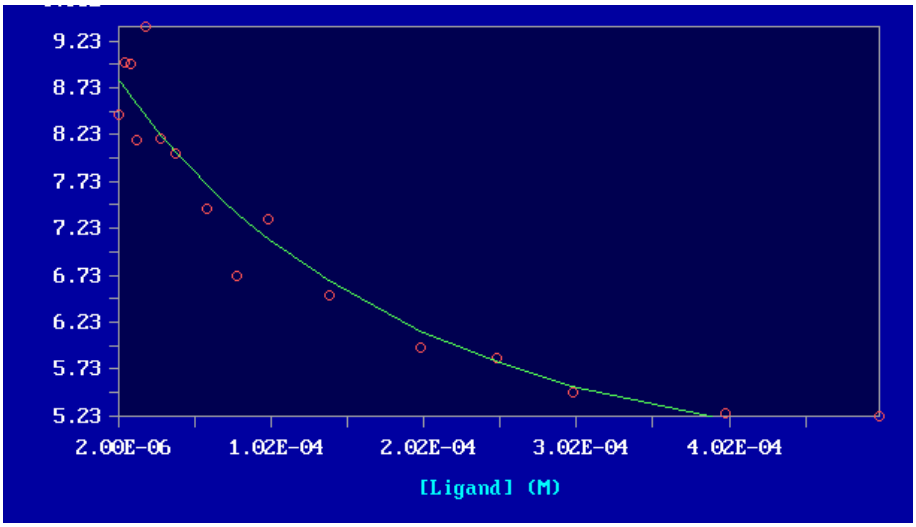

Slika 41. Primjer logaritamske krivulje titracije BSA s AgNP.

Dobivene krivulje ukazuju na stvaranje kompleksa u omjeru 1:1, bez indikacija stvaranja kompleksa većeg reda. Iz dobivene logaritamske krivulje izračunat je logaritam konstante vezanja (log K_a) (SPECFIT User Manual, 1993). Veće vrijednosti konstanti vezanja ukazuju na jače vezanje i veću stabilnost kompleksa.

Izračunate konstante vezanja (dane kao log K_a vrijednosti) između albumina i različitih AgNP u četiri različita medija (UW, FP, FO i FPNaCl), te konstante vezanja između AGP i AgNP u UW i FP navedene su u Tablici 20.

Tablica 20. Konstante vezanja BSA i različitih AgNP, te AGP i različitih AgNP. Rezultati su izraženi kao srednje log K_a vrijednosti najmanje 3 neovisna mjerenja uz navedene standardne devijacije.

AgNP	**log K_a**					
	BSA				AGP	
	UW	FO	FP	FPNaCl	UW	FP
AOT10sph	4,3 ± 0,10	3,9 ± 0,1	3,6 ± 0,06	3,3 ± 0,07	3,3 ± 0,10	2,8 ± 0,15
PVP10sph	3,7 ± 0,20	3,9 ± 0,00	3,6 ± 0,06	3,7 ± 0,07	3,8 ± 0,14	3,4 ± 0,07
TW10sph	3,2 ± 0,06	4,2 ± 0,07	3,8 ± 0,06	3,6 ± 0,14	3,7 ± 0,06	3,6 ± 0,06
Brij10sph	3,3 ± 0,06	3,5 ± 0,14	3,2 ± 0,06	3,6 ± 0,14	2,5 ± 0,14	3,0 ± 0,17
PLL10sph	3,2 ± 0,15	3,0 ± 0,32	3,9 ± 0,00	3,7 ± 0,06	3,5 ± 0,16	3,0 ± 0,21
CTA10sph	3,6 ± 0,06	3,7 ± 0,00	3,4 ± 0,10	3,3 ± 0,07	3,3 ± 0,00	3,2 ± 0,12
CIT10sph	3,4 ± 0,10	3,7 ± 0,07	3,7 ± 0,11	3,3 ± 0,07	3,1 ± 0,06	3,2 ± 0,15
BSA10sph	3,0 ± 0,06	3,3 ± 0,14	3,6 ± 0,06	3,3 ± 0,07	3,3 ± 0,10	3,0 ± 0,20
AOT50sph	3,2 ± 0,06	3,6 ± 0,07	3,5 ± 0,06	3,7 ± 0,07	2,9 ± 0,06	3,0 ± 0,06
CIT50sph	3,4 ± 0,15	3,7 ± 0,07	3,6 ± 0,17	3,6 ± 0,14	3,2 ± 0,00	3,2 ± 0,12
CTA50sph	2,8 ± 0,32	3,7 ± 0,14	3,7 ± 0,00	3,9 ± 0,21	2,9 ± 0,06	3,0 ± 0,06
PVP50sph	3,5 ± 0,06	3,5 ± 0,00	4,0 ± 0,06	3,5 ± 0,07	3,0 ± 0,15	3,1 ± 0,06
Brij50sph	3,0 ± 0,12	3,2 ± 0,07	2,9 ± 0,15	2,9 ± 0,00	3,4 ± 0,12	3,2 ± 0,00
TW50sph	3,1 ± 0,12	3,5 ± 0,07	3,5 ± 0,12	3,5 ± 0,07	2,6 ± 0,15	2,8 ± 0,06
PVP50tri	3,6 ± 0,06	3,5 ± 0,07	3,3 ± 0,06	3,3 ± 0,07	3,7 ± 0,06	3,6 ± 0,06
AOT50tri	3,6 ± 0,06	3,4 ± 0,1	3,8 ± 0,21	3,1 ± 0,2	2,5 ± 0,14	3,0 ± 0,17
PVP50cube	2,9 ± 0,2	3,2 ± 0,1	3,0 ± 0,1	2,9 ± 0,1	3,5 ± 0,16	3,0 ± 0,21

Već brzim pregledom uočljivo je da je varijacija izmjerenih log K_a vrijednosti za pojedini protein vrlo mala, te za BSA varira od 2,8 do 4,2, a za AGP od 2,4 do 3,8. Statističkom obradom podataka nije uočena značajna razlika u log K_a vrijednostima između AgNP s nominalnim promjerom oko 50 nm i AgNP s nominalnim promjerom oko 10 nm, iako je većina AgNP10sph imala neznatno veće log K_a vrijednosti od dobivenih za

AgNP50sph. To je vjerojatno posljedica veće dostupne površine za vezanje kod AgNP10sph. Što se tiče površinske strukture AgNP, AOT10sph pokazuju neznatno veći afinitet za BSA od drugih čestica, dok PVP50sph pokazuju neznatno manji afinitet za BSA od ostalih AgNP. Afinitet AgNP za AGP je nešto manji u odnosu na afinitet vezanja BSA, što može biti posljedica glikozilacije AGP. Od svih AgNP, samo Tween10sph pokazuju neznatno veći afinitet, a CTA10sph i PVP50cube neznatno manji afinitet za AGP u odnosu n BSA. Također nije dobivena statistički značajna korelacija između log K_a vrijednosti za BSA i za AGP, što ukazuje na različite mehanizme interakcija ova dva proteina s nanočesticama (poglavlje 7, Tablica 22,).

Uslijed nepostojanja statistički značajne povezanosti log K_a vrijednosti s pojedinačnim fizikalnim varijablama provedena je 2D grafička analiza njihove povezanosti (Slika 42). U tu svrhu, za AgNP izračunate su vrijednosti specifične površine (poglavlje 7, Tablica 24). 2D grafička analiza prikazana na Slici 42 stavlja u odnos specifičnu površinu AgNP, njihov ζ potencijal i log K_a vrijednost.

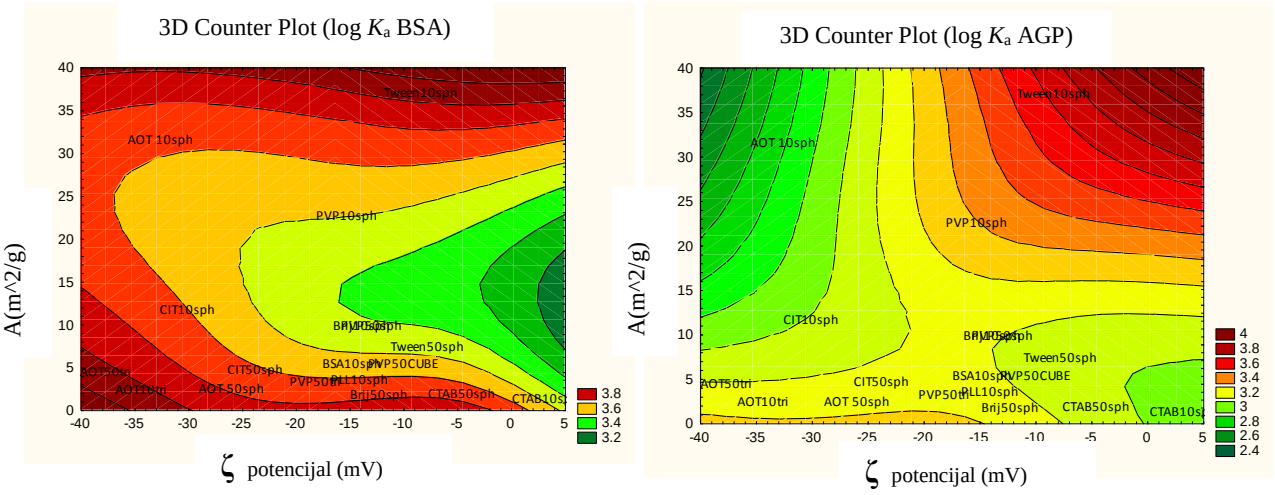

Slika 42. Grafička analiza povezanosti specifične površine i ζ potencijala različitih AgNP s log K_a vrijednostima za BSA i AGP.

Uočljivo je da očekivan gotovo sve AgNP10 imaju relativno veliku specifičnu površinu dok suprotno vrijedi za AgNP50. Također je vidljivo da čestice s negativno nabijenim stabilizatorima imaju nešto veći negativan ζ potencijal, dok čestice s neutralnim ili pozitivnim stabilizatorima imaju mali negativan ζ potencijal. AGP je pri pH 7,4 jako negativno nabijen pa se snažnije veže na pozitivno nabijene i neutralne čestice manjeg promjera koje imaju veću specifičnu površinu dostupnu za vezanje. BSA, koji je pri pH 7,4 slabo negativno nabijen, se

podjednako veže i na AgNP s negativnim, i na AgNP s pozitivnim i s neutralnim stabilizatorima pri čemu podjednaku ulogu imaju ζ potencijal i specifična površina AgNP. Ekstremne vrijednosti ζ potencijala te mali d_H odnosno velika specifična površina AgNP povećavaju i log K_a vrijednosti za BSA. Neselektivnost vezanja BSA u odnosu na ζ potencijal i specifičnu površinu AgNP proizlazi iz činjenice da je BSA istovremeno polianion i polikation koji lako može prilagoditi svoju tercijarnu strukturu tako da optimizira interakcije bočnih aminokiselinskih lanaca koje su nositelji naboja. Stoga se u slučaju BSA pri vezanju na AgNP očekuju veće i raznolikije promjene sekundarne/tercijarne strukture u odnosu na AGP.

4.3.2. Konformacijske promjene albumina i α-1-kiselog glikoproteina uslijed vezanja na površinu različitih srebrnih nanočestica

Poznato je da se struktura proteina, a posebno konformacija, može promijeniti prilikom vezanja na AgNP. Spektroskopijom cirkularnog dikroizma (CD) ispitane su promjene u tercijarnoj strukturi BSA i AGP uslijed njihovog vezanja na različite AgNP kako je opisano u Materijalima i metodama (Poglavlje 3.4.3.). BSA je neglikozilirani protein s visokim sadržajem α-heliksa i niskim sadržajem β-ploča u svojoj tercijarnoj strukturi, dok je AGP visoko glikoziliran protein sa 45% šećera u ukupnoj strukturi te mnogo većim sadržajem β-ploča u svojoj tercijarnoj strukturi. Slika 43 prikazuje prosječne CD spektar BSA i α1aGP u FP. CD spektri snimljeni su u rasponu od 190 do 250 nm.

Spektar BSA je snimljen pri koncentraciji od 2 μM (5 ponavljanja) s karakterističnim signalom na 208 nm koji ukazuje na visoki sadržaj α-heliksa u strukturi proteina. Spektar AGP, snimljen kod jednake koncentracije od 2 μM (7 ponavljanja), pokazuje minimum na 215 nm koji je karakterističan za strukturu proteina s većim sadržajem β-ploča. Primjenom Beta Structure Selection (BeStSel) metode, iz CD spektra kvantitatiziran je omjer osam strukturalnih elemenata u proteinu (α heliks 1, α heliks 2, anti 1 ploče, anti 2 ploče, anti 3 ploče, zavojnice i ostali).

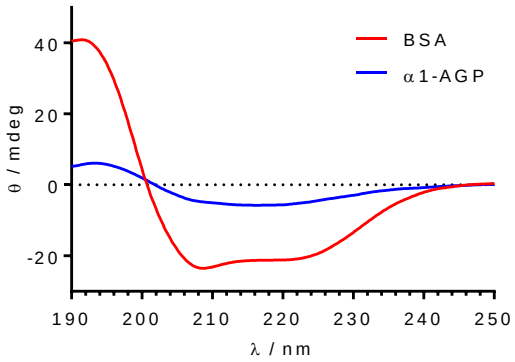

Slika 43. CD spektri čistih proteina BSA i AGP u FP mediju.

Zbog programskog modela kojim su CD spektri analizirani, frakcijski sadržaj sastava proteinske sekundarne strukture je uvijek 100%, pa smanjenje sadržaja jedne vrste sekundarne strukture povećava sadržaj ostalih vrsta. Usporedbom zastupljenosti strukturnih elemenata čistog proteina koji je snimljen kao kontrolni uzorak i proteina u interakciji s AgNP dobiven je uvid u utjecaj površinske strukture sintetiziranih AgNP na sekundarnu strukturu BSA i AGP. Koncentracija testiranih AgNP povećavana je od 10 μM do 500 μM pri čemu nije uočena značajnija promjene povećavanjem koncentracije AgNP iznad 100 μM. Tipične promjene u CD spektru proteina uslijed interakcije s AgNP prikazuje Slika 44.

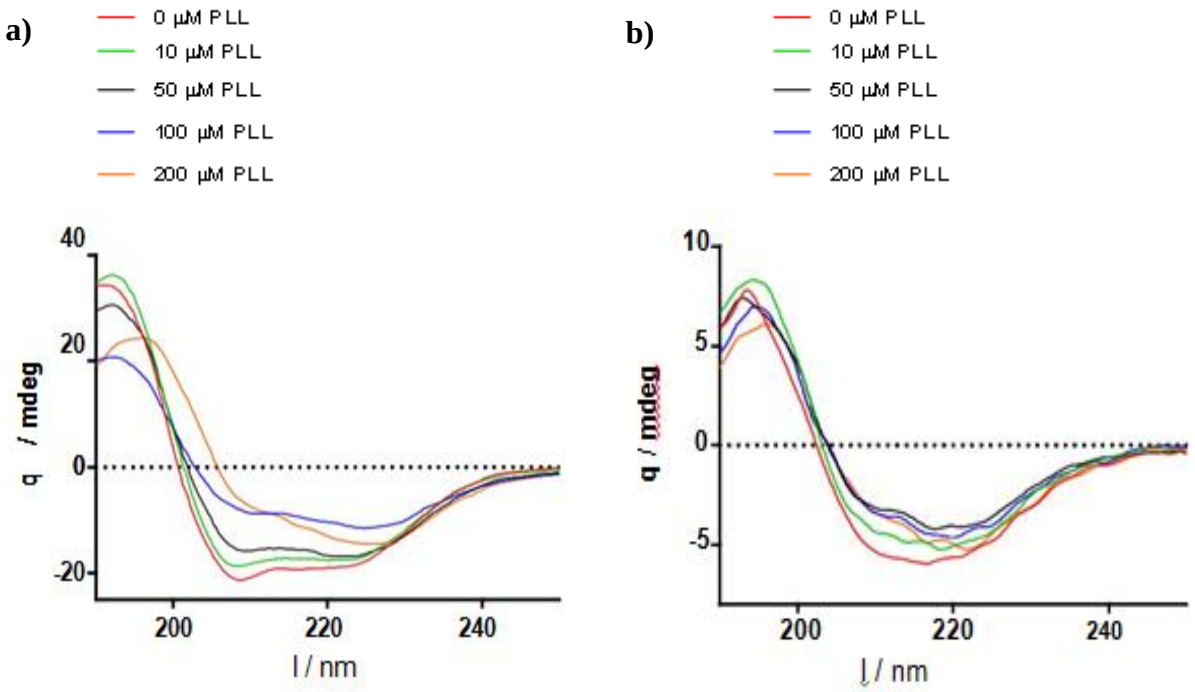

Slika 44. Promjene u CD spektrima BSA (a) i AGP (b) uslijed njihove interakcije s PLL10sphAgNP.

Rezultati strukturnih promjena BSA i AGP uslijed njihove interakcije s različitim AgNP prikazani su u Slikama 45-48. Pošto je u fiziološkim uvjetima serumska koncentracija BSA 600-700 μM i pošto je promjena sekundarne/tercijarne strukture slabo ovisna o koncentraciji BSA u razmatranje je uzet samo slučaj u kojem je koncentracija BSA 100 μM. Na Slikama 54 – 61, poglavlje 7 prikazane su promjene u strukturi proteina BSA i AGP nakon interakcije s AgNP pri koncentracijama od 10 μM i 50 μM. Povećanjem veličine AgNP evidentna je promjena u strukturi proteina. Veće AgNP imaju manji učinak na strukturne promjene BSA. Interakcija AGP s AgNP10 i AgNP50 vrstama pokazuje da najmanji utjecaj na strukturu AGP ima PVP10sph, CIT10sph i CTA10sph (Slike 47 i 48). I kod AGP su manje konformacijske promjene izazvale veće AgNP pri čemu je najmanja promjena uzrokovana interakcijom AGP s Tween50sph i Brij50sph.

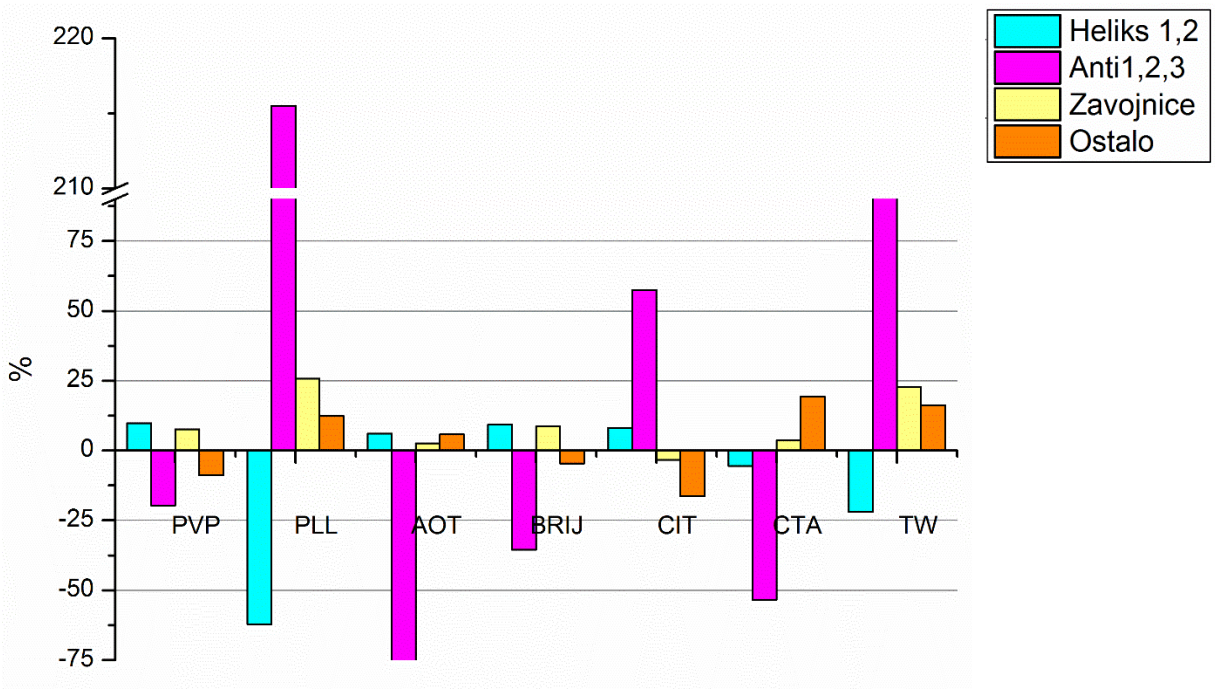

Slika 45. Promjena strukuture BSA u interakciji s AgNP10 u koncetraciji od 100 μM.

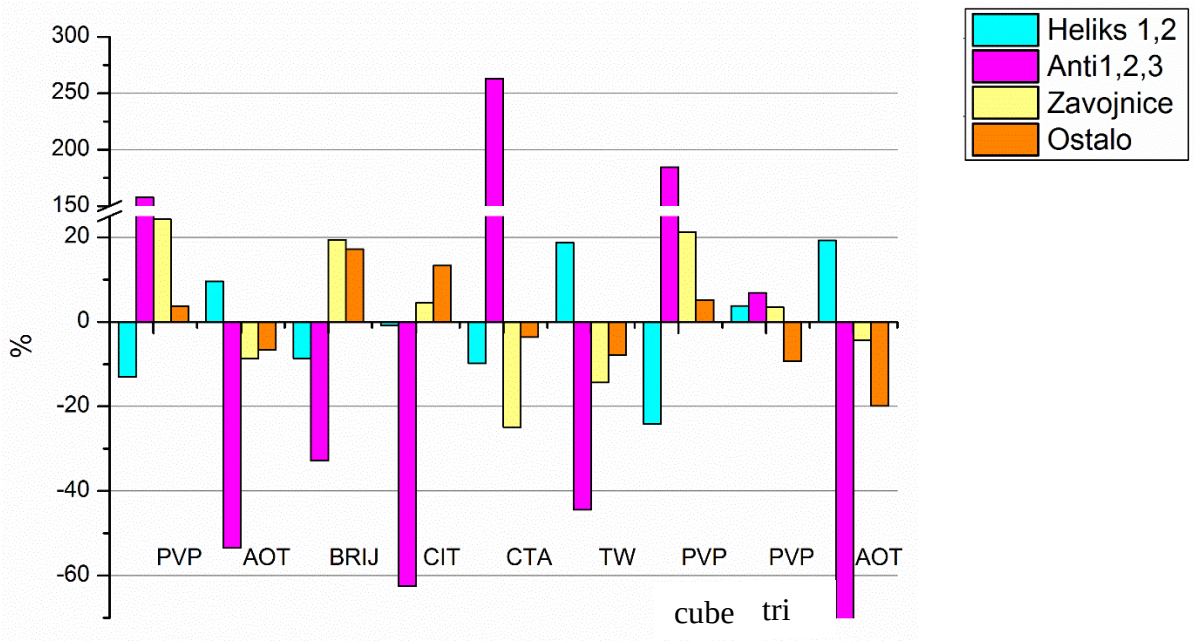

Slika 46. Promjena strukuture BSA u interakciji s AgNP50 u koncetraciji od 100 μM.

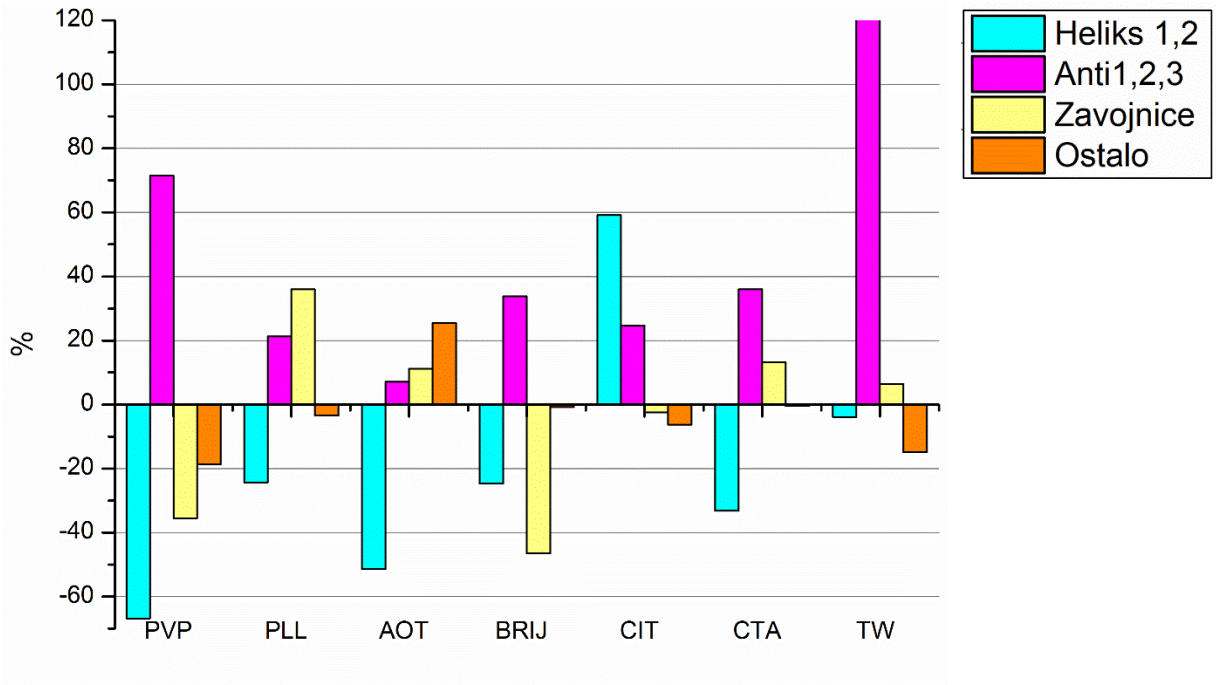

Slika 47. Promjena strukuture AGP u interakciji s AgNP10 u koncetraciji od 100 μM.

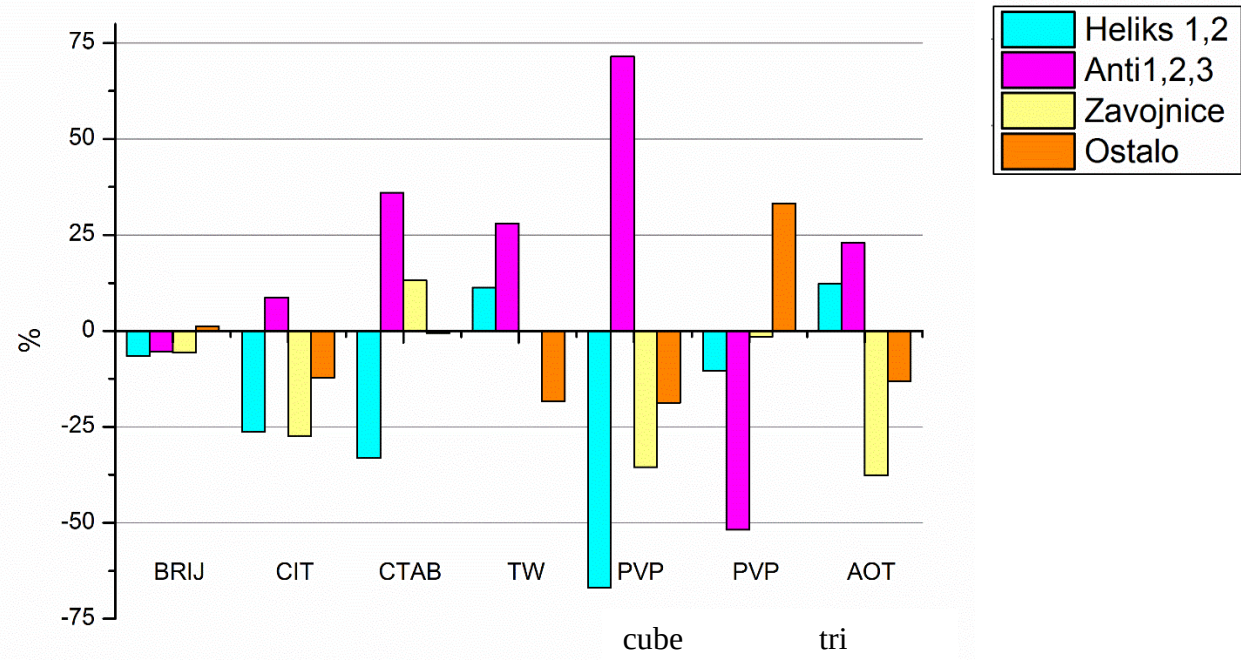

Slika 48. Promjena strukuture AGP u interakciji s AgNP50 u koncetraciji od 100 μM.

Najveće promjene parametara sekundarne/tercijarne strukture BSA nakon njegovog vezanja na AgNP se odnose na promjene udjela β nabranih ploča i α heliksa pri čemu porast udjela β nabranih ploča najčešće prati pad udjela α heliksa i obratno. β nabrane ploče kao i α heliksi su strukture koje nastaju stvaranjem vodikovih veza među atomima u peptidnim vezama: broj vodikovih veza promjenom udjela jednih i drugih struktura se neznatno mijenja no, vodikove veze djeluju na promijenjenim udaljenostima unutar primarne aminosekvence što određuje vrsta/mehanizam interakcije BSA s pojedinom nanočesticom. AgNP s pozitivno nabijenim stabilizatorom poput PLL10, CTA50 i PVP50sph/cube najčešće su utjecale na porast udjela β nabranih ploča jer su povećale udaljenost peptidnih veza unutar primarne aminosekvence između kojih nastaju vodikove veze, dok AgNP s negativno nabijenim stabilizatorom poput AOT umjereno umanjuju udio β nabranih ploča te smanjuju udaljenost peptidnih veza unutar primarne aminosekvence između kojih nastaju vodikove veze. U slučaju AgNP s nenabijenim stabilizatorima promjene sekundarne i tercijarne strukture su zanemarive. Najvjerojatnije BSA vezanjem na AgNP mijenja sastav ovojnice koja okružuje nanočestice tj. uklanja negativne protu-ione koji daju negativni ζ potencijal. Interakcija s molekulama stabilizatora može objasniti različite promjene sekundarne/tercijarne strukture BSA u ovisnosti o vrsti stabilizatora na površini AgNP na koju se BSA veže (Rocha i dr., 2008). Dok α heliksi diktiraju cilindričku distribuciju bočnih lanaca aminokiselina, β nabrane ploče određuju njihovu trans-plošnu raspodjelu: kako su kod BSA bočni lanci pri fiziološkom pH uglavnom negativno nabijeni to bi moglo objasniti nestajanje α heliksa i nastajanje β

nabranih ploča vezanjem BSA na nanočestice s lužnatim stabilizatorom.Uslijed velike očekivane raznolikosti interakcija BSA s AgNP, što je utvrđeno u prethodnim poglavljima, za pretpostaviti je da će se teško moći povezati fizikalno-kemijske varijable s promjenama tercijarne strukture BSA izazvanim njegovim vezanjem na nanočestice. Iz tog je razloga analiza provedena primjenom 2D prikaza koji povećava izglede za pronalaženje složenijih oblika povezanosti promjena sekundarne/tercijarne strukture s fizikalno-kemijskim varijablama (Slika 48). U slučaju BSA vezu između promjene sekundarne/tercijarne strukture i fizikalno-kemijskih svojstava moguće je uočiti samo za slučaj promjene udjela α-heliksa u odnosu na d_H i log K_a vrijednosti. Za AgNP za koje su svojstvene velike d_H i log K_a vrijednosti, te za AgNP s malim d_H i log K_a vrijednostima, vezanjem BSA udio α-heliksa se u tercijarnoj strukturi povećava. Drugim riječima, slabo vezanje BSA na male AgNP, te snažno vezanje BSA na velike AgNP dovodi do porasta udjela α-heliksa. Ovisno o metodi mjerenja log K_a, nije isključeno da je u slučaju velikih AgNP koje snažno vežu BSA došlo do stvaranja višeslojne proteinske korone. Nešto bolja veza između mjera tercijarne strukture i fizikalno-kemijskih svojstava uočena je u slučaju 10 uM koncentracije BSA no ta se koncentracija teško može povezati s fiziološkim uvjetima pa su odgovarajući prikazi ispušteni.

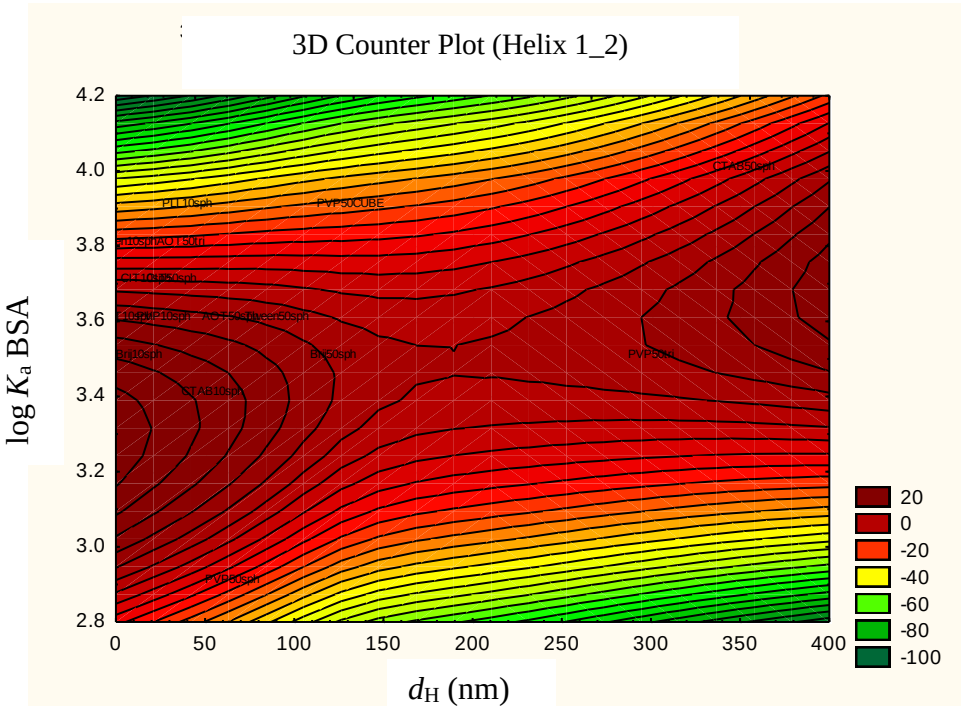

Slika 49. Povezanost promjene sekundarne/tercijarne strukture BSA s fizikalno-kemijskim svojstvima AgNP pri koncentraciji od 100 μM u FP mediju.

Nešto veći broj statistički značajnih korelacija između promjena sekundarne/tercijerne strukture AGP i fizikalno-kemijskih svojstava AgNP ukazuje na veću uniformnost interakcija

AGP s AgNP u odnosu na interakcije BSA. Osim d_H, sva ostala fizikalno-kemijska svojstva su bar u nekim slučajevima povezana s parametrima promjene sekundarne/tercijarne strukture AGP. AGP se u serumu pri fiziološkim stanjima nalazi u oko 10 puta nižim koncentracijama nego BSA, ali se njegova koncentracija drastično mijenja u svim drugim stanjima. Detaljnom analizom rezultata vidljivo je da log K_a i specifična površina koreliraju s promjenom udjela β nabranih ploča nakon vezanja AGP na AgNP što ukazuje na moguću povezanost mehanizama vezanja AGP i mehanizama nastajanja β nabranih ploča te na relativno malu raznoliku navedenih mehanizama. Moguće je da je specifična površina važan čimbenik u vezanju AGP na AgNP i mehanizamu nastanka β nabranih ploča pri čemu zeta potencijal AgNP ima manju ulogu nego li što je to slučaj kod vezanja BSA. Promjene sekundarne/tercijarne strukture AGP nakon njegovog vezanja su puno manje izražene u odnosu na promjene sekundarne/tercijarne strukture BSA. Najveće promjene parametara sekundarne/tercijarne strukture AGP nakon njegovog vezanja, isto kao i kod BSA, se odnose na promjene udjela β nabranih ploča i α heliksa pri čemu porast udjela β nabranih ploča najčešće prati pad udjela α heliksa i obratno. Zbog malih razlika u promjenama sekundarne/tercijarne strukture AGP u ovom se slučaju teško može poopćiti utjecaj vrste stabilizatora na te promjene. Hipotezu da je specifična površina važan čimbenik u vezanju i mehanizamu nastanka β nabranih ploča kod AGP podržava i činjenica da primjena Tween detergenta dovodi do najvećeg povećanja udjela β nabranih ploča. Jednostavna veza poput smanjenja napetosti površine koje je izraženije kod AgNP s velikom spcifičnom površinom koje sadrže surfaktante na svojoj površini može objasniti takvo ponašanje. Čini se da β nabrane ploče bolje od α heliksa prekrivaju slobodnu površinu, pogotovo ako je ona nenabijena. Ipak, za očekivati je bilo da bi AgNP koje u svom sastavu sadrže lužnate stabilizatore više utjecale na nastajanje β nabranih ploča kao i na snažnije vezanje negativno nabijenog AGP.

S obzirom na veću uniformnost interakcija AGP s AgNP u ovom je slučaju bilo moguće doći do prikladnih 2D prikaza povezanosti promjene sekundarne/tercijarne strukture AGP prilikom vezanja s fizikalno kemijskim varijablama AgNP. Za 2D prikaze su korištene sva četiri dostupna fizikalno-kemijska svojstva (zeta potencijal, konstanta vezanja, hidrodinamički promjer i specifična površina) a izabrane su one koje daju najjasniji uvid u povezanost sekundarne/tercijarne strukture s odabranim varijablama (Slika 50). Izmjereni promjer AgNP i njihova specifična površina su međuovisni ali im međuovisnost nije linearna što se vidi iz činjenice da čak niti ne koreliraju. Iako su i specifična površina i hidrodinamički promjer AgNP povezani, povezanost parametara promjene sekundarne/tercijarne strukture i tih svojstava za AGP u nekim slučajevima daje jasniju sliku ako se upotrijebi d_H, a u drugima

ako se upotrijebi specifična površina. AgNP kojima su svojstvene visoke vrijednosti specifične površine (mali d_H), velika log K_a vrijednosti za AGP i izražen negativni zeta potecijal, povezane su s visokim udjelom β nabranih ploča i niskim udjelom α heliksa (Slika 50). Ovakvo je ponašanje svojstveno i za vezanje BSA na male AgNP. Čini se da male AgNP snažno vežu različite proteine iz otopine pri čemu ti proteini oblažu nanočestice u formi β nabranih ploča te ih stabiliziraju. AgNP kojima je svojstven izraženi negativni ζ potencijal, niže vrijednosti log K_a za AGP i mala specifična velik (visok d_H), pokazuju veći udio α heliksa i manji udio β nabranih ploča. Zbog velikog promjera vjerojatnost aglomeracije je, u ovom slučaju, relativno velika. Udio zavoja kao i udio ostalih sekundarnih/tercijarnih struktura se relativno malo mijenja prilikom vezanja na nanočestice.

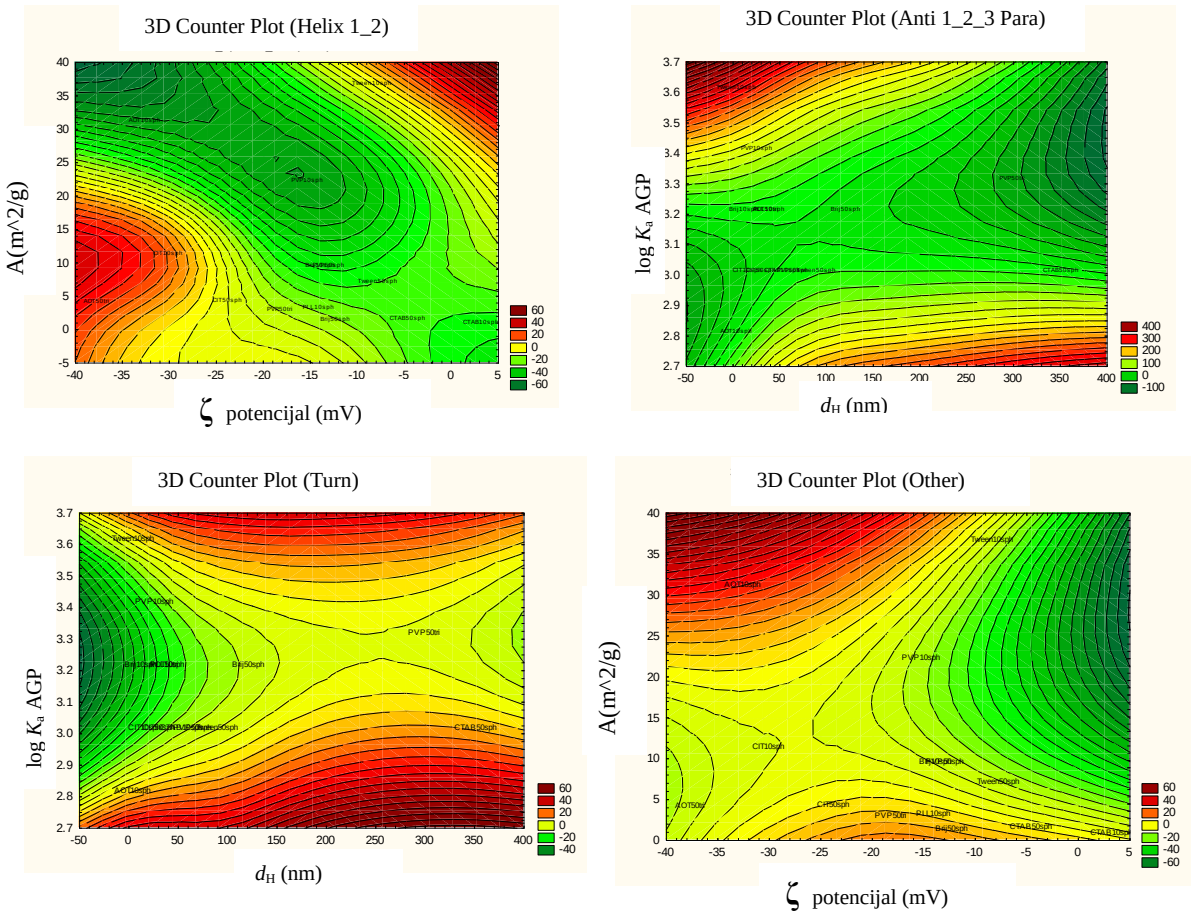

Slika 50. Povezanost promjena sekundarne/tercijarne strukture AGP s fizikalno-kemijskim svojstvima AgNP pri koncentraciji od 100 μM u FP mediju.

Sposobnost NP da izazovu značajne promjene sekundarne/tercijarne strukture pokazane i za AGP i za BSA slučaju bi bilo razumno ispitati i kod ostalih klinički značajnih strukturnih proteina poput različitih amiloida ili Tau proteina.

5. ZAKLJUČAK

Na modelu citratom stabiliziranih AgNP prosječne veličine oko 50 nm (CIT50sph) definirani su protokoli za sintezu, karakterizaciju i određivanje stabilnosti AgNP u različitim medijima. U svrhu procjene stabilnost CIT50sph ispitan je utjecaj pH medija, elektrolita, ionske jakosti i prisustva površinski aktivnih tvari na stabilnost AgNP. Značajno povećanje ili smanjenje pH vrijednosti medija smanjilo je apsolutnu vrijednost ζ potencijala AgNP. Budući da se AgNP presvučeni s citratom elektrostatički stabiliziraju negativno nabijenim citratnim ionima, povećanje pH disperzijskog medija dovodi do povećanja negativnog zeta potencijala na površini AgNP i povećavanja jačine odbojnih sila čime je povećana stabilnost CIT50sph. Praćenjem otapanja CIT50sph u medijima različitih pH vrijednosti evidentno je umjereno otapanje AgNP pri pH 9, dok je pri pH 3 zabilježeno značajno povećanje brzine oslobađanja Ag^+ iona s površine CIT50sph. Učinak ionske jakosti medija značajno utječe na stabilnost AgNP. Suspenzija AgNP je destabilizirana povećanjem ionske jakosti, kada kompleksiranje kationa s citratnim karboksilnim skupinama na površini AgNP dovodi do aglomeracije čestica. Nadalje, AgNP se otapa u mnogo većoj mjeri u svim otopinama elektrolita nego u UW. Rezultati jasno pokazuju da prisutnost površinski aktivnih tvari u sustavima gdje se AgNP mogu osloboditi sprječava njihovu aglomeraciju, sedimentaciju i otapanje pri neutralnom pH i niskoj ionskoj jakosti. To naglašava veći potencijal oslobađanja AgNP-a iz bilo kojeg sustava u kojem se koriste surfaktanti. Međutim, sustavi okoliša su uglavnom složeni i obično karakterizirani visokom ionskom jakosti. Važno je naglasiti da interakcija AgNP sa surfaktantom prisutnim u otpadnim vodama potencijalno može povećati otapanje i oslobađanje AgNP čime se povećava izloženost biljnih, životinjskih i ljudskih organizama učincima AgNP vrsta.

Primjenom različitih sintetskih postupaka sintetizirano je šesnaest vrsta različitih AgNP sferičnog, trokutastog i kubičnog oblika u veličinama od ~10 nm i ~50 nm pri čemu je korišteno osam različitih, pozitivnih, negativnih i neutralnih stabilizatora. Primjena različitih površinskih stabilizatora tijekom sinteze nanočestica srebra utjecala je na stabilnost AgNP što je dokazano DLS, TEM, UV-VIS, fluorescencijom i CD mjerenima u UW, FO, FP, FPNaCl. Povećanjem složenosti medija od UW do FPNaCl evidentan je porast promjera nanočestica i zeta potencijala što ukazuje na nestabilnost AgNP u biološkim uvjetima. Hidrodinamički promjer (d_H) dominantno zastupljenih nanočestica najmanji je u UW, dok promjenom medija prema FPNaCl dolazi do značajnog povećanja pri čemu postoji poveznica između vrste površinskog stabilizatora i nominalne veličine sintetizirane čestice u odnosu na stabilnost otopine. Naime, najveće promjene hidrodinamičkog promjera zabilježene su kod CTA10/50sph a najmanje kod TW10sph i Brij10sph pri čemu je za AgNP50 evidentno veće

povećanje promjera. Vidljivo je da u CTA50sph, Brij50sph i AOT10tri promjer raste značajno iznad 100 nm te se više i ne može govoriti o nanočesticama. Navedeno ukazuje na mogućnost da će pripremljene nanočestice u fiziološkim uvjetima imati relativno velik promjer, najvjerojatnije više od 100 nm u slučaju primjene nabijenih površinskih stabilizatora i pripreme čestica s nominalnim promjerom od 50 nm, a manje od 100 nm u slučaju primjene nenabijenih površinskih stabilizatora nominalnim promjerom od 10 nm. Nadalje, osim povećanja hidrodinamičkog promjera s porastom ionske jakosti i primjenom pufera, dolazi do smanjenja vriejdnosti zeta potencijala nanočestica prema nuli što ukazuje na prelazak srebra iz nanosrebra u ionsko srebro. Sve navedeno ukazuje na moguću nestabilnost srebrnih nanočestica u biološkim tekućinama. Rezultati upućuju da su kombinacija naboja i jačine adsorpcijskog učinka stabilizatora zajedno s njihovom molekularnom strukturom važni čimbenici koji utječu na stabilnost AgNP u elektrolitskim otopinama. Važno je istaknuti da dodatak BSA u istraživanim medijima dovodi do stabilizacije AgNP (Tablica 21) neovisno o kemijskom sastavu, strukturi i sastavu površine te zeta potencijalu AgNP.

Tablica 21. Utjecaj različitih površinskih stabilizatora na stabilnost AgNP.

Stabilizator	**FPNaCl vs. UW**	**FPNaCl +BSA vs. UW**
CIT	Stabilna diserzija; $\|\zeta\|$ smanjen Nema morfoloških promjena	Stabilna disperzija; $\|\zeta\|$ smanjen; Lokalizirane AgNP uz BSA
AOT	Izražena alomeracija; $\|\zeta\|$ smanjen Morfološke promjene	Stabilna disperzija; $\|\zeta\|$ smanjen Lokalizirane AgNP uz BSA
CTA	Djelomična stabilizacija; $\|\zeta\|$ smanjen, promjena potencijala Morfološke promjene	Stabilna disperzija; $\|\zeta\|$ smanjen Lokalizirane AgNP uz BSA
Brij	Izražena alomeracija; $\|\zeta\|$ povećan Morfološke promjene	Stabilna disperzija; $\|\zeta\|$ smanjen AgNP dispergirane po TEM mrežici
TW	Parcijalna stabilizacija; $\|\zeta\|$ povećan; Morfološke promjene	Stabilna disperzija; $\|\zeta\|$ smanjen Lokalizirane AgNP uz BSA
PVP	Stabilna disperzija; $\|\zeta\|$ smanjen Nema morfoloških promjena	Stabilna disperzija; $\|\zeta\|$ smanjen Lokalizirane AgNP uz BSA
PLL	Izražena aglomeracija $\|\zeta\|$ smanjen, promjena potencijala Morfološke promjene	Stabilna disperzija; $\|\zeta\|$ povećan Lokalizirane AgNP uz BSA
BSA	Stabilna disperzija; $\|\zeta\|$ povećan Nema morfoloških promjena	Stabilna disperzija; $\|\zeta\|$ smanjen AgNP dispergirane po TEM mrežici

Veličina čestica ima veliku ulogu što je potvrđeno evaluacijom antibakterijskog djelovanja AgNP. Naime, AgNP10sph bile su toksičnije protiv *S. aureus* i *E. coli* u odnosu na AgNP50sph, neovisno o tipu površinskog stabilizatora. Međutim, veća antibakterijska

učinkovitosti AgNP10sph, odgovara većem postotku slobodnih Ag^+ iona u odnosu na AgNP50sph što znači da najveću ulogu u toksičnosti AgNP imaju bioraspoloživi Ag^+ ioni. Osim navedenog, važan faktor za sintezu antibakterijski učinkovitih AgNP je njihov zeta potencijal i topljivost čija se modulacije postiže odabirom odgovarajućeg površinskog stabilizatora. U danim eksperimentalnim uvjetima, uloga površinskog stabilizatora u modulaciji oslobađanja Ag^+ iona bila je važnija od učinaka usmjeravanja interakcija AgNP-bakterija zeta potencijal AgNP-a. Ispitivane AgNP su učinkovita antimikrobna sredstva, pri čemu su mehanizmi toksičnosti temeljeni na njihovoj topivosti, zeta potencijalu i veličini.
Konstante vezanja proteina na AgNP su reda veličine log K_a od 2,6 do 4,2 pri čemu ne ovise o vrsti medija te nije uočena značajna razlika između različitih AgNP. Vezanje AgNP i AGP je po jačini slično onome između AGP i lijekova poput primjerice indometacina, irbesatrana, haloperidola, estrona, epirubicina (Israili i Dayton; 2001), a između AgNP i BSA po jačini onome između BSA i flavonoida poput primjerice diosmetina, flavona, tamariksetina (Rimac, 2017).

Obzirom da AgNP10 imaju veću specifičnu površinu u odnosu na AgNP50, neznatno snažnije se vežu za protein. Nadalje, čestice s negativno nabijenim stabilizatorima imaju veći negativan ζ potencijal, pa će se slabije vezati na AGP koji je pri pH 7,4 jako negativno nabijen. BSA, koji je pri pH 7,4 slabo negativno nabijen, a istovremeno je i polianion i polikation koji lako može prilagoditi svoju tercijarnu strukturu s ciljem optimizacije interakcijskih uvjeta, AgNP se podjednako veže na BSA neovisno o površinskom stabilizatoru. S obzirom na svojstvo prilagodbe proteinske strukutre, za BSA su uočene veće promjene sekundarne/tercijarne strukture u odnosu na AGP. Prilikom interakcije AgNP s proteinima važno je osigurati nepromjenjenu funkciju proteina. AgNP koje pokazuju najniži učinak na protein u obliku promjena u strukturiranim domenama definiraju se kao biokompatibilni. AgNP koji pokazuju jači učinak na strukturne domene proteina treba dodatno ispitati kako bi se definirala specifičnost i selektivnost nastale promjene s ciljem procjene sposobnosti za buduću terapeutsku upotrebu.

6. LITERATURA

1. Abou-Zeid, O.K., Al-Shihi, O.I.K., (2008). Characterization of subdomain IIA binding site of human serum albumin in its native, unfolded, and refolded states using small molecular probes. *Journal of the American Chemical Society* 130, 10793-10801.
2. Abramson, F.P., Lutz, M.P., (1986). The kinetics of induction by rifampin of alpha 1-acid glycoprotein and antipyrine clearance in the dog. *Drug Metab Dispos* 14, 46-51.
3. Abramson, FP. (1988). Dose-response behavior of the induction of alpha 1-acid glycoprotein by phenobarbital in the dog. *Drug Metab Dispos* 16, 546-550.
4. Abriata, L.A., (2011). A simple spreadsheet program to simulate and analyze the far-UV Circular Dichroism spectra of Proteins. *J Chem Ed* 88, 1268-1273.
5. Aggarwal, P., Hall, J.B., McLeland, C.B., Dobrovolskaia, M.A., McNeil, S.E., (2009). Nanoparticle interaction with plasma proteins as it relates to particle biodistribution, biocompatibility and therapeutic efficacy. *Adv Drug Deliv Rev* 61, 428–437.
6. Aguilar, Z., (2012). Nanomaterials for medical applications. Elsevier Inc. Oxford, UK.
7. Agnihotria, S., Mukherjiabc, S., Mukherji, S., (2014). Size-controlled silver nanoparticles synthesized over the range 5–100 nm using the same protocol and their antibacterial efficacy. *RSC Adv* 4, 3974-3983.
8. Ahamed, M., Karns, M., Goodson, M., Rowe, J., Hussain, S.M., Schlager, J.J., Hong, Y., (2008). DNA damage response to different surface chemistry of silver nanoparticles in mammalian cells. *Toxicol Appl Pharmacol* 233, 404–410.
9. Allen, J.J., Barron, A.R., Bott, S., Bovet, C., Boyd, J., Bratt, A., Chiang, P.T., Cisneros, B., Conn, C., (2012). Introduction to Atomic Absorption Spectroscopy. U: *Physical Methods in Chemistry and Nano Science*. Rice University, Houston, Texas.
10. Alexander, J.W. (2009). History of the medical use of silver. *Surg. Infect.* 10, 289-92.
11. Allen, P.C., Hill, E.A., Stokes, A.M., (1977). Alpha1-acid glycoprotein in plasma proteins: analytical and preparative techniques. *Blackwell Scientific*; Oxford, UK.
12. Alvarez-Puebla, R. A., Arceo, E., Goulet, P. J. G., Garrido J. J., Aroca, R. F., (2005). Role of Nanoparticle Surface Charge in Surface-Enhanced Raman Scattering. *The Journal of Physical Chemistry B* 109, 3787–3792.
13. Arora, S., Jain, J. M. Rajwade, Paknikar, K.M., (2009). Interactions of silver nanoparticles with primary mouse fibroblasts and liver cells. *Toxicol Appl Pharmacol*. 236, 310–318.
14. Asharani, P.V., Hande, M.P. (2009). Valiyaveettil, S. Anti-proliferative activity of silver nanoparticles. *BMC Cell Biology* 17, 10-65.

15. Asharani, P.V., Kah, L., Mun, G., Hande, M.P., Valiyaveettil, S., (2009). Cytotoxicity and genotoxicity of silver nanoparticles in human cells. *ACS Nano* 3, 279–290.
16. Atkins, P., Julio de Paula., (2009). *Physical Chemistry*. Eighth Edition. Published in Great Britain by Oxford University Press.
17. Aubert, J.P., Loucheux-Lefebvre, M.H., (1976). Conformational study of alpha1-acid glycoprotein. *Arch Biochem Biophys* 175, 400-409
18. Auffan, M., Rose J, Wiesner MR, Bottero J-Y., (2009). Chemical stability of metallic nanoparticles: A parameter controlling their potential cellular toxicity in vitro. *Environmental Pollution* 157, 1127–1133.
19. Bannunah, A.M., Vllasaliu, D., Lord, L., Stolnik, S., (2014). Mechanisms of Nanoparticle Internalization and Transport Across an Intestinal Epithelial Cell Model: Effect of Size and Surface Charge. *Mol. Pharmaceutics* 11, 4363–4373.
20. Barbero, F., Russo. L., Vitali, M., Paella, J., Salvo, I., Borrajo, M.L., Busquets-Fité M., Grandori R., Bastús N.G., Casals E., Puntes V., (2017). Formation of the Protein Corona: The Interface between Nanoparticles and the Immune System. *Seminars in Immunology* 34, 52-60.
21. Baroli, B., Ennas M.G., Loffredo F., Isola M., Pinna R., López-Quintela M.A., (2007). Penetration of metallic nanoparticles in human full-thickness skin. *Journal of Investigative Dermatology* 127, 1701-1712.
22. Beaty, R.D., Kerber, J.D., (2002). Concepts, Instrumentation and Techniques in Atomic Absorption Spectrophotometry. The Perkin-Elmer Corporation Norwalk, CT, U.S.A.
23. Beer, C., Foldbjerg, R. Hayashi, Y., Sutherland, D.S., Autrup, H., (2012). Toxicity of silver nanoparticles - nanoparticle or silver ion? *Toxicol Lett* 208, 286–292.
24. Benn, T. M. and Westerhoff, P. (2008). Nanoparticle silver released into water from commercially available sock fabrics. *Environmental Science & Technology* 42, 4133–4139.
25. Bennemann, K.H., Koutecky, J., (1984). Small Particles and Inorganic Clusters, North Holland, Amsterdam. Small Particles and Inorganic Clusters, Freie Universität Berlin, Germany.
26. Bhol, K.C., Schechter, P.J., (2005). Topical nanocrystalline silver cream suppresses inflammatory cytokines and induces apoptosis of inflammatory cells in a murine model of allergic contact dermatitis. *Br. J. Dermatol* 152, 1235-1242
27. Bhol, K.C., Schechter, P.J., (2007). Effects of nanocrystalline silver (NPI 32101) in a rat model of ulcerative colitis. *Digestive Dis. Sci*. 52, 2732-2742.

28. Bilberg, K.,. Hovgaard, M.B., Besenbacher, F., Baatrup, E., (2012). In vivo toxicity of silver nanoparticles and silver ions in zebrafish (Danio rerio). *J Toxicol* 2012, 293784–293793.
29. Biou, D., Chanton, P., Konan D., Seta, N., N'Guyen, H., Feger, J., Durand, G., (1989). Microheterogeneity of the carbohydrate moiety of human alpha 1-acid glycoprotein in two benign liver diseases: alcoholic cirrhosis and acute hepatitis. *Clin Chim Acta* 186, 59-66.
30. Biou, D., Bauvy, C., N'Guyen, H., Codogno, P., Durand, G., Aubery, M., (1991). Alterations of the glycan moiety of human alpha 1-acid glycoprotein in late-term pregnancy. *Clin Chim Acta* 204, 1-12.
31. Bondarenko, O., Juganson, K., Ivask, A., Kasemets, K., Mortimer, M., Kahru, A. (2013). Toxicity of Ag, CuO i ZnO nanoparticles to selected environmentally relevant test organisms i mammalian cells in vitro: a critical review, Arch. Toxicol. 87, 1181–1200.
32. Borm, P. J., Robbins, D., Haubold, S., Kuhlbusch, T., Fissan, H., Donaldson, K., Schins, R., Stone, V., Kreyling, W., Lademann, J., Krutmann, J., Warheit, D., Oberdorster, E., (2006). The potential risks of nanomaterials: a review carried out for ECETOC, Particle and Fibre Toxicology 14, 3-11.
33. Boulos, S.P., Davis, T.A., Yang, J.A., Lohse, S. E., Alkilany, A.M., Holland, L. A., Murphy, C.J. (2013). Nanoparticle − Protein Interactions: A Thermodynamic and Kinetic Study of the Adsorption of Bovine Serum Albumin to Gold Nanoparticle Surfaces. Langmuir 29, 14984-14996.
34. Boxall, A.B.A., Chaudhry, Q., Sinclair, C., Jones, A., Aitken, R., Jefferson, B., Watts, C. (2007). Current and future predicted environmental exposure to engineered nanoparticles. Central Science Laboratory, Sand Hutton, York, UK.
35. Branca, M., Gamba, A., Manitto, P., Monti, D., Speranza, G., (1983). The binding of bilirubin to albumin a study using spin-labelled bilirubin. Biochim BiophysActa 742, 341-351.
36. Breaven, G.H., D'Albis, A., and Gratzer, W.B. (1973). EurJBiochem. 33,500-509.
37. Brkić A. L., Milić, M., Pongrac, I.M., Marjanovič, A.M., Mlinarić, H., Pavičić, I., Gajović, S., Vinković Vrček, I., (2017). Impact of surface functionalization on the uptake mechanism and toxicity effects of silver nanoparticles in HepG2 cells. Food and Chemical Toxicology 107, 349-361.
38. Brown, J. R. and Shockley, P., (1982). In Lipid Protein Interactions. (eds Jost, P. and Griffith,O.H.) JohnWiley & Sons, NewYork.

39. Brust, M., Bethell, D., Schiffrin, D.J., Kiely, C.J., (1995). Novel gold dithiol nano-networks with non-metallic electronic properties. Advanced materials 7, 795-797.
40. Brust, M., Walker, M., Bethell, D., Schiffrin, D.J., Whyman, R. (1994). Synthesis of thiol-derivatised gold nanoparticles in a two-phase Liquid–Liquid system. J. Chem. Soc., Chem. Commun 0, 801-802.
41. Burrell, R.E., Heggers, J.P., Davis, G.J., Wright, J.B. (1999). Efficacy of silver-coated dressings as bacterial barriers in a rodent burn sepsis model. Wounds 11, 64-71.
42. Byko, M. (2005). From Electric Corsets to Self-Cleaning Pants: The Materials Science and Engineering of Textiles 57, 14-18.
43. Cantor, C.R., Schimmel, P.R. (1980). Biophysical Chemistry: Part II Techniques for the Study of Biological Structure and Function. W.H. Freeman & Company: Oxford.
44. Capjak, I., Avdičević, Z.M., Sikirić, D.M., Jurašin, D.D., Hozić, A., Pajić, D., Dobrović, S., Goessler, W., Vrček, V.I., (2018). Behavior of silver nanoparticles in wastewater: systematic investigation on the combined effects of surfactants and electrolytes in the model systems. Environmental Science: Water Research & Technology 4, 2146-2159.
45. Carlson, C., Hussain, S.M., Schrand, A.M., Braydich-Stolle, L.K., Hess, K.L., Jones, R.L., Schlager, J.J., (2008). Unique cellular interaction of silver nanoparticles: size-dependent generation of reactive oxygen species. J Phys Chem B 112, 13608–13619.
46. Carter, D.C. and Ho, J.X., (1994). Structure of serum albumin. Adv Protein Chern 45, 153-203.
47. Casals, E., Pfaller, T., Duschl, A., Oostingh, G.J., Puntes, V. (2010). Time evolution of the nanoparticle protein corona. ACS Nano 2010, 4, 3623–3632.
48. Ceciliani, F. and Pocacqua V. (2007). The acute phase protein alpha1-acid glycoprotein: a modelfor altered glycosylation during diseases. Curr Protein Pept Sci 8, 91-108.
49. Cedervall, T., Lynch I.,, Lindman, S., Berggard, T., Thulin, E., Nilsson, H., Dawson, K. A., Linse., S., (2007). Understanding the nanoparticle–protein corona using methods to quantify exchange rates and affinities of proteins for nanoparticles. Proc Natl Acad Sci U S A. 104, 2050-2055.
50. Cedervall, T., Lynch I., Foy M., Berggad T., Donnelly S., Cagney G., Linse S., Dawson K. (2007). Detailed identification of plasma proteins adsorbed on copolymer nanoparticles. Angew Chem Int Ed 46, 5754–5756.
51. Chanana, M., Rivera-Gil P., Correa-Duarte M.A., LizMarzán L.M., Parak W.J., (2013). Physicochemical Properties of Protein-Coated Gold Nanoparticles in Biological Fluids and Cells before and after Proteolytic Digestion. Angew Chem Int Ed 52, 4179–4183.

52. Chaturvedi, P.N. and Dave, N.K. (2012). Shah Applications of nano-catalyst in new era. Journal of Saudi Chemical Society 16, 307-325.
53. Chaturvedi, S., Dave, P.N., Shah, N.K. (2012). Applications of nano-catalyst in new era. Journal of Saudi Chemical Society 16, 307–325.
54. Chemistry (2017). Dostupno na: https://www2.chemistry.msu.edu/faculty/reusch/virttxtjml/spectrpy/UV-VIS/spectrum.htm, (pristupljeno: svibanj 2017.).
55. Chen, Y. H. and Yeh, C.S. (2002). Laser ablation method: use of surfactants to form the dispersed Ag nanoparticles. Colloids and Surfaces A: Physicochemical and Engineering Aspects Volume 197, 133–139.
56. Chen, M., Wang, L.-Y., Han, J.-T., Zhang, J.-Y., Li, Z.-Y., Qian, D.-J. (2006). Preparation and Study of Polyacryamide-Stabilized Silver Nanoparticles through a One-Pot Process. The Journal of Physical Chemistry B 110, 11224–11231.
57. Chernousova, S., Epple, M. (2013). Silver as antibacterial agent: ion, nanoparticle, and metal. Angew Chem Int Ed Engl. 52, 1636-53.
58. Chou, K.S. and Lai, Y.S. (2004). Effect of polyvinyl pyrrolidone molecular weights on the formation of nanosized silver colloids. Mater. Chem. Phys 83, 82-88.
59. Churchman, A.H., Wallace, R., Milne, S.J., Brown, A.P., Brydson, R., Beales, P.A., (2013). Serum albumin enhances the membrane activity of ZnO nanoparticles. Chem Commun 49, 4172–4174.
60. Colombo, S., Buclin, T, Decosterd, L.A., Telenti, A., Furrer, H., Lee B.L., Biollaz, J., Eap, C.B., (2006). Orosomucoid (alpha1-acid glycoprotein) plasma concentration and genetic variants: effects on human immunodeficiency virus protease inhibitor clearance and cellular accumulation. Clin Pharmacol Ther 80, 307-318.
61. Conde, J., Dias, J.T., Grazú, V., Moros, M., Baptista, P.V., de la Fuente, J.M., (2014). Revisiting 30 years of biofunctionalization and surface chemistry of inorganic nanoparticles for nanomedicine. Frontiers Chem 2, 2-48.
62. Corbo, C., Molinaro, R., Parodi, A., Furman, N.E.T., Salvatore, F., Tasciotti, E., (2016). The impact of nanoparticle protein corona on cytotoxicity, immunotoxicity and target drug delivery. Nanomedicine 11(1):81–100.
63. Cui, M.H., Liu, R.X., Deng, Z.Y., Ge, G.L., Liu, Y., Xie, L.M., (2014). Quantitative Study of Protein Coronas on Gold Nanoparticles with Different Surface Modifications Nano Research 7, 345–352.

64. Curry S. (2009). Lessons from the crystallographic analysis of the small molecule binding to human serum albumin. Drug Metab Pharmacokinet 24, 342-57.
65. Curry, S., Brick, P., Franks, N.P., (1999). Fatty acid binding to human serum albumin: new insights from crystallographic studies. Biochimica et Biophysica Acta 1441, 131-140
66. Cushing, B.L., Kolesnichenko, V.L. , O'Connor, C.J., (2004). Recent Advances in the Liquid-Phase Syntheses of Inorganic Nanoparticles. Chem.Rev 104, 3893-3946.
67. Diederichs J.E. (1996). Plasma protein adsorption patterns on liposomes: establishment of analytical procedure. Electrophoresis 17, 607–611.
68. Ding, F., Radic, S., Chen, R., Chen, P., Geitner, N.K., Brown, J.M., Ke, P. C., (2013). Direct observation of a single nanoparticle-ubiquitin corona formation. Nanoscale 5, 9162–9169.
69. Docter, D., Westmeier, D., Markiewicz, M., Stolte, S., Knauer, S.K., Stauber, R.H., (2015). The nanoparticle biomolecule corona: lessons learned– challenge accepted? Chem. Soc. Rev 44, 6094-6121.
70. Dominguez-Medina, S., Blankenburg, J., Olson, J., Landes, C.F., Link, S. (2013). Adsorption of a Protein Monolayer via Hydrophobic Interactions Prevents Nanoparticle Aggregation under Harsh Environmental Conditions. ACS Sustainable Chem Eng 7, 833–842.
71. Duche, J.C., Urien, S., Simon, N., Malaurie, E., Monnet, I., Barre, J., (2000). Expression of the genetic variants of human alpha-1-acid glycoprotein in cancer. Clin Biochem 33, 197-202.
72. Duncan, T.V. (2011). "Applications of nanotechnology in food packaging and food safety: barrier materials, antimicrobials and sensors", J Colloid Interface Sci 363, 1-24.
73. Duran, N., Silveira, C.P., Duran, M., Martinez, D., (2015). Silver nanoparticle protein corona and toxicity: a mini-review. Journal of Nanobiotechnology 13, 55-72.
74. Durán, N., Durán, M., Seabra, A.B., Fávaro, W.J., Nakazato, G., (2016). Silver nanoparticles: a new view on mechanistic aspects on antimicrobial activity. Nanomed. Nanotechnol. Biol. Med. 12, 789–799.
75. Dziendzikowska, K., Gromadzka-Ostowska, J., Lankoff, A., Oczkowski, M., Krawczyńska, A., Chwastowska, J., Sadowska-Bratek, M., Chajduk, E., Wojewódzka, M., Dušinská, M., Kruszewski, M., (2012). Time-dependent biodistribution and excretion of silver nanoparticles in male. Wistarrats. J. Appl. Toxicol 32, 920–928.

76. Eap, C.B., Fischer, J.F., Baumann, P., (1991). Variations in relative concentrations of variants ofhuman alpha 1-acid glycoprotein after acute-phase conditions. Clin Chim Acta 203, 379-385.
77. Eigler, D.M. and Schweizer E.K. (1990). Positioning single atoms with a scanning tunnelling microscope. Nature 344, 524-526.
78. El-Badawy, A., Feldhake, R., Venkatapathy, R., (2010). State-Of-The-Science Review: Everything NanoSilver and More. U.S. Environmental Protection Agency, Washington.
79. El-Badawy, A.M., Silva, R.G., Morris, B., Scheckel, K.G., Suidan, M.T., Tolaymat, T.M. (2011). Surface Charge-Dependent Toxicity of Silver Nanoparticles. Environ. Sci. Technol. 45, 283-287.
80. Elechiguerra, J.L., Burt, J.L., Morones, J.R, Camacho-Bragado, A., Gao, X., Lara, H.H., Yacaman, M.J., (2005). Interaction of silver nanoparticles with HIV-1. Journal of Nanobiotechnology 3, 6-16.
81. Elliott, H.G., Elliott, M.A., Watson, J, Steele, L, Smith, K.D., (1995). Chromatographic Investigation of the Glycosylation Pattern of Alpha-1-Acid Glycoprotein Secreted by the HEPG2 Cell Line; a Putative Model for Inflammation. Biomed Chrom 9, 199-204.
82. Elzey, S. and Grassian, V.H., (2010). Agglomeration, isolation and dissolution of commercially manufactured silver nanoparticles in aqueous environments. Journal of Nanoparticle Research 12, 1945–1958.
83. Empa & TSV Schweiz Textilverband. (2011). Nano textiles – Grundlagen und Leitprinzipien zur effizienten Entwicklung nachhaltiger Nanomaterialien, Ausga
84. Enciklopedija (2017). Dostupno na: http://www.enciklopedija.hr/natuknica.aspx?ID=4486#top, pristup travanj 2017.
85. Eskandari, K., Kamali, M., Ramezani, M., Safiri, Z., Keihan, A.H., Rashidiani, J., Kooshki, H, Zarei, H., (2013). The Effect of Hydrophobicity and Hydrophilicity of Gold Nanoparticle on Proteins Structure and Function. International Journal of Bio-Inorganic Hybrid Nanomaterials 3, 465-470
86. European Commission (2011). Commission Recommendation on the definition of nanomaterial. Official Journal of the European Union, Brussels.
87. European Commission (2013). Communication from the Commission to the European Parliament, the Council and the European Economic and Social Committee. Second regulatory review on nanomaterials. Brussels.
88. European Commission (2014). Communication from the Scientific Committee on Emerging and Newly Identified Health Risks (SCENIHR). Opinion on Nanosilver:

safety, health and environmental effects and role in antimicrobial resistance. Brussels, effects and rolein antimicrobial resistance. Brussels.

89. European Commission (2015). Communication from the Scientific Committee on Emerging and Newly Identified Health Risks (SCENIHR). Opinion on the Guidance on the Determination of Potential Health Effects of Nanomaterials Used in Medical Devices. Brussels.
90. Evans, F., Wennerstrom, H., (1994). Polymers in Colloidal Systems. In The Colloidal Domain: Where Physics, Chemistry, Biology, and Technology Meet; Wiley-VCH: New York.
91. Fan, L. and Guo, R., (2008). Growth of Dendritic Silver Crystals in CTA/SDBS Mixed-Surfactant Solutions. Crystal Growth & Design 8, 2150–2156.
92. Fey, G.H., Fuller, G.M. (1987). Regulation of acute phase gene expression by inflammatory mediators. Mol Biol Med 4, 323-338.
93. Filip, Z., Jan, K., Vendula, S., Jana, K. Z., Kamil, M., Kamil, K., (2013). Albumin and α1-acid glycoprotein: old acquaintances. Expert Opin Drug Metab Toxicol 9, 943-954.
94. Filipović, I., Lipanović, S. (1987). Opća i anorganska kemija. Školska knjiga, Zagreb.
95. Finsy, R., (1994). Particle sizing by quasi-elastic light-scattering. Adv. Colloid Interface Sci 52, 79–143.
96. Fleischert, C.C. and Payne, C.K., (2014). Nanoparticle–Cell Interactions: Molecular Structure of the Protein Corona and Cellular Outcomes. Acc. Chem. Res 47, 2651–2659.
97. Fornes, J.A. (1985). Secondary minimum analysis in the DLVO theory. Colloid Polym Sci 263, 1004–1007.
98. Fournier, T., Medjoubi, N.N., Porquet, D., (2000). Alpha-1-acid glycoprotein. Biochim Biophys Acta 1482, 157-171.
99. Fournier, T., Vranckx, R., Mejdoubi, N., Durand, G., Porquet, D., (1994). Induction of rat alpha-1-acid glycoprotein by phenobarbital is independent of a general acute-phase response. Biochem Pharmacol 48, 1531-1535.
100. Gamer, A.O., Leibold, E., Van-Ravenzwaay, B. (2006). The in vitro absorption of microfine zinc oxide and titanium dioxide through porcine skin. Toxicology in Vitro 3, 301-307.
101. Gebauer, J.S., Malissek, M., Simon, S., Knauer, S.K., Maskos, M., Stauber, R.H., Peukert, W., Treuel, L. (2012). Impact of the Nanoparticle–Protein Corona on Colloidal Stability and Protein Structure. Langmuir 28, 9673–9679.

102. Generalić, E. (2017). "Zeta potencijal." Englesko-hrvatski kemijski rječnik. Dostupno na: https://glossary.periodni.com/dictionary.php?en=zeta+potencijal, (prostupljeno: svibanj 2017.)
103. Georgios, A.S. and Sotiris, E., (2011). Pratsinis Engineering nanosilver as an antibacterial, biosensor and bioimaging material. Curr Opin Chem Eng 1, 3–10.
104. Goesmann, H. and Feldmann, C., (2010). Nanoparticulate Functional Materials. Angew Chem Int Ed 49, 1362–1395.
105. Goppert, T.M. and Muller, RH., (2005). Adsorption kinetics of plasma proteins on solid lipid nanoparticles for drug targeting. Int J Pharm 302, 172–186.
106. Gornik, O. and Lauc, G., (2008). Glycosylation of serum proteins in inflammatory diseases. Dis Markers 25, 267–278.
107. Grand View Research, Report. (2015). Silver Nanoparticles Market By Application (Electronics & electrical, healthcare, food & beverages, textiles) and segment forecasts to 2022.
108. Gray, R.D. and Stroupe, S.D., (1978). Kinetics and mechanism of bilirubin binding to human serum albumin. J Biol Chem 25, 4370–4377.
109. Greenfield, N.J. (2006). Using Circular Dichroism spectra to estimate protein secondary structure. Nat. Protoc 1, 2876-2890.
110. Gurunathan, S., Han, J.W., Kwon, D.N., Kim, J.H., (2014). Enhanced antibacterial and antibiofilm activities of silver nanoparticles against Gram-negative and Gram-positive bacteria. Nanoscale Res. Lett. 9, 373-390.
111. Guzmán, M.G., Dille, J., Godet, S. (2009). Synthesis of silver nanoparticles by chemical reduction method and their antibacterial activity. International Journal of Chemical and Biomolecular Engineering 2, 3-11.
112. Hackenberg, A., Scherzed, A., Kessler, M., Hummel, S., Technau, A., Froelich, K., Ginzkey, C., Koehler, C., Hagen, R., Kleinsasser, N., (2011). Silver nanoparticles: evaluation of DNA damage, toxicity and functional impairment in human mesenchymal stem cells. Toxicol Lett 201, 27–33.
113. Hage, D.S. and Austin, J., (2000). High-performance affinity chromatography and immobilized serum albumin as probes for drug - and hormone-binding. J Chromatogr B Biomed Sci Appl 739, 39-54.
114. Hanada, K., Yamanaka, E., Yamamoto, N., Minami, H., Kawai, S., Sasaki Y., Ogata, H., (2011). Effects of surgery and chronic disease states on the concentrations and phenotype

distribution of alpha1-acid glycoprotein: studies in patients with breast cancer and patients with chronic inflammatory disease. Int J Clin Pharmacol Ther 49, 415-421.

115. Hashimoto, S., Asao, T., Takahashi, J., Yagihashi, Y., Nishimura, T., Saniabadi, A.R., Poland, D.C., van Dijk, W., Kuwano, H., Kochibe, N., Yazawa, S., (2004). alpha1-acid glycoprotein fucosylation as a marker of carcinoma progression and prognosis. Cancer 101, 2825-2836.
116. Hassan, P.A., Rana, S., Verma, G. (2015) Making sense of Brownian motion: colloid characterization by dynamic light scattering. Langmuir 31, 3-12.
117. Hayashi, T., Era, S., Kawai, K, Imai, H., Nakamura, K., Onda, E., Yoh, M., (2000). Observation for redox state of human serum and aqueous humor albumin from patients with senile cataract. Pathophysiology 6, 237-43.
118. He, D., Dorantes-Aranda, J.J., Waite, T.D. (2012). Silver Nanoparticle-Algae Interactions: Oxidative Dissolution, Reactive Oxygen Species Generation and Synergistic Toxic Effects. Environ Sci Technol 46, 8731–8738.
119. Hedberg, J., Lundin, M., Lowe, T., Blomberg, E., Wold, S., Wallinder, I.O., (2012). Interactions between surfactants and silver nanoparticles of varying charge. Journal of Colloid and Interface Science 369, 193–201.
120. Hegyi, G., Kardos, J., Kovács, M., Málnási-Csizmadia, A., Nyitray, L., Pál, G., Radnai, L., Reményi, A., Venekei, I., (2013). Molecular forces stabilising ligand binding. U: Introduction to Practical Biochemistry. ELTE Faculties of Science Student Foundation, Eötvös Loránd University, Macarska.
121. Henglein, A. (1998). Colloidal Silver Nanoparticles: Photochemical Preparation and Interaction with O2, CCl4, and Some Metal Ions. Chem. Mater 10, 444–540.
122. Higai, K., Aoki, Y., Azuma, Y, Matsumoto, K. (2005). Glycosylation of site-specific glycans of α1-acid glycoprotein and alterations in acute and chronic inflammation. Biochim Biophys Acta 1725, 128-135.
123. Hochepied, T., Berger, F.G., Baumann, H., Libert, C., (2003). Alpha(1)-acid glycoprotein: an acute phase protein with inflammatory and immunomodulating properties. Cytokine Growth Factor Rev 14, 25-34.
124. Hotze, E.M., Labille, J., Alvarez, P., Wiesner, M.R., (2008). Environ Sci Technol 42, 4175–4180.
125. Huang, R., Carney, R.P., Stellacci, F., Lau, B.L.T., (2013). Protein–nanoparticle interactions: the effects of surface compositional and structural heterogeneity are scale dependent. Nanoscale 5, 6928-6935.

126. Hunter, R.J. (2001). Double Layer Interaction and Particle Coagulation. InFoundations of Colloid Science, 2nd ed.; Oxford University Press: NewYork.
127. Hussain, S.M., Braydich-Stolle, L.K., Schrand, A.M., Murdock, R.C., Yu, K.O., Mattie, D.M., Schlager, J.J., Terrones, M. (2009). Adv Mater 21, 1549–1559.
128. Israili, Z.H and Dayton, PG., (2001). Human alpha-1-glycoprotein and its interactions with drugs. Drug Metab Rev 33, 161-235.
129. Janes, R.W. (2005). Bioinformatics analyses of Circular Dichroism protein reference databases. Bioinformatics 21, 4230-4238.
130. Jezequel, M., Set,a N.S., Corbic, M.M., Feger, J.M., Durand, G.M. (1988). Modifications of concanavalin A patterns of alpha 1-acid glycoprotein and alpha 2-HS glycoprotein in alcoholic liver disease. Clin Chim Acta 176, 49-57.
131. Jiang, J., Oberdörster, G., Biswas, P. (2009). Characterization of size, surface charge, and agglomeration state of nanoparticle dispersions for toxicological studies. J. Nanopart. Res 11, 77–89.
132. Jhonsi, M.A., Kathiravan, A., Renganathan, R. (2009). Spectroscopic studies on the interaction of colloidal capped CdS nanoparticles with bovine serum albumin. Colloids Surf B Biointerfaces 72, 167–172.
133. Joseph, K.S., Moser, A.C., Basiaga, S.B.G., Schiel, J.E., Hage, D.S., (2009). Evaluation of alternatives to warfarin as probes for Sudlow site I of human serum albumin: characterization by high-performance affinity chromatography. J Chromatogr A 1216, 3492-500.
134. Jurašin, D., Dutour Sikirić, M. (2014). Higher Oligomeric Surfactants — From Fundamentals to Applications, in Oligomerization of Chemical i Biological Compounds, InTech.
135. Jurašin, D.D., Čurlin, M., Capjak, I., Crnković, T., Lovrić, M., Babič, M., Horàk, D., Vrček I.V., (2016). Sufrace coating affects behavior of metalic nanoparticle in a bilogical environment. Beilstein Journal of Nanotechnology 7, 246-262.
136. Kaiser, J.P., Roesslein, M., Diener, L., Wichser, A., Nowack, B., Wick. P. (2017). Cytotoxic effects of nanosilver are highly dependent on the chloride concentration and the presence of organic compounds in the cell culture media. J Nanobiotechnology 15, 5-16.
137. Kato, H. (2012). Size Determination of Nanoparticles by Dynamic Light Scattering, Nanomaterials: Processing and Characterization with Lasers, Subhash Chandra Singh, Haibo Zeng, Chunlei Guo, and Weiping Cai, Wiley-VCH Verlag GmbH & Co.

138. Kelly, S.M., Jess, T.J., Price, N.C., (2005). How to study proteins by Circular Dichroism. Biochimica et Biophysica Acta 1751, 119-139.
139. Khan, Z., Al-Thabaiti, S.A, Obaid, Y.A., Al-Youbi, A.O., (2011). Preparation and characterization of silver nanoparticles by chemical reduction method. Colloids and Surfaces B: Biointerfaces 82, 513–517.
140. Khrapunov, S. (2009). Circular dichroism spectroscopy has intrinsic limitations for protein secondary structure analysis. Anal Biochem 389, 174-176
141. Kim, H.R., Andrieux, K., Delomenie, C., Chacun, H., Appel, M., Desmaele, D., Taran, F., Georgin, D., Couvreur, P., Taverna, M,. (2007). Analysis of plasma protein adsorption onto PEGylated nanoparticles by complementary methods: 2-DE, CE and Protein Labon-chip system. Electrophoresis 28, 2252–2261.
142. Kim, H.S. and Wainer, I.W., (2008). Rapid analysis of the interactions between drugs and human serum albumin (HSA) using high-performance affinity chromatography (HPAC). J Chromatogr B Biomed Sci Appl 870, 22-26.
143. Kim, J.S., Kuk, E., Yu, K.N., Kim, J.H., Park, S.J., Lee, H.J., Kim, S.H., Park, Y.H., Hwang, C.Y., Kim, Y.K., Lee, Y.S., Jeong, D.H., Cho, M.H., (2007). Antimicrobial effects of silver nanoparticles. Nanomed. Nanotechnol. Biol. Med 3, 95–101.
144. Kirsch, R., Frith, L., Black, E., Hoffenberg, R., (1968). Regulation of albumin synthesis and catabolism by alteration of dietary protein. Nature 217,578-579.
145. Kittler, S., Greulich, C., Gebauer, J.S., Diendorf, J., Treuel, L., Ruiz, L., Gonzalez-Calbet, J. M., Vallet-Regi, M, Zellner, R., Koller, M., Epple, M., (2010). The influence of proteins on the dispersability and cell-biological activity of silver NP. Journal of Materials Chemistry 20, 512-518.
146. Klein, J. (2007). Probing the interaction of proteins and nanoparticles. PNAS 104, 2029-2030.
147. Klevens, R.M., Edwards, J.R., Richards, C.L.Jr, Horan, T.C., Gaynes, R.P., Pollock, D.A., Cardo, D.M., (2007). Estimating health care-associated infections and deaths in US hospitals. Public Health Rep 122, 160-166.
148. Kopecky, V.Jr., Ettrich, R., Hofbauerova, K., Baumruk, V., (2003). Structure of human alpha1-acid glycoprotein and its high-affinity binding site. Biochem Biophys Res Commun 300, 41-46.
149. Korbekandi, S.I. (2012). Nanotechnology and Nanomaterials » "The Delivery of Nanoparticles", Chapter 1 Silver Nanoparticles. InTech, Rijeka, Croatia.

150. Koshkina, O., Lang, T., Thiermann, R., Docter, D., Roland, H.S., Secker, C., Schlaad, H., Weidner, S., Mohr, B., Maskos, M., Bertin, A., (2015). Temperature-Triggered Protein Adsorption on Polymer-Coated Nanoparticles in Serum. Langmuir 31, 8873−8881.
151. Kragh-Hansen, U. (1983). Relations between high-affinity binding sites for L-tryptophan, diazepam, salicylate and Phenol Red on human serum albumin. Biochem J 209, 135-4.
152. Kragh-Hansen, U., Chuang, V.T.G, Otagiri, M., (2002). Practical aspects of the ligand-binding and enzymatic properties of human serum albumin. Biol Pharm Bull 25, 695-704.
153. Kratochwil, N.A., Huber, W., Mueller, F., Kansy, M., Gerber, P.R., (2004). Predicting plasma protein binding of drugs – revisited. Curr Opin Drug Discov Devel 4, 507-512.
154. Kremer, J.M., Wilting, J., Jansen, L.H., (1988). Drug binding to human alpha 1-acid glycoprotein in health and disease Pharmacol Rev 40, 1-47.
155. Kruszewski, M., Gradzka, I., Bartlomiejczyk, T., Chwastowska, J., Sommer, S., Grzelak, A., Zuberek, M., Lankoff, A., Dusinska, M., Wojewodzka, M., (2013). Oxidative DNA damage corresponds to the long term survival of human cells treated with silver nanoparticles. Toxicol Lett 219, 151–159.
156. Kubista, M., Sjöback, R., Eriksson, S., Albinsson, B., (1994). Exprimental Correction for the Inner-filter Effect in Fluorescence Spectra. Analyst 119, 417-419.
157. Kubo, A., Capjak, I., Vinković Vrček, I., Bondarenko, O.M., Kurvet, I., Vija, H., Ivask, A., Kasemets, K., Kahru, A., (2018). Antimicrobial potency of differently coated 10 and 50 nm silver nanoparticles against clinically relevant bacteria Escherichia coli and Staphylococcus aureus. Colloids and Surfaces B: Biointerfaces 170, 401–410.
158. Kulkarni, A.B, Reinke, R, Feigelson, P., (1985). Acute phase mediators and glucocorticoids elevatealpha 1-acid glycoprotein gene transcription J Biol Chem. 260, 15386-15389.
159. Kuribayashi, T., Tomizawa, M., Seita, T., Tagata, K., Yamamoto, S., (2011). Relationship between production of acute-phase proteins and strength of inflammatory stimulation in rats. Lab Anim 45, 215-218.
160. Kvıtek, L., Panaček A., Soukupova, J., Kolar, M., Večerova, R., Prucek, R., Holecova, M., Zboril R., (2008). Effect of Surfactants and Polymers on Stability and Antibacterial Activity of Silver Nanoparticles (NPs). J. Phys. Chem 112, 5825-5834.

161. Kwon K.S., Yu M.H. (1997). Effect of glycosylation on the stability of alpha1-antitrypsin toward urea denaturation and thermal deactivation. Biochim Biophys Acta. 1335, 265-272.
162. Laera, S., Ceccone, G., Rossi, F., Gilliland, D., Hussain, R., (2011). Measuring protein structure and stability of protein-nanoparticle systems with Synchrotron Radiation Circular Dichroism. Nano Letters 11, 4480-4484.
163. Lansdown, A. B. G. (2006). Silver in health care: antimicrobial effects and safety in use. Curr. Probl. Dermatol. 2006, 33, 17-34.
164. Lansdown, A. B. G. (2010). Silver in healthcare. Its antimicrobial efficacy and safety in use, Vol. 6, Royal Society of Chemistry, Cambridge.
165. Lee, J.S., Lytton-Jean, A.K., Hurst, S.J., Mirkin, C.A., (2007). Nanoparticle Oligonucleotide Conjugates Based on DNA with Triple Cyclic Disulfide Moieties. Nano Lett 7, 2112–2115.
166. Lehmann, S., Harris, D.A. (1997). Blockade of glycosylation promotes acquisition of scrapielike properties by the prion protein in cultured cells. J Biol Chem 272, 21479-21487
167. Lentechm (2017). Dostupno na: (http://www.lenntech.com/periodic/elements/ag.ht (pristupljeno: ožujak 2017.)
168. Leo, B.F., Chen, S., Kyo, Y., Herpoldt, K.-L., Terrill, N.J., Dunlop, I. E., McPhail, D. S., Shaffer, M. S., Schwander, S., Gow, A., Zhang, J., Chung, K. F., Tetley, T. D., Porter, A. E., Ryan, M. P., (2013). The stability of silver nanoparticles in a model of pulmonary surfactant. Environ. Sci. Technol 47, 11232–11240.
169. Levard, C., Michel, F.M., Wang, Y., Choi, Y., Eng, P., Brown, G.E.Jr., (2011). Probing Ag nanoparticle surface oxidation in contact with (in)organics: an X-ray scattering and fluorescence yield approach. J. Synchrot. Radiat 18, 871−878.
170. Levard, C., Hotze, E.M., Lowry, G.V., Brown, Jr. GE., (2012). Environmental Transformations of Silver Nanoparticles: Impact on Stability and Toxicity. Environ Sci Technol 46, 6900−6914.
171. Li, H., Xia, H., Wang, D., Tao, X. (2013). Simple synthesis of monodisperse, quasi-spherical, citrate-stabilized silver nanocrystals in water. Langmuir 29, 5074-5079.
172. Li, X., Lenhart, J. J., Walker, H.W., (2012. Aggregation kinetics and dissolution of coated silver nanoparticles Langmuir 28, 1095–1104.
173. Li, Y., Luo, L., Rasool, N., Kang, CY., (1993). Glycosylation is necessary for the correct folding of human immunodeficiency virus gp120 in CD4 binding. J Virol 67, 584-588.

174. Lim, P., Asharani, P.H., (2012). Enhanced genotoxicity of silver nanoparticles in DNA repair deficient mammalian cells. Front Genet 3, 1–12.
175. Linnert, T., Mulvaney, P. and Henglein, A., (1993). Surface chemistry of colloidal silver: surface plasmon damping by chemisorbed iodide, hydrosulfide (SH-), and phenylthiolate. The Journal of Physical Chemistry 97, 679–682.
176. Lindman, S., Lynch, I., Thulin, E., Nilsson, H., Dawson, K.A., Linse, S., (2007). Systematic investigation of the thermodynamics of HSA adsorption to N-iso-propylacrylamide/ N-tert-butylacrylamide copolymer nanoparticles. Effects of particle size and hydrophobicity. Nano Lett 7, 914–920.
177. Litovchick, A., Rando, R.R., (2003). Stereospecificity of short Rev-derived peptide interactions with RRE IIB RNA. RNA 9, 937-948.
178. Liu, J.; Hurt and R. H., (2010). Ion release kinetics and particle persistence in aqueous nano-silver colloids. Environ. Sci. Technol 44, 2169− 2175.
179. Liu, P., Sun, Y., Wang, Q., Sun, Y., Li, H., Duan, Y., (2014). Intracellular trafficking andcellular uptake mechanism of mPEG-PLGA-PLL and mPEG-PLGA-PLL-Galnanoparticles for targeted delivery to hepatomas. Biomaterials 35, 760-770.
180. López-Heras, M., Theodorou, I.R., Leo, B.F., Ryan, M.P., Porter, A.E.,(2015). Towards understanding the antibacterial activity of Ag nanoparticles: electron microscopy in the analysis of the materials-biology interface in the lung. Environ. Sci. Nano 2, 312–326.
181. Louie, A.Y. and Meade, T.J., (1999). Metal complexes as enzyme inhibitors. Chem Rev. 99, 2711-34.
182. Lu, W., Senapati, D., Wang, S., Tovmachenko, O., A.K. Singh, H. Yu, Ray, P.C., (2010). Effect of surface coating on the toxicity of silver nanomaterials on human skin keratinocytes. Chem Phys Lett 487, 92–96.
183. Lück, M., Paulke, B.R., Schröder, W., Blunk, T., Müller, R.J. (1998). Analysis of plasma protein adsorption on polymeric nanoparticles with different surface characteristics. Biomed. Mater. Res 39, 478–485.
184. Lundqvist, M., Stigler J., Cedervall T., Berggard T., Flanagan M.B., Lynch I., Elia G., Dawson, K., (2011). The evolution of the protein corona around nanoparticles: a test study. ACS Nano. 5, 7503–7509.
185. Lundqvist, M., Stigler, J., Elia G, Lynch I, Cedervall T, Dawson K.A. (2008). Nanoparticle size and surface properties determine the protein corona with possible implications for biological impacts. Proc Natl Acad Sci, 105, 14265–14270.

186. Luterotti, S., Bicanic, D., (2013). Odabrane teme iz bioanalitike. 4. Izdanje. Farmaceutsko-biokemijski fakultet Sveučilišta u Zagrebu, Zagreb.
187. Lutz, H.-P., Luisi, P.L., (1983). Correction for Inner Filter Effects in Fluorescence Spectroscopy. Helvetica Chim Acta 66 (190), 1929-1935.
188. Lynch, I. and Dawson K.A., (2008). Protein–nanoparticle interactions. NanoToday 3, 40–47.
189. Lynch, I., Cedervall, T., Lundqvist, M., Cabaleiro-Lago C, Linse S, Dawson, K.A., (2007). The nanoparticle–protein complex as a biological entity; a complex fluids and surface science challenge for the 21st century. Adv Colloid Interface Sci. 134–135, 167–174.
190. MacCuspie, R. I. (2011). Colloidal stability of silver nanoparticles in biologically relevant conditions. J. Nanopart. Res. 13, 2893–2908.
191. Mafuné, F., J. Kohno J, Y. Takeda, T. Kondow, Sawabe, H. (2000). Formation and size control of sliver nanoparticles by laser ablation in aqueous solution J. Phys. Chem. B 104 9111-9117.
192. Malina, D., Sobczak-Kupiec, A., Wzorek, Z., Kowalski, Z., (2012). Silver nanoparticles synthesis with different concentrations of polyvinylpyrrolidone. Digest Journal of Nanomaterials and Biostructures 7, 1527-1534.
193. Marambio-Jones, C., Hoek, E.M.V. (2010). A review of the antibacterial effects of silver nanomaterials i potential implications for human health i the environment. J. Nanopart. Res. 12, 1531–1551.
194. Mariam, J., Dongre P.M., Kotharu, D.C., (2011). Study of interaction of silver nanoparticles with bovine serum albumin using fluorescence spectroscopy. Journal of Fluorescence 21, 2193-2199.
195. Marucco, A.; Catalano, F.; Fenoglio, I.; Turci, F.; Martra, G., Fubini, B., (2015). Possible Chemical Source of Discrepancy between in Vitro and in Vivo Tests in Nanotoxicology Caused by Strong Adsorption of Buffer Components. Chem. Res. Toxicol. 28, 87–91.
196. Mavon, A., Miquel, C., Lejeune, O., Payre, B., Moretto, P., (2007). In vitro percutaneous absorption and in vivo stratum corneum distribution of an organic and a mineral sunscreen. Skin Pharmacology and Physiology 1, 10-20.
197. McShan, D., Paresh C. Ray, and Hongtao Y., (2014). Molecular Toxicity Mechanism of Nanosilver. J Food Drug Anal. 22, 116–127.

198. Means, G.E, Bender, M.L.m (1975). Acetylation of human serum albumin by p-nitrophenyl acetate. Biochemistry 14, 4989-94.
199. Means, G.E., Wu, HL., (1979). The reactive tyrosine residue of human serum albumin: characterization of its reaction with diisopropylfluorophosphate. Arch Biochem Biophys 194, 526-30.
200. Medical dictionary, Dostupno na: http://medical-dictionary.thefreedictionary.com/blood (pristupljeno: 12.04.2017.)
201. Métraux, G.S., Mirkin, C.A., (2005). Rapid thermal synthesis of silver nanoprisms with chemically tailorable thickness. Adv. Mater 17, 412-415.
202. Mie, G., (1908). Beiträge zur Optik trüber Medien, speziell kolloidaler Metallösungen. *Annalen der Physik*, 330, 377–445.
203. Milić, M., Leitinger, G., Pavičić, I., Zebić Avdičević, M., Dobrović, S., Goesslere, W., Vinković Vrček, I., (2014). Cellular uptake and toxicity effects of silvernanoparticles in mammalian kidney cells. J. Appl. Toxicol 35, 581–592.
204. Moerz, S.T., Kraegeloh, A., Chanana, M., Kraus T. (2015). Formation Mechanism for Stable Hybrid Clusters of Proteins and Nanoparticles. ACS Nano 9, 6696–6705.
205. Monopoli, M.P., D. Walczyk, A. Campbell, G. Elia, I. Lynch, F.B. Bombelli, Dawson, K.A. (2011). Physical-Chemical Aspects of Protein Corona: Relevance to in Vitro and in Vivo Biological Impacts of Nanoparticles. J. Am. Chem. Soc 133, 2525–2534.
206. Morones, J.R., Elechiguerra, J.L., Camacho, A., Holt, K., Kouri, J.B., Ramírez, J.T., Yacaman, M.J., (2005) The bactericidal effect of silver nanoparticles. Nanotechnology 6, 2346-53.
207. Nadworny, P.L., Wang, J., Tredget, E.E., Burrell, R.E., (2010). Anti-inflammatory activity of nanocrystalline silver-derived solutions in porcine contact dermatitis. Journal of Inflammation 7, 13-33.
208. Nakanishi, K., Sakiyama, T., Imamura, K., (2001). On the adsorption of proteins on solid surfaces, a common but very complicated phenomenon. J Biosci Bioeng 91, 233–244.
209. Nallathambya, P.D., Xu., X. H., (2010). Study of cytotoxic and therapeutic effects of stable and purified silver nanoparticles on tumor cells. Nanoscale 2, 942-952.
210. Nanotechnology (2017). A Brief Overview. Dostupno na:
211. http://barrett-group.mcgill.ca/tutorials/nanotechnology/nano02.htm (pristupljeno: 02.06.2017.).
212. Berger, M., (2007). Nanotechnology Risks-The Real Issues, nanoWERK 1, 1-7.

213. Nel, A.E., Mädler, L., Velegol, D., Xia T, Hoek EMV, Somasundaran P, Klaessig F, Castranova V, Thompson M., (2009). Understanding biophysicochemical interactions at the nano-bio interface. Nature Materials 8 543-557.
214. Nielsen, A.H., Vollertsen, J., H.S. Jensen, H.I. Madsen, Hvitved-Jacobsen, T., (2008). Aerobic and anaerobic transformations of sulfide in a sewer system - Field study and model simulations. Water Environ. Res 80, 16−25.
215. Nishi, K., Komine Y, Fukunaga N, Maruyama T, Suenaga A, Otagiri M., (2006). Involvement of disulfide bonds and histidine 172 in a unique beta-sheet to alpha-helix transitionof alpha 1-acid glycoprotein at the biomembrane interface. Proteins 63, 611-620.
216. Nowack, B., Bucheli, T. D., (2007). Occurrence, behavior and effects of nanoparticles in the environment. Environmental Pollution 50, 5-22.
217. Nowack, B., Krug, H.F., Height, M. (2011). 120 years of nanosilver history: implications for policy makers. Environ. Sci. Technol. 45, 1177-1183.
218. Oettl, K, Satuber, RE., (2007). Physiological and pathological changes in the redox state of human serum albumin critically influence its binding properties. Br J Pharmacol 151, 580-590.
219. Otagiri, M. A. (2005). molecular functional study on the interactions of drugs with plasma proteins. Drug Metab Pharmacokinet 20, 309-323.
220. Özmetin, C., Copur, M., Yartasi, A., Kocakerim, M. M. Kinetic Investigation of Reaction Between Metallic Silver i Nitric Acid Solutions. *Chemical Engineering & Technology*, 2000, 23, 707–711.
221. Pacioni, N.L., Borsarelli, C.D., Reyand Alicia, Veglia, V., (2015). Synthetic Routes for the Preparation of Silver Nanoparticles. A Mechanistic Perspective. Chapter Silver Nanoparticle Applications. Part of the series Engineering Materials, Springer, Switzerland.
222. Pal, S., Tak, Y.K., Song, J.M., (2007). Does the antibacterial activity of silver nanoparticles depend on the shape of the nanoparticle? A study of the Gram-negative bacterium Escherichia coli. Appl. Environ. Microbiol 73, 1712-1720.
223. Pappas, S. (2014). Facts About Silver. Live Science Contributor. Dostupno na: http://www.livescience.com/37040-silver.html
(pristupljeno: ožujak 2017.)

224. Paresh-Chandra, R. (2011). Size and Shape Dependent Second Order Nonlinear Optical Properties of Nanomaterials and Its Application in Biological and Chemical Sensing. Chem Rev 110, 5332–5365.
225. Park, E-J, Yi J, Kim, Y, Choi, K, Park, K., (2009). Toxicol In Vitro. 24, 872–878.
226. Park, M.V., Neigh, D.Z., Vermeulen, J.P., de la Fonteyne, LJ., Verharen, H.W., Briedé, J.J., van Loveren, H., de Jong, W.H., (2011). The effect of particle size on the cytotoxicity, inflammation, developmental toxicity and genotoxicity of silver nanoparticles. Biomaterials 32, 9810–9817.
227. Percival, S.L., Bowler, P.G., Dolman, J., (2007). Antimicrobial activity of silver-containing dressings on wound microorganisms using an in vitro biofilm model. Int. Wound. J 4, 186-191.
228. Peters, T. (1996). All about albumin; biochemistry, genetics and medical applications. Academic Press; San Diego, CA.
229. Peters, T., Anfinsen, C.B., (1950). Net production of serum albumin by liver slices. J Biol Chem 186, 805-13.
230. Petersen, C.E., Ha C.E., Harohalli K., Feix, J.B., Bhagavan, N.V., (2000). A Dynamic model for bilirubin binding to human serum albumin. J Biol Chem 275, 20985-95.
231. Petitpas, I., Bhattacharya, A.A., Twine, S., East, M., Curry, S., (2001). Crystal structure analysis of warfarin binding to human serum albumin: anatomy of drug site I. JBiol Chem 276, 22804-22809.
232. Pfeiffer, C., Rehbock, C., Huhn, D., Carrillo-Carrion, C., Aberasturi, D. J., Merk, V., Barcikowski S., Parak,W. J., (2014). Interaction of colloidal nanoparticles with their local environment: the (ionic) nanoenvironment around nanoparticles is different from bulk and determines the physico-chemical properties of the nanoparticles. Journal of The Royal Society Interface, 11, 96 – 109.
233. Pisani C., Gaillard J., Odorico M., Nyalosaso J., Charnay C., Guari Y., Chopineau, J., Devoisselle, J.M., Armengaud, J., Prat, O., (2017). The timeline of corona formation around silica nanocarriers highlights the role of the protein interactome. Nanoscale 9, 1840-1851.
234. Pokutta, S., Herrenknecht, K., Kemler, R., Engel, J., (1994). Conformational changes of the recombinant extracellular eomain of E-cadherin upon calcium binding. Eur. J. Biochem 223, 1019-1026
235. Pongrac, I., Pavičić, I., Brkić Ahmed, L., Babič, M., Horak, D., Vinković Vrček, I., Gajović, S., (2016). Oxidative stress response in neural stem cells exposed to different

superparamagnetic iron oxide nanoparticles. International Journal of Nanomedicine 11, 1701–1715.

236. Pongrac, I., Brkić Ahmed, L., Mlinarić, H., Jurašin, D.D., Pavičic, I., Marjanović Čermak, A.M., Milić, M., Gajović, S., Vinković Vrček, I., (2018). Surface coating affects uptake of silver nanoparticles in neural stem cells. Journal of trace elements in medicine and biology. 50, 684-692.
237. Puthusserickal, A.H., Rana, S., Verma, G., (2015). Making Sense of Brownian Motion: Colloid Characterization by Dynamic Light Scattering. Langmuir 1, 3−12.
238. Rahban, M., Divsalar, A., Saboury, A.A., Golestani, A., (2010). Nanotoxicity and Spectroscopy Studies of Silver Nanoparticle: Calf Thymus DNA and K562 as Targets. J Phys Chem C 114, 5798–5803.
239. Rahman, M., Laurent, S., Tawil, N., Yahia, L., Mahmoudi, M., (2013). Nanoparticle and Protein Corona. U: Protein-Nanoparticle Interactions. Springer-Verlag Berlin Heidelberg.
240. Ramanathan, M., Shrestha, L.,K., Mori, T., Ji, Q., Hill, J.P., Ariga, K., (2013). Amphiphile nanoarchitectonics: from basic physical chemistry to advanced applications. Phys Chem Chem Phys. 15, 10580-611.
241. Ratte, H.T., (1999). Bioaccumulation and toxicity of silver compounds: A review. Environ. Toxicol.Chem 18, 89−108.
242. Ravindran, A., Singh, A., Raichur, A.M., Chandasekaran, N., Mukherjee, A., (2010). Studies on ionteraction of colloidal Ag nanoparticles with bovine serum albumin (BSA). Colloids and Surfaces Biointerfaces 76, 32-37.
243. Reidy, B., Haase, A., Luch, A., Dawson, K.A., Lynch, I., (2013). Mechanisms of Silver Nanoparticle Release, Transformation and Toxicity: A Critical Review of Current Knowledge and Recommendations for Future Studies and Applications. Materials 6, 2295-2350.
244. Rimac, H.(/2017). Interakcije flavonoida i odabranih ksenobiotika pri vezanju na humani serumski albumin. Doktorska disertacija, Farmaceutsko biokemijski fakultet, Sveučilište u Zagrebu, Zagreb.
245. Rocha, S., Thünemann, A.F., Pereira, D.C.M., Coelho, M., Möhwald, H., Brezesinski, G. (2008). Influence of Fluorinated and Hydrogenated Nanoparticles on the Structure and Fibrillogenesis of Amyloid beta-Peptide. Biophysical Chemistry, Elsevier, 137, 35-42.

246. Rosei, F., (2004). Nanostructured surfaces: challenges and frontiers in nanotechnology. J. Phys.: Condens 16, 1373–1436.
247. Rosslein, M., Liptrott, N.J., Owen, A., Boisseau, P., Wick, P., Herrmann, I.K. (2017). Sound understanding of environmental, health and safety, clinical, and market aspects is imperative to clinical translation of nanomedicines. Nanotoxicology 11, 147–149.
248. Ryman-Rasmussen, J.P., Riviere, J.E., Monteiro-Riviere, N. A., (2006). Penetration of intact skin by quantum dots with diverse physicochemical properties. Toxicological Sciences 91, 159-165
249. Sabella, S., Carney, R.P., Brunetti, V., Malvindi, M.A., Al-Juffali, N., Vecchio, G.,Janes, S.M., Bakr, O.M., Cingolani, R., Stellacci, F., Pompa, P.P., (2014). A generalmechanism for intracellular toxicity of metal-containing nanoparticles. Nanoscale 6, 7052-7061.
250. Sahoo, B., Goswami, M., Nag, S, Maiti S., (2007). Spontaneous formation of a protein corona prevents the loss of quantum dotfluorescence in physiological buffers. Chem Phys Lett 445, 217–220.
251. Sakthivel, R. and Prasanna, V., (2012). Solid state synthesis of nano-mineral particles. International Journal of Mining Science and Technology 22, 651–655.
252. Saptarshi, S.R., Duschl A., Lopata A.L., (2013). Interaction of NP with proteins: relation to bio-reactivity of the nanoparticle. Journal of Nanobiotechnology 11, 26-38.
253. Sharma, V.K., Siskova, K.M., Zboril, R., Gardea-Torresdey, J. L., (2014). Organic-coated silver nanoparticles in biological and environmental conditions: fate, stability and toxicity Adv. Colloid Interface Sci. 204, 15–34.
254. Sasahara, K., Demura, M., Nitta, K., (2002). Equilibrium and kinetic folding of Hen Egg-White Lyzozyme under acidic conditions. Proteins 49, 472-482
255. Schmid, K., (1989). Human plasma alpha 1-acid glycoprotein--biochemical properties, theamino acid sequence and the structure of the carbohydrate moiety, variants andpolymorphism. Prog Clin Biol Res 300, 7-22.
256. Schmid, K., Nimerg, R.B., Kimura, A., Yamaguchi, H., Binette, J.P., (1977). The carbohydrate units of human plasma alpha1-acid glycoprotein. Biochim Biophys Acta 492, 291-302.
257. Schmid, O., Stoeger, T. (2016). Surface area is the biologically most effective dose metric for acute nanoparticle toxicity in the lung. Journal of Aerosol Science 99, 133-143.
258. Schönfeld, D.L., Ravelli, R.B.G., Mueller, U., Skerra, A., (2008). The 1.8-Å Crystal Structure of α1-Acid Glycoprotein (Orosomucoid) Solved by UV RIP Reveals the Broad

Drug-Binding Activity of This Human Plasma Lipocalin. Journal of Molecular Biology 384, 393–405.

259. Shannahan, J.H., Lai, X., Ke, P.C., Podila, R., Brown, J.M., Witzmann, F.A., (2013). Silver Nanoparticle Protein Corona Composition in Cell Culture Media. PLoS One. 8, 74001 – 74011.
260. Sheehan, D., (2009). Physical Biochemistry: Principles and Applications. Wiley-Blackwell, Ireland.
261. Shiyan, S.D., Bovin N., (1977). Carbohydrate composition and immunomodulatory activity of different glycoforms of α1-acid glycoprotein. Glycoconj J 14, 631-638.
262. Shrivastava S., Bera, T., Singh, K.S., Singh, G., Ramchandrarao, P., Dash, D., (2009). Characterization of antiplatelet properties of silver nanoparticles. ACS Nano 3, 1357–1364.
263. Shrivastava, S., T. Bera, A. Roy, Singh, G., P. Ramachandrarao, Dash, D., (2007). Characterization of enhanced antibacterial effects of novel silver nanoparticles. Nanotechnology 18, 225103-225112.
264. Silvestre, C., (2011). Duraccio, D., and Sossio, C., (2011). Food packaging based on polymer nanomaterials. Progress in Polymer Science 36, 1766–1782.
265. Simberg, D., Park J.H., Karmali P.P., Zhang W.M., Merkulov S., McCrae K., Bhatia S.N., Sailor M., Ruoslahti E., (2009). Differential proteomics analysis of the surface heterogeneity of dextran ironoxide nanoparticles and the implications for their in vivo clearance. Biomaterials 30, 3926–3933.
266. Simo, A., Polte, J., Pfänder, N., Vainio, U. Emmerling, F. Rademann, K., (2012). Formation Mechanism of Silver Nanoparticles Stabilized in Glassy Matrices. J. Am. Chem. Soc 134, 18824–18833.
267. Skoglund, S., Lowe, T. A., Hedberg, J., Blomberg, E., Wallinder, I. O., Wold S., Lundin, M., (2013). Effect of laundry surfactants on surface charge and colloidal stability of silver nanoparticles. Langmuir 29, 8882–8891.
268. Skoog, D.A., Holler, F.J., Crouch, S.R., (2007). Principles of Instrumental Analysis Sixth Edition. Thomson Brooks/Cole. Thomson Learning Academic Resource Center. Kanada.
269. Smulders, E., Rybinski, W., Sung, E., Rähse, W., Steber, J., Nordskog, A. (2007). Laundry Detergents, Ullmann's Encyclopedia of Industrial Chemistry, Wiley-VCH.
270. Som, C., Wick, P., Krug, H., Nowack, B., (2011). Environmental and health effects of nanomaterials in nanotextiles and façade coatings Environ Int, 37, 1131-1142.

271. Soukupova, L., Kvitek, A., Panacek, T., Nevecna R., Zboril, R. , (2008). Comprehensive study on Surfactant Role on Silver Nanoparticles (NPs) Prepared via Modified Tollens Process. Materials Chemistry and Physics Vol. 111, No. 1, 77-81.
272. SPECFIT Global Analysis System With Expanded Factor Analysis & Marquardt Least Squares Minimization User Manual. (1993). Chapel Hill, SAD, Specfit Software Associates.
273. Fewtrell, L., (2014). Silver: water disinfection and toxicity. Centre for Research into Environment and Health. Dostupno na: http://www.who.int/water_sanitation_health/dwq/chemicals/Silver_water_disinfection_toxicity_2014V2.pdf (pristupljeno: svibanj 2017.).
274. Sreerama, N., Woody, R.W.,(2004). Computation and analysis of protein Circular Dichroism spectra. Methods in Enzymology 383, 318-351.
275. Steiner, RF., Roth, J., and Robbins, J., (1966). The Binding of Thyroxine by Serum Albumin as Measured by Fluorescence Quenching. J Biol Chem 241, 560-567.
276. Stekleneva, N.I., Shevtsova, A.I., Brazaluk O.Z., Kulinich, A.O. , (2010). Expression and structuralfunctional alterations of α-1-acid glycoprotein at the pathological state. Biopolymers and Cell 26, 265-272.
277. Stern, S.T., McNeil, S.E., (2008). Nanotechnology safety concerns revisited. Toxicological Sciences 101, 4-21. Stoimenov, P.K., Klinger, R.L., Marchin, G.L., Klabunde, K.J., (2002). Metal oxide nanoparticles as bactericidal agents. Langmuir 18, 6679–6686.
278. Sukhov, N. L., Ershov, N. B., Mikhalko, V. K. and Gordeev, A.V., (1997). Absorption spectra of large colloidal silver particles in aqueous solution. Russian Chemical Bulletin 46, 197–199.
279. Sun, R.W., Chen, R., Chung, N.P., Ho, C.M., Lin, C.L., Che, C.M., (2005). Silver nanoparticles fabricated in HEPES buffer exhibit cytoprotective activities toward HIV-1 infected cells. Chem. Commun 40,5059-5061.
280. Taguchi, K., Nishi, K., Tuan, G.C.V., Maruyama, T., Otagiri, M., (2013). Molecular Aspects of Human Alpha-1 Acid Glycoprotein — Structure and Function. Chapter 6. IntechOpen Limited, London, UK.
281. Tanga, X., Tsujia, M., Jiangc, P., Nishioa, M., Janga, S-M., Yoona, S-H., (2009). Rapid and high-yield synthesis of silver nanowires using air-assisted polyol method with chloride ions. Colloids and Surfaces A: Physicochemical and Engineering Aspects 338, 33–39.

282. Tavanti, F., Pedone, A., Menziani, M.C., (2015). Competitive Binding of Proteins to Gold Nanoparticles Disclosed by Molecular Dynamics Simulations. J. Phys. Chem 119, 22172−22180.
283. Technical note - Dynamic Light Scattering: An Introduction in 30 Minutes (2014) . http://www.malvern.com/en/pdf/secure/TN101104DynamicLightScatteringIntroduction.pdf (pristupljeno travanj 2017.)
284. Teeguarden, J.G., Hinderliter, P.M.,Orr,G.,Thrall, B.D. , Pounds, J.G., (2007). Particokinetics in vitro: dosimetry considerations for in vitro nanoparticle toxicity assessments. Toxicol Sci 95,300–312.
285. Tesseromatis, C., Alevizou, A.E., Tigka, R, Kotsiou, A., (2011). Acute-Phase Proteins: Alpha -1- Acid Glycoprotein. Chapter 11, DOI: 10.5772/22640.nema nista na internetu
286. Tejamaya, M., Römer, I., Merrifield, R. C., Lead, J. R., (2012). Stability of citrate, PVP, and PEG coated silver nanoparticles in ecotoxicology media.Environ. Sci. Technol 46, 7011–7017.
287. McWilliams, A., (2016) . The Maturing Nanotechnology Market: Products and Applications. BCC Research. Wellesley MA USA
288. Theilgaard-Mönch, K., Jacobsen L.C., Rasmussen, H., Niemann C.U., Udby, L., Borup, R., Gharib, M., Arkwright, P.D., Gombart, A.F., Calafat, J., Porse, B.T., Borregaard, N., (2005). Highly glycosylated α1-acid glycoprotein is synthesized in myelocytes, stored in secondary granules, and released by activated neutrophils. J Leukoc Biol 78, 462-470.
289. Thierry, F., Najet, M., Dominique, P., (2000). Alpha-1-acid glycoprotein. Elsevier Science, Biochimica et Biophysica Acta 1482, 157-171.
290. Toduka, Y., Toyooka, T., Ibuki, Y., (2012). Flow cytometric evaluation of nanoparticlesusing side-scattered light and reactive oxygen species-mediated Fluorescence - Correlation with genotoxicity. Environ. Sci. Technol. 46, 7629-7636.
291. Treuel, L., Nienhaus, G.U., (2012). Toward a molecular understanding of nanoparticle–protein interactions. Biophys Rev 4, 137–147.
292. Unrine, J.M., Colman, B.P., Bone, A.J., Gondikas, A.P., Matson, C.W., (2012). Biotic and Abiotic Interactions in Aquatic Microcosms Determine Fate and Toxicity of Ag Nanoparticles. Environ Sci Technol 46, 6915–6924.
293. Urbach, A.R., (2010). Circular Dichroism spectroscopy in the undergraduate curriculum. J Chem Ed 87, 891-893.

294. Usawadee, S., Morteza, M., Lionel, M., Jatuporn, S., Heinrich, H., (2014). Protein Corona Composition of Superparamagnetic Iron Oxide Nanoparticles with Various Physico-Chemical Properties and Coatings. Sci. Rep 4, 5020-5029
295. Van de Hulst, H.C., (1957). Light scattering by small particles. *New York: John Wiley & Sons*.
296. Van Oijen, A., (2008). Binding and kinetics. BCMP201.
297. Vance, M. E., Kuiken, T., Vejerano, E. P., McGinnis, S. P., Hochella, M. F., Rejeski, D., Hull, M. S., (2015). Nanotechnology in the real world: Redeveloping the nanomaterial consumer products inventory. Beilstein Journal of Nanotechnology 6, 1769-1780.
298. Varshney, A., Ahmad, B., Khan, R.H., (2008). Comparative studies of unfolding and binding of ligands to human serum albumin in the presence of fatty acid: spectroscopic approach. Int J Biol Macromol 42, 483-490.
299. Ventola, C. L., (2015). The Antibiotic Resistance Crisis: Part 1: Causes and Threats. Pharmacy and Therapeutics 40, 277–283.
300. Vidic, J.; Haque, F.; Guigner, J. M.; Vidy, A.; Chevalier, C., Stankic, S., (2014). Effects of water and cell culture media on the physicochemical properties of ZnMgO nanoparticles and their toxicity toward mammalian cells. Langmuir 30, 11366–11374.
301. Vinković Vrček, I., Žuntar, I., Petlevski, R., Pavičić, I., Dutour Sikirić, M., Čurlin, M., Goessler, W., (2014.). Comparison of In Vitro Toxicity of Silver Ions and Silver Nanoparticles on Human Hepatoma Cells. Environ Toxicol 31, 679-692.
302. Wadhera, A., Fung, M., (2005). Systemic argyria associated with ingestion of colloidal silver. Dermatology Online Journal. 1, 11-12.
303. Walczyk, D., Baldelli Bombelli, F., Monopoli, M.P., Lynch, I., Dawson, K.A., (2010). What the Cell ―Sees‖ in Bionanoscience. J Am Chem Soc 132, 5761–5768.
304. Walkey, C.D., Olsen, J.B., Guo, H., Emili A., Chan, W.C.W., (2012). Nanoparticle Size and Surface Chemistry Determine Serum Protein Adsorption and Macrophage Uptake. J Am Chem Soc 134, 2139–2147.
305. Walkey, C.D., Chan, W.C., (2012). Understanding and controlling the interaction of nanomaterials with proteins in a physiological environment. Chem Soc Rev 41, 2780–2799.
306. Walser, T., Demou, E., Lang, D.J., Hellweg, S., (2011). Prospective environmental life cycle assessment of nanosilver t-shirts. Environ. Sci. Technol 45, 4570 – 4578.

307. Wang, H., Wu, L., Reinhard, B.M., (2012). Scavenger receptor mediated endocytosis ofsilver nanoparticles into J774A.1 macrophages is heterogeneous. ACS Nano 6, 7122-7132.
308. Watanabe, H., Tanase, S., Nakajou, K., (2000). Role of Arg-410 and Tyr-411 in human serum albumin for ligand binding and esterase-like activity. Biochem J 349,813-819.
309. Wijnhoven, S.W.P., Peijnenburg, W.J.G.M., Herberts, C.A., Hagens, W.I., Oomen, A.G., Heugens, E.H.W., Roszek, B., Bisschops, J., Gosens, I., Van de Meent, D., Dekkers, S., de Jong, W.H., van Zijverden, M., Sips, A.J.A.M., Geertsma, R.E., (2009). Nanosilver – a review of available data and knowledge gaps in human and environmental risk assessment. Nanotoxicology 3, 109-138.
310. Williams, D.B., Carter, B.,(2009). Transmission Electron Microscopy A Textbook for Materials Science. Springer 1, 3-22.
311. Wright, J.B., Lam, K., Hansen, D., Burrell, R.E., (1999). Efficiacy of topical silver against fungal burn wound pathogens. Am. J. Infect. Control 27, 344-350.
312. Wu,T.W.,Wu, J.,Li,R.K.,Mickle,D., Carey, D., (1991). Albumin-bound bilirubins protect human ventricular myocytes against oxyradical damage.Biochem CellBiol 69, 683-688
313. Xiu, Z.-M., Ma, J., Alvarez, P. J. J. (2011). Differential Effect of Common Ligands and Molecular Oxygen on Antimicrobial Activity of Silver Nanoparticles versus Silver Ions. Environ. Sci. Technol 45 , 9003−9008
314. Yallapu, M.M., Ebeling, M.C., Jaggi, M., Chauhan, S.C., (2013). Plasma Proteins Interaction with Curcumin Nanoparticles: Implications in Cancer Therapeutics. Curr Drug Metab 14, 504–515.
315. Yallapu, M.M., Ebeling, M.C., Jaggi, M., Chauhan, S.C., (2013). Plasma Proteins Interaction with Curcumin Nanoparticles: Implications in Cancer Therapeutics. Curr Drug Metab. 14,504–515.
316. Yang, X., Gondikas, A.P. , Marinakos, S.M. , Auffan, M., Liu, J.,Hsu-Kim, H.,Meyer, J.N., (2012). Mechanism of Silver Nanoparticle Toxicity Is Dependent on Dissolved Silver and Surface Coating in Caenorhabditis elegans. Environ Sci Technol 46, 1119–1127.
317. Yin, Y., Li, Z.Y., Zhong, Z., Gates, B., Xia,Y., Venkateswaran, S., (2002). Synthesis and characterization of stable aqueous dispersions of silver nanoparticles through the Tollens process. Journal of Materials Chemistry 12, 522–527.
318. Yonezawa, S., Onoue S., Kimizuka, N., (2000). Preparation of Highly Positively Charged Silver Nanoballs and Their Stability. Langmuir 16, 5218–5220.

319. Yonezawa, T., Onoue, S., Kimizuka, N., (2005). Colloids and Surfaces A: Physicochemical and Engineering Aspects 256, 111–115.
320. Yu, D. and Yam, V.W., (2005). Hydrothermal-induced assembly of colloidal silver spheres into various nanoparticles on the basis of HTAB-modified silver mirror reaction. J Phys Chem B 109, 5497-5503.
321. Zhang, L., Gu, F.X., Chan, J.M., Wang, A.Z., Langer, R.S., Farokhzad, O.C., (2008). Nanoparticles in Medicine: Therapeutic Applications and Developments. Clinical Pharmacology Therapeutics 83, 761-769.
322. Zeng, X.Y., Zhang, Q.K., Yu, R.M., Lu, C.Z., (2010). A new transparent conductor: Silver nanowire film buried at the surface of a transparent polymer. Adv. Mater 22, 4484–4488.
323. Zetasizer NanoUser Manual. Malvern Instruments .
324. Zhang, W., Zhang Q., Wang F., Yuan L., Xu Z., Jiang F., Liu Y., (2015). Comparison of interactions between human serum albumin and silver nanoparticles of different sizes using spectroscopic methods. Luminiscence 30, 397-404.
325. Zheng, X., Zhu, L., Yan, A.,Wang,X.,Xie. Y., (2003). Controlling synthesis of silver nanowires and dendrites in mixed surfactant solutions. J. Colloid Interface Sci 268, 357–361.
326. Zook, J.M., Halter, M.D., Cleveland, D., Long, S.E., (2012). Disentangling the effects of polymer coatings on silver nanoparticle agglomeration, dissolution and toxicity to determine mechanisms of nanotoxicity. Springer, Nanopart Res 14,1165-1174.
327. Zook, J.M., MacCuspie, R.I., Locasicio L.E., Halter M.D., Elliott J.T., (2011). Stable Nanoparticle Aggregates/Agglomerates of Different Sizes and the Effect of Their Size on Hemolytic Cytotoxicity. Nanotoxicology 5, 517–530.

7. DODATNI PRIKAZI REZULTATA

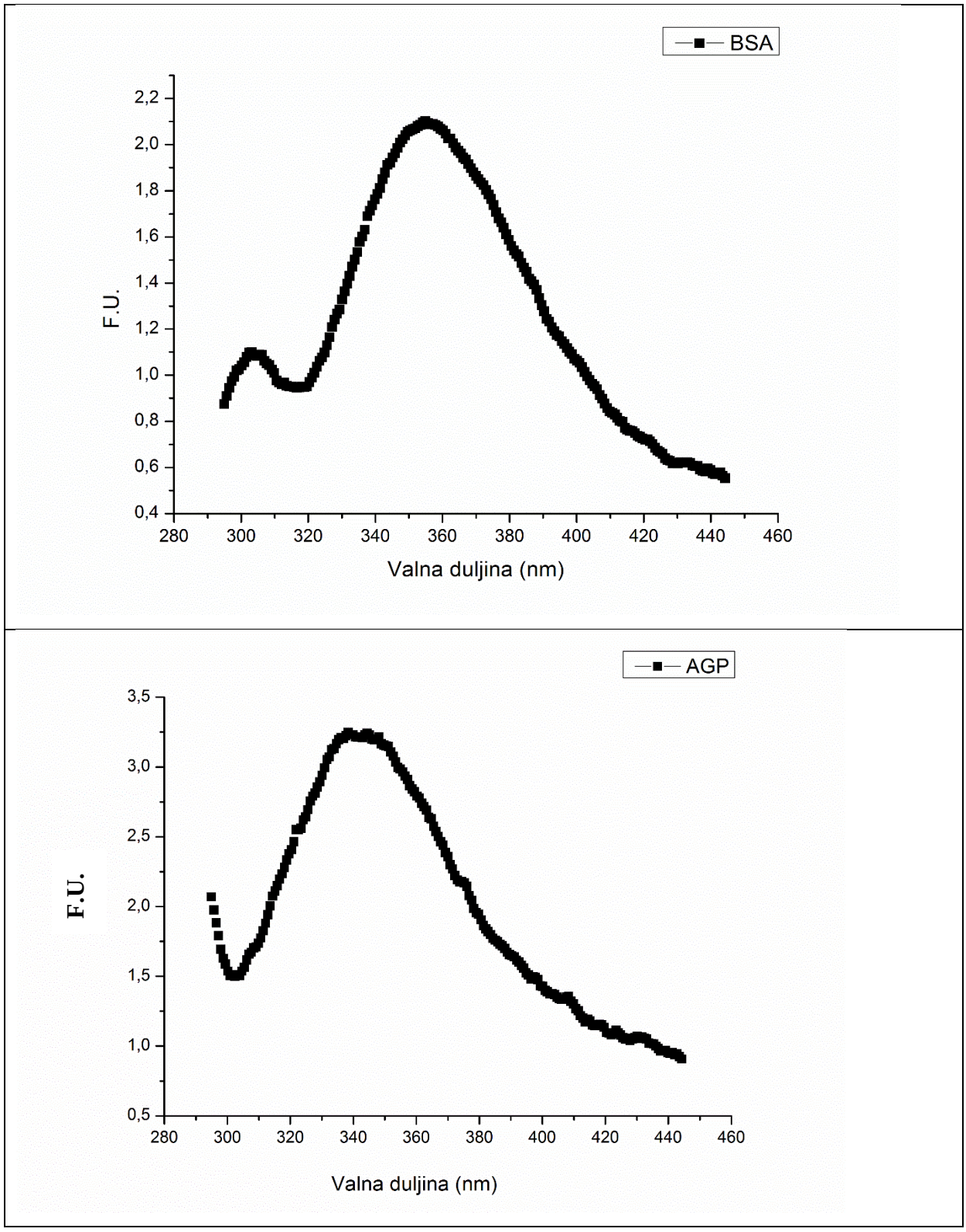

Slika 51. Fluorescencijski spektri proteina BSA (0,1 μM) i AGP (0,2 μM).

AOT10sph

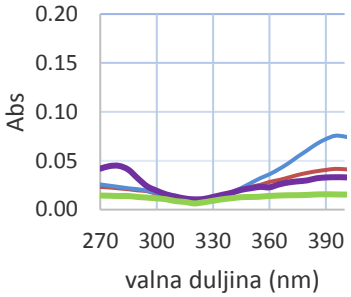

PVP10sph

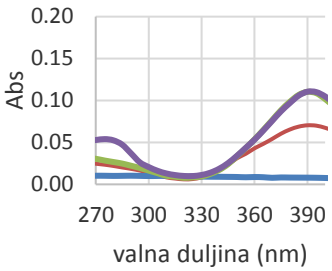

TW10sph

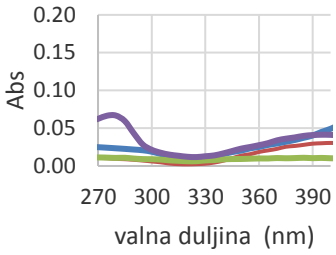

PLL10sph

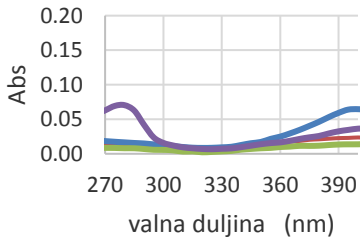

CTA10sph

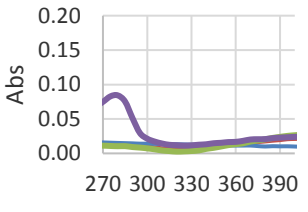

CIT10sph

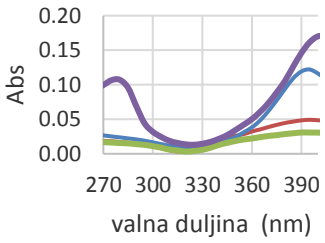

BSA10sph

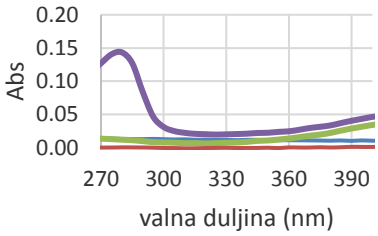

Brij10sph

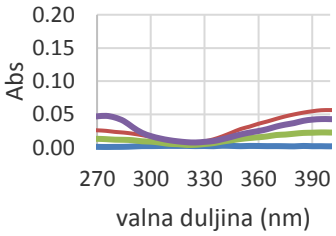

AOT 50sph

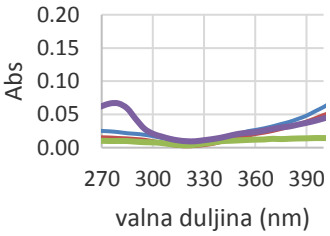

CIT50sph

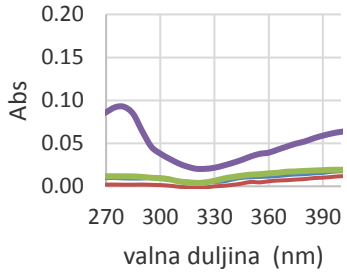

CTA50sph

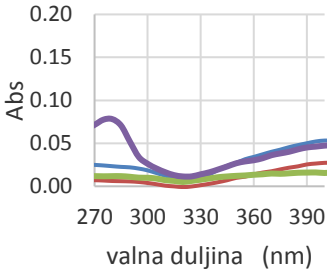

PVP50sph

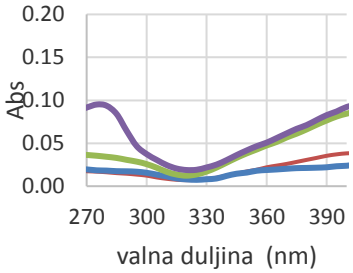

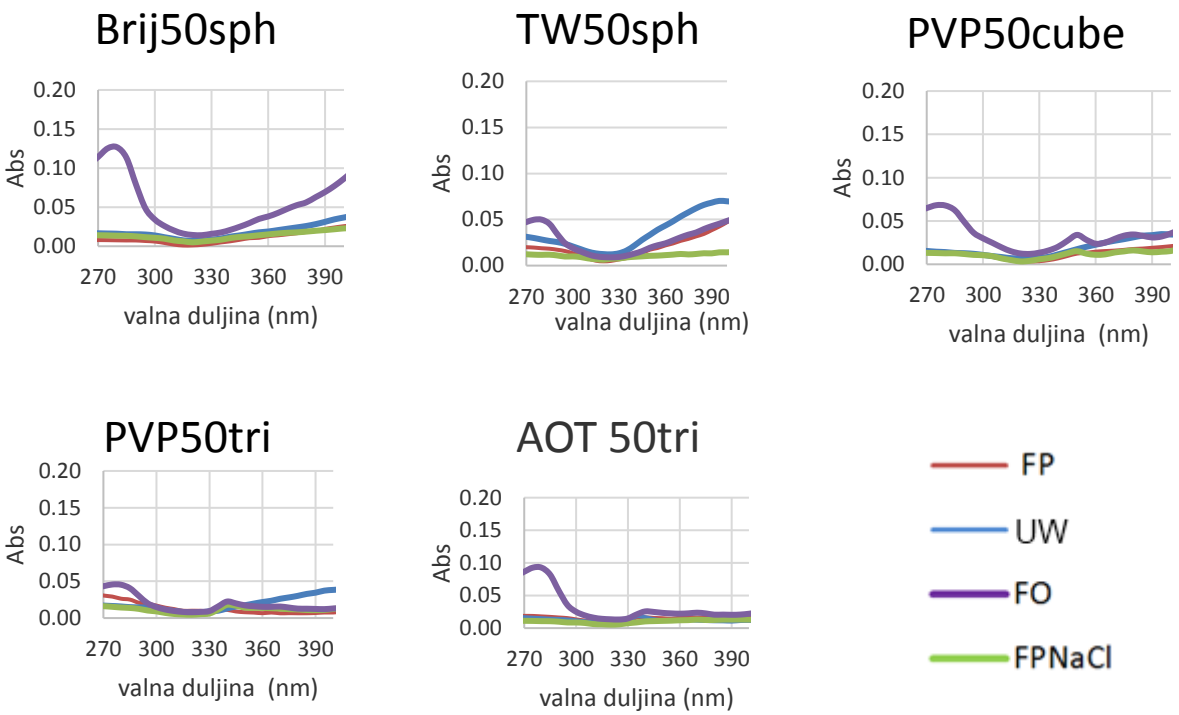

Slika 52. UV-VIS spektri nanočestica srebra u UW, FP, FO i FPNaCl pri koncentraciji AgNP od 10μM (270 nm – 390 nm)

AOT10sph

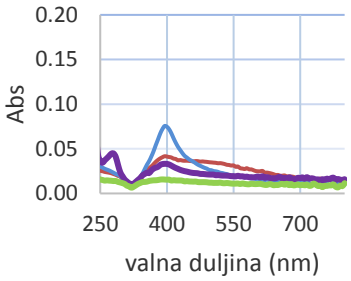

PVP10sph

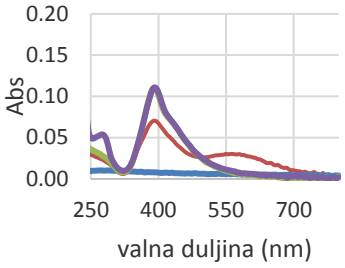

TW10sph

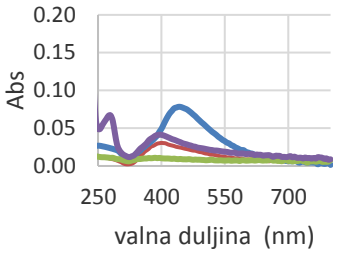

PLL10sph

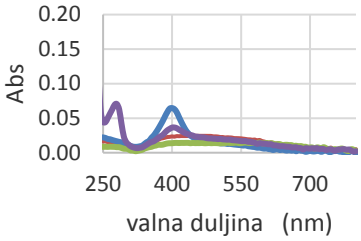

CTA10sph

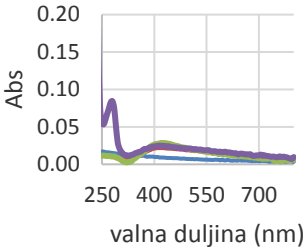

CIT10sph

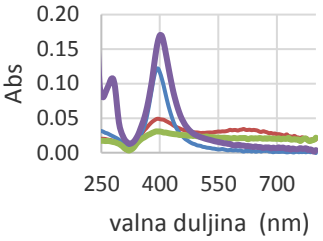

BSA10sph

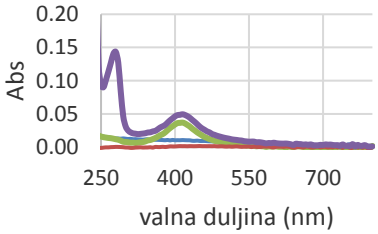

Brij10sph

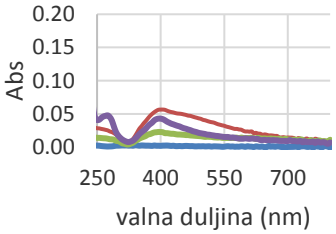

AOT 50sph

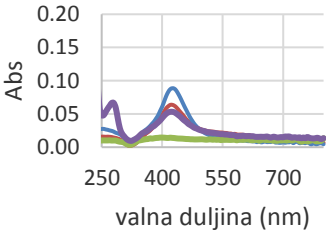

CIT50sph

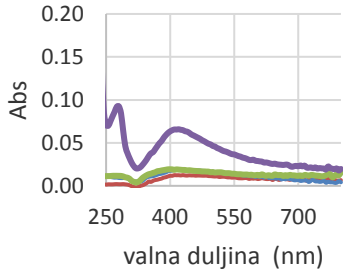

CTA50sph

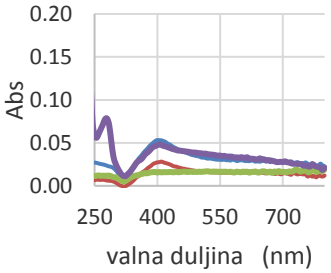

PVP50sph

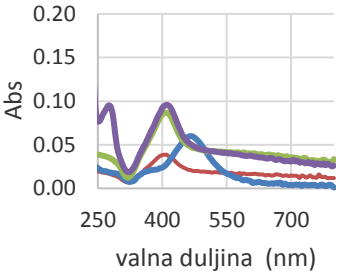

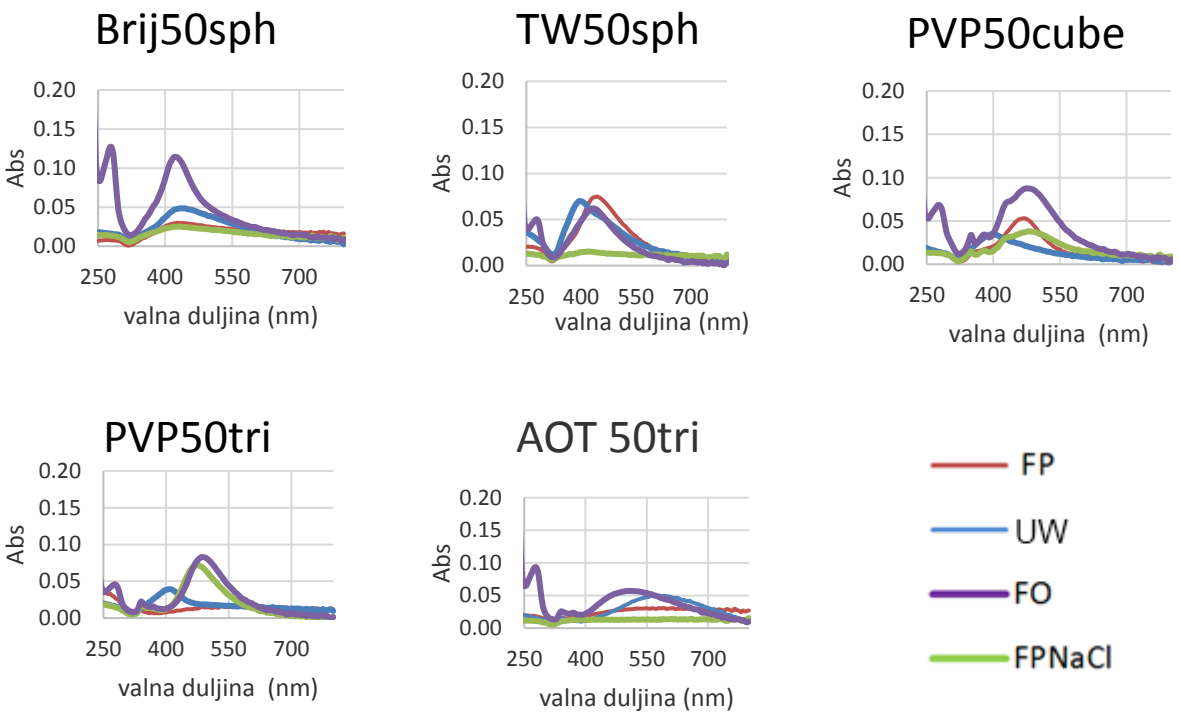

Slika 53. UV-VIS spektri nanočestica srebra u UW, FP, FO i FPNaCl pri koncentraciji AgNP od 10μM (250 nm – 800 nm)

Tablica 22. Korelacije fizikalno kemijskih varijabli u FP. (PB_pKa.sta). Korelacije su značajne ako je p <.05000.

	d_H (nm)	ζ (mV)	A(m^2/g)	logKaBSA	logKaAGP
dH(nm)	1,0000	-,1983	-,3454	,3132	-,0714
	p= ---	p=,430	p=,160	p=,206	p=,778
ζ (mV)	-,1983	1,0000	-,0772	-,1887	,0821
	p=,430	p= ---	p=,761	p=,453	p=,746
A(m^2/g)	-,3454	-,0772	1,0000	-,0225	,2898
	p=,160	p=,761	p= ---	p=,930	p=,243
log K_a BSA	,3132	-,1887	-,0225	1,0000	,0408
	p=,206	p=,453	p=,930	p= ---	p=,872
log K_a AGP	-,0714	,0821	,2898	,0408	1,0000
	p=,778	p=,746	p=,243	p=,872	p= ---

Tablica 23. Antimikrobna učinkovitost (minimalna baktericidna koncentracija, MBC) različito obloženih 10 nm i 50 nm AgNP i $AgNO_3$ prema E. coli i S. aureus nakon 4 h i 24 h inkubacije u deioniziranoj vodi.

AgNP	*Escherichia coli* MG1655		*Staphylococcus aureus* 6538	
	4 h MBC ± SD (mg Ag/L)	24 h MBC ± SD (mg Ag/L)	4 h MBC ±SD (mg Ag/L)	24 h MBC ± SD (mg Ag/L)
$AgNO_3$	0,02±0,01	0,02±0,01	0,16±0,10	0,05±0,02
CIT10sph	0,20±0,09	0,14±0,09	2,75±1,66	0,35±0,13
AOT10sph	0,08±0,04	0,07±0,04	1,00±0,35	0,18±0,07
PVP10sph	0,16±0,11	0,05±0,02	1,75±0,82	0,29±0,14
TW10sph	0,35±0,20	0,26±0,21	9,38±3,61	0,89±0,33
CTA10sph	0,25±0,18	0,11±0,03	2,13±0,75	0,50±0,18
PLL10sph	0,13±0,09	0,08±0,05	1,81±0,80	0,35±0,13
CIT50sph	0,19±0,07	0,21±0,17	7,50±2,89	0,56±0,07
AOT50sph	0,83±0,29	0,31±0,15	8,75±2,50	2,13±1,92
PVP50sph	0,58±0,41	0,28±0,21	3,38± 1,11	0,38±0,22
TW50sph	4,17±1,44	3,75±2,17	10,00± 0,00	6,50±3,35
CTA50sph	5,00±0,00	0,63±0,27	10,00±0,00	3,44±1,88

Prikazani podaci su prosjek od 3-5 ponovljenih mjerenja. Mapiranje topline: od crvene do zelene što prikazuje slijed od toksičnije do manje toksične.

Tablica 24. Specifična površina čestica izražena kao m^2 po g uzorka

AgNP	specifična površina /m^2 po g uzorka			
	UW	**FO**	**FP**	**FPNaCl**
AOT 10sph	30,2	3,68	30,53	6,49
PVP10sph	62,1	67,16	21,63	46,53
Tween10sph	99,6	96,26	36,05	22,82
PLL10sph	44,4	17,28	2,54	0,02
CTA10sph	49,4	1,56	0,27	2,19
CIT10sph	25,2	16,29	10,68	1,75
BSA10sph	5,8	3,26	4,37	2,08
AOT 50sph	2,8	4,64	1,49	5,79
CIT50sph	3,7	11,30	3,67	1,04
CTA50sph	2,2	1,24	0,92	1,08
PVP50sph	4,5	6,42	8,86	1,97
Brij50sph	13,2	4,74	0,74	0,04
Tween50sph	8,9	5,83	6,40	1,82
PVP50tri	9,2	0,88	2,25	2,87
AOT50tri	7,3	1,33	3,50	3,54
PVP50CUBE	6,3	4,59	4,39	5,04

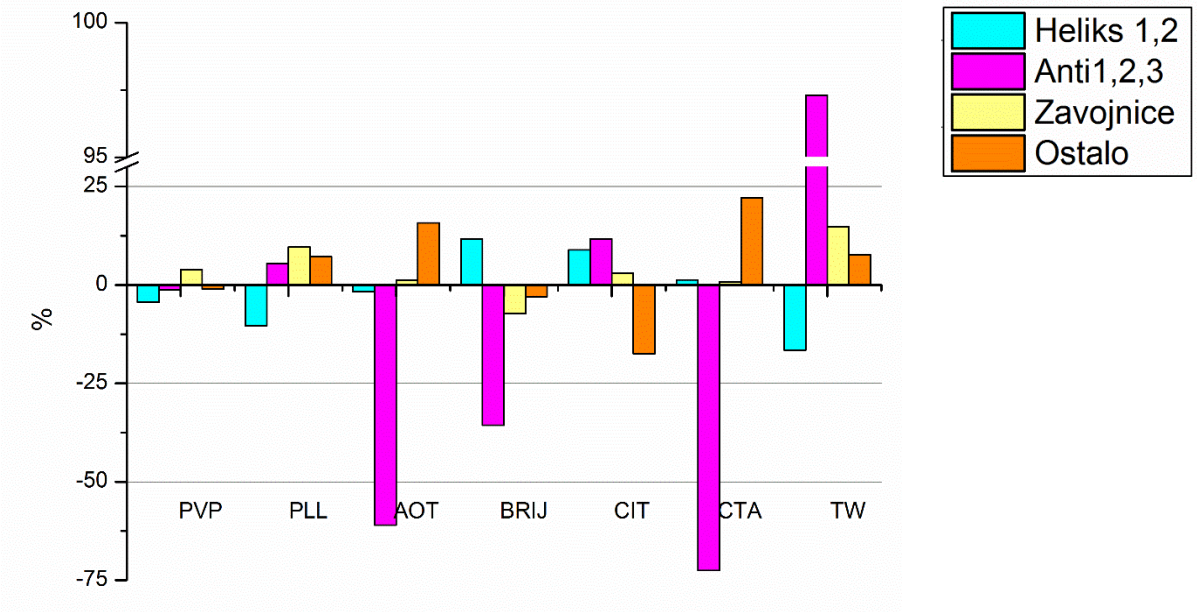

Slika 54. Promjena strukuture BSA u interakciji s AgNP10 u koncetraciji od 10 μM.

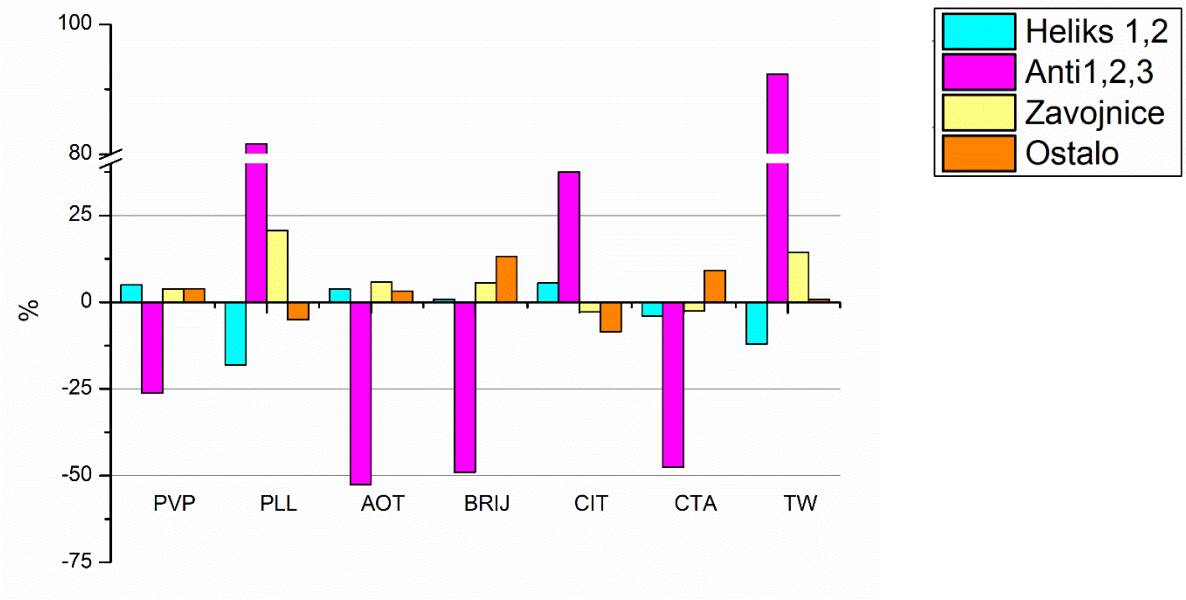

Slika 55. Promjena strukuture BSA u interakciji s AgNP10 u koncetraciji od 50 μM.

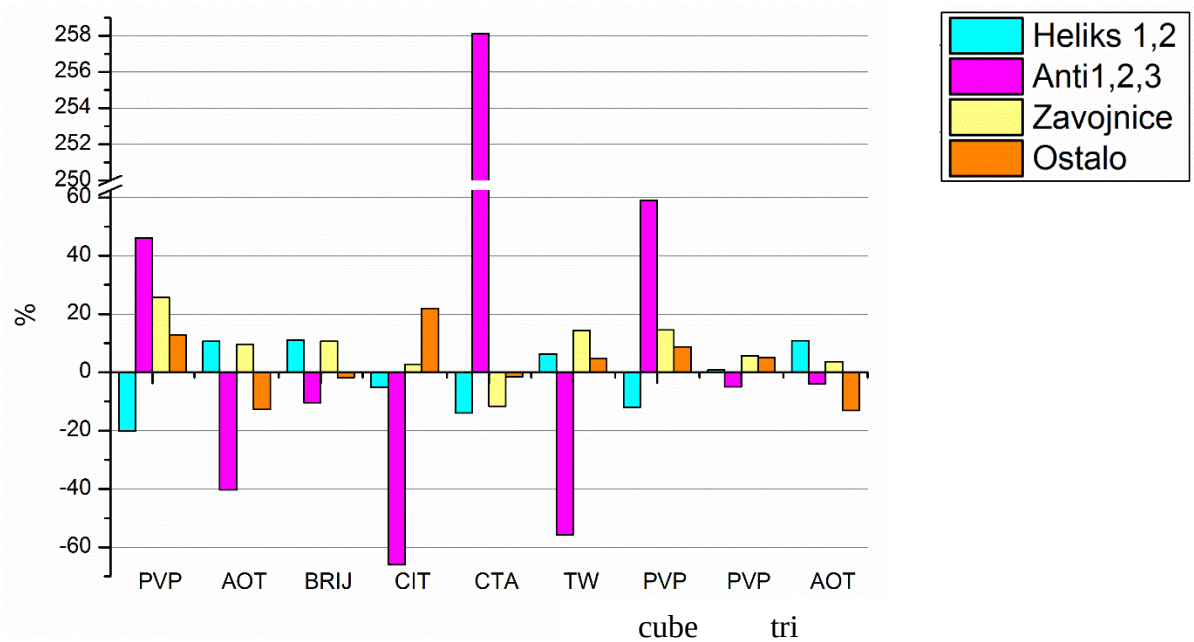

Slika 56. Promjena strukuture BSA u interakciji s AgNP50 u koncetraciji od 10 μM.

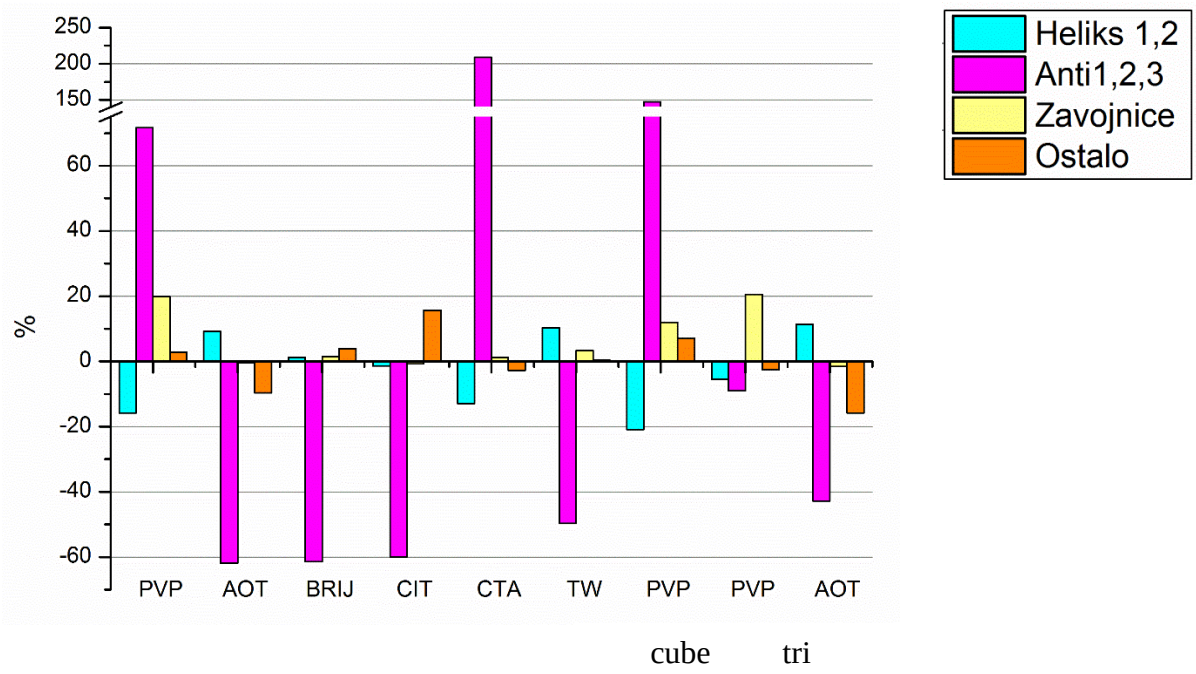

Slika 57. Promjena strukuture BSA u interakciji s AgNP50 u koncetraciji od 50 μM.

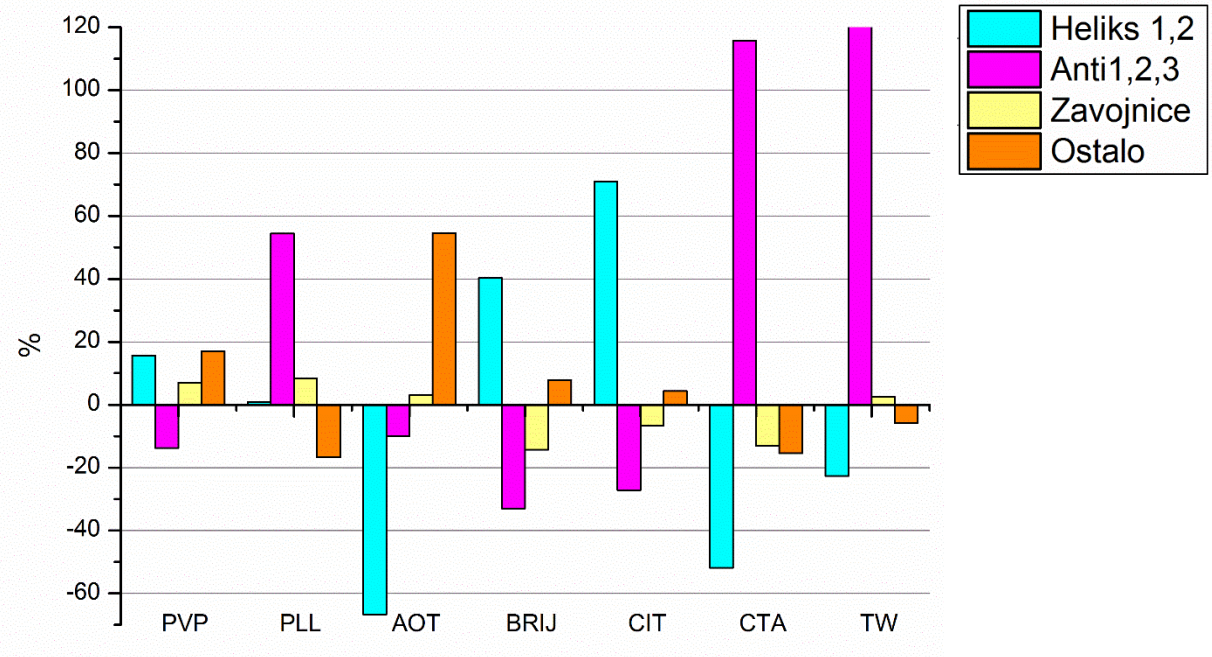

Slika 58. Promjena strukuture AGP u interakciji s AgNP10 u koncetraciji od 10 μM.

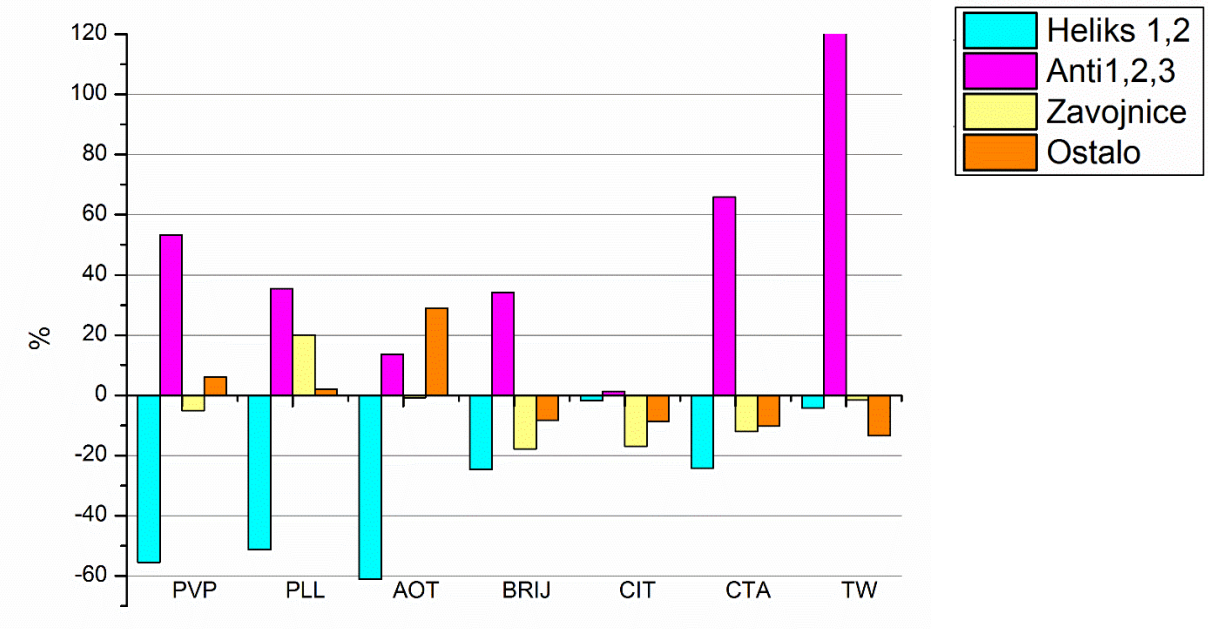

Slika 59. Promjena strukuture AGP u interakciji s AgNP10 u koncetraciji od 50 μM.

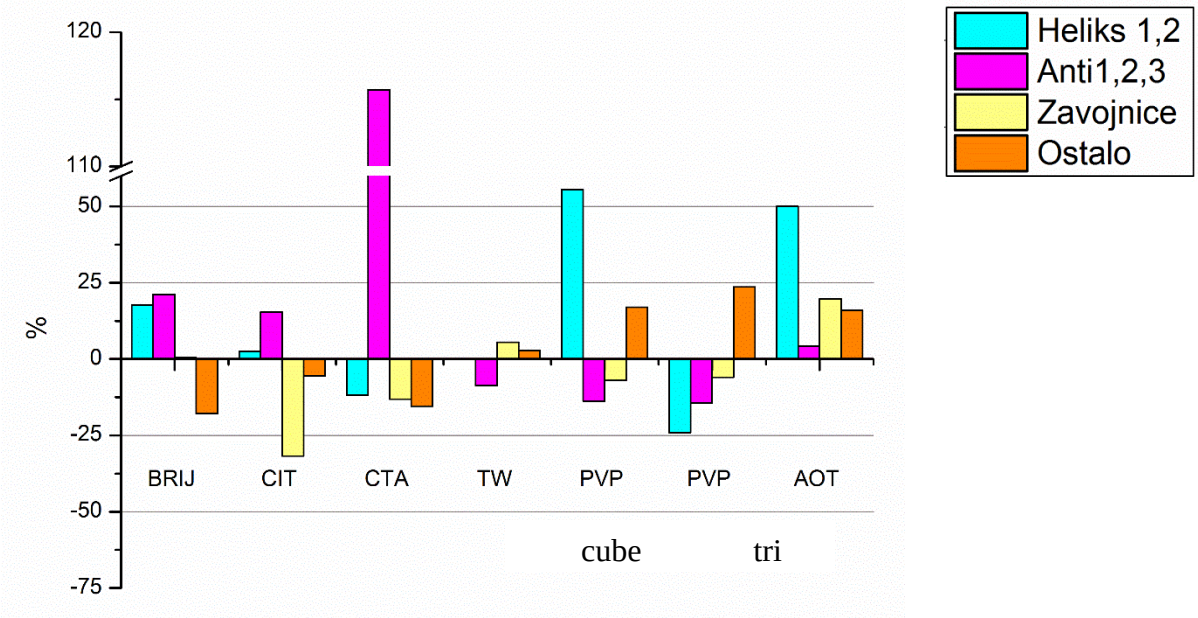

Slika 60. Promjena strukuture AGP u interakciji s AgNP50 u koncetraciji od 10 μM.

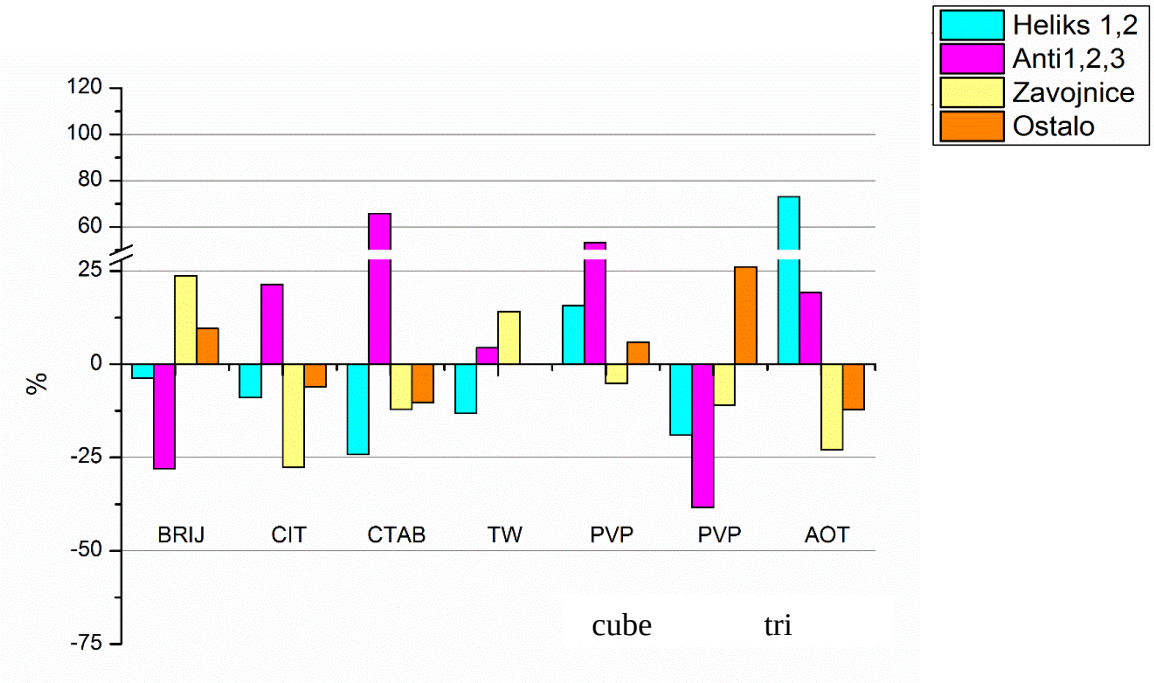

Slika 61. Promjena strukuture AGP u interakciji s AgNP50 u koncetraciji od 50 μM.

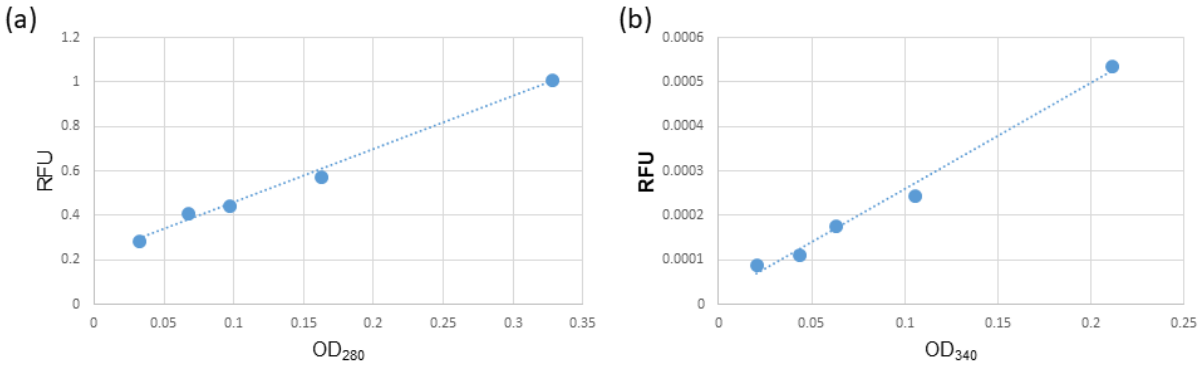

Slika 62. Odnos intenziteta fluorescencije prema absorbanciji kod različitih koncentracija AgNP (u rasponu od 10 do 1000 μM).

PRILOZI

Ovaj prilog sadrži tri izvorna znanstvena rada objavljena u časopisima zastupljenim u bazama Current Contents koji obrađuju rezultate iznesene u ovom doktorskom radu, te jedan pregledni znanstveni rad objavljen u časopisu iz Web of Science baze:

1. Domazet Jurašin, Darija; Ćurlin, Marija; Capjak, Ivona; Crnković, Tea; Lovrić, Marija; Babič, Michal; Horák, Daniel; Vinković Vrček, Ivana; Gajović, Srećko. Surface coating affects behavior of metallic nanoparticles in a biological environment. // Beilstein Journal of Nanotechnology. (2016) , 7; 246-262. (izvorni znanstveni rad)
2. Capjak, Ivona; Šupraha Goreta, Sandra; Domazet Jurašin, Darija; Vinković Vrček, Ivana. How protein coronas determine the fate of engineered nanoparticles in biological environment. Arhiv za higijenu rada i toksikologiju. 68 (2017) , 4; 245-253. (pregledni znanstveni rad)
3. Kubo, Anna-Liisa; Capjak, Ivona; Vinković Vrček, Ivana; Bondarenko, Olesja M.; Kurvet, Imbi; Vija, Heiki; Ivask, Angela; Kasemets, Kaja; Kahru, Anne. Antimicrobial potency of differently coated 10 and 50 nm silver nanoparticles against clinically relevant bacteria Escherichia coli and Staphylococcus aureus. // Colloids and surfaces. B, Biointerfaces. 170 (2018) , 1 October; 401-410. (izvorni znanstveni rad)
4. Capjak, Ivona; Zebić Avdičević, Maja; Dutour Sikirić, Maja; Domazet Jurašin, Darija; Amela Hozić, Amela; Pajić, Damir; Dobrović, Slaven; Goessler, Walter; Vinkovic Vrcek, Ivana. Behavior of silver nanoparticles in wastewater: systematic investigation on the combined effects of surfactants and electrolytes in the model systems. // Environmental Science: Water Research and Technology. 4 (2018); 2146-2159. (izvorni znanstveni rad)

BEILSTEIN JOURNAL OF NANOTECHNOLOGY

Surface coating affects behavior of metallic nanoparticles in a biological environment

Darija Domazet Jurašin[1], Marija Ćurlin[2], Ivona Capjak[3], Tea Crnković[4], Marija Lovrić[2], Michal Babič[5], Daniel Horák[5], Ivana Vinković Vrček[*6,§] and Srećko Gajović[2]

Full Research Paper

Open Access

Address:
[1]Division of Physical Chemistry, Ruđer Bošković Institute, Bijenička cesta 54, 10 000 Zagreb, Croatia, [2]School of Medicine, Croatian Institute for Brain Research, University of Zagreb, Šalata 3, 10 000 Zagreb, Croatia, [3]Croatian Institute of Transfusion Medicine, Petrova 3, 10 000 Zagreb, Croatia, [4]Faculty for Pharmacy and Biochemistry, University of Zagreb, Ante Kovačića 1, 10 000 Zagreb, Croatia, [5]Institute of Macromolecular Chemistry, Academy of Sciences of the Czech Republic, Heyrovský Sq. 2, 162 06 Prague 6, Czech Republic and [6]Institute for Medical Research and Occupational Health, Ksaverska cesta 2, 10 000 Zagreb, Croatia

Email:
Ivana Vinković Vrček[*] - ivinkovic@imi.hr

* Corresponding author
§ Tel.: +385 1 4682540; Fax: +385 1 4673303

Keywords:
biological fluids; colloidal stability; maghemite; nanoparticles; protein interaction; silver; surface coating

Beilstein J. Nanotechnol. **2016,** *7,* 246–262.
doi:10.3762/bjnano.7.23

Received: 11 November 2015
Accepted: 04 February 2016
Published: 15 February 2016

Associate Editor: M. Stenzel

Abstract

Silver (AgNPs) and maghemite, i.e., superparamagnetic iron oxide nanoparticles (SPIONs) are promising candidates for new medical applications, which implies the need for strict information regarding their physicochemical characteristics and behavior in a biological environment. The currently developed AgNPs and SPIONs encompass a myriad of sizes and surface coatings, which affect NPs properties and may improve their biocompatibility. This study is aimed to evaluate the effects of surface coating on colloidal stability and behavior of AgNPs and SPIONs in modelled biological environments using dynamic and electrophoretic light scattering techniques, as well as transmission electron microscopy to visualize the behavior of the NP. Three dispersion media were investigated: ultrapure water (UW), biological cell culture medium without addition of protein (BM), and BM supplemented with common serum protein (BMP). The obtained results showed that different coating agents on AgNPs and SPIONs produced different stabilities in the same biological media. The combination of negative charge and high adsorption strength of coating agents proved to be important for achieving good stability of metallic NPs in electrolyte-rich fluids. Most importantly, the presence of proteins provided colloidal stabilization to metallic NPs in biological fluids regardless of their chemical composition, surface structure and surface charge. In addition, an assessment of AgNP and SPION behavior in real biological fluids, rat whole blood (WhBl) and blood plasma (BlPl), revealed that the composition of a biological medium is crucial for the colloidal stability and type of metallic NP transformation. Our results highlight the importance of physicochemical characterization and stability evaluation of metallic NPs in a variety of biological systems including as many NP properties as possible.

Introduction

Functional nanomaterials, including nanoparticles, nanocrystals, and nanoclusters, are promising tools for new medicinal applications, particularly for clinical use in disease diagnosis and treatment [1,2]. However, only a few nanomaterials are currently in use for medical purposes [3], for example silver nanoparticles (AgNPs) and superparamagnetic iron oxide nanoparticles (SPIONs). AgNPs are exploited in medicine for biocidal therapy owing to their antibacterial, antifungal, antiviral, and anti-inflammatory properties. In addition, they attract great interest for application in a variety of other commercial products, such as mobile phones, textiles, food storage containers, refrigerators, and cosmetics [1,2]. SPIONs are exploited in numerous in vitro and in vivo biomedical applications, but the most important is their use in imaging and drug delivery systems [4]. The biomedical applications of AgNPs and SPIONs imply uptake into the body, which consequently leads to interactions with protein-containing biological fluids [5,6]. Therefore, it is of increasing interest to systematically collect detailed information on their physicochemical properties and behavior in a biological environment. Despite a considerable number of studies on the colloidal stability of AgNPs and SPIONs in cell culture media, in natural water, or in the formulation of consumer products [2,7-14], general conclusions and a clear understanding of their fate in living organisms are still lacking.

In comparison to the bulk material, the colloidal stability of the nanoparticulate form of metal is usually more complicated. In colloidal systems, there are several possible interactions between the surface atoms of NPs and the molecules present in the media like dissolution, adsorption, binding, and aggregation, all influencing biological impacts by affecting reactive oxygen species generation, cellular uptake and NP biodistribution [15-18]. Metallic NPs usually aggregate in media with high electrolyte content that correspond to biological fluids [19-27]. NP agglomeration is intended in some applications, such as in immunoassays [28], while many others require stable colloidal dispersions of NPs at high physiological ionic strength [29]. Stabilization of metallic NPs at high electrolyte content, i.e., in biological media, may be achieved by electrostatic or steric repulsions [30-32].

Various types of surface coatings have been shown to affect NP properties, particularly to improve their biocompatibility and stability against agglomeration [30,33-35]. Proteins or biologically-compatible surfactants may serve as desirable barriers preventing NPs from agglomeration in biomedical applications [18]. Moreover, when NPs enter a biological fluid, electrostatic, dispersive, and covalent interactions cause proteins to adsorb on NP surfaces, leading to the formation of a dynamic protein corona [30,36-38]. The nature and the concentration of these proteins not only determine the behavior and biological identity of the NPs, but consequently biouptake, biodistribution and possible unwanted biological side effects [39-41]. It has already been shown that the size of the NP correlates with the uptake and toxicity of metallic NPs [41,42], whereas differences in surface coatings influence cytotoxicity and surface charge [43]. However, it is still unclear how different surface coatings affect the interaction of NPs with biological environments and the formation of the protein corona.

Because AgNPs and SPIONs with various coatings are used in many nanotherapeutic and consumer products [44], it has become critical to fill the knowledge gap surrounding the mechanisms of colloidal destabilization including the role of surface coating in the biocompatibility of metallic NP. The systematically collected and thoroughly analyzed data presented in this study will provide further insight into the behavior of AgNPs and SPIONs in complex biological media and the influence of surface properties on their colloidal stability. Furthermore, the obtained results contribute to the understanding of principal factors governing the behavior of metallic NPs in modelled and real biological fluids.

The aim of this study was to analyze the colloidal stability and behavior of differently coated AgNPs and SPIONs under conditions close to those found in biological fluids. A systematic investigation was performed using a set of eight kinds of AgNPs and three kinds of SPIONs, each of similar size but stabilized with different surface coatings. For the purpose of systematic investigation, surface coatings were chosen following several criteria: (a) to include non-ionic as well as positively and negatively charged coatings, (b) to employ coatings of different chemical functionality, i.e., polymers, surfactants, small ionic molecules, (c) to include coatings of different hydrophilic–hydrophobic balance in molecular structure. The selected coating agents enabled us to investigate the influence of electrostatic and/or steric effects on the stabilization of NPs. Thus, AgNPs were produced with the following coatings (Figure 1): trisodium citrate (CITAgNP), sodium bis(2-ethylhexyl) sulfosuccinate (AOTAgNP), cetyltrimethylammonium bromide (CTAAgNP), poly(vinylpyrrolidone) (PVPAgNP), poly(L-lysine) (PLLAgNP), bovine serum albumin (BSAAgNPs), Brij 35 (BrijAgNP) and Tween 20 (TweenAgNP). The SPIONs were prepared as uncoated γ-Fe_2O_3 NPs (UNSPIONs), and coated with D-mannose (MANSPIONs) or poly(L-lysine) (PLLSPIONs). Three media for NP dispersion were investigated: ultrapure water (UW), biological cell culture medium without addition of protein (BM), and BM supplemented with common serum protein (BMP). In

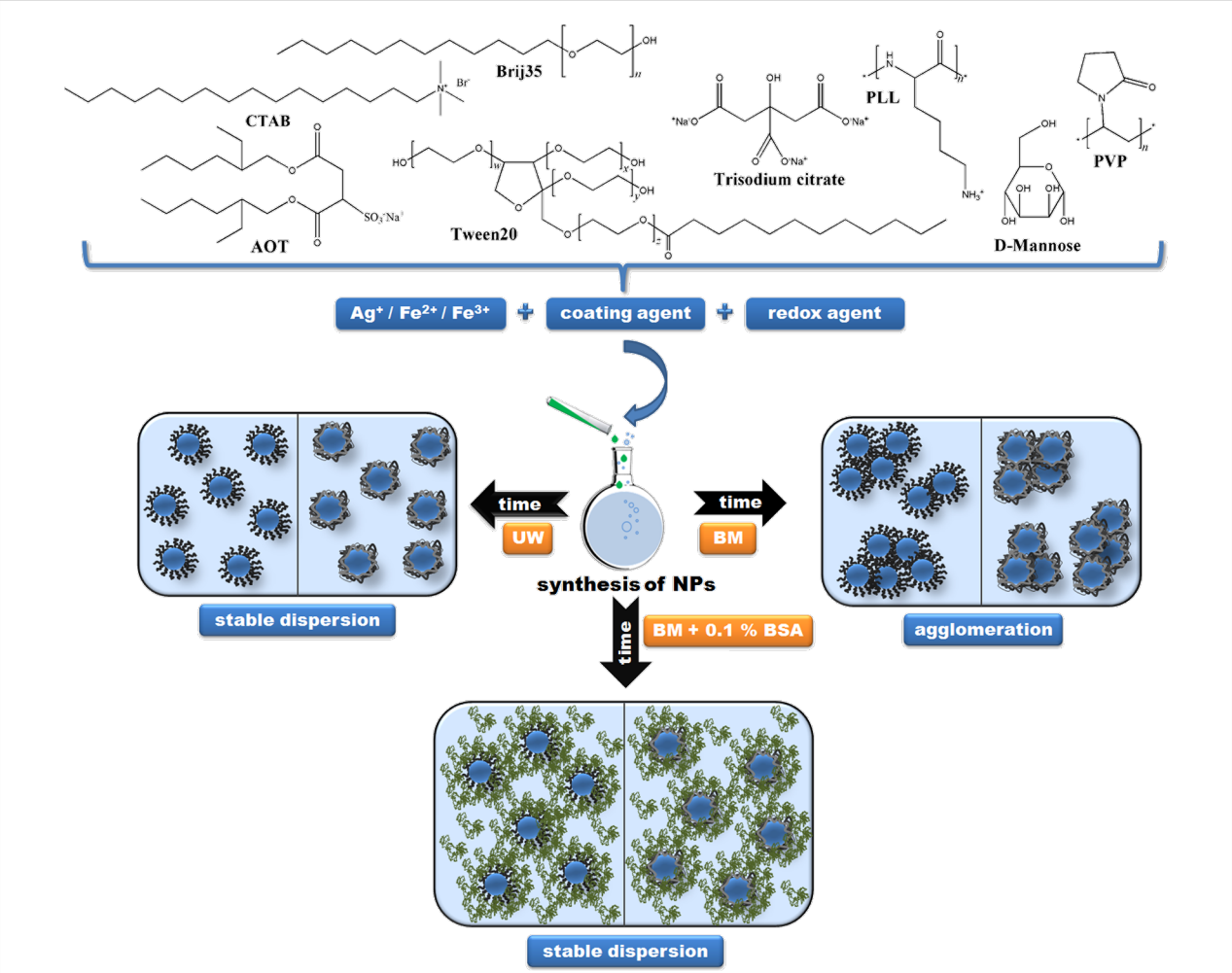

Figure 1: Experimental setup for stability evaluation of differently coated metallic nanoparticles in different media (UW - ultrapure water, BM - biological cell culture medium without addition of protein, BMP - BM supplemented with common serum protein).

addition, the behavior of NPs was investigated in real biological fluids: whole blood (WhBl) and blood plasma (BlPl) taken from Wistar rats. Dulbecco's modified Eagle's medium (DMEM), as a common cell culture medium for a broad range of mammalian cells, was used as a model biological fluid. Bovine serum albumin (BSA) served as a model serum protein due to its biological relevance and high significance in biomedical applications. Albumin is the most abundant protein in mammalian blood plasma and has outstanding buffering ability [3,45]. In addressing the effects of surface coating on the stability and behavior of NPs in selected model biological environments, three types of widely used measurement techniques were employed: dynamic light scattering (DLS), electrophoretic light scattering (ELS) and transmission electron microscopy (TEM). We expect our results to be applicable in a wide variety of different NP types, allowing for robust interpretation and predictive tools in nanobioscience and nanobiotechnology.

Results and Discussion

In this study, the role of surface coating agents on the behavior of well-characterized silver and superparamagnetic iron oxide NPs [46] in different biological environments was investigated in adherence to the experimental scheme presented in Figure 1.

Characteristics of prepared AgNPs and SPIONs

As the first step, the physicochemical properties of freshly synthesized NPs were carefully evaluated in UW using DLS, ELS and TEM. Table 1 and Table 2 summarize the hydrodynamic diameters (d_H) obtained for both volume- and intensity-weighted distributions of differently coated AgNPs and SPIONs under study. DLS measurements in UW showed that both the volume and the intensity size distributions were monomodal only for AOTAgNPs. Volume-weighted size distributions were bimodal for all of the other investigated NPs, with the exception of CTAAgNPs for which distributions showed three peak

Table 1: Hydrodynamic diameter (d_H) obtained from size distributions by volume and intensity of differently coated silver nanoparticles in ultrapure water (UW) and biological medium (BM) after 1 h at 25 °C. Coating agents: trisodium citrate (CITAgNP), sodium bis(2-ethylhexyl) sulfosuccinate (AOTAgNP), poly(vinylpyrrolidone) (PVPAgNP), Brij 35 (BrijAgNP), Tween 20 (TweenAgNP), bovine serum albumin (BSAAgNP), poly(L-lysine) (PLLAgNP), and cetyltrimethylammonium bromide (CTAAgNP).

NPs type	medium	d_H (nm)	% mean volume	d_H (nm)	% mean intensity
CITAgNPs	UW	12.1 ± 2.8 96.3 ± 10.3	97.1 2.7	15.0 ± 1.8 144.3 ± 11.7	11.6 87.8
	BM	13.4 ± 2.5 63.3 ± 7.2	85.5 14.1	16.1 ± 2.9 101.4 ± 16.3	8.0 89.9
AOTAgNPs	UW	19.9 ± 0.5	99.4	27.8 ± 0.4	96.5
	BM	409.0 ± 74.1 5351 ± 128	93.2 7.3	295.4 ± 75.0 5144 ± 228	98.4 2.0
PVPAgNPs	UW	4.9 ± 1.7 33.5 ± 4.0	98.7 1.2	6.2 ± 1.1 69.5 ± 2.9	11.3 86.5
	BM	4.1 ± 1.3 37.9 ± 2.6	98.5 1.6	5.4 ± 1.4 78.9 ± 10.7	9.2 89.4
BrijAgNPs	UW	24.1 ± 14.3 129.3 ± 56.4	62.1 37.6	26.9 ± 2.1 164.7 ± 4.8	2.4 97.4
	BM	269.5 ± 25.6 56.5 ± 7.9 5220 ± 126	82.5 10.2 7.5	246.9 ± 19.2 56.5 ± 10.8 4974 ± 219	91.5 3.4 4.5
TweenAgNPs	UW	5.5 ± 0.3 36.1 ± 2.5	98.8 1.2	6.9 ± 0.5 68.9 ± 3.6	20.4 79.3
	BM	11.3 ± 2.4 98.3 ± 15.9 5019 ± 307	92.6 4.5 3.7	13.7 ± 3.1 143.7 ± 38.9 4448 ± 543	7.8 84.2 7.2
BSAAgNPs	UW	12.8 ± 8.1 65.7 ± 26.1	89.8 8.7	85.9 ± 22.3 12.4 ± 0.8	96.7 1.8
	BM	15.6 ± 4.4 47.3 ± 8.7	60.6 84.8	25.1 ± 14.5 128.6 ± 28.8	13.4 86.5
PLLAgNPs	UW	7.4 ± 1.3 55.7 ± 13.4	96.2 3.7	8.9 ± 1.7 115.7 ± 15.4	2.9 88.1
	BM	686.6 ± 133.8 5289 ± 214	95.0 4.7	542.4 ± 135.7 5038 ± 105	97.1 2.8
CTAAgNPs	UW	17.4 ± 5.4 81.5 ± 7.6 193.6 ± 36.8	88.1 2.9 8.7	22.3 ± 5.7 — 182.9 ± 17.4	6.0 — 91.6
	BM	27.9 ± 5.4 71.8 ± 7.1 602.0 ± 57.2	40.9 10.6 51.4	32.3 ± 6.7 — 418.8 ± 72.7	4.2 — 95.6

Table 2: Hydrodynamic diameter (d_H) obtained from size distributions by volume and intensity of uncoated superparamagnetic iron oxide nanoparticles (UNSPIONs) and coated with poly(L-lysine) (PLLSPIONNs) or D-mannose (MANSPION) in ultrapure water (UW) and biological medium (BM) after 1 h at 25 °C.

NPs type	medium	d_H (nm)	% mean volume	d_H (nm)	% mean intensity
UNSPIONs	UW	62.0 ± 13.8 105.6 ± 28.8	77.1 22.3	48.9 ± 19.4 130.3 ± 30.0	82.3 17.1
	BM	765.7 ± 170.4 5380.5 ± 72.3	95.1 4.6	670.7 ± 200.1 5060.2 ± 899.9	92.5 6.8
PLLSPIONs	UW	50.7 ± 24.2 279.7 ± 144.2	37.7 61.6	53.6 ± 23.4 254.8 ± 112.4	44.8 54.9
	BM	138.8 ± 35.1 688.6 ± 167.3	16.3 76.7	153.3 ± 42.2 610.4 ± 185.6	35.7 61.3
MANSPIONs	UW	43.8 ± 20.9 130.3 ± 30.1	85.8 15.9	70.9 ± 39.3 —	97.6 —
	BM	131.6 ± 29.7 723.0 ± 170.6 5322.4 ± 198.3	1.6 93.7 4.8	137.6 ± 29.3 636.2 ± 193.6 5209.7 ± 192.1	5.3 93.7 1.0

maximums. In terms of size, the majority of AgNPs had a d_H that ranged from 5 to 25 nm. As expected, the intensity-based size distributions yielded different results than the volume-based values. For example, a volume of more than 95% of PLLAgNPs had a mean size of 7.4 ± 1.3 nm, while intensity-weighted distribution showed a mean value of 115.7 ± 15.4 for ca. 88.1% of PLLAgNPs (Table 1). As already noted, it is known that intensity size distributions are subject to scattering interferences because the intensity of scatter light is much greater for large agglomerates compared to small particles. In accordance with the obtained DLS data, TEM images in UW showed monodisperse AOTAgNPs, PVPAgNPs, TweenAgNPs and PLLAgNPs, whereas other AgNPs were polydispersed (Figure 2). All of the AgNPs visualized by the TEM were spherically shaped except rod-like CITAgNPs (Figure 2).

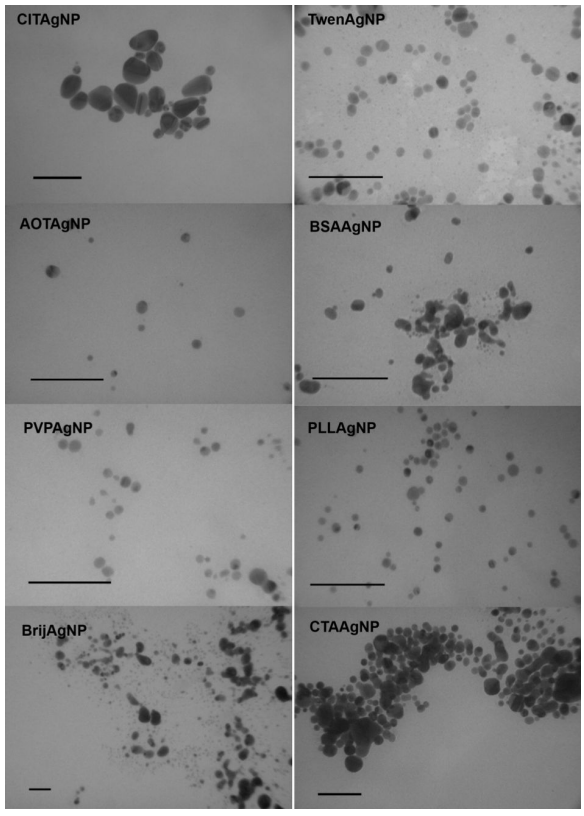

Figure 2: Transmission electron micrographs (TEM) of different silver nanoparticles coated with trisodium citrate (CITAgNP), sodium bis(2-ethylhexyl) sulfosuccinate (AOTAgNP), poly(vinylpyrrolidone) (PVPAgNP), Brij 35 (BrijAgNP), Tween 20 (TweenAgNP), bovine serum albumin (BSAAgNP), poly(L-lysine) (PLLAgNP), and cetyltrimethylammonium bromide (CTAAgNP). Scale bars are 100 nm.

The DLS measurements showed that SPIONs had two particle populations in UW: one with d_H of about 50 nm and another with d_H larger than 100 nm at peak maximum (Table 2). The initially synthesized SPIONs were much smaller than 10 nm as observed by TEM [4,47]. The results presented in Table 2 and Figure 3 clearly indicate a formation of SPION aggregates in UW. As it has been documented that SPIONs lose colloidal stability over time [47], the aggregates were expected considering that the SPIONs were synthesized 40–60 days prior to DLS and TEM experiments.

The ELS data, presented in Figure 4, showed that nine out of the eleven studied NPs had negative ζ-potential in UW, al-

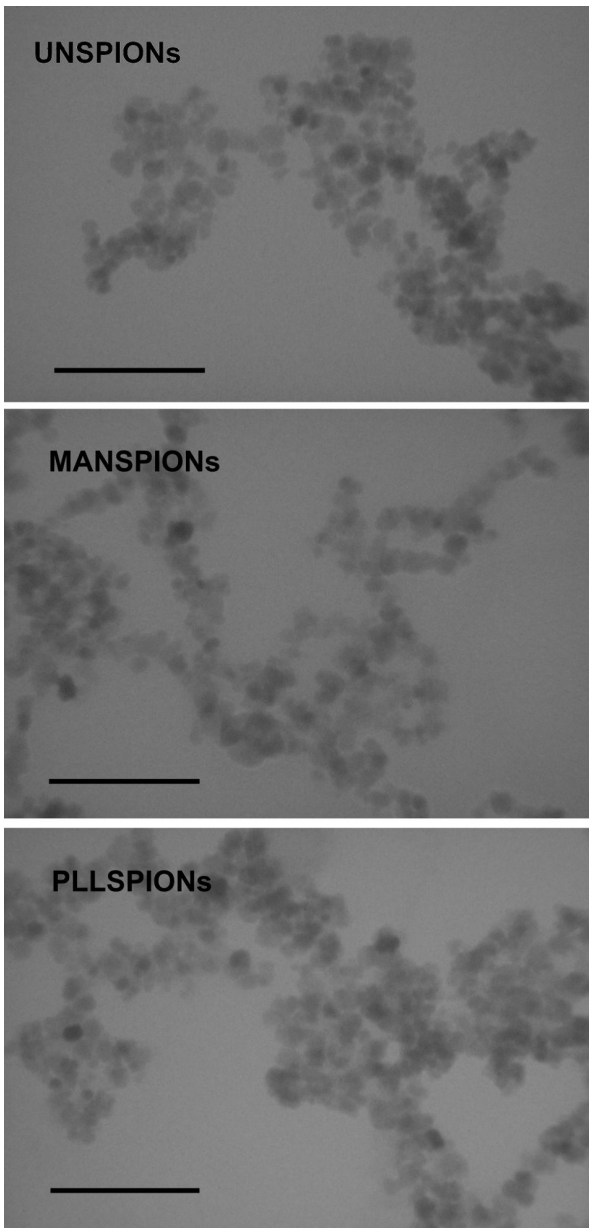

Figure 3: Transmission electron micrographs (TEM) of differently coated superparamagnetic iron oxide nanoparticles: uncoated (UNSPION) and coated with D-mannose (MANSPION) and poly(L-lysine) (PLLSPION). Scale bars are 100 nm.

though one of our "synthetic" goals was to prepare positively, neutral and negatively coated, i.e., charged metallic NPs (Figure 1). The coating of AgNPs with PLL and CTA led to positively charged AgNPs characterized by ζ-potentials of 23.6 ± 4.0 and 38.5 ± 2.9 mV, respectively. Both of these coating agents are positively charged at pH 6–7, which was used in this study. For PLLSPIONs, the negatively charged surface of the maghemite core was only partially compensated by positive PLL resulting in a ζ-potential value of −5.4 ± 0.4 mV. As expected, the use of negatively charged coating agents CIT, AOT and MAN resulted in NPs bearing an overall negative charge of −38.5 ± 2.9, −27.8 ± 1.9 and −26.9 ± 1.1 mV, respectively. For AgNPs coated with uncharged molecules; PVP, Tween 20 and Brij 35, we expected a ζ-potential close to zero. However, all of the three mentioned AgNPs were characterized by slightly negative ζ-potentials ranging from −6 to −19 mV. Since we employed a borohydride reduction of $AgNO_3$ during AgNP synthesis, the BH_4^- anions left over after synthesis were obviously attached next to the surface coatings of PVPAgNPs, BrijAgNPs and TweenAgNPs and led to a slightly negative ζ-potential. Synthesis of AgNPs using BSA as coating agent also resulted in NPs with a slightly negative surface charge.

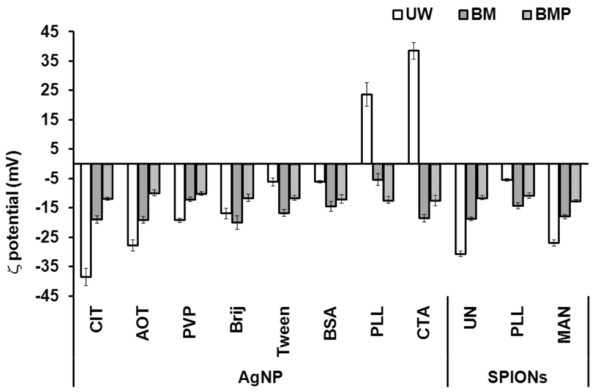

Figure 4: Zeta-potential (ζ) values of differently coated silver (AgNPs) and superparamagnetic iron oxide nanoparticles (SPIONs) in ultrapure water (UW), biological medium (BM) and biological medium supplemented with 0.1% bovine serum albumin (BMP) after 1 h at 25 °C. Coating agents: trisodium citrate (CIT), sodium bis(2-ethylhexyl) sulfosuccinate (AOT), poly(vinylpyrrolidone) (PVP), Brij 35 (Brij), Tween 20 (Tween), bovine serum albumin (BSA), poly(L-lysine) (PLL), cetyltrimethylammonium bromide (CTA) and D-mannose (MAN).

Agglomeration behavior of different AgNPs and SPIONs in biological media

The DLS and ELS methods were used to quantify the agglomeration of differently coated AgNPs and SPIONs in DMEM, a model biological media (BM), while TEM provided a visual presentation of NPs. Although the terms aggregation and agglomeration are used interchangeably, this study uses the term agglomeration because many recent studies have shown that NPs tend to agglomerate in aqueous biological matrices characterized by high ionic strength and neutral pH, such as phosphate-buffered saline and cell culture media [19-26,30]. The term aggregation indicates strongly bonded or fused particles and agglomeration indicates more weakly bonded particles.

All of the obtained results for the agglomeration of differently coated AgNPs and SPIONs in BM are given in Table 1 and Figures 4–6. One would have expected that the stabilization

would have been more effective using ionic coating agents when compared to non-ionic surfactants and polymers, but the explanation for the agglomeration behavior of the investigated AgNPs and SPIONs is not as straightforward. For CITAgNPs, PVPAgNPs and BSAAgNPs, the results clearly showed good colloidal stability, i.e., the size distributions in BM were similar to those obtained for dispersions in UW (Table 1).

However, the absolute value of the ζ-potential for BSAAgNPs increased after dispersion in BM. Conversely, the ζ-potential for CITAgNPs and PVPAgNPs decreased compared to that measured in UW (Figure 4). It would be expected that, when the ζ-potential approaches zero, interparticle repulsion decreases as does the stability of the dispersion. CITAgNPs are stabilized primarily through electrostatic repulsions, while bulky ligands such as PVP and BSA provide additional steric hindrances. Our results, in accordance with previously published data [48], imply that CIT, PVP and BSA provided colloidal stability for AgNPs irrespective to the type of surface interactions. It is interesting that we have recently observed [49] a significant agglomeration of CITAgNPs in phenol red-free DMEM (product number 12-709, Lonza, Verviers, Belgium) and in RPMI-1640 medium (product number R5886, Sigma-Aldrich, Munich, Germany) [50]. Both of these formulations contained HEPES as the buffering agent, while the media used in the recent work, where much like in this study no agglomeration of CITAgNPs [48] was observed, were buffered with phosphate buffer (PB). The most common buffering agents are PB and HEPES, which significantly differ in their chemical composition. Consequently, the behavior and stability of NPs in PB might be completely different from that in HEPES buffering system [21]. As phosphate, and not HEPES, is a normal constituent of mammalian blood and other body fluids, DMEM buffered with PB was chosen as the model BM.

Other AgNPs and all of the SPIONs agglomerated almost immediately after addition to the media, as can be seen from Figure 5. Thus, the high ionic strength of BM caused an agglomeration expected to be close to diffusion-limited. Moreover, the fast agglomeration of investigated NPs in BM was visible even to the naked eye. Immediately after the addition of clear NP stock solution into the BM, a cloudy black precipitate

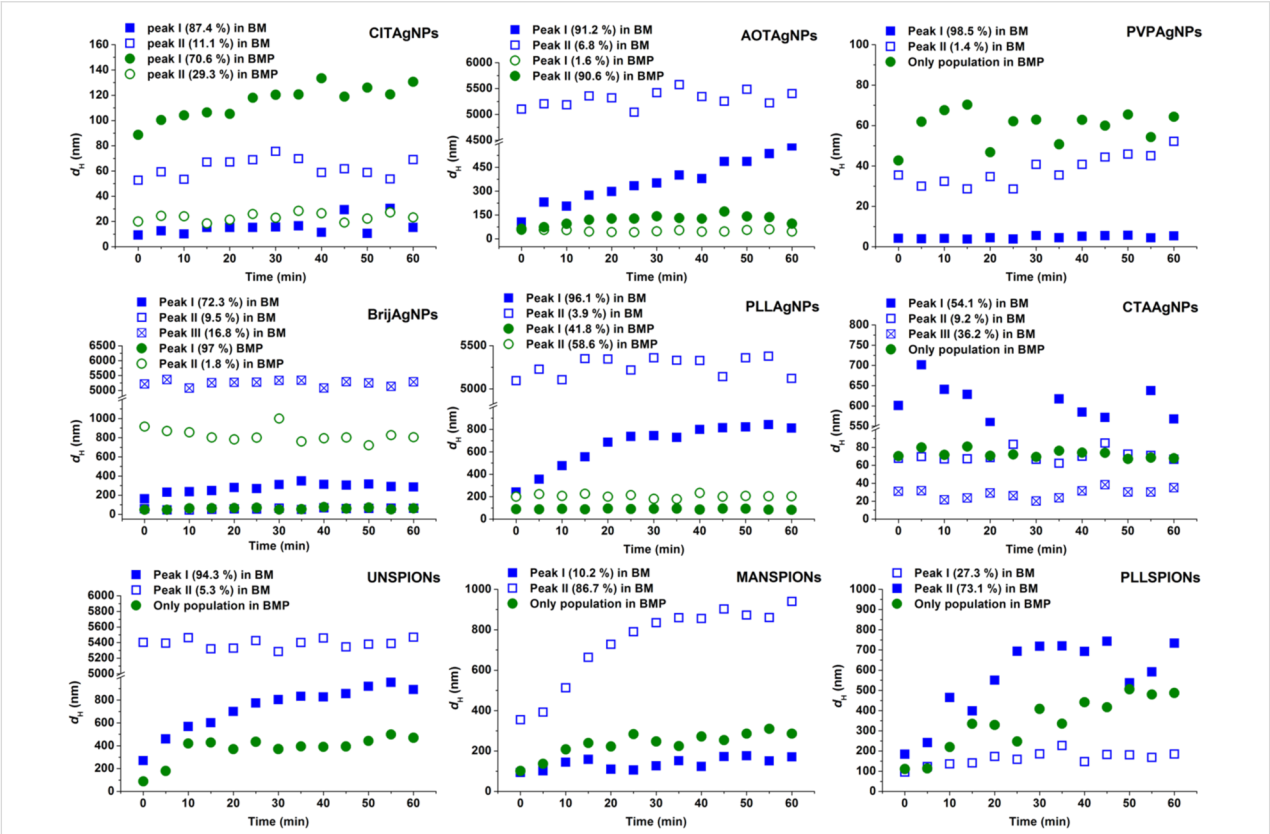

Figure 5: Temporal evolution of the hydrodynamic diameter (d_H) obtained from size distributions by volume of differently coated metallic nanoparticles in biological media (BM) and biological media supplemented with 0.1% bovine serum albumin (BMP) over a period of 1 h at 25 °C. Results are presented for silver nanoparticles coated with trisodium citrate (CITAgNP), sodium bis(2-ethylhexyl) sulfosuccinate (AOTAgNP), poly(vinylpyrrolidone) (PVPAgNP), Brij 35 (BrijAgNP), poly(L-lysine) (PLLAgNP), cetyltrimethylammonium bromide (CTAAgNP); and superparamagnetic iron oxide nanoparticles uncoated (UNSPION) and coated with D-mannose (MANSPIONs) and poly(L-lysine) (PLLSPION).

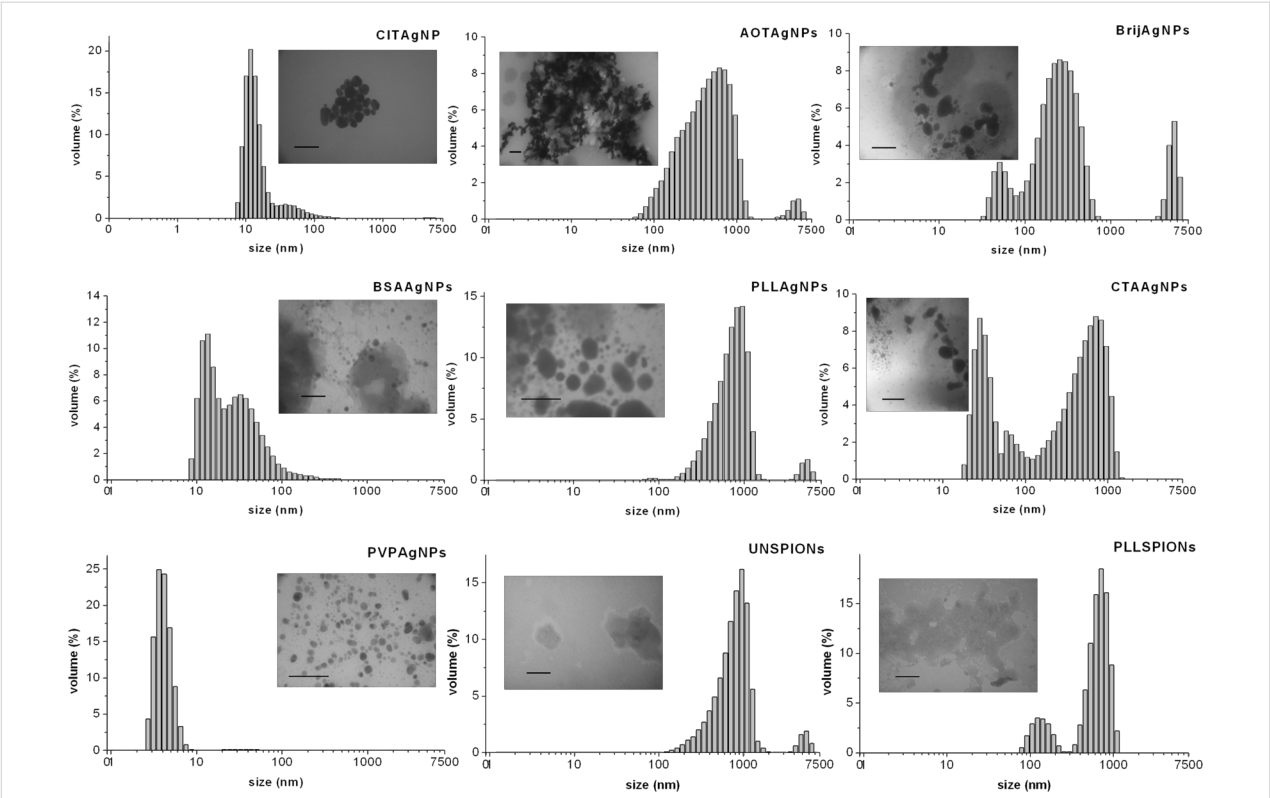

Figure 6: Transmission electron micrographs (TEM) and corresponding size distributions by volume of differently coated metallic nanoparticles in biological media after 1 h at 25 °C. Results are presented for silver nanoparticles coated with trisodium citrate (CITAgNP), sodium bis(2-ethylhexyl) sulfosuccinate (AOTAgNP), Brij 35 (BrijAgNPs), bovine serum albumin (BSAAgNPs), poly(L-lysine) (PLLAgNP), cetyltrimethylammonium bromide (CTAAgNP), and poly(vinylpyrrolidone) (PVPAgNP) and superparamagnetic iron oxide nanoparticles uncoated (UNSPION) and coated with poly(L-lysine) (PLLSPION). Scale bars are 100 nm.

was observed at the bottom of the flask. AOTAgNPs, BrijAgNPs, PLLAgNPs, UNSPIONs and MANSPIONs showed the most pronounced agglomeration in BM and clusters of ca. 5 µm were observed (Table 1, Figure 6). As can be seen from the TEM micrographs and corresponding size distributions (Figure 6), agglomerated NPs are characterized by very high polydispersity. The CTAB and Tween coatings prevented severe agglomeration of AgNPs in BM due to steric repulsion effects. According to the volume-weighted size distribution data, less than 10% of TweenAgNPs population agglomerated in BM, while 50% of CTAAgNPs was agglomerated to clusters of about 600 nm (Table 1). Interestingly, PLL prevented a harsh agglomeration of SPIONs, but not of the AgNPs. It is known that NP coating agents can lose their stabilizing effect at high ionic strength due to complexation with counter ions. Consequently, van der Waals attraction forces induce aggregation of unprotected NPs [3]. Thus, the chemical nature of the surface-capping agents played a significant role in the conservation of colloidal stability of metallic NPs in BM. The observed differences in ζ-potential in BM compared to UW provide an additional important explanation [21]. Dispersion in BM resulted in a net-negatively-charged layer on the surfaces of all of the studied NPs, while absolute values of the ζ-potential were decreased in BM for all NPs except for BrijAgNPs, TweenAgNPs, BSAAgNPs and PLLSPIONs. This observation may explain the good colloidal stability of BSAAgNPs and PLLSPIONs in BM, moderate stability of TweenAgNPs, and instability of PLLAgNPs, but is contradictory to the observed behavior of BrijAgNPs. The electrostatic stabilization effect, playing the key role for CITAgNPs was also important for PVPAgNPs characterized by the negative ζ-potential imparted by adsorbed BH_4^-, a residual side product from AgNPs synthesis. In addition, PVPAgNPs were stabilized by steric repulsion of PVP molecules. However, BH_4^- anions were also attached to the BrijAgNPs and TweenAgNPs coatings, but adsorption of Tween 20 and Brij 35 surfactants to the AgNPs surfaces was much weaker, thus providing lower colloidal stability compared to PVP. This has already been described previously [51]. It is important to note that charge reversal was noticed in the ζ-potential measurements of positively charged PLLAgNPs and CTAAgNP after dispersion in BM, which affected their stability and heavily increased the possibility of their agglomeration. Lower stability of PLLAgNPs compared to CTAAgNPs could be explained by the much more negative ζ-potential value of

CTAAgNPs in BM. The DLS results agree well with the complementary information obtained by TEM observation (Figure 6). The TEM images provide evidence that no changes in the morphology or size of the CITAgNPs, PVPAgNPs and BSAAgNPs occurred upon dispersion in BM. Conversely, after being dispersed in the BM, all of the other studied NPs exhibited disordered and agglomerated morphologies (Figure 6). Small AgNP nanospheres coated with AOT, Brij, Tween, PLL and CTAB, and SPIONs were strongly damaged and had irregular surfaces (Figure 6).

In summary, different coating agents used on AgNPs and SPIONs imparted different colloidal stabilities in the same biological media. The obtained data clearly show that a combination of negative charge and high adsorption strength of coating agents alongside molecular structure are important factors that impart good colloidal stability of metallic NPs in electrolyte-rich fluids. Moreover, DLS, ELS and TEM proved to be sufficient and fast screening methods for a colloidal stability evaluation of metallic NPs in biological environments.

Effect of albumin on the dispersibility of AgNPs and SPIONs in biological media

When suspended in biological fluids, NPs rapidly interact with proteins that form a dynamical layer all over the NP surface, known as a protein corona (PC) [36,37,39]. Subsequently, the formation of PC modifies the physicochemical properties of NPs, while proteins may undergo conformational and functional changes [52-56]. Consequently, the presence of proteins in dispersion media alters the physicochemical behavior and stability of NPs. DLS data, shown in Table 3 and Figure 5, suggest that BSA stabilized the dispersion of both types of studied metallic NPs in BMP.

A similar stabilizing effect of BSA against the aggregation of nanoparticles was previously reported [3,5,30,57,58]. Although the presence of BSA prevents NP agglomeration, the d_H obtained from size distributions by volume increased by a factor of two and more for all NPs upon suspension in BMP due to the bulky globular nature of the BSA coating. This can be seen by comparing data from Table 1, Table 2 and Table 3. The very

Table 3: Hydrodynamic diameter (d_H) obtained from size distributions by volume and intensity of differently coated silver (AgNPs) and superparamagnetic iron oxide nanoparticles (SPIONs) in biological medium supplemented with 0.1% bovine serum albumin (BMP) after 1 h at 25 °C. Coating agents: trisodium citrate (CIT), sodium bis(2-ethylhexyl) sulfosuccinate (AOT), poly(vinylpyrrolidone) (PVP), Brij 35 (Brij), Tween 20 (Tween), bovine serum albumin (BSA), poly(L-lysine) (PLL), cetyltrimethylammonium bromide (CTA) and D-mannose (MAN).

NPs type	d_H (nm)	% mean vol	d_H (nm)	% mean intensity
CITAgNPs	114.2 ± 12.9 22.4 ± 2.9	82.3 17.7	117.8 ± 9.5 —	99.9 —
AOTAgNPs	47.8 ± 8.9 671.0 ± 140.4	1.7 0.1	63.4 ± 27.0 548.9 ± 126.4	7.1 20.4
PVPAgNPs	59.6 ± 11.4	0.2	82.9 ± 20.7	36.2
BrijAgNPs	59.2 ± 9.4 848.3 ± 9.6 4304 ± 204	2.7 0.3 0.3	91.7 ± 14.0 — 4882 ± 187	74.6 — 8.9
TweenAgNPs	55.2 ± 6.8	0.9	87.8 ± 10.9	70.4
BSAAgNPs	86.5 ± 17.5	0.2	124.6 ± 26.7	41.4
PLLAgNPs	85.6 ± 17.6 208.4 ± 14.8	41.2 56.7	34.3 ± 7.8 174.9 ± 8.4	2.3 97.7
CTAAgNPs	71.8 ± 6.4	0.9	99.7 ± 10.6	72.5
UNSPIONs	43.1 ± 6.4 417.6 ± 41.7	0.1 0.1	54.7 ± 19.4 489.8 ± 69.7	4.3 29.7
PLLSPIONs	537.9 ± 64.3	0.3	382.1 ± 28.5	69.8
MANSPIONs	30.5 ± 15.9 778.1 ± 179.7	0.1 0.3	31.8 ± 14.8 680.4 ± 237.7	3.1 41.3

heterogeneous size distribution for different NPs indicates non-uniform surface coverage depending on surface coating. Thus, the BSA molecules clustered and adsorbed on the NP surface variously for different AgNPs and SPIONs, resulting in a thickness variation. Moreover, the BSA coating is likely to include many surface regions that retain adsorbed coating agents, remaining from the original synthesis. For CITAgNPs, PVPAgNPs, TweenAgNPs, BSAAgNPs and PLLSPIONs, characterized by a bimodal size distribution in UW, interaction with BSA led to a monomodal size distribution in which all NPs were covered by several BSA molecules. For the NPs that were agglomerated in BM, the addition of BSA inhibited completely or significantly reduced the agglomeration process. It is clearly visible from Figure 5 that the d_H obtained from size distributions by volume was constant and significantly lower in BMP compared to BM for AOTAgNBPs, BrijAgNPs, PLLAgNPs, and CTAAgNPs after 1 h. The observed increase in the mean d_H for CITAgNPs, UNSPIONs, MANSPIONs and PLLSPIONs in the BMP after 1 h is not a result of agglomeration, but rather an indication of a slower adsorption of BSA molecules to NP surfaces depending on the interchange of the coating agent with BSA. Such an assumption was further confirmed by TEM that clearly showed non-agglomerated, well-dispersed NPs in the BMP (Figure 7). This highlights the difficulties of using the DLS technique for extracting changes in the actual size of NP core when taking into account surface coatings, which can agglomerate/cluster on the NP surface. BSA may be bound by a relatively strong covalent bond between the NPs surface and cysteine groups or via protein–protein electrostatic or depletion interactions. If both interactions take place simultaneously, the thickness of a PC will vary depending on the type of NP.

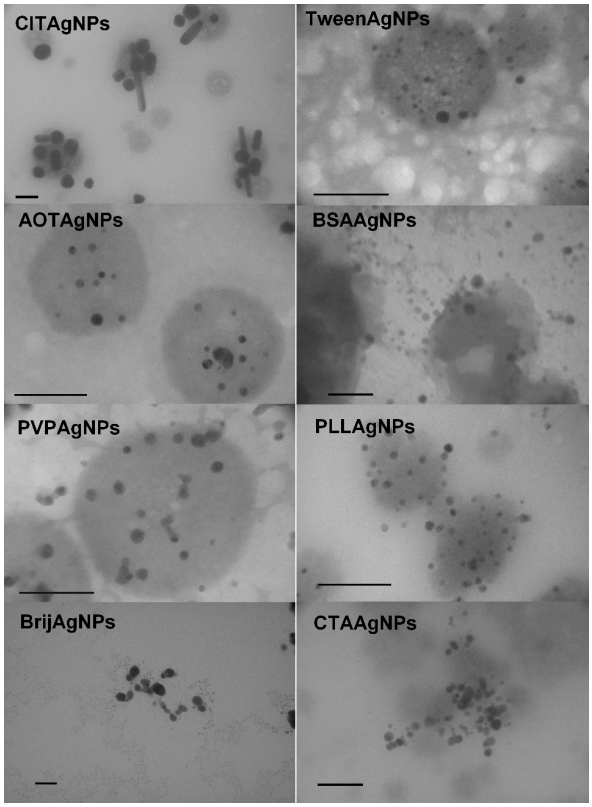

Figure 7: Transmission electron micrographs (TEM) of different silver nanoparticles coated with trisodium citrate (CITAgNP), sodium bis(2-ethylhexyl) sulfosuccinate (AOTAgNP), poly(vinylpyrrolidone) (PVPAgNP), Brij 35 (BrijAgNP), Tween 20 (TweenAgNP), bovine serum albumin (BSAAgNP), poly(L-lysine) (PLLAgNP), and cetyltrimethylammonium bromide (CTAAgNP) in biological media supplemented with 0.1% bovine serum albumin (BMP) after 1 h. Scale bars are 100 nm.

The ELS data showed that all of the NPs had very similar potential values in BMP regardless of the coating agent, ranging from −9.9 to −12.4 mV (Figure 4). The decrease of absolute values of the ζ-potential toward zero in the BMP compared to BM imply that the BSA coating itself was the main source of particle stability in the BMP, as this protein is just slightly negatively charged at physiological pH values. The measured ζ-potentials were very close to the values determined for pure BSA dispersions, −7.5 ± 0.04 mV, which is not surprising taking into account the relatively high protein concentration. Thus, BSA conjugates provided an enhanced electrostatic repulsion against the agglomeration of metallic NPs in DMEM. The BSA has negative charges above its isoelectric point (pH 4.78) [59] and the electrostatic forces dominate over hydrophobic interactions. Accordingly, the attractive forces between the positively charged AgNPs and the negatively charged BSA led to protein adsorption, but questions remained about why the repulsive forces between the negatively charged NPs and BSA did not prevent protein adsorption. Besides a negatively charged surface at physiological pH, the structure of BSA is also characterized by positively charged lysine and cysteine [60]. Therefore, its interaction with NPs is hardly trivial.

The most important observation of this study is that BSA enables a colloidal stabilization of metallic NPs in biological fluids regardless of their chemical composition, surface structure and surface charge. This is also evident from the micrographs typically visualized by TEM for NPs dispersed in BMP (Figure 7). These images show that NPs are well-dispersed, but can be found only on grid areas where drops of BMP settled. Only BSAAgNPs and BrijAgNPs were dispersed all over the TEM grid.

Our results are in good agreement with recently published data for stabilization of different metallic NPs in protein-containing media [3,54,61-64]. The mechanisms of PC adsorption and the way how the PC is arranged at the NP surface are crucial for

gaining an understanding of the biological reactivity of NPs in vivo [61]. In principle, the protection against colloidal agglomeration offered by BSA could be used in different nanotechnological applications, but also highlights the facilitated transport of nanoparticles across the bloodstream. This study clearly shows that surface coating strongly affects colloidal stability and behavior of metallic NPs in biological environment as presented in Table 4.

Behavior of NPs in blood and blood plasma

The implications of the PC on the bioactivity nanomaterials in vivo are enormous. Biological fluids are complex environments in which it is difficult even to predict all of the possible NP modifications and interactions. In such an environment, the dynamic adsorption of different biomolecules onto the surface of metallic NPs is a well-established fact, which irreversibly changes the nature of the original NPs [61,65].

In order to examine how differently coated metallic NPs behave in more complex biological fluids, PVPAgNPs, BSAAgNPs, AOTAgNPs and PLLAgNPs were dispersed in rat whole blood (WhBl) and blood plasma (BlPl). After incubation for 1 h, samples were examined by TEM as described in the Experimental section. The TEM micrographs showed rather unexpected features (Figure 8). All of the AgNPs except PVPAgNPs, which were initially small and exhibited spherical shape, were transformed depending on the media. AOTAgNPs and BSAAgNPs significantly changed their shape and size in WhBl, but stayed very well dispersed in BlPl. On the contrary, the morphology of PLLAgNPs and PVPAgNPs changed in BlPl, but remained unchanged in WhBl (Figure 8). The BSAAgNPs formed square- and rectangular-shaped agglomerates larger than 200 nm in WhBl. Similarly shaped structures were found for PLLAgNPs in BlPl, while PVPAgNPs formed large hexagonal nanocomposites in BlPl (Figure 8). Interest-

Table 4: Summarized effects of different coating agents on the stability of silver and maghemite nanoparticles in model biological medium after 1 h. UW - ultrapure water, BM - biological cell culture medium without addition of protein, BMP - BM supplemented with common serum protein.

coating agent	BM compared with UW	BMP compared with BM
trisodium citrate (CIT)	stable dispersion, $\|\zeta\|$ decreased, no morphology changes	stable dispersion, $\|\zeta\|$ decreased, localized in BMP areas on TEM grid
sodium bis(2-ethylhexyl) sulfosuccinate (AOT)	pronounced aggregation, $\|\zeta\|$ decreased, morphology changes (irregular shapes)	stable dispersion, $\|\zeta\|$ decreased, localized in BMP areas
cetyltrimethylammonium bromide (CTA)	partial stabilization, $\|\zeta\|$ decreased, charge reversal, morphology changes (irregular shapes)	stable dispersion, $\|\zeta\|$ decreased, localized in BMP areas on TEM grid
Brij 35 (Brij)	pronounced aggregation, $\|\zeta\|$ increased, morphology changes (irregular shapes)	stable dispersion, $\|\zeta\|$ decreased, dispersed over the TEM grid
Tween 20 (Tween)	partial stabilization, $\|\zeta\|$ increased, morphology changes (irregular shapes)	stable dispersion, $\|\zeta\|$ decreased, localized in BMP areas on TEM grid
poly(vinylpyrrolidone) (PVP)	stable dispersion, $\|\zeta\|$ decreased, no morphology changes	stable dispersion, $\|\zeta\|$ decreased, localized in BMP areas on TEM grid
poly(L-lysine) (PLL)	pronounced aggregation for AgNPs, $\|\zeta\|$ decreased, charge reversal, partial stabilization for SPIONs, $\|\zeta\|$ increased, morphology changes (irregular shapes)	stable dispersion, $\|\zeta\|$ increased, localized in BMP areas on TEM grid
bovine serum albumin (BSA)	stable dispersion, $\|\zeta\|$ increased, no morphology changes	stable dispersion, $\|\zeta\|$ decreased, dispersed over the TEM grid
D-mannose (MAN)	pronounced aggregation, $\|\zeta\|$ decreased, morphology changes (irregular shapes)	stable dispersion $\|\zeta\|$ decreased localized in BMP areas on TEM grid

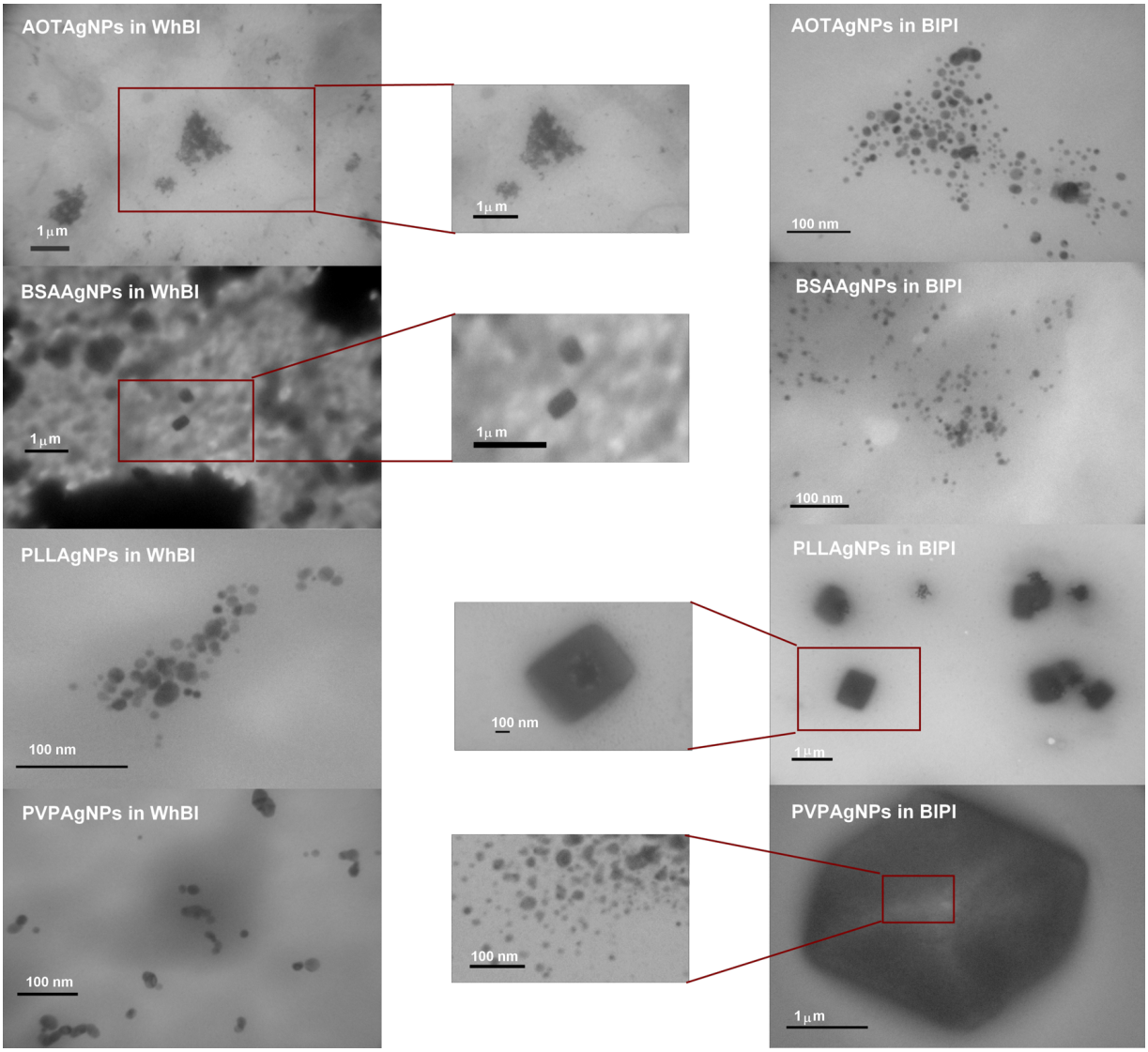

Figure 8: Transmission electron micrographs (TEM) of different silver nanoparticles coated with sodium bis(2-ethylhexyl) sulfosuccinate (AOTAgNP), bovine serum albumin (BSAAgNP), poly(L-lysine) (PLLAgNP), and poly(vinylpyrrolidone) (PVPAgNP) in whole blood (WhBl) and blood plasma (BlPl) of Wistar rats after 1 h.

ingly, AOTAgNPs were associated in triangle clusters formed of small, separated NPs (Figure 8).

It has been very well established that the shape of metallic NPs may be controlled using different surfactants [66,67]. The choice and addition of surfactants may successfully control the synthesis of nanodiscs, triangular nanoplates or nanospheres. In recent years, solution-phase methods developed rapidly toward a reproducible preparation of metallic NPs with controlled shape [66]. A typical synthesis of nanocrystals can be divided into three levels: nucleation, evolution of nuclei into seed, and growth of seed into nanocrystals. The mechanism behind such a synthesis is extremely complicated, but the type of coating agent proved to be crucial for the final shape of a nanocrystal [66]. The micrographs presented in Figure 8 suggest that our initially small AgNPs appeared as seeds in WhBl or BlPl, where further growth to nanocomposites was accomplished. Thus, our results indicate an in vivo synthesis of metallic nanocrystals in mammalian organisms, similarly to that already described in microorganisms [68].

There are many examples of in vivo formation of nanomaterials (NMs) in biological systems [68]. The most common process is the biomineralization of bones and shells [69]. It is interesting that the shape of these bionanomaterials is usually induced by an engulfing organic matrix [69]. Different microorganisms, such as magnetotactic bacteria or diatoms, are also able to produce nanocrystals in vivo [70-74]. The biosynthesis

of metallic NMs with controlled morphology is governed by using different bacterial strains [68]. For example, *Pseudomonas stutzeri* AG259, a metal-accumulating bacterium, is able to synthesize AgNPs through its detoxification process after exposure to silver [75]. It is somewhat intriguing that we observed similar AgNPs forms in WhBl and BlPl (Figure 8) as already described for *Pseudomonas stutzeri* AG259 [75].

The reason for the observed differences between WhBl and BlPl is unclear, but it implies that NP stability and morphology can be significantly changed with only small changes in the composition of the biological medium. Our results point out that an accurate characterization of physicochemical parameters and behavior of NPs in a particular biological environment is imperative for clinical relevance to target organ groups. As a consequence, the development of nanomaterials for theragnostics is an ambitious goal with many parameters to assess.

Conclusion

The lack of fundamental knowledge about the biocompatibility of metal-based nanomaterials and their effect and behavior in biological systems may restrict the capability to establish principles used as regulatory guidance and design safe nanomaterials. The detection and assessment of the colloidal stability of metallic NPs is vital. The presented work describes a systematically conducted experimental approach consisting of techniques that, although simple, are sufficient to perform a fast screening of the biocompatibility and colloidal stability of metallic NPs in biological environments. The obtained results have shown that the agglomeration behavior of metallic NPs in aqueous solutions with the pH and ionic strength close to biological fluids depends on the surface coating. This study confirmed that the presence of proteins such as BSA plays a major role in the colloidal stabilization of metallic NPs in biological fluids. Data on the behavior of differently coated NPs in whole blood and blood plasma highlights the importance of investigating the behavior and effects of metallic NPs in a variety of biological fluids in addition to including as many of the NPs properties as possible. It is not superfluous to stress that a systematic study of the stability and behavior for various NPs in addition to the best possible characterization of NPs would enable clear conclusions and predictions about the effects of NPs in a variety of biological systems.

Experimental

Chemicals and materials

If not otherwise stated, chemicals were obtained from Sigma-Aldrich Chemie GmbH (Munich, Germany). Dulbecco's modified Eagle's medium (DMEM) with 4.5 $g \cdot L^{-1}$ glucose without L-glutamine and sodium dihydrogen phosphate as buffering agent (product number 12-614Q) was obtained from Lonza (Verviers, Belgium). Bovine serum albumin (product number A-7906, Sigma-Aldrich Chemie GmbH, Steinheim, Germany) was used as received without further purification. The plastic and glassware used for chemical analysis were from Sarstedt (Belgium). Osmium tetroxide was purchased from Agar Scientific (Stansted, UK) and TAAB epoxy resin (medium hard) from Aldermaston (Berkshire, UK). All dilutions were made with ultrapure water (18.2 MΩ·cm), obtained from a GenPureUltraPure water system (TKA Wasseraufbereitungssysteme GmbH, Niederelbert, Germany).

Synthesis of metallic nanoparticles

The syntheses of AgNPs and SPIONs with different surface coatings were conducted as previously described [49] using structurally diverse surface coatings: trisodium citrate (CIT), sodium bis(2-ethylhexyl) sulfosuccinate (AOT), cetyltrimethylammonium bromide (CTA), poly(vinylpyrrolidone) (PVP), poly(L-lysine) (PLL), bovine serum albumin (BSA), Brij 35 (Brij), Tween 20 (Tween) and D-mannose (MAN).

Silver nanoparticles coated with sodium bis(2-ethylhexyl) sulfosuccinate (AOTAgNP), cetyltrimethylammonium bromide (CTAAgNP), poly(vinylpyrrolidone) (PVPAgNP), poly(L-lysine)(PLLAgNP), and Tween 20 (TweenAgNP) were synthesized by reducing $AgNO_3$ with $NaBH_4$. Briefly, the solutions of capping agent were prepared by dissolving appropriate amounts of capping agent in ultra-pure water. Then, 9.2 mL of 50 mM $AgNO_3$ was added dropwise and dissolved by constant stirring on an IKA RCT basic magnetic stirrer plate (IKA Werke, Germany). To this solution, a volume of 2 mL of 0.4 M $NaBH_4$ solution was added dropwise (about 1 drop/s). The final concentrations of AOT, CTAB, PVP, PLL, and Tween were 500, 500, 75, 20 and 6 mM, respectively. The reaction mixture was stirred vigorously at room temperature for 45 min. After the synthesis, silver colloids were centrifuged at 11,000*g* for 20 min. After decanting the supernatant, the residue was suspended in ultrapure water and kept at 4 °C in the dark. BrijAgNPs were synthesized by mixing an aqueous solution of $AgNO_3$ (0.09 mL, 50 mM), Brij 35 (5 mL, 0.45 mM) and hydrogen peroxide (0.105 mL, 30 wt %) with 44.5 mL ultrapure water. The mixture was vigorously stirred at room temperature in the presence of air. The final volume was kept at 50 mL. To this mixture, $NaBH_4$ (0.4 mL, 200 mM) was rapidly injected, generating a colloid that was pale yellow. After 30 min, the colloid darkened to a deep-yellow color indicating the formation of AgNPs. CITAgNPs were synthesized via the following protocol: 200 µL of the aqueous solution of ascorbic acid (AsA) with a concentration of 0.1 mM was added into 190 mL of boiling water, followed by boiling for an additional 1 min. Then, 3.8 mL of the aqueous solution of sodium citrate (35.4 mM) and 1.2 mL of the aqueous solution of $AgNO_3$ (50 mM) were consecutively added

to 5 mL of water under stirring at room temperature. After 5 min of incubation at room temperature, the citrate–AgNP mixture solution was injected into the boiling aqueous solutions of AsA (just after 1 min boiling after AsA addition to boiling water). The final concentrations of reactants were 0.673 mM for sodium citrate, 0.3 mM for $AgNO_3$ and 0.1 μM for AsA. The color of the reaction solution quickly changed from colorless to yellow. The transparent and yellow reaction solution was further boiled for 1 h under stirring to warrant formation of uniform quasi-spherical AgNPs. Purification of AgNPs was performed by centrifugation of colloidal solution two times at 11,000*g* for 30 min. Supernatant was decanted and precipitate was redispersed in ultrapure water by sonification. Silver nanoparticles directly conjugated to bovine serum albumin (BSAAgNPs) were prepared as follows: 7.6 mL of 50 mM $AgNO_3$ was added dropwise under stirring to 33 mL of ultrapure water containing dissolved 90 mg of BSA. Then, sodium borohydride (1 mL, 0.397 M) was added to an aqueous solution of $AgNO_3$ and BSA under vigorous stirring. The molar ratio of Ag^+:BSA and Ag^+:BH_4^- were 28:1 and 1:1, respectively. The reaction volume was 40 mL, and contained 13.50 μmol BSA. The reaction was allowed to proceed for 1 h, and the product was purified by precipitation at −5 °C using ultracentrifugation.

Three different maghemite nanoparticles (γ-Fe_2O_3NPs), uncoated, coated with poly(L-lysine) and D-mannose, were prepared by coprecipitation of $FeCl_2$ and $FeCl_3$ using ammonium hydroxide, followed by the oxidation of the resulting magnetite with sodium hypochlorite [46,47]. The obtained superparamagnetic maghemite (γ-Fe_20_3) was referred as uncoated γ-Fe_2O_3NPs (UNSPIONs). The post-synthesis coating of maghemite with D-mannose (MANSPIONs) or poly(L-lysine) (PLLSPIONs) was achieved [46] by addition of D-mannose or poly(L-lysine) to the primary uncoated maghemite cores [4].

Analytical methods

As described in [49], the size and charge of NPs were measured by dynamic (DLS) and electrophoretic light scattering (ELS), respectively, using Zetasizer Nano ZS (Malvern, UK). Visualization of NPs were done using a transmission electron microscope (TEM, Zeiss 902A). Total silver concentrations in AgNPs were determined using an Agilent Technologies 7500cx inductively coupled plasma mass spectrometer (ICPMS) (Waldbronn, Germany).

Characterization of nanoparticles and dispersion protocols

Careful characterization and colloidal stability evaluation of each NP type was conducted using several different dispersion protocols: ultrapure water (UW), DMEM high glucose as model biological medium (BM), BM supplemented with 0.1 or 1% BSA (BMP), whole blood (WhBl) and blood plasma (BlPl) taken from the Wistar rat. The aim was to investigate the behavior of each NP after 1 h in different biological environments. In each dispersion experiment, NPs were applied at total metal concentration of 1 or 10 $mg \cdot L^{-1}$.

The stock solution of BSA in DMEM was freshly prepared for each experiment and then diluted to the desired concentrations. Differently coated metallic NPs were dispersed in BSA solutions to the final concentration of 1 $mg \cdot L^{-1}$ just before DLS measurements. Among the most important parameters of colloidal systems is their particle size, which can be used as an indicator of their stability. DLS is the most common and versatile technique for measuring size distribution of NPs in solutions (Murdock et al. [53]). However, conventional DLS has its limitations. The main interferences in the biological matrix originate from the light scattering of different biological components and a mixture of different sizes of fractal-shaped agglomerates. In our model BMP system, the effect of BSA scattering requires cautious and thoughtful analysis of DLS results. The pure BSA in DMEM had a volume-weighted mean size of 7.4 ± 0.8 nm, while d_H obtained from size distributions by intensity was shown to be 9.6 ± 0.9 nm, as expected for a globular protein of 66 kDa [60]. Thus, the BSA scattering is the most significant in interpretation of DLS results for small, non-agglomerated NPs with sizes close to BSA. That was not the issue in the present study. The size of the measured metallic NPs in all BMP systems was at least two-fold larger than d_H of BSA therefore no overlaps of the peak maximums were observed. On the other hand, due to the low concentration of metallic NP, the volume peak area (%) in all of the BMP systems was significantly smaller compared to BSA. Conversely, size distribution by intensity showed more realistic peak ratios. To address this problem to some extent, BSA levels 2.4 (1% BSA) and 24 (0.1% BSA) times lower than physiological concentrations ([BSA] = 375 μM) were added to the BM (in order to prepare BMPs). In order to present results in a transparent way and obtain accurate conclusions from the DLS measurements, size distribution by intensity and volume were used in analyzing the results. Intensity-weighted size distribution is the first order result from a DLS experiment calculated from the scatter intensity of each particle in solution. On the other hand, intensity distributions can be biased towards larger particles since the intensity of particle light scatter varies with the 6th power of particle diameter. In order to avoid overestimations arising from the scattering of larger particles, volume-weighted size distributions are often used. In addition, d_H obtained from size distributions by volume was presented so results could be comparable with our previously published studies. It should be noted that the data was sometimes compiled from different syn-

thesis batches of NPs, leading to some discrepancy in the size distributions of the various control samples.

For dispersions of NPs in whole blood (WhBl) and blood plasma (BlPl), whole blood and blood plasma were obtained from healthy twelve weeks old male Wistar rats. Animals were killed by narketan/xilapan anesthesia following the whole blood collection by cardiac puncture. The experiment was approved by the Ethics Committee for Animal Studies of the Institute for Medical Research and Occupational Health according to European and Croatian legislation on animal experimentation and International Council for Laboratory Animal Science ethical guidelines for researchers, respectively. Then, different NPs were dispersed in 1 mL of WhBl or BlPl at a final metal concentration of 10 $mg \cdot L^{-1}$ and agitated for 1 h on a digital waving rotator (Thermo Scientific, USA). After incubation, suspensions were diluted 50 times before further analysis. It should be noted that DLS and ELS measurements were impossible in WhBl and BlPl suspensions.

TEM samples were prepared by depositing a drop of the NPs suspension after 1 h of incubation at room temperature on a Formvar® coated copper grid and air-drying at room temperature.

Acknowledgements

We thank the European Commission for financial support of this investigation within the GlowBrain project (FP7-REGPOT–2012–CT2012–316120) and the Czech Science Foundation (project 16-01128J). We thank Mrs. Iris Elezović for her great help during preparation of samples for TEM, and Mr. Makso Herman for his advices during writing.

References

1. Tai, J.-T.; Lai, C.-S.; Ho, H.-C.; Yeh, Y.-S.; Wang, H.-F.; Ho, R.-M.; Tsai, D.-H. *Langmuir* **2014,** *30,* 12755–12764. doi:10.1021/la5033465
2. Lohse, S. E.; Murphy, C. J. *J. Am. Chem. Soc.* **2012,** *134,* 15607–15620. doi:10.1021/ja307589n
3. Dominguez-Medina, S.; Blankenburg, J.; Olson, J.; Landes, C. F.; Link, S. *ACS Sustainable Chem. Eng.* **2013,** *1,* 833–842. doi:10.1021/sc400042h
4. Babič, M.; Horák, D.; Trchová, M.; Jendelová, P.; Glogarová, K.; Lesný, P.; Herynek, V.; Hájek, M.; Syková, E. *Bioconjugate Chem.* **2008,** *19,* 740–750. doi:10.1021/bc700410z
5. Kittler, S.; Greulich, C.; Gebauer, J. S.; Diendorf, J.; Treuel, L.; Ruiz, L.; Gonzalez-Calbet, J. M.; Vallet-Regi, M.; Zellner, R.; Köller, M.; Epple, M. *J. Mater. Chem.* **2010,** *20,* 512–518. doi:10.1039/B914875B
6. Yen, H.-J.; Hsu, S.-H.; Tsai, C.-L. *Small* **2009,** *5,* 1553–1561. doi:10.1002/smll.200900126
7. Liu, J. Y.; Hurt, R. H. *Environ. Sci. Technol.* **2010,** *44,* 2169–2175. doi:10.1021/es9035557
8. Walters, C.; Pool, E.; Somerset, V. *Toxicol. Environ. Chem.* **2013,** *95,* 1690–1701. doi:10.1080/02772248.2014.904141
9. Pettibone, J. M.; Gigault, J.; Hackley, V. A. *ACS Nano* **2013,** *7,* 2491–2499. doi:10.1021/nn3058517
10. MacCuspie, R. I.; Allen, A. J.; Hackley, V. A. *Nanotoxicology* **2011,** *5,* 140–156. doi:10.3109/17435390.2010.504311
11. Loza, K.; Diendorf, J.; Sengstock, C.; Ruiz-Gonzalez, L.; Gonzalez-Calbet, J. M.; Vallet-Regi, M.; Köller, M.; Epple, M. *J. Mater. Chem. B* **2014,** *2,* 1634–1643. doi:10.1039/c3tb21569e
12. Liu, J. Y.; Sonshine, D. A.; Shervani, S.; Hurt, R. H. *ACS Nano* **2010,** *4,* 6903–6913. doi:10.1021/nn102272n
13. Liu, J. Y.; Wang, Z. Y.; Liu, F. D.; Kane, A. B.; Hurt, R. H. *ACS Nano* **2012,** *6,* 9887–9899. doi:10.1021/nn303449n
14. Stebounova, L. V.; Guio, E.; Grassian, V. H. *J. Nanopart. Res.* **2011,** *13,* 233–244. doi:10.1007/s11051-010-0022-3
15. Hotze, E. M.; Labille, J.; Alvarez, P.; Wiesner, M. R. *Environ. Sci. Technol.* **2008,** *42,* 4175–4180. doi:10.1021/es702172w
16. Hussain, S. M.; Braydich-Stolle, L. K.; Schrand, A. M.; Murdock, R. C.; Yu, K. O.; Mattie, D. M.; Schlager, J. J.; Terrones, M. *Adv. Mater.* **2009,** *21,* 1549–1559. doi:10.1002/adma.200801395
17. Park, E.-J.; Yi, J.; Kim, Y.; Choi, K.; Park, K. *Toxicol. In Vitro* **2010,** *24,* 872–878. doi:10.1016/j.tiv.2009.12.001
18. Zook, J. M.; MacCuspie, R. I.; Locascio, L. E.; Halter, M. D.; Elliott, J. T. *Nanotoxicology* **2011,** *5,* 517–530. doi:10.3109/17435390.2010.536615
19. Tejamaya, M.; Römer, I.; Merrifield, R. C.; Lead, J. R. *Environ. Sci. Technol.* **2012,** *46,* 7011–7017. doi:10.1021/es2038596
20. Vidic, J.; Haque, F.; Guigner, J. M.; Vidy, A.; Chevalier, C.; Stankic, S. *Langmuir* **2014,** *30,* 11366–11374. doi:10.1021/la501479p
21. Marucco, A.; Catalano, F.; Fenoglio, I.; Turci, F.; Martra, G.; Fubini, B. *Chem. Res. Toxicol.* **2015,** *28,* 87–91. doi:10.1021/tx500366a
22. Leo, B. F.; Chen, S.; Kyo, Y.; Herpoldt, K.-L.; Terrill, N. J.; Dunlop, I. E.; McPhail, D. S.; Shaffer, M. S.; Schwander, S.; Gow, A.; Zhang, J.; Chung, K. F.; Tetley, T. D.; Porter, A. E.; Ryan, M. P. *Environ. Sci. Technol.* **2013,** *47,* 11232–11240. doi:10.1021/es403377p
23. Li, X.; Lenhart, J. J.; Walker, H. W. *Langmuir* **2012,** *28,* 1095–1104. doi:10.1021/la202328n
24. MacCuspie, R. I. *J. Nanopart. Res.* **2011,** *13,* 2893–2908. doi:10.1007/s11051-010-0178-x
25. Sharma, V. K.; Siskova, K. M.; Zboril, R.; Gardea-Torresdey, J. L. *Adv. Colloid Interface Sci.* **2014,** *204,* 15–34. doi:10.1016/j.cis.2013.12.002
26. Jiang, J.; Oberdörster, G.; Biswas, P. *J. Nanopart. Res.* **2009,** *11,* 77–89. doi:10.1007/s11051-008-9446-4
27. Gebauer, J. S.; Treuel, L. *J. Colloid Interface Sci.* **2011,** *354,* 546–554. doi:10.1016/j.jcis.2010.11.016
28. Thanh, N. T. K.; Rosenzweig, Z. *Anal. Chem.* **2002,** *74,* 1624–1628. doi:10.1021/ac011127p
29. Schulze, C.; Kroll, A.; Lehr, C.-M.; Schäfer, U. F.; Becker, K.; Schnekenburger, J.; Schulze Isfort, C.; Landsiedel, R.; Wohlleben, W. *Nanotoxicology* **2008,** *2,* 51–61. doi:10.1080/17435390802018378
30. Gebauer, J. S.; Malissek, M.; Simon, S.; Knauer, S. K.; Maskos, M.; Stauber, R. H.; Peukert, W.; Treuel, L. *Langmuir* **2012,** *28,* 9673–9679. doi:10.1021/la301104a
31. Segets, D.; Marczak, R.; Schäfer, S.; Paula, C.; Gnichwitz, J.-F.; Hirsch, A.; Peukert, W. *ACS Nano* **2011,** *5,* 4658–4669. doi:10.1021/nn200465b
32. Kohut, A.; Voronov, A.; Peukert, W. *Langmuir* **2007,** *23,* 504–508. doi:10.1021/la062465u
33. Gilbert, B.; Huang, F.; Zhang, H.; Waychunas, G. A.; Banfield, J. F. *Science* **2004,** *305,* 651–654. doi:10.1126/science.1098454

34. Min, Y.; Akbulut, M.; Kristiansen, K.; Golan, Y.; Israelachvili, J. *Nat. Mater.* **2008,** *7,* 527–538. doi:10.1038/nmat2206
35. Zook, J. M.; Halter, M. D.; Cleveland, D.; Long, S. E. *J. Nanopart. Res.* **2012,** *14,* 1165. doi:10.1007/s11051-012-1165-1
36. Treuel, L.; Nienhaus, G. U. *Biophys. Rev.* **2012,** *4,* 137–147. doi:10.1007/s12551-012-0072-0
37. Walczyk, D.; Bombelli, F. B.; Monopoli, M. P.; Lynch, I.; Dawson, K. A. *J. Am. Chem. Soc.* **2010,** *132,* 5761–5768. doi:10.1021/ja910675v
38. Moerz, S. T.; Huber, P. *Langmuir* **2014,** *30,* 2729–2737. doi:10.1021/la404947j
39. Monopoli, M. P.; Walczyk, D.; Campbell, A.; Elia, G.; Lynch, I.; Bombelli, F. B.; Dawson, K. A. *J. Am. Chem. Soc.* **2011,** *133,* 2525–2534. doi:10.1021/ja107583h
40. Lynch, I.; Salvati, A.; Dawson, K. A. *Nat. Nanotechnol.* **2009,** *4,* 546–547. doi:10.1038/nnano.2009.248
41. Shannahan, J. H.; Lai, X.; Ke, P. C.; Podila, R.; Brown, J. M.; Witzmann, F. A. *PLoS One* **2013,** *8,* e74001. doi:10.1371/journal.pone.0074001
42. Park, M. V. D. Z.; Neigh, A. M.; Vermeulen, J. P.; de la Fonteyne, L. J. J.; Verharen, H. W.; Briedé, J. J.; van Loveren, H.; de Jong, W. H. *Biomaterials* **2011,** *32,* 9810–9817. doi:10.1016/j.biomaterials.2011.08.085
43. El Badawy, A. M.; Silva, R. G.; Morris, B.; Scheckel, K. G.; Suidan, M. T.; Tolaymat, T. M. *Environ. Sci. Technol.* **2011,** *45,* 283–287. doi:10.1021/es1034188
44. European Commission. Communication from the Commission to the European Parliament, the Council and the European Economic and Social Committee. Second regulatory review on nanomaterials. Brussels, 3.10.2012, COM (2012) 572 final.
45. Martin, M. N.; Allen, A. J.; MacCuspie, R. I.; Hackley, V. A. *Langmuir* **2014,** *30,* 11442–11452. doi:10.1021/la502973z
46. Horák, D.; Babič, M.; Jendelová, P.; Herynek, V.; Trchová, M.; Pientka, Z.; Pollert, E.; Hájek, M.; Syková, E. *Bioconjugate Chem.* **2007,** *18,* 635–644. doi:10.1021/bc060186c
47. Horák, D.; Babič, M.; Jendelová, P.; Herynek, V.; Trchová, M.; Likavčanová, K.; Kapcalová, M.; Hájek, M.; Syková, E. *J. Magn. Magn. Mater.* **2009,** *321,* 1539–1547. doi:10.1016/j.jmmm.2009.02.082
48. Vinković Vrček, I.; Žuntar, I.; Petlevski, R.; Pavičić, I.; Dutour Sikirić, M.; Ćurlin, M.; Goessler, W. *Environ. Toxicol.* **2014,** in press. doi:10.1002/tox.22081
49. Vinković Vrček, I.; Pavičić, I.; Crnković, T.; Jurašin, D.; Babič, M.; Horák, D.; Lovrić, M.; Ferhatović, L.; Ćurlin, M.; Gajović, S. *RSC Adv.* **2015,** *5,* 70787–70807. doi:10.1039/C5RA14100A
50. Milić, M.; Leitinger, G.; Pavičić, I.; Zebić Avdičević, M.; Dobrović, S.; Goessler, W.; Vinković Vrček, I. *J. Appl. Toxicol.* **2015,** *35,* 581–592. doi:10.1002/jat.3081
51. Kvítek, L.; Panáček, A.; Soukupová, J.; Kolář, M.; Večeřová, R.; Prucek, R.; Holecová, M.; Zbořil, R. *J. Phys. Chem. C* **2008,** *112,* 5825–5834. doi:10.1021/jp711616v
52. Churchman, A. H.; Wallace, R.; Milne, S. J.; Brown, A. P.; Brydson, R.; Beales, P. A. *Chem. Commun.* **2013,** *49,* 4172–4174. doi:10.1039/c3cc37871c
53. Murdock, R. C.; Braydich-Stolle, L.; Schrand, A. M.; Schlager, J. J.; Hussain, S. M. *Toxicol. Sci.* **2008,** *101,* 239–253. doi:10.1093/toxsci/kfm240
54. Cedervall, T.; Lynch, I.; Lindman, S.; Berggård, T.; Thulin, E.; Nilsson, H.; Dawson, K. A.; Linse, S. *Proc. Natl. Acad. Sci. U. S. A.* **2007,** *104,* 2050–2055. doi:10.1073/pnas.0608582104
55. Maiorano, G.; Sabella, S.; Sorce, B.; Brunetti, V.; Malvindi, M. A.; Cingolani, R.; Pompa, P. P. *ACS Nano* **2010,** *4,* 7481–7491. doi:10.1021/nn101557e
56. Simón-Vázquez, R.; Lozano-Fernández, T.; Peleteiro-Olmedo, M.; González-Fernández, Á. *Colloids Surf., B* **2014,** *113,* 198–206. doi:10.1016/j.colsurfb.2013.08.047
57. Ravindran, A.; Singh, A.; Raichur, A. M.; Chandrasekaran, N.; Mukherjee, A. *Colloids Surf., B* **2010,** *76,* 32–37. doi:10.1016/j.colsurfb.2009.10.005
58. Yang, Q.; Liang, J.; Han, H. *J. Phys. Chem. B* **2009,** *113,* 10454–10458. doi:10.1021/jp904004w
59. Patil, S.; Sandberg, A.; Heckert, E.; Self, W.; Seal, S. *Biomaterials* **2007,** *28,* 4600–4607. doi:10.1016/j.biomaterials.2007.07.029
60. Peters, T., Jr. *All About Albumin: Biochemistry, Genetics and Medical Applications,* 1st ed.; Academic Press, Inc.: San Diego, CA, USA, 1996.
61. Saptarshi, S. R.; Duschl, A.; Lopata, A. L. *J. Nanobiotechnol.* **2013,** *11,* 26. doi:10.1186/1477-3155-11-26
62. Dobrovolskaia, M. A.; Patri, A. K.; Zheng, J.; Clogston, J.; Ayub, D.; Aggarwal, P.; Neun, B. W.; Hall, J. B.; McNeil, S. E. *Nanomedicine* **2009,** *5,* 106–117. doi:10.1016/j.nano.2008.08.001
63. Alkilany, A. M.; Nagaria, P. K.; Hexel, C. R.; Shaw, T. J.; Murphy, C. J.; Wyatt, M. D. *Small* **2009,** *5,* 701–708. doi:10.1002/smll.200801546
64. Khullar, P.; Singh, V.; Mahal, A.; Dave, P. N.; Thakur, S.; Kaur, G.; Singh, J.; Singh Kamboj, S.; Singh Bakshi, M. *J. Phys. Chem. C* **2012,** *116,* 8834–8843. doi:10.1021/jp300585d
65. Casals, E.; Pfaller, T.; Duschl, A.; Oostingh, G. J.; Puntes, V. *ACS Nano* **2010,** *4,* 3623–3632. doi:10.1021/nn901372t
66. Xia, Y.; Xiong, Y.; Lim, B.; Skrabalak, S. E. *Angew. Chem., Int. Ed.* **2008,** *48,* 60–103. doi:10.1002/anie.200802248
67. Goesmann, H.; Feldmann, C. *Angew. Chem., Int. Ed.* **2010,** *49,* 1362–1395. doi:10.1002/anie.200903053
68. Klaus-Joerger, T.; Joerger, R.; Olsson, E.; Granqvist, C.-G. *Trends Biotechnol.* **2001,** *19,* 15–20. doi:10.1016/S0167-7799(00)01514-6
69. Lowenstam, H. A. *Science* **1981,** *211,* 1126–1131. doi:10.1126/science.7008198
70. Spring, S.; Schleifer, K.-H. *Syst. Appl. Microbiol.* **1995,** *18,* 147–153. doi:10.1016/S0723-2020(11)80386-3
71. Schüler, D.; Frankel, R. B. *Appl. Microbiol. Biotechnol.* **1999,** *52,* 464–473. doi:10.1007/s002530051547
72. Kajander, E. O.; Çiftçioglu, N. *Proc. Natl. Acad. Sci. U. S. A.* **1998,** *95,* 8274–8279. doi:10.1073/pnas.95.14.8274
73. Rivadeneyra, M.-A.; Delgado, G.; Soriano, M.; Ramos-Cormenzana, A.; Delgado, R. *Curr. Microbiol.* **1999,** *39,* 53–57. doi:10.1007/PL00006827
74. Keefe, W. E. *Infect. Immun.* **1976,** *14,* 590–592.
75. Klaus, T.; Joerger, R.; Olsson, E.; Granqvist, C.-G. *Proc. Natl. Acad. Sci. U. S. A.* **1999,** *96,* 13611–13614. doi:10.1073/pnas.96.24.13611

Review DOI: 10.1515/aiht-2017-68-3054

How protein coronas determine the fate of engineered nanoparticles in biological environment

Ivona Capjak[1], Sandra Šupraha Goreta[2], Darija Domazet Jurašin[3], and Ivana Vinković Vrček[4]

Croatian Institute of Transfusion Medicine[1], University of Zagreb, Faculty of Pharmacy and Biochemistry[2], Ruđer Bošković Institute[3], Institute for Medical Research and Occupational Health[4], Zagreb, Croatia

[Received in October 2017; Similarity Check in October 2017; Accepted in December 2017]

Nanomedicine is a booming medical field that utilises nanoparticles (NPs) for the development of medicines, medical devices, and diagnostic tools. The behaviour of NPs *in vivo* may be quite complex due to their interactions with biological molecules. These interactions in biological fluids result in NPs being enveloped by dynamic protein coronas, which serve as an interface between NPs and their environment (blood, cell, tissue). How will the corona interact with this environment will depend on the biological, chemical, and physical properties of NPs, the properties of the proteins that make the corona, as well as the biological environment. This review summarises the main characteristics of protein corona and describes its dynamic nature. It also presents the most common analytical methods to study the corona, including examples of protein corona composition for the most common NPs used in biomedicine. This knowledge is necessary to design NPs that will create a corona with a desired efficiency and safety in clinical use.

KEY WORDS: *hard corona; nano-bio interface; nanomedicine; soft corona*

Nanomedicine is a growing medical field that utilises nanomaterials for new applications in medicine, including their clinical use in disease diagnosis and treatment (1-3). According to the European Commission (4), *'Nanomaterial' means a natural, incidental or manufactured material containing particles, in an unbound state or as an aggregate or as an agglomerate and where, for 50 % or more of the particles in the number size distribution, one or more external dimensions is in the size range 1-100 nm*. However, in medicine the term *nanoparticle* includes particles with dimensions of up to 1000 nm.

Due to a large surface-area-to-volume ratio, nanoparticles (NPs) have exceptional functional and structural properties that make them suitable to carry many diagnostic and therapeutic agents (5). Recent advances in nanomedicine have resulted in the development of biodegradable nanodrug delivery systems, nanocrystals for magnetic resonance imaging (MRI), and luminescent NPs for multiplexed molecular diagnostics (1, 3, 5, 6).

Because of the small size, NPs can enter almost every part of the body, including tissues, organs, and organelles (mitochondria, lysosomes, and endosomes) by different routes (e.g., inhalation, ingestion, injection, or physical contact with cuts or wounds) (2, 3, 7-9).

There are many types of NPs, including polymeric NPs, liposomes, carbon nanotubes, quantum dots, or metal-based NPs (gold, silver iron oxide, silica, titanium dioxide, etc.). Owing to the exceptional properties, these NPs may be used for targeted drug and contrast delivery, photothermal therapy, optical sensing, biochromatography, bioanalytical electrochemistry, biocidal agents and coatings, or a variety of bioassays (1-3, 5).

Their distribution, excretion, metabolism, and pharmacokinetics may be quite complex and pose a challenge for developing safe and effective nano-based biomedical agents. One of the key issues to resolve is rapid NP uptake and clearance by the reticuloendothelial system (RES), active *vs*. passive targeting, and penetration into tumour tissues (5).

Even though thousands of research papers have already been published on the interaction between NPs and biological systems, little is still known about the mechanistic details of these interactions (5). What are the biological interfaces that facilitate the interaction between NPs and cell components? This question should be addressed from the perspective of colloidal chemistry (10).

Blood as a biological medium contains more than a thousand biomolecules like proteins, lipids, and nucleic acids (1, 10). As soon as NPs enter the medium, ions, small molecules, proteins, and cells compete to adsorb on the NP surface due to its high reactivity (11). Plasma proteins have a critical role in creating nano-bio interfaces, as they opsonise NPs and form coronas (5, 12-16).

What kind of a protein corona forms around an NP's surface will depend on the NP's properties (size, shape, composition, surface functional groups, and surface charges), biophysical properties of the biological medium (blood, interstitial fluid, or cell cytoplasm), and the time of interaction. In other words, how will proteins adsorb on

Correspondence to: Ivana Vinković Vrček, Institute for Medical Research and Occupational Health, Ksaverska cesta 2, 10000 Zagreb
E-mail: *ivinkovic@imi.hr*

NPs will depend not only on protein-NP interaction but also on protein-protein interactions.

Once formed, a protein corona will determine the physicochemical behaviour of an NP. Its properties are more important in determining the biological response (agglomeration, cellular uptake, circulation lifetime, signalling, kinetics, transport, accumulation, and toxicity) than NP's properties. In other words, to find out what will be the distribution, metabolism, and elimination of NPs in the body before it is applied in clinical practice, one needs to determine how protein corona affects them.

Knowing how to control the formation of the protein corona is crucial for most clinical uses of NPs (9, 10, 17, 18). This review summarises the current knowledge on the nano-bio interface between NPs and proteins.

Dynamic nature of protein corona

When NPs come in contact with biological components, a nano-bio interface is formed. What makes it dynamic is a number of physicochemical interactions and thermodynamic exchanges between NP and biomolecular surfaces (7, 19-21). The dynamic nature of the nano-bio interface between NPs and proteins is best described by *soft* and *hard* coronas (Figure 1). Proteins with higher affinity for NP surface will exchange easily and quickly forming the *hard* corona, while proteins with low affinity exchange slowly forming the *soft* corona (19). The *hard* corona proteins interact directly with NP surface, while the *soft corona* proteins interact with the hard corona proteins via weak protein-protein interactions. The time needed for corona formation differs between the *hard* and *soft* corona. The *hard* corona is formed very quickly, within seconds or a minute, while the formation of the *soft* corona may take hours or even days, as proteins with higher affinity replace those with lower affinity (21). This process depends on protein concentrations and the composition of the biological environment.

Some suggest that even at low plasma concentrations, corona proteins will completely envelope the surface of an NP and modify its nature and physicochemical properties (19). Soft corona proteins can also interact with the hard corona proteins, as they desorb from NP surface and free the slot for other biomolecules to interact. All these exchanges are based on competitive adsorption and desorption of proteins, which depends on interaction time, protein concentrations, and their adsorption affinity for the NP. These exchanges, known as the *Vroman effect* (22, 23) have two stages. In the early stage, proteins adsorb rapidly with the highest association rates, and in the late stage proteins with short residence times are being replaced by proteins with slower association rates but longer residence times (24).

This dynamic nano-bio system is determined by hydrodynamic, electrostatic, electrodynamic, solvent, and steric interactions (Table 1) (25, 26).

This is why the nano-bio interface changes continuously in a biological environment (Figure 2), especially in the living cells, where different cell products are being secreted. When NPs move from one biological compartment to another, protein corona will change its profile. Some proteins form only transient complexes with NPs, while

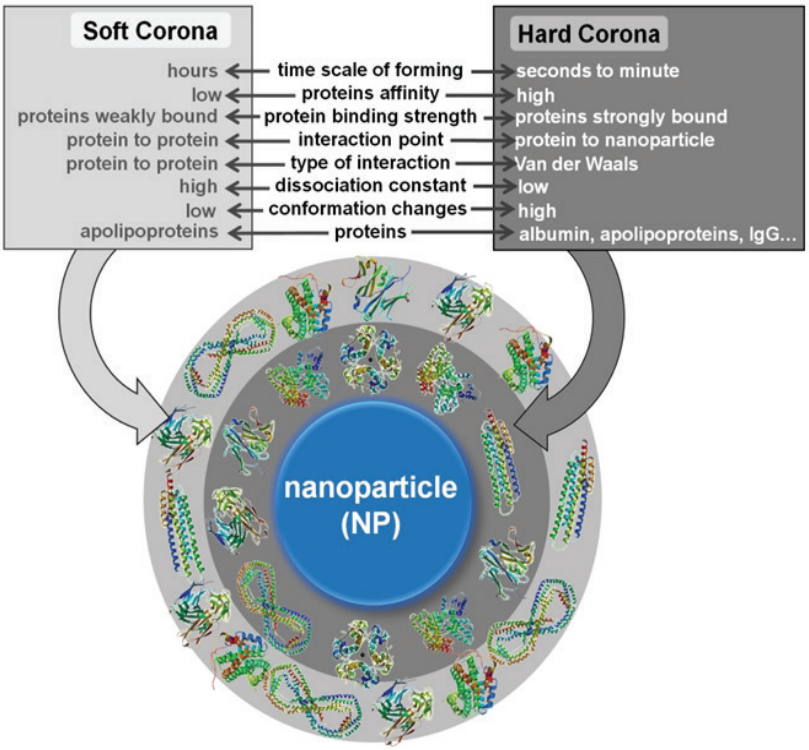

Figure 1 *Nano-bio interface: properties of protein corona on NP surface*

Table 1 *Main forces at the nano-bio interface (26)*

Force	Range (nm)	Origin and properties
Hydrodynamic interactions	10^2-10^6	Long-range interactions; induced by particles moving in a viscous fluid, bulk transport, shear, lift, and Brownian diffusion; Increases the collision between NPs and other surfaces in the system
Electrostatic interactions	1-100	Coulomb interactions; induced by attraction or collision between charged interfaces and counter- or repel co-ions; characterized by the formation of an electrostatic double layer
Electrodynamic interactions	1-100	Van der Waals interactions that describe interactions between randomly oriented dipoles, between dipole and induced dipole, and fluctuating dipole and induced dipole
Solvent interactions	1-10	Interactions between lyophobic or lyophilic materials and solvent molecules
Steric interactions	1-100	Repulsive interactions with other interfaces; induced by adsorbed polymer layers on NPs surface; increase stability of individual NPs, but can interfere in cellular uptake

others will be tightly bound, depending on the specific NP type and the biological fluids in which NPs are suspended.

Protein adsorption on and interaction with NPs may induce conformational changes or crowding of proteins on the NPs surface or the formation of reactive oxygen species (ROS) that will cause oxidative damage to the adsorbed proteins (26). If a hydrophobic or charged protein sequence interacts with a hydrophobic or charged part of NP surface, this will induce thermodynamically favourable changes. Conformational changes of proteins induced by their interaction with NPs are typically irreversible (21) and may affect the downstream protein-protein interaction, cellular signalling, and DNA transcription, which directly affect enzyme activity (24). At the same time, protein binding that changes the shape, size, and surface charge of NPs will directly affect the agglomeration, cellular uptake, circulation lifetime, signalling, kinetics, transport, accumulation, and toxicity of NPs in a biological environment (10, 27).

A complex consisting of an NP and its protein corona is a new entity that cells can *see* (10, 28). For easier understanding, hard and soft coronas are usually presented as layers (Figure 1). The outer layer (soft corona) does not allow the inner layer (hard corona) to interact with the cell

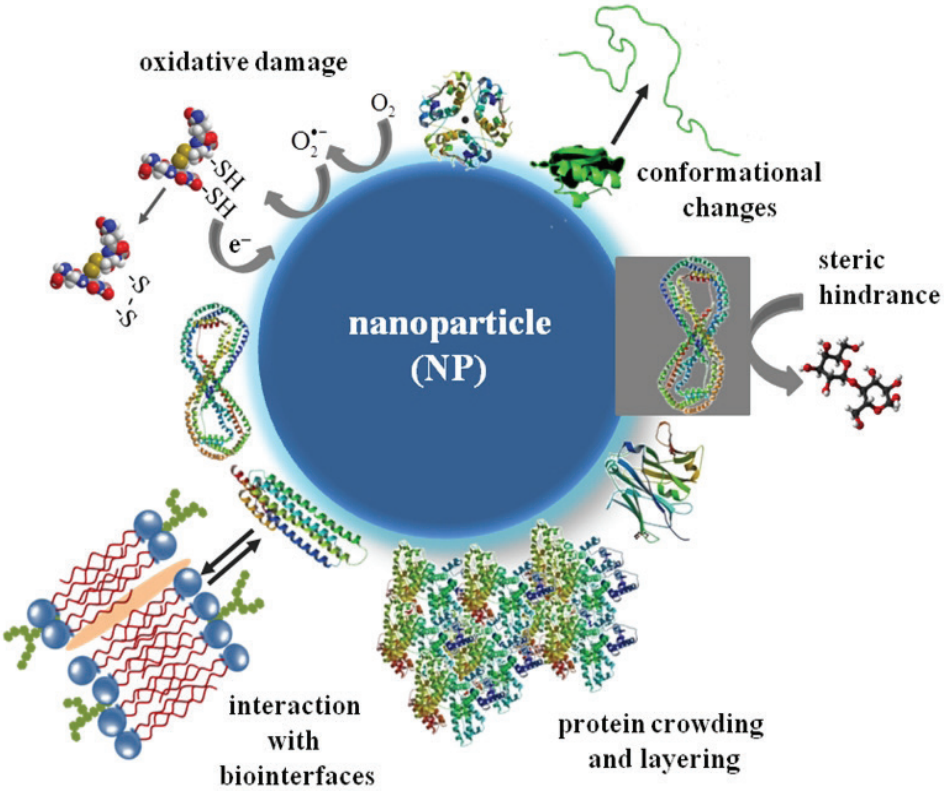

Figure 2 *Changes in the structure and function of NPs and proteins caused by events occurring at the nano-bio interface [inspired by (10)]*

medium (6, 7, 11, 14, 18, 29). Of course, this will depend on the thickness of the outer layer.

Figure 3 shows the types of interactions between NPs and the biological medium. These interactions promote or inhibit: (a) the adsorption of ions, detergents, and other molecules from the medium, (b) attachment/detachment of proteins, (c) competitive binding, (d) steric hindrance on the NPs surface, (e) formation of two or more layers on NP surface, (e) NP dissolution and/or degradation, (f) surface reconstruction, and (g) accumulation and/or agglomeration of NPs (12, 27, 30, 31).

The most important physicochemical properties of an NP that define protein corona formation and fate are chemical composition, shape, curvature, surface functionalisation and structure, porosity, crystallinity, heterogeneity, roughness, and hydrophobicity/hydrophilicity (2-4). Furthermore, effective surface charge, aggregation state, stability, biodegradability, and dissolution properties of the NP surface layer are also important parameters that need to be considered for the investigation of the nano-bio interface (4, 32). For example, surface curvature of an NP affects protein-binding affinities. Greater curvature makes the corona thicker but decreases protein-protein interactions and conformational changes of the adsorbed proteins. Higher surface charge increases corona thickness as well as conformational changes of proteins (13, 27, 30, 31, 33). It may also trigger protein denaturation (27). Higher hydrophobicity increases corona thickness and conformational changes of proteins, as well as the opsonisation rate (14, 34).

All these properties and interactions (Figures 2-3) determine the long-range and short-range forces governing the nano-bio interface (Table 1) (10, 35). Long-range forces originate from attractive van der Waals and repulsive electrostatic double-layer interactions, while short-range forces arise from charge, steric interactions, depletion, and solvent interactions (Table 2) (10, 35).

Understanding how each physicochemical parameter of an NP affects corona formation is a key to designing new, efficient, and secure nanomaterials. Then these properties can be optimised, NPs pre-coated, and their surfaces functionalised to obtain the nature of the protein corona that would render an NP biocompatible (23). One should also take into account environmental factors, such as temperature, pH, protein concentrations, and time of interaction. NPs may also change adsorption, accumulation, degradation, agglomeration, dissolution, distribution, and clearance patterns after the protein corona has been formed, while the proteins forming the corona may pass through conformational changes, free energy release, restructuration, or change their binding profile and kinetics (10, 36, 37).

Mechanistic investigation of protein corona

The properties of metallic NPs can be investigated with a range of spectroscopic, electrophoretic, and microscopic methods (Table 2). The same methods can also be used to study protein corona formation and composition. The most common methods for determining NP properties are the transmission electron microscopy (TEM), light scattering techniques, and UV-visible and fluorescence spectroscopy.

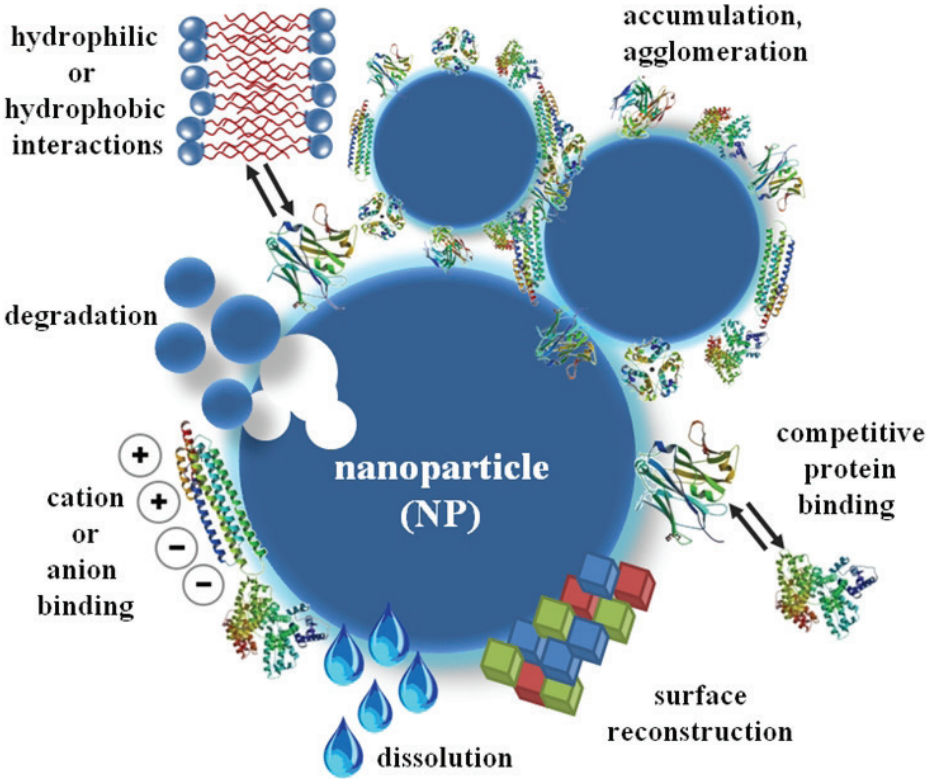

Figure 3 *Active interactions at the nano-bio interface [inspired by (10)]*

Table 2 *Analytical methods used to assess the of properties of NPs and their interactions at the nano-bio interface*

NP properties	Analytical technique	Brief analytical description
Size and charge	light scattering (dynamic and electrophoretic)	changes in the hydrodynamic diameter of NP upon binding to proteins
	analytical ultracentrifugation	changes in the hydrodynamic diameter of NP
Size, shape and structure	transmission electron microscopy (TEM)	visualisation of NPs
	atomic force microscopy (AFM)	visualisation of NPs
Structure	X-ray diffraction	determination of crystalline and chemical structure
Size, dissolution	UV-Vis spectroscopy	evaluation for surface plasmon resonance (SPR) peak
Dissolution, structure	inductively coupled plasma mass spectrometry (ICPMS)	determination of elemental composition
Surface area	Braunauer-Emmet-Teller method	measurement of specific surface area using adsorption of gas on the surface
Protein binding affinity	fluorescence spectroscopy	evaluation of changes in fluorescence spectra of proteins due to the NPs-protein interaction
	UV-Vis spectroscopy	evaluation of changes in absorption spectra due to the NPs-protein interaction
	isothermal calorimetry	determination of binding constant, thermodynamic parameters of NP-protein interactions
	quartz crystal balance	determination of changes in mass at the oscillating quartz surface in the NPs-protein complexes
	surface plasmon resonance	detection of change in oscillation of electrons on a metal surface in the NPs-protein complexes
	AFM	determination of adhesion forces and surface free energy during the protein corona formation
	fluorescence correlation spectroscopy	determination of binding characteristics depending on the fluctuation in florescence
Protein structural changes	circular dichroism spectroscopy	measurement of changes in secondary structure of proteins depending on chiral properties of proteins
	Fourier transformed infrared spectroscopy	measurement of adsorption of amide bonds in the proteins to derive structural change
	Raman spectroscopy	evaluation of molecular vibrations to predict structure
	nuclear magnetic resonance	determination of magnetic properties of atomic nuclei to predict structure
Composition of protein corona	capillary electrophoresis	separation of proteins and NPs-protein complexes using very small sample volumes
	LC-MS/MS	separation and identification of protein, accurate analysis of molecular weight (M_w) distribution
	polyacrylamide gel electrophoresis (PAGE)	identification of proteins

Newly synthesised metallic NPs are usually characterised in the medium used for their synthesis, such as water. Although quite demanding, NP evaluation in pure water is much less complicated than in any biological matrix.

Complexes that form between NPs and proteins are most often analysed with mass spectrometry (MS)-based proteomics. Spectroscopic methods like ultraviolet-visible (UV-Vis) and fluorescence spectroscopy, and circular dichroism (CD) are used to investigate nano-bio interface binding interactions due to their robustness and high sensitivity. UV-Vis spectroscopy can be used to measure the rate of protein binding as a function of change in plasmon λ_{max} over time. Fluorescence spectroscopy acquires the intrinsic fluorescence of the protein and can therefore measure binding to NPs. CD spectroscopy uses changes in the chiral properties of a protein to predict changes in its secondary structure. Measured interactions between plasma proteins and NPs can be quantified using several kinetic models and equations (38-40). All the methods described in Table 2 are quite accessible and straightforward to evaluate nano-bio interface in pure water or a simple buffer system. In complex media like blood plasma or cellular matrix, however, analytical performance and interpretation of results may become very complex.

Protein corona composition

The most extensively studied biological environment for protein corona is human blood plasma. Protein layer(s) that adsorb on NPs in blood can affect their uptake and distribution in the cells. For example, fibrinogen, immunoglobulin G (IgG), or complement factors are believed to promote phagocytosis and removal of NPs from the bloodstream, while human serum albumin (HSA) and apolipoproteins prolong their circulation time in blood (19).

In the early stage of corona formation, albumin, IgG, fibrinogen, and apolipoproteins seem to adsorb rapidly on metallic NPs in plasma (13, 35, 41). These proteins are found in the hard coronas of all studied NPs and are replaced by apolipoproteins and coagulation factors in the slow phase of corona formation (35). Changes in biological environment also reflect on a corona composition. Walkey and Chan (21) use the term *adsorbome* to denote a group of 125 most common plasma proteins in the corona. Table 3 lists some of them by the type of NP.

Only two to six of them strongly adsorb on metallic NPs. For most metallic NPs, the corona is dominated by albumin (42), which is at the same time the most abundant protein in plasma. Although it has a negative net charge at pH 7.4, albumin contains 60 positively charged lysine residues, which enable its interaction with both positively and negatively charged NPs. Albumin will form anionic corona complexes with NPs regardless of their net charge (36). These coronas are similar in size and effective surface charge, but their behaviour in contact with the cell will differ. Fleischert and Payne (36) believe that cationic NPs alter the structure of albumin proteins in the corona, while anionic NPs do not. These structural changes affect the behaviour of the albumin-NP complex at the cellular level, so that cell receptors bind coronas formed around anionic NPs and redirect those formed around cationic NPs to scavenger receptors. Another difference is that albumin adsorbs much more on the surface of anionic than cationic NPs (23% *vs.* 8% of surface coverage, respectively) (36).

Similar to albumin, fibrinogen was also identified in the corona of many NPs. Apolipoproteins will mainly adsorb on liposomes and polymeric NPs, as they have low affinity for metallic NPs. The main force involved in their interactions with NPs is hydrophobicity (29). Polymeric and hydrophobic NPs also attract proteins like transferrin, haptoglobin, fetuin A, kininogen, histidine-rich glycoprotein, and intrinsic clotting pathway factors. Most of these proteins will adsorb on metallic NPs (29).

Table 3 *Composition of protein corona by NP type*

NP type	Proteins detected in corona	Reference
Polystyrene NPs	coagulation factors, immunoglobulins, lipoproteins, acute phase proteins, complement proteins, plasminogen, anti-CD4, c4a, albumin	1, 23,42
Latex NPs	albumin, apolipoproteins, immunoglobulins, hemoglobin, haptoglobins	1, 23
Copolymer NPs	albumin, apolipoprotiens, fibrinogen, immunoglobulins, C4BP-α-chain	1
Supraparamagnetic iron oxide NPs	albumin, α-1-antitrypsin, fibrinogen chains, immunoglobulin chains, transferrin, transthyretin	1, 41, 42
Gold NPs	albumin, fibrinogen chains, apolipoprotein A1, transport proteins, coagulation factors, tissue development proteins	1, 23, 42
Carbon nanotubes	fibrinogen chains, immunoglobulin light chains, fibrin, albumin, ApoA1, complement, component proteins, fibronectin	1, 42
SiO_2 NPs	immunoglobulins, lipoproteins, complement proteins, coagulation proteins, acute phase proteins, cell proteins, serum proteins	1, 23, 19
TiO_2NPs, ZnONPs, SiO_2 NPs	albumin, immunoglobulins, fibrinogen, transferrin, apolipoprotein A1, complement proteins, immunoglobulin light chains, fibrin, albumin, fibronectin	1, 23
Magnetic NPs	albumin, apolipoprotein A1, complement factors, vitronectin, hemoglobin	1
Citrate-coated AgNPs	albumin, α-1-antiproteinase, α-2-HS-glycoprotein, apolipoprotein A1, serotransferrin, α-2-macroglobulin, α-fetoprotein, apolipoprotein B100, α-2-antiplasmin, complement C3, β-2-glycoprotein 1, fetuin-B, inter-α-trypsin inhibitor heavy chain H1, hemoglobin foetal subunit β, inter-α-trypsin inhibitor heavy chain H3, inter-α-trypsin inhibitor heavy chain H2, hemoglobin subunit α, complement factor B, hemopexin, serpin A3-6	46
AgNPs coated with polyvinylpyrrolidone	albumin, α-2-HS-glycoprotein, α-1-antiproteinase, apolipoprotein A1, serotransferrin, α-2-macroglobulin, α-fetoprotein, apolipoprotein B100, complement C3, α-2-antiplasmin, inter-α-trypsin inhibitor heavy chain H1, fetuin-B, β-2-glycoprotein 1, hemoglobin foetal subunit beta, inter-α-trypsin inhibitor heavy chain H3, inter-α-trypsin inhibitor heavy chain H2, vitamin D-binding protein, transthyretin, hemoglobin subunit α, complement factor B	46

Importance of protein corona for biomedical application of nanoparticles

As the NP-corona complex is actually "what the cell sees" (28), it is more important to determine the biological response (i.e., immunogenicity) to the complex than the properties of an NP alone (43). For most biomedical purposes, hard corona will likely improve the interaction between NPs and proteins, membranes, phospholipids, endocytic vesicles, organelles, and DNA (44-46).

Corona is what controls which type of biomolecule will it bind and how, how will the NP-corona complex interact with cells receptors, and what will its distribution and elimination be (45-46). For a nano-drug delivery system it is important to define the affinity, stoichiometry, kinetics, and the concentrations of NPs for their interaction with specific proteins. At the moment, however, we still have a lot to learn. The biggest challenge for researches is to find out how protein corona could contribute to nanodrug distribution *in vivo*.

Conflicts of interest

None to declare.

REFERENCES

1. Saptarshi SR, Duschl A, Lopata AL. Interaction of nanoparticles with proteins: relation to bio-reactivity of the nanoparticle. J Nanobiotechnol 2013;11:26. doi: 10.1186/1477-3155-11-26
2. Huang R, Carney RP, Stellacci F, Lau BL. Protein-nanoparticle interactions: the effects of surface compositional and structural heterogeneity are scale dependent. Nanoscale 2013;5:6928-35. doi: 10.1039/c3nr02117c
3. Jurašin DD, Ćurlin M, Capjak I, Crnković T, Lovrić M, Babič M, Horák D, Vinković Vrček I, Gajović S. Sufrace coating affects behavior of metallic nanoparticle in a bilogical environment. Beilstein J Nanotechnol 2016;7:246-62. doi: 10.3762/bjnano.7.23.
4. European Commission. Commission recommendation of 18 October 2011 on the definition of nanomaterial (Text with EEA relevance) (2011/696/EU) [displayed 3 November 2017]. Available at https://ec.europa.eu/research/industrial_technologies/pdf/policy/commission-recommendation-on-the-definition-of-nanomater-18102011_en.pdf
5. Lane LA, Qian X, Smith AM, Nie S. Physical chemistry of nanomedicine: understanding the complex behaviours of nanoparticles *in vivo*. Annu Rev Phys Chem 2015;66:521-47. doi: 10.1146/annurev-physchem-040513-103718
6. Ding F, Radic S, Chen R, Chen P, Geitner NK, Brown JM, Ke PC. Direct observation of a single nanoparticle-ubiquitin corona formation. Nanoscale 2013;5:9162-9. doi: 10.1039/c3nr02147e
7. Duran N, Silveira CP, Duran M, Martinez DST. Silver nanoparticle protein corona and toxicity: a mini-review. J Nanobiotechnology 2015;13:55. doi: 10.1186/s12951-015-0114-4
8. Docter D, Westmeier D, Markiewicz M, Stolte S, Knauer SK, Stauber RH. The nanoparticle biomolecule corona: lessons learned - challenge accepted? Chem Soc Rev 2015;44:6094-121. doi: 10.1039/C5CS00217F
9. Kononenko V, Narat M, Drobne D. Nanoparticle interaction with the immune system. Arh Hig Rada Toksikol 2015;66:97-108. doi:10.1515/aiht-2015-66-2582
10. Nel AE, Mädler L, Velegol D, Xia T, Hoek EMV, Somasundaran P, Klaessig F, Castranova V, Thompson M. Understanding biophysicochemical interactions at the nano-bio interface. Nat Mater 2009;8:543-57. doi: 10.1038/nmat2442
11. Tavanti F, Pedone A, Menziani MC. Competitive binding of proteins to gold nanoparticles disclosed by molecular dynamics simulations. J Phys Chem C 2015;119:22172-80. doi: 10.1021/acs.jpcc.5b05796
12. Cedervall T, Lynch I, Foy M, Berggad T, Donnelly S, Cagney G, Linse S, Dawson K. Detailed identification of plasma proteins adsorbed on copolymer nanoparticles. Angew Chem Int Ed 2007;46:5754-6. doi: 10.1002/anie.200700465
13. Lundqvist M, Stigler J, Elia G, Lynch I, Cedervall T, Dawson KA. Nanoparticle size and surface properties determine the protein corona with possible implications for biological impacts. Proc Natl Acad Sci 2008;105:14265-70. doi: 10.1073/pnas.0805135105
14. Cedervall T, Lynch I, Lindman S, Berggård T, Thulin E, Nilsson H, Dawson KA, Linse S. Understanding the nanoparticle-protein corona using methods to quantify exchange rates and affinities of proteins for nanoparticles. Proc Natl Acad Sci USA 2007;104:2050-5. doi: 10.1073/pnas.0608582104
15. Lynch I, Dawson KA, Linse S. Detecting cryptic epitopes created by nanoparticles. Sci STKE 2006;2006(327):pe14. doi: 10.1126/stke.3272006pe14
16. Gref R, Lück M, Quellec P, Marchand M, Dellacherie E, Harnisch S, Blunk T, Müller RH. 'Stealth' corona-core nanoparticles surface modified by polyethylene glycol (PEG): influences of the corona (PEG chain length and surface density) and of the core composition on phagocytic uptake and plasma protein adsorption. Colloids Surf B Biointerfaces 2000;18:301-13. doi: 10.1016/S0927-7765(99)00156-3
17. Kittler S, Greulich C, Gebauer JS, Diendorf J, Treuel L, Ruiz L, Gonzalez-Calbet JM, Vallet-Regi M, Zellner R, Köller M, Epple M. The influence of proteins on the dispersability and cell-biological activity of silver NP. J Mater Chem 2010;20:512-8. doi: 10.1039/B914875B
18. Koshkina O, Lang T, Thiermann R, Docter D, Stauber RH, Secker C, Schlaad H, Weidner S, Mohr B, Maskos M, Bertin A. Temperature-triggered protein adsorption on polymer-coated nanoparticles in serum. Langmuir 2015;31:8873-81. doi: 10.1021/acs.langmuir.5b00537
19. Monopoli MP, Walczyk D, Campbell A, Elia G, Lynch I, Bombelli FB, Dawson KA. Physical-chemical aspects of protein corona: relevance to *in vitro* and *in vivo* biological impacts of nanoparticles. J Am Chem Soc 2011;133:2525-34. doi: 10.1021/ja107583h
20. Miclăuş T, Bochenkov VE, Ogaki R, Howard KA, Sutherland DS. Spatial mapping and quantification of soft and hard protein coronas at silver nanocubes. Nano Lett 2014;14:2086-93. doi: 10.1021/nl500277c
21. Walkey CD, Chan WC. Understanding and controlling the interaction of nanomaterials with proteins in a physiological environment. Chem Soc Rev 2012;41:2780-99. doi: 10.1039/c1cs15233e

22. Vroman L, Adams AL, Fischer GC, Munoz PC. Interaction of high molecular-weight kininogen, factor-XII, and fibrinogen in plasma at interfaces. Blood 1980;55:156-9. PMID: 7350935
23. Aggarwal P, Hall JB, McLeland CB, Dobrovolskaia MA, McNeil SE. Nanoparticle interaction with plasma proteins as it relates to particle biodistribution, biocompatibility and therapeutic efficacy. Adv Drug Deliv Rev 2009;61:428-37. doi: 10.1016/j.addr.2009.03.009
24. Göppert TM, Müller RH. Polysorbate-stabilized solid lipid nanoparticles as colloidal carriers for of drugs to the brain: comparison of plasma protein adsorption patterns. J Drug Target 2005;13:179-87. doi: 10.1080/10611860500071292
25. Gebauer JS, Malissek M, Simon S, Knauer SK, Maskos M, Stauber RH, Peukert W, Treuel L. Impact of the nanoparticle-protein corona on colloidal stability and protein structure. Langmuir 2012;28:9673-9. doi: 10.1021/la301104a
26. Treuel L, Nienhaus GU. Toward a molecular understanding of nanoparticle-protein interactions. Biophys Rev 2012;4:137-47. doi 10.1007/s12551-012-0072-0
27. Lynch I, Dawson KA, Linse S. Detecting cryptic epitopes created by nanoparticles. Sci STKE 2006;2006(327):pe14. doi: 10.1126/stke.3272006pe14
28. Walczyk D, Bombelli FB, Monopoli MP, Lynch I, Dawson KA. What the cell "sees" in bionanoscience. J Am Chem Soc 2010;132:5761-8. doi: 10.1021/ja910675v
29. Gessner A, Waicz R, Lieske A, Paulke B-R, Mäder K, Müller RH. Nanoparticles with decreasing surface hydrophobicities: influence on plasma protein adsorption. Int J Pharm 2000;196:245-9. doi: 10.1016/S0378-5173(99)00432-9
30. Lundqvist M, Stigler J, Cedervall T, Berggard T, Flanagan MB, Lynch I, Elia G, Dawson K. The evolution of the protein corona around nanoparticles: a test study. ACS Nano 2011;5:7503-9. doi: 10.1021/nn202458g
31. Mahmoudi M, Lynch I, Ejtehadi MR, Monopoli MP, Bombelli FB, Laurent S. Protein-nanoparticle interactions: opportunities and challenges. Chem Rev 2011;111:5610-37. doi: 10.1021/cr100440g
32. Klein J. Probing the interaction of proteins and nanoparticles. Proc Natl Acad Sci USA 2007;104:2029-30. doi: 10.1073/pnas.0611610104
33. Gessner A, Lieske A, Paulke BR, Müller RH. Influence of surface charge density on protein adsorption on polymeric nanoparticles: analysis by two-dimensional electrophoresis. Eur J Pharm Biopharm 2002;54:165-70. doi: 10.1016/S0939-6411(02)00081-4
34. Lindman S, Lynch I, Thulin E, Nilsson H, Dawson KA, Linse S. Systematic investigation of the thermodynamics of HSA adsorption to N-iso-propylacrylamide/N-tert-butylacrylamide copolymer nanoparticles. Effects of particle size and hydrophobicity. Nano Lett 2007;7:914-20. doi: 10.1021/nl062743+
35. Rahman M. Nanoparticle and protein corona. In: Rahman M, Laurent S, Tawil N, Yahia L, Mahmoudi M, editors. Springer Series in Biophysics. Vol. 15. Protein-nanoparticle interactions. Chapter 2. Berlin Heidelberg: Springer-Verlag; 2013. p. 21-44.
36. Fleischert CC, Payne CK. Nanoparticle-cell interactions: molecular structure of the protein corona and cellular outcomes. Acc Chem Res 2014;47:2651-9. doi: 10.1021/ar500190q
37. Laera S, Ceccone G, Rossi F, Gilliland D, Hussain R, Siligardi G, Calzolai L. Measuring protein structure and stability of protein-nanoparticle systems. Nano Lett 2011;11:4480-4. doi: 10.1021/nl202909s
38. Eskandari K, Kamali M, Ramezani M, Safiri Z, Keihan AH, Rashidiani J, Kooshki H, Zarei H. The effect of hydrophobicity and hydrophilicity of gold nanoparticle on proteins structure and function. Int J Bio-Inorg Hybrid Nanomat 2013;2:465-70.
39. Cui M, Liu R, Deng Z, Ge G, Liu Y, Xie L. Quantitative study of protein coronas on gold nanoparticles with different surface modifications. Nano Res 2013;7:345. doi: 10.1007/s12274-013-0400-0
40. Boulos SP, Davis TA, Yang JA, Lohse SE, Alkilany AM, Holland LA, Murphy CJ. Nanoparticle-protein interactions: a thermodynamic and kinetic study of the adsorption of bovine serum albumin to gold nanoparticle surfaces. Langmuir 2013;29:14984-96. doi: 10.1021/la402920f
41. Sakulkhu U, Mahmoudi M, Maurizi L, Salaklang J, Hofmann H. Protein corona composition of superparamagnetic iron oxide nanoparticles with various physico-chemical properties and coatings. Scientific Rep 2014;4:5020. doi: 10.1038/srep05020
42. Karmali PP, Simberg D. Interactions of nanoparticles with plasma proteins: implication on clearance and toxicity of drug delivery systems. Expert Opin Drug Deliv 2011;8:343-57. doi: 10.1517/17425247.2011.554818
43. Lee YK, Choi E-J, Webster TJ, Kim S-H, Khang D. Effect of the protein corona on nanoparticles for modulating cytotoxicity and immunotoxicity. Int J Nanomedicine 2015;10:97-113. doi: 10.2147/IJN.S72998
44. Yallapu MM, Ebeling MC, Jaggi M, Chauhan SC. Plasma proteins interaction with curcumin nanoparticles: implications in cancer therapeutics. Curr Drug Metab 2013;14:504-15. PMCID: PMC4030727
45. Zook JM, Halter MD, Cleveland D, Long SE. Disentangling the effects of polymer coatings on silver nanoparticle agglomeration, dissolution and toxicity to determine mechanisms of nanotoxicity. J Nanopart Res 2012;14:1165. doi: 10.1007/s11051-012-1165-1
46. Shannahan JH, Lai X, Ke PC, Podila R, Brown JM, Witzmann FA. Silver nanoparticle protein corona composition in cell culture media. PLoS One 2013;8:e74001. doi: 10.1371/journal.pone.0074001

Kako proteinska korona određuje sudbinu nanočestica u biološkom okolišu

Nanomedicina je iznimno napredno medicinsko područje u kojem se iskorištavaju nanočestice za razvoj inovativnih lijekova, medicinskih pomagala i dijagnostičkih postupaka. U *in vivo* uvjetima ponašanje nanočestica može biti vrlo kompleksno zbog bliskih interakcija s biološkim molekulama. Zbog međudjelovanja nanočestica i proteina u biološkim tekućinama nastaje dinamička proteinska korona koja obavija nanočestice i tvori novo sučelje između nanočestica i okoliša u kojem se one nalaze (krv, stanice, tkiva). Ta međudjelovanja ovise o biološkim, kemijskim i fizikalnim svojstvima samih nanočestica i proteina, ali i samog biološkog okoliša. U ovom preglednom radu dan je prikaz glavnih karakteristika koji određuju proteinsku koronu te opis njezine dinamičke prirode. Prikazane su najvažnije analitičke metode za istraživanje proteinske korone te primjeri sastava proteinske korone za najčešće korištene vrste nanočestica u biomedicini. Takvo je znanje nužno za dizajn i razvoj učinkovitih i sigurnih nanomedicinskih proizvoda.

KLJUČNE RIJEČI: *nano-bio interakcije; nanomedicina; meka korona; tvrda korona*

Colloids and Surfaces B: Biointerfaces 170 (2018) 401–410

Contents lists available at ScienceDirect

Colloids and Surfaces B: Biointerfaces

journal homepage: www.elsevier.com/locate/colsurfb

Antimicrobial potency of differently coated 10 and 50 nm silver nanoparticles against clinically relevant bacteria *Escherichia coli* and *Staphylococcus aureus*

Anna-Liisa Kubo[a], Ivona Capjak[b], Ivana Vinković Vrček[c], Olesja M. Bondarenko[a], Imbi Kurvet[a], Heiki Vija[a], Angela Ivask[a], Kaja Kasemets[a], Anne Kahru[a,d,*]

[a] Laboratory of Environmental Toxicology, National Institute of Chemical Physics and Biophysics, Akadeemia tee 23, Tallinn 12618, Estonia
[b] Croatian Institute of Transfusion Medicine, Petrova 3, 10 000 Zagreb, Croatia
[c] Institute for Medical Research and Occupational Health, Ksaverska cesta 2, Zagreb, Croatia
[d] Estonian Academy of Sciences, Kohtu 6, Tallinn, Estonia

ARTICLE INFO

Keywords:
Library of silver nanoparticles
Biocides
Dissolution
Bioavailability
Recombinant Ag-sensor bacteria
Gram-negative and Gram-positive bacteria
Healthcare associated infections
Minimal bactericidal concentration
Flow cytometry
Nanoparticle-cell interactions

ABSTRACT

Silver nanoparticles (nanoAg) are effective antimicrobials and promising alternatives to traditional antibiotics. This study aimed at evaluating potency of different nanoAg against healthcare infections associated bacteria: Gram-negative *Escherichia coli* and Gram-positive *Staphylococcus aureus*. A library of differently coated nanoAg of two different sizes (10 and 50 nm) were prepared using coating agents poly-L-Lysine (PLL), cetyltrimethyl-ammonium bromide (CTAB), citrate (CIT), polyvinyl-pyrrolidone (PVP), polysorbate 80 (Tween 80), and dioctyl-sodium sulfosuccinate (AOT). Stability evaluation by means of agglomeration and dissolution behaviour was performed for all nanoAg under conditions relevant for this study.

Antibacterial properties of nanoAg were addressed by determining their minimal bactericidal concentrations (MBC) in deionised (DI) water to minimise the influence of silver speciation on its bioavailability. In parallel, $AgNO_3$ was analysed as an ionic control.

Studied nanoAg were efficient antimicrobials being remarkably more potent towards *E. coli* than to *S. aureus* (4 h MBC values for different nanoAg ranged from 0.08 to 5.0 mg Ag/L and 1.0–10 mg Ag/L, respectively). The toxicity of all nanoAg to *S. aureus* (but not to *E. coli*) increased with exposure time (4 h *vs* 24 h). 10 nm sized nanoAg released more Ag-ions and were more toxic than 50 nm nanoAg. Coating-dependent toxicity was more prominent for 50 nm nanoAg coated with Tween 80 or CTAB rendering the least toxic nanoAg. Obtained results showed that the antimicrobial effects of nanoAg were driven by shed Ag-ions, depended on target bacteria, exposure time and were the interplay of NP size, solubility and surface coating.

1. Introduction

The increased microbial resistance to antibiotics is a worldwide problem that significantly affects public health issue due to healthcare-associated infections (HAIs). O'Neill recently forecasted that the antimicrobial resistant bacteria (AMR) belonging to both, Gram-negative and Gram-positive bacteria [1] will kill more people than cancer by 2020 [2]. Unfortunately, prevention of HAIs is challenging due to rapid proliferation of bacteria and their profound ability to accommodate within unfavourable environment and develop resistance to nearly all existing antibiotics [3]. The use of silver nanoparticles (nanoAg) is one of the possibilities to combat the antibacterial resistance [1]. High antibacterial efficacy of nanoAg has often been demonstrated to originate from the effect of solubilised Ag-ions on the microbial membranes, specifically on the thiol-groups of proteins leading to enzyme inhibition [4] including enzymes of the respiratory chain [5]. Different nanoAg-based formulations have been recommended for high-touch surfaces in healthcare environment to avoid proliferation of pathogenic bacteria [6]. Also, as the risks of HAIs are often related with catheterization, silver-impregnated catheters are widely applied in acute-care hospitals [7]. In contrast to conventional antibiotics, bacterial resistance against silver has been reported just in a few hospital cases [8]. Additionally, synergic action of nanoAg with antibiotics commonly used against *E. coli* and *S. aureus* could be an effective antimicrobial strategy [9]. NanoAg are nowadays used as biocidal additives in many fields and in various products including dental resin composites, bone

* Corresponding author at: Laboratory of Environmental Toxicology, National Institute of Chemical Physics and Biophysics, Akadeemia tee 23, Tallinn 12618, Estonia.
E-mail address: anne.kahru@kbfi.ee (A. Kahru).

https://doi.org/10.1016/j.colsurfb.2018.06.027
Received 16 February 2018; Received in revised form 27 April 2018; Accepted 15 June 2018
Available online 18 June 2018
0927-7765/

Table 1
Coating/stabilising agents used in this study.

Name	Molecular structure	Molecular weight (g/mol)	Charge of the coating agent in deionised water	Conventional use
Trisodium citrate (CIT)	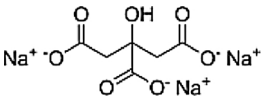	294.10 (dihydrate)	Negative	Buffering agent
Bis-2-ethylhexyl sulfosuccinate (AOT)	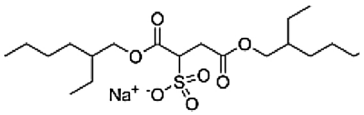	444.56 (Na-salt)	Negative	Anionic surfactant
Poly-vinylpyrrolidone (PVP)	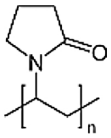	40000	Neutral	Nonionic polymer
Polysorbate 80 (Tween 80)	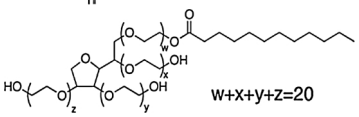	1310	Neutral	Nonionic surfactant
Cetyltrimethyl-ammonium bromide (CTAB)	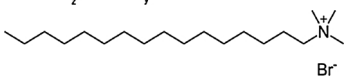	364.45	Positive	Cationic surfactant
Poly-L-lysine (PLL)	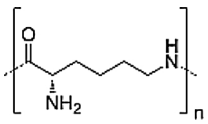	3000	Positive	Cationic polymer

cements, medical devices, water filters, textiles, detergents, soaps, toothpastes, wet wipes, washing machines, refrigerators, and many others [10,11]. According to the Nanotechnology Products Database (www.statnano.com), nanoAg are used in 75% nano enabled products for medical applications. The design of Ag-enabled biomedical nanomaterials is commonly performed by modulating the physico-chemical properties of nanoAg such as size, shape and surface properties [12,13]. Surface functionalisation is one of the important strategies to improve colloidal stability, controlled release of Ag-ions or targeted delivery of nanoAg [14]. Moreover, surface characteristics of nanoparticles (NPs) influence the interactions between NPs and microbes. A plethora of chemicals such as polymers, anionic, cationic or non-ionic surfactants, ionic liquids and reducing agents can be used to modulate NP surface properties providing protective, stabilising or functional surface coatings [14]. For metal-based NPs, such coatings control size and shape of NPs already during synthesis by interacting with metal ions and affecting the equilibrium of synthesis reaction, particle nucleation and growth rate [15]. According to Kvitek et al. [16], the aqueous dispersions of NPs can be stabilised (i) with the assistance of steric repulsion by using polymers (such as PVP) or non-ionic surfactants (Tween 80, Triton X-100); or (ii) by electrostatic repulsion using anionic (SDS) or cationic surfactants (CTAB).

A search in the Web of Science research platform (performed on Sep 15th 2017) on the use of coating/capping agents for stabilisation of nanoAg intended for use in biomedicine yielded altogether 4298 papers (Fig. S1). Literature search revealed that citrate (CIT) and polyvinylpyrrolidone (PVP) were the most frequently used coating materials (4.5 and 4.2% of the studies, respectively) followed by cetyltrimethyl-ammonium bromide (CTAB), dioctyl-sodium sulfosuccinate (AOT), poly-L-lysine (PLL) and polyoxyethylene sorbitan monolaurate (Tween 80). Other studies (~90%) reported the use of very diverse coating materials including different polymers (like PEG, chitosan, PVC, PEA, PAA, polypropylen), mineral-based materials (like HAP, silica, and iron oxide), surfactants, different biomolecules (like β-cyclodextrin, chitosan, cellulose, cysteine) or their combination. Chemicals applied as surface coating agents can protect NPs from direct interaction with the environment, oxidation [17], dissolution [18], or aggregation. However, stabilisation of NPs with functional coatings may significantly affect their biological activity. For example, Kvitek et al. [16] found a correlation between the stabilisation efficiency and increased antibacterial activity of SDS- and Tween 80-coated nanoAg concluding that non-aggregated NPs (but not spacious NPs aggregates) strongly interact with bacterial cell wall due to their high surface energy and mobility. Importantly, surface coating agent is not only attached to the NPs` surface, but exists also in free form in NPs suspensions [19]. Thus, the role (*e.g.*, potential toxicity) of coating agents should be addressed during evaluation of biological impact or toxicity of coated/stabilised NPs. Yet, the information on contribution of surface coatings to overall NPs biological effects is scarce [19].

This study aimed to evaluate antibacterial activity of differently coated nanoAg of two different sizes: 10 nm (10 nAg) and 50 nm (50 nAg). For this purpose, a library of 11 different nanoAg was prepared employing neutral (PVP and Tween 80), positively (PLL and CTAB) and negatively charged surface coatings (AOT and CIT). Biocidal activity of these nanoAg was evaluated against two clinically relevant pathogens: Gram-negative *Escherichia coli* and Gram-positive *Staphylococcus aureus*. Additionally, antibacterial effects of coatings themselves were investigated. The role of possible nanoAg dissolution on their biocidal effects was assessed by quantifying the released Ag-ions from nanoAg surface.

2. Materials and methods

2.1. Synthesis of silver nanoparticles

Silver nitrate ($AgNO_3$) was used as a precursor of nanoAg. Capping/coating agents used for stabilisation of nanoAg are described in Table 1. CIT-coated 10 nAg were synthesised as described by Li et al. [20]. Other types of 10 nAg were synthesised by reducing $AgNO_3$ with $NaBH_4$ as described in [21]. 50 nAg coated with AOT, PVP, Tween 80 or CTAB were prepared *via* chemical reduction of the complex cation $[Ag(NH_3)_2]^+$ by *D*-glucose [22], while CIT-coated 50 nAg were prepared as

described by Munro et al. [23]. High purity deionised (DI) water obtained from a Milli-Q® system (Merck Millipore, Darmstadt, Germany) was used as solvent in all synthesis. Detailed protocols are in the Supplementary material (SM).

2.2. Physico-chemical characterisation of silver nanoparticles

The hydrodynamic size and surface charge of nanoAg were measured by dynamic light scattering (DLS) and electrophoretic light scattering (ELS), respectively, at 173 °C using Zetasizer Nano ZS (Malvern, UK) equipped with a green laser (532 nm). The hydrodynamic diameter (d_H) was obtained as a value at peak maximum of size volume distribution functions. The d_H values for each sample are reported as an average of 10 measurements. The surface charge of the nanoAg was characterised by zeta (ζ)-potential values, which was calculated from the measured electrophoretic mobility by means of the Henry equation using the Smoluchowski approximation. Each sample was measured 5 times and the results are expressed as average values. The data were processed by Zetasizer software 6.32 (Malvern Instruments).

Visualisation of nanoAg was carried out using a transmission electron microscope (TEM, Zeiss 902 A, Germany) operated in bright field mode at an acceleration voltage of 80 kV. Images were recorded with a Canon PowerShot S50 camera attached to the microscope. TEM samples were prepared by depositing a drop of the nanoAg suspension after 1 h of incubation at room temperature on a Formvar® coated copper grid (Agar Scientific Ltd.) and air-drying at room temperature. TEM images were used for measurement of primary size of nanoAg. Size was determined from the cross-sectional area of the particles which was converted to an equivalent spherical diameter by using ImageJ software. Primary particles were distinguished from nanoAg aggregates by tracing it manually. Altogether at least 70 particles per particle type were measured.

Total Ag concentration in nanoAg colloidal suspensions was determined in acidified solutions (10% (v/v) HNO_3) using an Agilent Technologies 7500 cx inductively coupled plasma mass spectrometer (ICPMS) (Waldbronn, Germany). An Ag standard solution (1000 mg/L in 5% HNO_3) from Merck (Darmstadt, Germany) was used for calibration.

Stability of nanoAg in DI water was studied by ultraviolet-visible (UV–vis) spectral analysis. The absorbance spectra were recorded by the Multiskan Spectrum spectrophotometer (Thermo Electron Corporation, Finland) at wavelengths of 200–800 nm (measurement step 10 nm) on the 96-well polystyrene microplates (BD Falcon, USA), 200 µl per well, after the nanoAg suspension preparation (0 h) and incubation for 4 and 24 h at 30 °C in the dark without shaking. Prior to the UV–vis measurements, the samples were shaken for 1 min.

2.3. Quantification of dissolved silver in abiotic conditions by chemical method

Suspensions of nanoAg (1mg Ag/L) were incubated in DI water in conditions simulating the antibacterial test (but without bacteria added) on 12-well polystyrene plates (BD Falcon), 1.2 mL per well, for 4 h at 30 °C in the dark without shaking. Dissolved Ag-ions were separated from nanoAg by ultrafiltration [24] using Amicon-4 Ultra centrifugal filter units with 3 KDa cut-off (Merck Millipore, Darmstadt, Germany) and were quantified by graphite furnace atomic absorption spectrometry (AAS) (Perkin Elmer AAnalyst 600, Perkin Elmer, Shelton, USA) with Zeeman background correction. Standard Reference Material® 1643e Trace Elements in Water (NIST, USA) was used to confirm the reliability of analytical methods. The results were within ± 10% of the certified values.

2.4. Quantification of bioavailable silver using Ag-sensing bacteria

Quantification of bioavailable/intracellular silver in the test suspensions of nanoAg was performed according to Bondarenko et al. and Käosaar et al. [25,26] using recombinant luminescent sensor bacteria *E. coli* MC1061 (pSLcueR/pDNPcopAlux) responding dose-dependently by increased bioluminescence to Ag-ions that have entered bacterial cells [27]. In parallel, 'control' bacteria, *i.e.* constitutively luminescent bacteria *E. coli* MC1061 (pDNlux) [28] were used. Preparation of the test bacteria, test media and additional details of the assay are in SM.

2.5. Analysis of antibacterial efficiency of different nanoAg and their coatings

The antibacterial efficiency was evaluated using a spot assay as described in Kasemets et al. [29] and Suppi et al. [30] by estimating minimal bactericidal concentrations (MBC) of test compounds against *Escherichia coli* MG1655 (bacterial strain obtained from the *E. coli* genetic stock centre, Yale University) and *Staphylococcus aureus* (6538) (obtained from the American Type Culture Collection, ATCC). Briefly, after 4-h or 24-h exposure of test bacteria to the test compound in DI water, 3 µl of bacterial test suspension was pipetted as a 'spot' onto LB agar plates to assess the viability of the cells. In addition to the spot assay, the pure coatings were evaluated using bacterial growth inhibition assay according to ISO 20776-1 [31]. Preparation of test bacteria and details of the assays are in SM.

2.6. Flow cytometry analysis of nanoAg -bacteria interactions

Flow cytometry with BD Accuri™ (BD Biosciences) was used to determine the binding of nanoAg to bacterial cells essentially as described by Feng et al. [32]. Briefly, bacteria were exposed to nanoAg (2 or 8 mg Ag/L), 70% ethanol or $AgNO_3$ (0.2 mg Ag/L) at room temperature for 10 min without shaking. The bacteria were stained 15 min with 5 µM SYTO 9 (Invitrogen S34854 846177) or 7.5 µM propidium iodide (PI) (Fluka 81845) in the dark. For additional information, see SM.

2.7. Statistical analysis

R Language and Environment for Statistical Computing (http://www.R-project.org) was used for the analysis of variance (one-way ANOVA followed by a Tukey's honest significant difference post-hoc test) and a *t*-test in Microsoft Excel 2010 to determine statistically significant differences between the test values (nanoAg size, solubility, bioavailability, and MBC).

3. Results

3.1. Characterisation and stability evaluation of nanoAg

The library of nanoAg was prepared aiming two size groups: ~10 nm (further designated as 10 nAg) and ~50 nm (designated as 50 nAg). Six different coating agents were used for stabilisation of nanoAg (Table 1). The average primary size (TEM) of 10 nAg (irrespective of the coating) was 13 ± 5.8 nm and median size 12 nm, while 50 nAg had the average size 58 ± 39 nm and median size 49 nm (Fig. S2). 10 nAg and 50 nAg of the same coating were clearly distinguishable and different (Fig. S3).

NanoAg were characterised immediately after synthesis using DLS, ELS, and UV–vis spectrophotometry. Table 2 summarises data on d_H, polydispersity index (PdI) and ζ-potential values. All 10 nAg were characterised by d_H values in the range of 5.6–39.7 nm. The CIT-, AOT-PVP- and PLL- coated 10 nAg showed bimodal size distribution while Tween 80- and CTAB-coated 10 nAg had monomodal size distribution (Table 2). All 50 nAg, with the exception of Tween 80 coating, had bimodal size distribution. The CIT- and PVP-coated 50 nAg had

Table 2
Physico-chemical characteristics of differently coated silver nanoparticles (nanoAg) determined by transmission electron microscope (TEM), dynamic light scattering (DLS) and electrophoretic light scattering (ELS).

Intended primary size	Surface coating	Primary size (average, TEM, nm)	d_H * (nm)	Mean volume (%)	PdI†	ζ-potential (mV)
10 nm	CIT‡	12.9 ± 4.5	16.5 ± 0.8	97.6	0.17	−55.2 ± 2.1
			39.7 ± 2.7	2.4		
	AOT¥	10.8 ± 4.2	15.2 ± 5.3	96.6	0.15	−40.6 ± 6.5
			12.6 ± 0.9	3.4		
	PVPŁ	14.5 ± 5.2	15.0 ± 1.6	98.4	0.12	−18.0 ± 3.7
			31.2 ± 3.5	1.6		
	Tween 80	15.2 ± 6.9	15.8 ± 0.3	100	0.09	−27.2 ± 5.8
	CTAB#	10.8 ± 4.3	11.9 ± 1.6	100	0.08	+28.2 ± 1.5
	PLL**	13.5 ± 7.1	5.6 ± 0.8	91.8	0.10	+38.6 ± 6.9
			18.4 ± 1.6	8.2		
50 nm	CIT	72.7.0 ± 46	35.6 ± 3.2	91.8	0.27	−28.6 ± 0.7
			148.1 ± 28.8	8.2		
	AOT	50.4 ± 34	58.7 ± 28.0	62.8	0.31	−19.3 ± 2.6
			12.4 ± 5.4	37.2		
	PVP	37.6 ± 21	40.1 ± 8.2	76.1	0.34	−34.8 ± 0.9
			7.6 ± 2.5	14.7		
	Tween 80	56.0 ± 33	54.5 ± 1.1	100	0.17	−18.3 ± 0.9
	CTAB	75.3 ± 45	32.7 ± 15.6	56.7	0.38	+5.9 ± 0.8
			180.1 ± 92.9	43.3		

*d_H– hydrodynamic diameter, †PdI – polydispersity index, ‡CIT – Trisodium citrate, ¥AOT – Bis-2-ethylhexyl sulfosuccinate, ŁPVP – Poly-vinylpyrrolidone, Tween 80 – Polysorbate 80, #CTAB – Cetyltrimethyl-ammonium bromide, **PLL – Poly-L-lysine. Primary sizes of NPs (nm) were measured from TEM images by using ImageJ software. DLS values indicate hydrodynamic diameter (d_H, nm) obtained from size distributions by volume. Light scattering methods provided in addition ζ-potential (mV) and polydispersity index (PdI). All parameters were obtained by diluting nanoAg in DI water to a concentration of 10 mg/L immediately after the synthesis, at 25 °C.

predominant NPs population of ~40–60 nm size, while CTAB- and AOT-coated 50 nAg were more polydisperse, which is also obvious from measured PdI values. All attempts to prepare PLL-coated 50 nAg failed. Thus, this type of nanoAg was not included in this study.

All nanoAg were stable and well-dispersed in DI water for a period of 24 h with the exception of 50 nAg-CTAB that formed aggregates as evidenced also from the observed PdI 0.38 (Table 2; Fig. S2, D).

UV–vis absorption spectra of nanoAg showed the characteristic surface plasmon resonance (SPR) peaks for 10 nAg and 50 nAg at 390–395 nm and 400–440 nm, respectively (Fig. S4). Slight decrease in the intensity values of the SPR peaks can be explained by the nanoAg solubility [33]. Significant changes were observed only in the case of 50 nAg-CTAB, where the absorption band disappeared completely after 24 h of incubation due to significant agglomeration as evidenced also by DLS measurements (Fig. S4). Interestingly, the aggregation of 50 nAg-CTAB was facilitated only after dilution in DI water prior to the tests, whereas the stock solution of 50 nAg-CTAB (total Ag concentration of 1220 mg/L) prepared immediately after the synthesis, was stable for several months (data not shown). The poorer stability of 50 nAg-CTAB may be explained by their surface charge close to the neutral ζ-potential value.

3.2. Antibacterial properties of nanoAg against E. coli and S. aureus

Antimicrobial efficiency of nanoAg was evaluated using a spot assay and expressed as MBC.

4 h and 24 h MBC values are presented in Fig. 1 and Table S1 (SM).

Comparison of the antibacterial efficiency of differently sized nanoAg showed that 10 nAg were in general more potent antibacterial agents than 50 nAg to both *E. coli* (Fig. 1, upper panels) and *S. aureus* (Fig. 1, lower panels). However, in the case of CIT- and PVP-coated nanoAg the differences in size-dependent toxic effects were statistically not significant with the exception of 4 h-exposed *S. aureus* (Fig. 1; Table S1).

The toxicity of all studied nanoAg (except 50 nAg-Tween 80) towards *S. aureus* significantly increased with time, *i.e.*, 4 h *versus* 24 h (Fig. S5, lower panels). As a rule, the effect of prolonged incubation on toxicity was not observed in *E. coli*. Only 10 nAg-PVP, 50 nAg-CTAB and 50 nAg-AOT showed statistically different effect between 4 h and 24 h time points in *E. coli* (Fig. S5, upper panels). The same tendency, *i.e.* increase of toxic effect with time in case of *S. aureus,* was observed for $AgNO_3$ evidencing the role of released ionic Ag in nanoAg toxicity (Fig. S5, B; Table S1).

Comparison of the sensitivities of two different bacterial strains showed significantly higher susceptibility of Gram-negative *E. coli* than Gram-positive *S. aureus* to both nanoAg and ionic Ag (Fig S6). The difference was especially remarkable after 4 h of exposure, when MBC values for nanoAg to *E. coli* were in the range of 0.08–5 mg Ag/L and 1–10 mg Ag/L for *S. aureus* (Table S1). For both bacterial strains Ag-ions were remarkably more toxic than nanoAg. The 4 h MBC for Ag-ions to *E. coli* was 0.02 mg Ag/L and 0.16 mg Ag/L to *S. aureus* (Table S1). Thus, *E. coli* was up to 12-times more susceptible to nanoAg and 8-times more susceptible to Ag-ions than *S. aureus*. The same tendency was observed after 24 h of exposure, except for 50 nAg coated with AOT, PVP and Tween 80.

There was no clear trend on the effect of the coating on antibacterial efficacy. Among 10 nAg, the Tween 80-coated nanoAg induced the lowest toxic effects to *S. aureus* after 4 h exposure (Fig. 2), while *E. coli* was susceptible to all 10 nAg to a similar extent after 4 h. After 24 h of exposure, all studied 10 nAg exhibited similar antibacterial effects to both strains. Probably, the antibacterial effect was mainly driven by their small size. Results obtained for 50 nAg (Fig. 2, lower panels) implied that antimicrobial effect can be tuned using various coatings. Tween 80- and CTAB-coated 50 nAg showed lower antimicrobial potential as compared to CIT-, AOT- and PVP-coated 50 nAg.

3.3. The role of dissolved Ag-ions in antibacterial effects of nanoAg

Dissolution behaviour of nanoAg in DI water as determined by AAS showed that ionic Ag in nanoAg dispersions ranged from 0.8 to 6.5%. In general, 10 nAg released more Ag-ions (2.1–6.5%) than 50 nAg (0.8–3.0%) (Fig. 3). The highest content of Ag-ions was found in PVP and AOT-coated 10 nAg (~6.5%), while CTAB-coated 50 nAg released the lowest amount of Ag-ions (0.8%).

Biosensor data showed that the Ag bioavailability was highest for PLL-coated 10 nAg (12.6%) and lowest for CTAB-coated 50 nAg (0.2%)

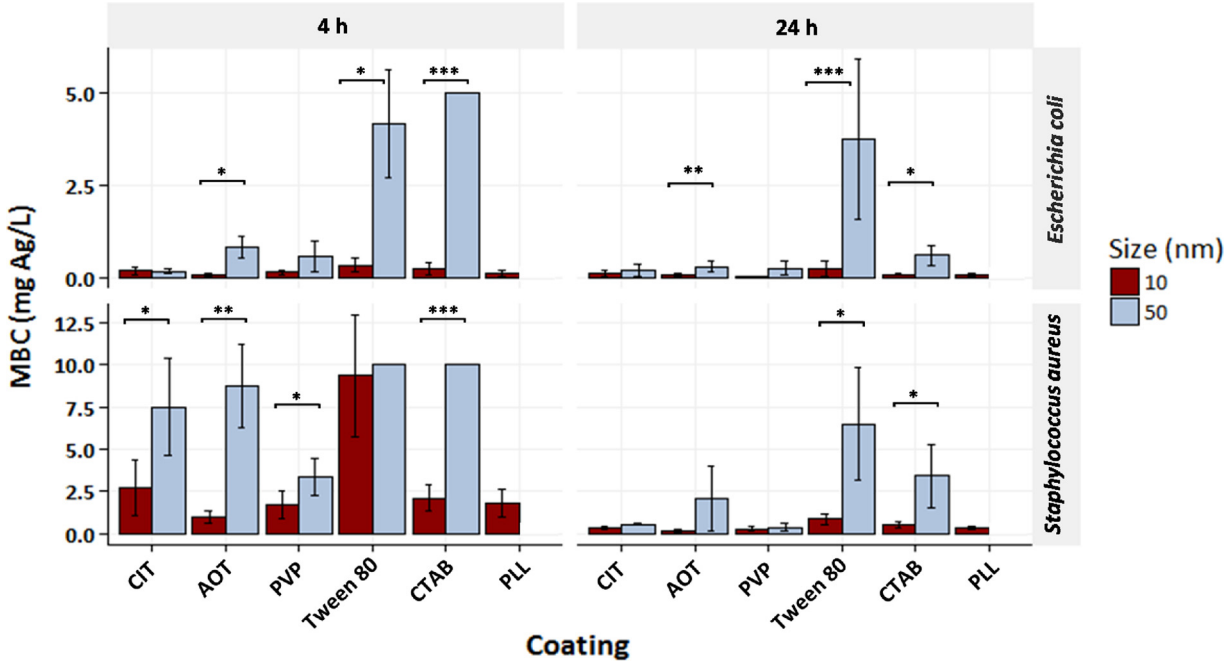

Fig. 1. Effect of particle size on minimal bactericidal concentration (MBC) of differently coated 10 nAg and 50 nAg to *Escherichia coli* (upper panels) and *Staphylococcus aureus* (lower panels). Data represent the average values of 3–5 experiments ± standard deviation (SD); ***p < 0.001, **p < 0.01, *p < 0.05. Data are plotted from Table S1.

(Fig. 3). Although the bioavailable fraction of Ag was, at first sight, comparable with its soluble fraction, biosensor and solubility data were significantly different for CIT-coated 10- and 50 nAg, CTAB-coated 10- and 50 nAg, Tween 80-coated 10- and 50 nAg and PLL-coated 10nAg (Fig. S7). For CIT-coated nanoAg, we hypothesize that CIT formed complexes with Ag-ions that were not bioavailable to Ag-sensor bacteria. In the case of PLL-coated 10 nAg, the bioavailability of dissolved Ag was ca 3-fold higher than their solubility as measured by AAS, indicating that biological factors (*e.g.*, cell-nanoAg interactions) might contribute to their bioavailability. Plotting of nanoAg solubility and bioavailability against their respective MBC values, a good correlation (log-log R^2 = 0.54–0.82) between antibacterial efficacy and solubilisation/bioavailability of nanoAg was observed (Fig. 4) suggesting that the antibacterial effect was mainly driven by shed Ag-ions.

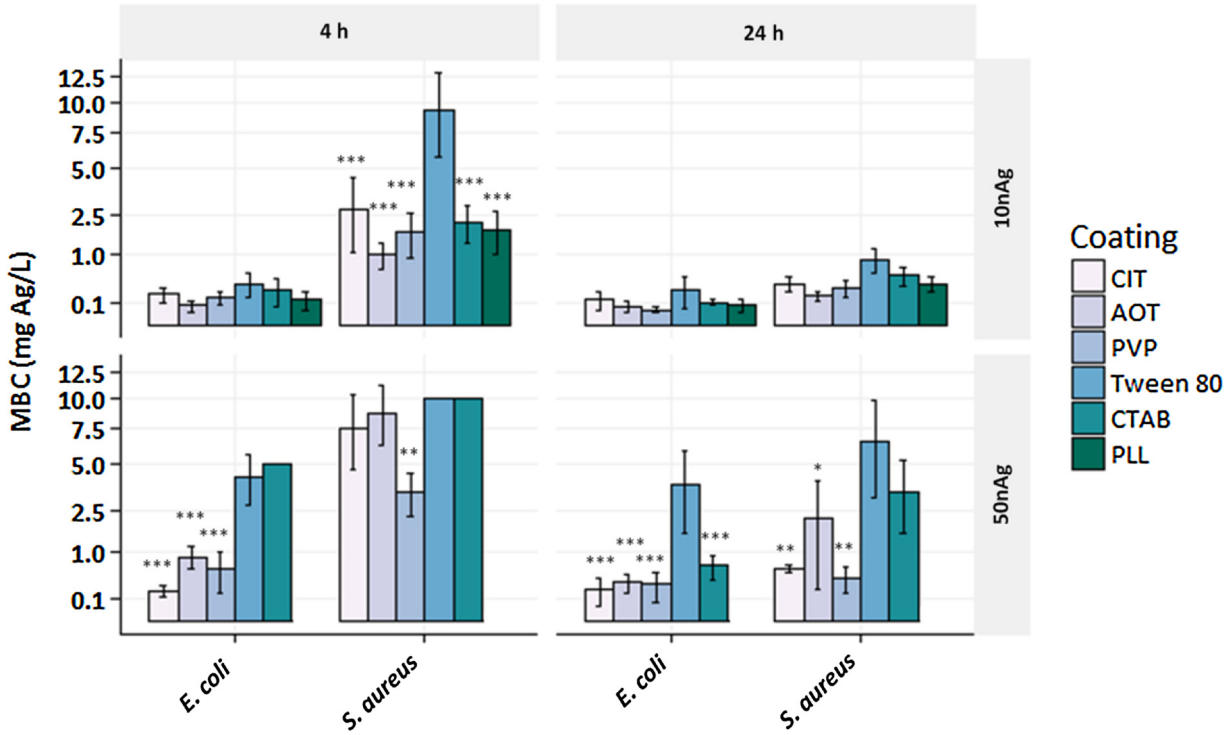

Fig. 2. The effect of coating on antimicrobial potency of 10 nAg (upper panels) and 50 nAg (lower panels) to *E. coli* and *S. aureus* exposed for 4 h (left panels) and 24 h (right panels). The statistical significance was compared to the least toxic compound (Tween 80) in the group: ***p < 0.001, **p < 0.01, *p < 0.05.

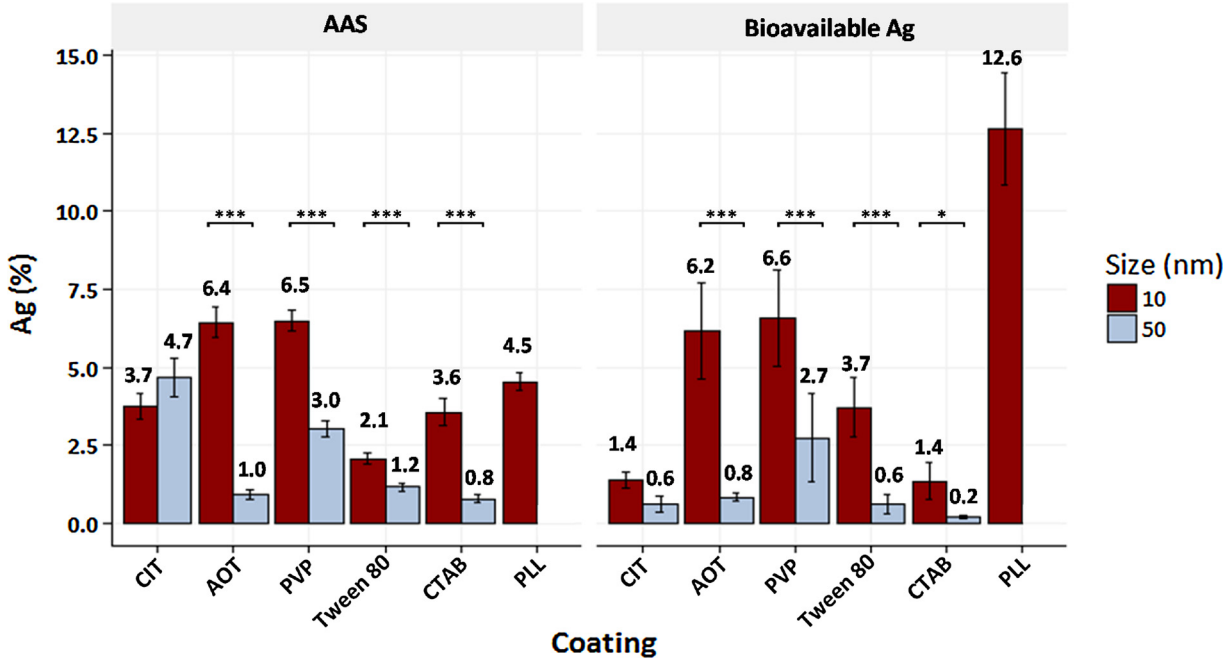

Fig. 3. Solubilility (measured by AAS) and bioavailability (determined by Ag-sensing bacteria) of different nanoAg and expressed as % of initial Ag content in nanoAg. Average values of at least three measurements ± SD are presented. Solubility analyses was performed at 1 mg Ag/L. Asterisks designate the statistical difference between 10 nAg and 50 nAg (***$p < 0.001$, **$p < 0.01$, *$p < 0.05$).

3.4. Antibacterial effects of coating agents

It is well-known that some of the coating materials used throughout this study, such as cationic polymer PLL [34] and cationic surfactant CTAB [35], can be inherently antibacterial. Thus, toxicity of pure AOT, CIT, CTAB, PLL, PVP and Tween 80 coatings was tested.

As shown in Table S2, all coating agents, except positively charged CTAB and PLL were not toxic to both bacterial strains up to the maximal tested concentrations (4000 mg/L).

Cationic polymer PLL and cationic surfactant CTAB proved toxic in both antibacterial assays with the EC_{50} values comparable to the toxicity of well-known cationic biocide benzalkonium chloride (MBC to both bacteria ranged between 1.3–2.5 mg/L, Tables S2 and S3). Our data were in agreement with previous articles on inherent toxicity of PLL and CTAB [34,35]. The toxicity of these coatings was similar to both strains with some exceptions. The antibacterial effects of PLL and AOT against *S. aureus* increased remarkably in time, which was not observed for *E. coli* (Table S2). Bacterial growth inhibition assay following ISO 20776-1 standard showed the toxicity of coatings to dividing cells (Table S3). The PVP, CIT and Tween 80 were not toxic to bacteria up to their maximal tested concentrations, while MBC and MIC values indicated slightly toxic effect of AOT to *S. aureus*, but not to *E. coli*. Similar to results obtained from the spot assay (Table S2), PLL and CTAB were inhibitory to both bacteria, with higher antimicrobial potency against Gram-positive *S. aureus* than against Gram-negative *E. coli* (Table S3).

Although the proportion of the coating in the formulations of nanoAg was small, we calculated, whether the toxic coatings PLL or CTAB may have contributed to the net toxicity of the 50 nAg-PLL and 50 nAg-CTAB (see SM). The calculations showed that the bactericidal concentrations of pure coatings (Table S2) were orders of magnitude higher than their concentration at the respective nanoAg MBCs (Table S1) indicating that the toxicity of those coatings was not contributing to the net antibacterial effects of respective nanoAg.

3.5. Flow cytometry analysis of particle-cell contact

Interaction of different nanoAg types with bacteria was evaluated using flow cytometry analysis. Bacterial cells were exposed to 2 and 8 mg/L nanoAg for 10 min. The SSC shift of SYTO 9-stained cell population was measured to study binding of nanoAg to cells [36], while fluorescence intensity after PI staining was indicating cell viability by determining the number of dead cells and cells with damaged membranes (Fig. S8).

PI staining indicated that viability of control cells (non-treated) was 91.7% for *E. coli* and 96.2% for *S. aureus* (Fig. 5, B). For all nanoAg, no binding to both bacterial strains was observed at lower nanoAg concentration (2 mg Ag/L, data not shown). Higher applied nanoAg concentration (8 mg Ag/L) led to binding of four different nanoAg types to *E. coli*, but binding above 10% was observed only for 10 nAg-PLL (Fig. 5, A). In the case of *S. aureus,* 10 nAg-PLL and all 50 nAg interacted with cells (Fig. 5, A).

The effect of nanoAg on cellular viability (10 min exposure) is shown in Fig. 5, B. In general, the damaging effects of nanoAg were smaller to *S. aureus* than to *E. coli*, while CTAB-coated 10 nAg showed highest toxic potential for *S. aureus* (Fig. 5, B). Interestingly, this was not reflected in the MBC values (Table S1). Thus, apparently some cells with damaged membranes (PI positive cells) were able to form colonies even after 4 h exposure to nanoAg. Remarkably, in the case of *S. aureus*, CTAB and PLL-coated nanoAg decreased cellular viability more than other nanoAg types of comparable sizes (Fig. 5, B). For example, the 50 nAg-CTAB damaged 35.3% of *S. aureus* cells, whereas the damage caused by other 50 nAg was below 16%. Thus, positively charged coating contributed to the membrane damage of *S. aureus* but not of *E. coli*. While *E. coli* cells were readily killed by Ag-ions released from nanoAg and cell-particle contact did not play the major role, cell-particle contact and particle charge obviously played significant role to the nanoAg effects on *S. aureus* cell damage.

4. Discussion

This study was conducted to provide systematic data on

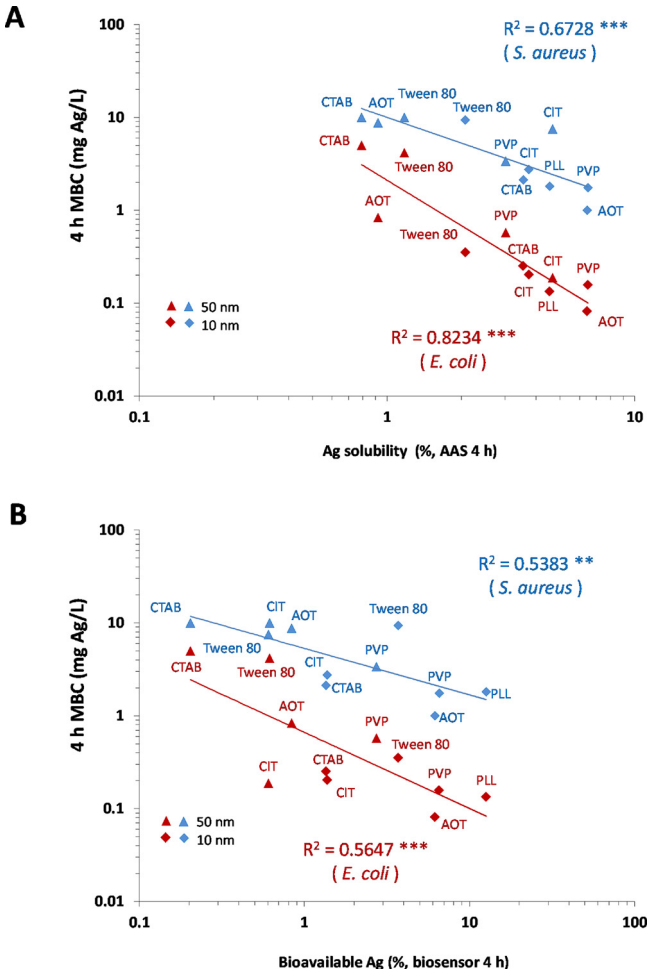

Fig. 4. Antibacterial effect (4 h MBC) of differently coated 10 nAg and 50 nAg to *Escherichia coli* and *Staphylococcus aureus versus* (A) solubility of nanoAg (%) as quantified by AAS and *versus* (B) bioavailability of nanoAg as quantified by Ag-sensing biosensor bacteria. A log-log correlation and respective correlation coefficients (R^2) are presented. The statistical significance of the calculated correlation coefficients (r) was estimated at different confidence levels (P) and designated as follows: $|r| > 0$, *P = 90%, **P = 95%, *** P = 99%, respectively.

antimicrobial potency of nanosilver by synthesising a library of differently coated nanoAg of two different sizes (10 and 50 nm). As microbial models, we chose *E. coli* and *S. aureus* representing Gram-negative and Gram-positive potentially pathogenic bacteria, respectively. Selection of these bacterial strains was based on the fact that the most often isolated bacteria in 15 000 HAI cases in 29 EU/EEA Member States were *E. coli* (15.9%) and *S. aureus* (12.3%) in the period between 2011–2012 [37]. *S. aureus* also belongs to the six problematic pathogens associated with multi-drug-resistant infections [38].

To evaluate the effect of NPs' surface properties, different surface coatings were employed in preparation of nanoAg library. Effect of Ag-ions (in the form of $AgNO_3$) was determined for comparative purposes.

Antibacterial evaluation of the nanoAg was performed in DI water to diminish the effects of organic components from the growth media on the colloidal stability (aggregation/agglomeration, protein adsorption, dissolution) of nanoAg [25,26,39–41]. The importance of absence of interfering compounds affecting speciation of silver for the interpretation of the toxic effects of silver NPs was stressed also in the recent review by Le Ouay and Stellacci [42].

Obtained data confirmed the main paradigm of nanotechnology, *i.e.* the small particle size yielded higher antimicrobial potency. Thus, 10 nAg were more toxic to tested bacteria than 50 nAg, irrespective of the coatings used for their stabilisation. As expected, nanoAg were less potent towards both *E. coli* and *S. aureus* as compared to Ag-ions (Table S1; Fig. S6). In addition, *S. aureus* was less susceptible than *E. coli* to all nanoAg types (Fig. S6), being in agreement with our previously published data from the similar test format [39]. Contrary to the effect observed for *E. coli*, the antibacterial effects of both nanoparticulate and ionic Ag forms to *S. aureus* increased with time (Table S1; Fig. S5). The difference in nanoAg toxicity between Gram-negative and -positive bacteria was especially remarkable after shorter (4 h) as compared to longer (24 h) exposure times (Fig. S6, B). The difference in toxicological profile of different nanoAg (and Ag-ions) for Gram-negative and -positive bacteria might be due to the fact that peptidoglycan layer in the cell walls of Gram-positive bacteria is 30 nm thick, while this layer is only 2–3 nm thick in the Gram-negative bacteria [1]. The thicker peptidoglycan layer may act as a barrier protecting the cell from penetration of nanoAg or/and Ag-ions into the cytoplasm ensuring the lower sensitivity of Gram-positive as compared to Gram-negative bacteria [43,44]. The difference in the thickness of this layer may also explain the longer time needed to gain equal antibacterial efficiency of nanoAg/Ag-ions against *S. aureus* than against *E. coli* (Fig. S5; Table S1). In addition, high sensitivity of Gram-negative bacteria towards nanoAg can be explained with the higher leakage of proteins from Ag destabilised membrane of *E. coli* as compared to *S. aureus* [45].

As expected, the antibacterial effects of nanoAg were in good correlation with the release of Ag-ions from the nanoAg surface (Fig. 4). Indeed, higher antibacterial potency of 10 nAg compared to 50 nAg was correlated with the higher % of free Ag-ions in the 10 nAg dispersions compared to 50 nAg (Figs. 3 and 4) being in good agreement with previously published data [46]. Ag-ions may additionally destabilise and rupture bacterial cell membranes [47–51]. For example, Ivask et al. demonstrated that the most nanoAg-affected proteins in *E. coli* were clusters of membrane proteins [33]. It has been reported that after disrupting the membranes, nanoAg inactivated the enzymes of respiration chain [5,52], released Ag-ions affected DNA and intracellular proteins, caused formation of intracellular reactive oxygen species (ROS) and enhanced the penetration of nanoAg into the cell [53].

Although there was a good correlation between the release of Ag-ions from nanoAg and their antibacterial action (Fig. 4), not all toxic effects were explained by Ag-ions. We hypothesise that toxicity may also have arisen from the toxicity of coatings themselves or from binding of nanoAg to the cells allowing higher local concentrations of released Ag-ions. Indeed, some of the coating agents can destabilise the bacterial membranes [54] and act as antimicrobials [55] leading to synergistic effect of coated nanoAg. For example, CTAB may permeabilise bacterial membranes [56,57], while PLL, a widely used food preservative, can disrupt bacterial membranes, generate ROS [58] and prevent *E. coli* growth at concentrations as low as ~70 μM [59]. Our data revealed that both coating agents, PLL and especially CTAB (but no other coatings tested in this study) were toxic to bacteria (Tables S2 and S3). However, the bactericidal concentrations of coatings were generally orders of magnitude higher than their concentrations in nanoAg toxicity test, indicating that the toxicity of coatings was not the obvious cause for the increased nanoAg toxicity.

Another important factor for observed effects could be the surface charge. The bacterial cell surface has negative surface charge as demonstrated in earlier studies [60] and confirmed also by us: the ζ potential of *S. aureus* and *E. coli* surface was −42 and −52 mV, respectively. Interestingly, CTAB and PLL-coated nanoAg with positive surface charge (Table 1) that were initially expected to be more antibacterial than nanoAg with negative surface charge, due to their higher potential for attachment to negatively charged bacterial cells, didn't demonstrate superior antimicrobial effects (Fig. 2). Thus, our data disagree with previously reported data on remarkably increased toxicity of nanoAg coated by positively charged branched PEI to *E. coli* [33]. However, positively charged nanoAg were superior in damaging membranes of *S. aureus* upon short exposures (Fig. 5, B), showing that

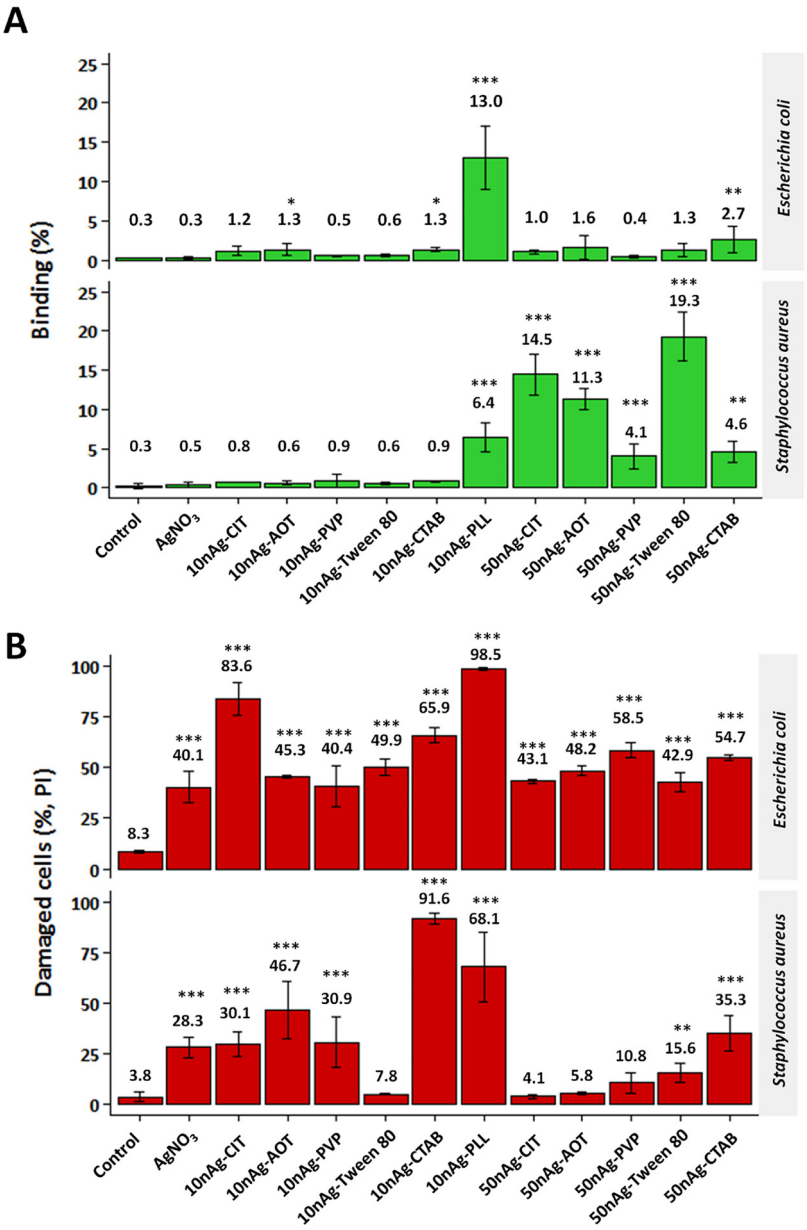

Fig. 5. Flow cytometry analysis of interactions between different nanoAg (8 mg Ag/L) or $AgNO_3$ (0.2 mg Ag/L) and bacteria determined by the SSC shift of SYTO 9-stained cells (A) and effect of nanoAg (8 mg Ag/L) or $AgNO_3$ (0.2 mg Ag/L) on viability of bacterial cells measured by propidium iodide (PI) stained cells (B). Asterisks show the statistical difference compared to control: ***$p < 0.001$, **$p < 0.01$, *$p < 0.05$.

positive charge is important but not a deciding factor for the actual bactericidal effect. Analogously, *E. coli* cells interacted with positively charged PLL-coated nanoAg (Fig. 5, A), which significantly increased their bioavailability for *E. coli* (Fig. 3). However, the direct charge-related effect of this interaction on toxicity was negligible, compared to the toxic effects caused by shed Ag-ions. Thus, in our experimental conditions, the role of nanoAg coatings in modulation of the release of Ag-ions (Fig. 3) was way more important than their NP-cell interactions directing effects. As a rule, within the same size category, the CTAB- and Tween 80-coated nanoAg were least soluble and least toxic to both bacterial strains, while PVP-, CIT- and AOT-coated nanoAg were most soluble and most efficient antibacterials (Fig. 4).

Thus, the strongest modulator of the antimicrobial effect was particle size which determined also dissolution behaviour of nanoAg: smaller nanoAg were significantly more toxic being more soluble. The effect of coating agents on antibacterial activity of nanoAg was only indirect modulator of nanoAg toxicity, mainly due to modulation of their solubility. This was particularly obvious in the case of 50 nAg and *S. aureus*. We also do not exclude a synergistic toxic effect of released Ag-ions and coatings.

5. Conclusions

To design efficient antimicrobial silver-based nanomaterials, focus should be set on the fine-tuning of solubilisation of NPs. For this purpose, the selection of smaller size of nanoAg could be recommended. If Gram-negative bacteria (*E. coli*) are the target, all types of coating/capping agents seem to be applicable. However, for Gram-positive bacteria (*S. aureus*), Tween 80 and similar agents should be avoided. In the case of Gram-positive bacteria, more time might be needed for the antibacterial action of nanoAg than for the Gram-negative bacteria due to the differences in the cell wall composition between these two bacteria types. Finally and contrary to the common view, positively charged nanoAg did not exhibit superior antibacterial properties

compared to the negatively charged nanoAg, suggesting that solubility might be more important determinant of antibacterial acitivity than the surface charge as such.

Conflict of interest

The authors declare no conflict of interest.

Acknowledgements

Estonian Research Council Grants IUT 23-5, PUT1015, Croatian Science Foundation grant number HRZZ-IP-2016-06-2436 and COST Action AMiCI (CA15114) are acknowledged for the support.

Appendix A. Supplementary Material

Supplementary Material related to this article can be found, in the online version, at doi:https://doi.org/10.1016/j.colsurfb.2018.06.027.

References

[1] M.K. Rai, S.D. Deshmukh, A.P. Ingle, A.K. Gade, Silver nanoparticles: the powerful nanoweapon against multidrug-resistant bacteria, J. Appl. Microbiol. 112 (2012) 841–852, http://dx.doi.org/10.1111/j.1365-2672.2012.05253.x.
[2] J. O'Neill, Antimicrobial resistance: tackling a crisis for the health and wealth of nations, Rev. Antimicrob. Resist. (2014) 1–16, http://dx.doi.org/10.1038/510015a.
[3] C.L. Ventola, The antibiotic resistance crisis: part 1: causes and threats, PTA Peer-Rev. J. Formul. Manag. 40 (2015) 277–283. Article.
[4] S.Y. Liau, D.C. Read, W.J. Pugh, J.R. Furr, A.D. Russell, Interaction of silver nitrate with readily identifiable groups: relationship to the antibacterial action of silver ions, Lett. Appl. Microbiol. 25 (1997) 279–283, http://dx.doi.org/10.1046/j.1472-765X.1997.00219.x.
[5] K.B. Holt, A.J. Bard, Interaction of silver(I) ions with the respiratory chain of Escherichia coli: an electrochemical and scanning electrochemical microscopy study of the antimicrobial mechanism of micromolar Ag, Biochemistry 44 (2005) 13214–13223, http://dx.doi.org/10.1021/bi0508542.
[6] M. Ahonen, A. Kahru, A. Ivask, K. Kasemets, S. Kõljalg, P. Mantecca, I.V. Vrček, M.M. Keinänen-Toivola, F. Crijns, Proactive approach for safe use of antimicrobial coatings in healthcare settings: opinion of the cost action network AMiCI, Int. J. Environ. Res. Public Health 14 (2017), http://dx.doi.org/10.3390/ijerph14040366.
[7] P. Dallas, V.K. Sharma, R. Zboril, Silver polymeric nanocomposites as advanced antimicrobial agents: classification, synthetic paths, applications, and perspectives, Adv. Colloid Interface Sci. 166 (2011) 119–135, http://dx.doi.org/10.1016/j.cis.2011.05.008.
[8] J.L. Hobman, L.C. Crossman, Bacterial antimicrobial metal ion resistance, J. Med. Microbiol. 64 (2015) 471–497, http://dx.doi.org/10.1099/jmm.0.023036-0.
[9] A.R. Shahverdi, A. Fakhimi, H.R. Shahverdi, S. Minaian, Synthesis and effect of silver nanoparticles on the antibacterial activity of different antibiotics against Staphylococcus aureus and Escherichia coli, Nanomed. Nanotechnol. Biol. Med. 3 (2007) 168–171, http://dx.doi.org/10.1016/j.nano.2007.02.001.
[10] S. Prabhu, E.K. Poulose, Silver nanoparticles: mechanism of antimicrobial action, synthesis, medical applications, and toxicity effects, Int. Nano Lett. 2 (2012) 32, http://dx.doi.org/10.1186/2228-5326-2-32.
[11] M.E. Vance, T. Kuiken, E.P. Vejerano, S.P. McGinnis, M.F. Hochella, D.R. Hull, Nanotechnology in the real world: redeveloping the nanomaterial consumer products inventory, Beilstein J. Nanotechnol. 6 (2015) 1769–1780, http://dx.doi.org/10.3762/bjnano.6.181.
[12] D. Yohan, B.D. Chithrani, Applications of nanoparticles in nanomedicine, J. Biomed. Nanotechnol. 10 (2014) 2371–2392, http://dx.doi.org/10.1166/jbn.2014.2015.
[13] J. Piella, N.G. Bastús, V. Puntes, Size-controlled synthesis of sub-10-nanometer citrate-stabilized gold nanoparticles and related optical properties, Chem. Mater. 28 (2016) 1066–1075, http://dx.doi.org/10.1021/acs.chemmater.5b04406.
[14] V. Labhasetwar, D.L. Leslie-Pelecky, Biomedical Applications of Nanotechnology, (2007), http://dx.doi.org/10.1002/9780470152928.
[15] P.C. Ray, Size and shape dependent second order nonlinear optical properties of nanomaterials and their application in biological and chemical sensing, Chem. Rev. 110 (2010) 5332–5365, http://dx.doi.org/10.1021/cr900335q.
[16] L. Kvítek, A. Panáček, J. Soukupová, M. Kolář, R. Večeřová, R. Prucek, M. Holecová, R. Zbořil, Effect of surfactants and polymers on stability and antibacterial activity of silver nanoparticles (NPs), J. Phys. Chem. C 112 (2008) 5825–5834, http://dx.doi.org/10.1021/jp711616v.
[17] W. Lu, D. Senapati, S. Wang, O. Tovmachenko, A.K. Singh, H. Yu, P.C. Ray, Effect of surface coating on the toxicity of silver nanomaterials on human skin keratinocytes, Chem. Phys. Lett. 487 (2010) 92–96, http://dx.doi.org/10.1016/j.cplett.2010.01.027.
[18] Z. Adamczyk, M. Oćwieja, H. Mrowiec, S. Walas, D. Lupa, Oxidative dissolution of silver nanoparticles: a new theoretical approach, J. Colloid Interface Sci. 469 (2016) 355–364, http://dx.doi.org/10.1016/j.jcis.2015.12.051.
[19] Y. Zhang, B. Newton, E. Lewis, P.P. Fu, R. Kafoury, P.C. Ray, H. Yu, Cytotoxicity of organic surface coating agents used for nanoparticles synthesis and stability, Toxicol. In Vitro 29 (2015) 762–768, http://dx.doi.org/10.1016/j.tiv.2015.01.017.
[20] H. Li, H. Xia, D. Wang, X. Tao, Simple synthesis of monodisperse, quasi-spherical, citrate-stabilized silver nanocrystals in water, Langmuir 29 (2013) 5074–5079, http://dx.doi.org/10.1021/la400214x.
[21] I. Vinković Vrček, I. Pavičić, T. Crnković, D. Jurašin, M. Babič, D. Horák, M. Lovrić, L. Ferhatović, M. Ćurlin, S. Gajović, Does surface coating of metallic nanoparticles modulate their interference with *in vitro* assays? RSC Adv. 5 (2015) 70787–70807, http://dx.doi.org/10.1039/C5RA14100A.
[22] J. Soukupová, L. Kvítek, A. Panáček, T. Nevěčná, R. Zbořil, Comprehensive study on surfactant role on silver nanoparticles (NPs) prepared via modified tollens process, Mater. Chem. Phys. 111 (2008) 77–81, http://dx.doi.org/10.1016/j.matchemphys.2008.03.018.
[23] C.H. Munro, W.E. Smith, M. Garner, J. Clarkson, P.C. White, Characterization of the surface of a citrate-reduced colloid optimized for use as a substrate for surface-enhanced resonance raman scattering, Langmuir 11 (1995) 3712–3720, http://dx.doi.org/10.1021/la00010a021.
[24] A. Colombo, M. Saibene, E. Moschini, P. Bonfanti, M. Collini, K. Kasemets, P. Mantecca, Teratogenic hazard of BPEI-coated silver nanoparticles to Xenopus laevis, Nanotoxicology 11 (2017) 405–418, http://dx.doi.org/10.1080/17435390.2017.1309703.
[25] O. Bondarenko, K. Juganson, A. Ivask, K. Kasemets, M. Mortimer, A. Kahru, Toxicity of Ag, CuO and ZnO nanoparticles to selected environmentally relevant test organisms and mammalian cells in vitro: a critical review, Arch. Toxicol. 87 (2013) 1181–1200, http://dx.doi.org/10.1007/s00204-013-1079-4.
[26] S. Käosaar, A. Kahru, P. Mantecca, K. Kasemets, Profiling of the toxicity mechanisms of coated and uncoated silver nanoparticles to yeast Saccharomyces cerevisiae BY4741 using a set of its 9 single-gene deletion mutants defective in oxidative stress response, cell wall or membrane integrity and endocyt, Toxicol. In Vitro 35 (2016) 149–162, http://dx.doi.org/10.1016/j.tiv.2016.05.018.
[27] A. Ivask, O. Bondarenko, N. Jepihhina, A. Kahru, Profiling of the reactive oxygen species-related ecotoxicity of CuO, ZnO, TiO2, silver and fullerene nanoparticles using a set of recombinant luminescent Escherichia coli strains: differentiating the impact of particles and solubilised metals, Anal. Bioanal. Chem. 398 (2010) 701–716, http://dx.doi.org/10.1007/s00216-010-3962-7.
[28] A. Leedjärv, A. Ivask, M. Virta, A. Kahru, Analysis of bioavailable phenols from natural samples by recombinant luminescent bacterial sensors, Chemosphere 64 (2006) 1910–1919, http://dx.doi.org/10.1016/j.chemosphere.2006.01.026.
[29] K. Kasemets, S. Suppi, K. Künnis-Beres, A. Kahru, Toxicity of CuO nanoparticles to yeast Saccharomyces cerevisiae BY4741 wild-type and its nine isogenic single-gene deletion mutants, Chem. Res. Toxicol. 26 (2013) 356–367, http://dx.doi.org/10.1021/tx300467d.
[30] S. Suppi, K. Kasemets, A. Ivask, K. Künnis-Beres, M. Sihtmäe, I. Kurvet, V. Aruoja, A. Kahru, A novel method for comparison of biocidal properties of nanomaterials to bacteria, yeasts and algae, J. Hazard. Mater. 286 (2015) 75–84, http://dx.doi.org/10.1016/j.jhazmat.2014.12.027.
[31] ISO 20776-1:2006 Clinical Laboratory Testing and in Vitro Diagnostic Test Systems – Susceptibility Testing of Infectious Agents and Evaluation of Performance of Antimicrobial Susceptibility Test Devices – Part 1 2006.
[32] Z.V. Feng, I.L. Gunsolus, T.A. Qiu, K.R. Hurley, L.H. Nyberg, H. Frew, K.P. Johnson, A.M. Vartanian, L.M. Jacob, S.E. Lohse, M.D. Torelli, R.J. Hamers, C.J. Murphy, C.L. Haynes, Impacts of gold nanoparticle charge and ligand type on surface binding and toxicity to Gram-negative and Gram-positive bacteria, Chem. Sci. 6 (2015) 5186–5196, http://dx.doi.org/10.1039/C5SC00792E.
[33] A. Ivask, A. Elbadawy, C. Kaweeteerawat, D. Boren, H. Fischer, Z. Ji, C.H. Chang, R. Liu, T. Tolaymat, D. Telesca, J.I. Zink, Y. Cohen, P.A. Holden, H.A. Godwin, Toxicity mechanisms in Escherichia coli vary for silver nanoparticles and differ from ionic silver, ACS Nano 8 (2014) 374–386, http://dx.doi.org/10.1021/nn4044047.
[34] T. Yoshida, T. Nagasawa, Epsilon-poly-L-lysine: microbial production, biodegradation and application potential, Appl. Microbiol. Biotechnol. 62 (2003) 21–26, http://dx.doi.org/10.1007/s00253-003-1312-9.
[35] K. Nakata, T. Tsuchido, Y. Matsumura, Antimicrobial cationic surfactant, cetyltrimethylammonium bromide, induces superoxide stress in Escherichia coli cells, J. Appl. Microbiol. 110 (2011) 568–579, http://dx.doi.org/10.1111/j.1365-2672.2010.04912.x.
[36] J.T. Buchman, A. Rahnamoun, K.M. Landy, X. Zhang, A.M. Vartanian, L.M. Jacob, C.J. Murphy, R. Hernandez, C.L. Haynes, Using an environmentally-relevant panel of Gram-negative bacteria to assess the toxicity of polyallylamine hydrochloride-wrapped gold nanoparticles, Environ. Sci. Nano 5 (2018) 279–288, http://dx.doi.org/10.1039/C7EN00832E.
[37] European Centre for Disease Prevention and Control, Point Prevalence Survey of Healthcare Associated Infections and Antimicrobial Use in European Acute Care Hospitals, ECDC, Stockholm, 2013.
[38] H.W. Boucher, G.H. Talbot, J.S. Bradley, J.E. Edwards, D. Gilbert, L.B. Rice, M. Scheld, B. Spellberg, J. Bartlett, Bad bugs, no drugs: no ESKAPE! An update from the infectious diseases society of America, Clin. Infect. Dis. 48 (2009) 1–12, http://dx.doi.org/10.1086/595011.
[39] S. Suppi, K. Kasemets, A. Ivask, K. Künnis-Beres, M. Sihtmäe, I. Kurvet, V. Aruoja, A. Kahru, A novel method for comparison of biocidal properties of nanomaterials to bacteria, yeasts and algae, J. Hazard. Mater. 286 (2015) 75–84, http://dx.doi.org/10.1016/j.jhazmat.2014.12.027.
[40] A. Jemec, A. Kahru, A. Potthoff, D. Drobne, M. Heinlaan, S. Böhme, M. Geppert, S. Novak, K. Schirmer, R. Rekulapally, S. Singh, V. Aruoja, M. Sihtmäe, K. Juganson,

A. Käkinen, D. Kühnel, An interlaboratory comparison of nanosilver characterisation and hazard identification: harmonising techniques for high quality data, Environ. Int. 87 (2016) 20–32, http://dx.doi.org/10.1016/j.envint.2015.10.014.
[41] N. Durán, C.P. Silveira, M. Durán, D.S.T. Martinez, Silver nanoparticle protein corona and toxicity: a mini-review, J. Nanobiotechnol. 13 (2015) 55, http://dx.doi.org/10.1186/s12951-015-0114-4.
[42] B. Le Ouay, F. Stellacci, Antibacterial activity of silver nanoparticles: a surface science insight, Nano Today. 10 (2015) 339–354, http://dx.doi.org/10.1016/j.nantod.2015.04.002.
[43] M. López-Heras, I.G. Theodorou, B.F. Leo, M.P. Ryan, A.E. Porter, Towards understanding the antibacterial activity of Ag nanoparticles: electron microscopy in the analysis of the materials-biology interface in the lung, Environ. Sci. Nano 2 (2015) 312–326, http://dx.doi.org/10.1039/C5EN00051C.
[44] J.S. Kim, E. Kuk, K.N. Yu, J.H. Kim, S.J. Park, H.J. Lee, S.H. Kim, Y.K. Park, Y.H. Park, C.Y. Hwang, Y.K. Kim, Y.S. Lee, D.H. Jeong, M.H. Cho, Antimicrobial effects of silver nanoparticles, Nanomed. Nanotechnol. Biol. Med. 3 (2007) 95–101, http://dx.doi.org/10.1016/j.nano.2006.12.001.
[45] S. Kim, H. Lee, D. Ryu, Antibacterial activity of silver-nanoparticles against Staphylococcus aureus and Escherichia coli, Korean J. Microbiol. Biotechnol. 39 (2011) 77–85.
[46] A. Ivask, I. Kurvet, K. Kasemets, I. Blinova, V. Aruoja, S. Suppi, H. Vija, A. Käkinen, T. Titma, M. Heinlaan, M. Visnapuu, D. Koller, V. Kisand, A. Kahru, Size-dependent toxicity of silver nanoparticles to bacteria, yeast, algae, crustaceans and mammalian cells in vitro, PLoS One 9 (2014), http://dx.doi.org/10.1371/journal.pone.0102108.
[47] D. McShan, P.C. Ray, H. Yu, Molecular toxicity mechanism of nanosilver, J. Food Drug Anal. 22 (2014) 116–127, http://dx.doi.org/10.1016/j.jfda.2014.01.010.
[48] N. Durán, M. Durán, M.B. de Jesus, A.B. Seabra, W.J. Fávaro, G. Nakazato, Silver nanoparticles: a new view on mechanistic aspects on antimicrobial activity, Nanomed. Nanotechnol. Biol. Med. 12 (2016) 789–799, http://dx.doi.org/10.1016/j.nano.2015.11.016.
[49] K. Theophel, V.J. Schacht, M. Schlüter, S. Schnell, C.-S. Stingu, R. Schaumann, M. Bunge, The importance of growth kinetic analysis in determining bacterial susceptibility against antibiotics and silver nanoparticles, Front. Microbiol. 5 (2014) 544, http://dx.doi.org/10.3389/fmicb.2014.00544.
[50] J.R. Morones-Ramirez, J.A. Winkler, C.S. Spina, J.J. Collins, Silver enhances antibiotic activity against Gram-negative bacteria, Sci. Transl. Med. 5 (2013), http://dx.doi.org/10.1126/scitranslmed.3006276.Silver.
[51] S. Gurunathan, J.W. Han, D.-N. Kwon, J.-H. Kim, Enhanced antibacterial and antibiofilm activities of silver nanoparticles against Gram-negative and Gram-positive bacteria, Nanoscale Res. Lett. 9 (2014) 373, http://dx.doi.org/10.1186/1556-276X-9-373.
[52] S. Ninganagouda, V. Rathod, D. Singh, J. Hiremath, A.K. Singh, J. Mathew, M. Ul-Haq, Growth kinetics and mechanistic action of reactive oxygen species released by silver nanoparticles from Aspergillus niger on Escherichia coli, Biomed. Res. Int. 2014 (2014), http://dx.doi.org/10.1155/2014/753419.
[53] M.A. Ansari, H.M. Khan, A.A. Khan, M.K. Ahmad, A.A. Mahdi, R. Pal, S.S. Cameotra, Interaction of silver nanoparticles with Escherichia coli and their cell envelope biomolecules, J. Basic Microbiol. 54 (2014) 905–915, http://dx.doi.org/10.1002/jobm.201300457.
[54] G. Kaur, S.K. Mehta, Developments of polysorbate (Tween) based microemulsions: preclinical drug delivery, toxicity and antimicrobial applications, Int. J. Pharm. 529 (2017) 134–160, http://dx.doi.org/10.1016/j.ijpharm.2017.06.059.
[55] C.K. Nielsen, J. Kjems, T. Mygind, T. Snabe, R.L. Meyer, Effects of tween 80 on growth and biofilm formation in laboratory media, Front. Microbiol. 7 (2016) 1–10, http://dx.doi.org/10.3389/fmicb.2016.01878.
[56] K. Rajagopal, P.K. Singh, R. Kumar, K.F. Siddiqui, CTAB-mediated, single-step preparation of competent Escherichia coli, Bifidobacterium sp. and Kluyveromyces lactis cells, Meta Gene 2 (2014) 807–818, http://dx.doi.org/10.1016/j.mgene.2014.10.002.
[57] S.L. Lai, C.-H. Chen, K.-L. Yang, Enhancing the fluorescence intensity of DNA microarrays by using cationic surfactants, Langmuir 27 (2011) 5659–5664, http://dx.doi.org/10.1021/la2004694.
[58] R. Ye, H. Xu, C. Wan, S. Peng, L. Wang, H. Xu, Z.P. Aguilar, Y. Xiong, Z. Zeng, H. Wei, Antibacterial activity and mechanism of action of ε-poly-L-lysine, Biochem. Biophys. Res. Commun. 439 (2013) 148–153, http://dx.doi.org/10.1016/j.bbrc.2013.08.001.
[59] K. Colville, N. Tompkins, A.D. Rutenberg, M.H. Jericho, Effects of poly(L-lysine) substrates on attached Escherichia coli bacteria, Langmuir 26 (2010) 2639–2644, http://dx.doi.org/10.1021/la902826n.
[60] P.K. Stoimenov, R.L. Klinger, G.L. Marchin, K.J. Klabunde, Metal oxide nanoparticles as bactericidal agents, Langmuir 18 (2002) 6679–6686, http://dx.doi.org/10.1021/la0202374.

Environmental Science
Water Research & Technology

PAPER

View Article Online
View Journal

Cite this: DOI: 10.1039/c8ew00317c

Behavior of silver nanoparticles in wastewater: systematic investigation on the combined effects of surfactants and electrolytes in model systems†

Ivona Capjak,[a] Maja Zebić Avdičević,[b] Maja Dutour Sikirić,[c] Darija Domazet Jurašin,[c] Amela Hozić,[c] Damir Pajić,[d] Slaven Dobrović,[b] Walter Goessler[e] and Ivana Vinković Vrček *[f]

Received 16th May 2018,
Accepted 19th October 2018

DOI: 10.1039/c8ew00317c

rsc.li/es-water

Due to the wide and increasing application of engineered silver nanoparticles (AgNPs) in commercial products, their release and disposal into aquatic environmental compartments is unavoidable. The final environmental fate of AgNPs depends on their stability, behavior and lifetime in a particular system. This study aimed to systematically investigate the aggregation and dissolution behavior of AgNPs in model aquatic systems including a range of different pH values, different concentrations of mono- and divalent electrolytes, and the presence of non-ionic, anionic and cationic surfactants used in commercial detergents. The investigation was performed by a combination of surface plasmon resonance (SPR) techniques, dynamic light scattering (DLS) and electrophoretic light scattering (ELS) methods, inductively coupled plasma mass spectroscopy (ICPMS), transmission electron microscopy (TEM), and atomic force microscopy (AFM). The obtained results highlighted the importance of pH, ionic strength and interaction with surfactants relevant to the laundry cycle to the stability and environmental fate of citrate-coated AgNPs. An important implication of this study is that the interaction of AgNPs with surfactants present in wastewater effluents could potentially become more environmentally hazardous due to the increased persistence and dissolution of AgNPs.

Water impact

Due to their biocidal activity, the increasing use of silver nanoparticles (AgNPs) in consumer products inevitably leads to their release into the aquatic environment. More comprehensive and analytical data on the behavior and fate of AgNPs under specific exposure scenarios are needed for risk assessment of their commercial use. This systematic investigation discloses the combined effects of surfactants and electrolytes on the stability and mobility of AgNPs in aqueous media relevant for wastewater effluents.

Introduction

According to inventories and publications on the use of nanotechnology in consumer products, silver nanoparticles (AgNPs) belong to the most popular nanomaterials found in these products.[1–5] Indeed, more than 25% of nano-based consumer products contain AgNPs.[2] The wide application of engineered AgNPs is constantly increasing due to their broad-spectrum biocidal activity and relatively low production costs.[2,3,5] Alongside the textile, food, cosmetic and electronic industries, AgNP-based items are increasingly used also for drinking water and wastewater treatment applications.[6–8] Due to such excessive production and use, the disposal and release of AgNPs into water bodies is inevitable.[8–13] Many, the majority of, studies on modelling AgNP release into the environment have suggested sewer systems and WWTPs as the most probable sink after release from domestic and industrial sources.[14] Thus, sewage sludge, wastewater, and waste incineration represent the most prominent ways of release of nanomaterials into the environment.[14–17] Although removal of Ag from wastewaters can be very efficient (up to 99%), the concentration of AgNPs released from European sewage treatment plants has been predicted at the ppm level.[18] The fact that sewage sludge is used in agriculture as fertilizer further complicates the risk

[a] Croatian Institute of Transfusion Medicine, Petrova 3, 10 000 Zagreb, Croatia
[b] University of Zagreb, Faculty of Mechanical Engineering and Naval Architecture, Ivana Lučića 5, Zagreb, Croatia
[c] Ruđer Bošković Institute, Bijenička cesta 54, 10 000 Zagreb, Croatia
[d] University of Zagreb, Faculty of Science, Physics Department, Bijenička cesta 32, 10000 Zagreb, Croatia
[e] University of Graz, Institute of Chemistry, Universitätsplatz 1/1, 8010 Graz, Austria
[f] Institute for Medical Research and Occupational Health, Ksaverska cesta 2, 10 000 Zagreb, Croatia. E-mail: ivinkovic@imi.hr; Fax: +385 1 4673303; Tel: +385 1 4682540

† Electronic supplementary information (ESI) available. See DOI: 10.1039/c8ew00317c

assessment of engineered AgNPs and other nanomaterials.[14] Although the current environmental concentrations of AgNPs are in the ng L^{-1} range,[19] any prediction of near-future environmental exposure to AgNPs is quite uncertain due to the unpredictable AgNP market and production volume. Thus, concern about the presence of AgNPs in the aquatic environment is rising due to the known toxic effects of silver to aquatic animals.[12,20,21] It has now been well-established that the main environmental exposure pathway for silver nanomaterials is through the wastewater system.[8] Upon reaching water bodies, the stability and reactivity of AgNPs may undergo different transformation processes, such as aggregation, agglomeration, dissolution, complexation, adsorption or desorption.[11–13,22] The behavior and lifetime of AgNPs in a particular system are highly affected by different physicochemical parameters like pH, ionic strength, and the presence of organic components.[9,13,23,24] The effect of these factors, including the acidity, electrolyte composition, and presence of natural organic matter, on the fate of different nanoparticles in the aquatic environment has been extensively studied.[11,12,24–32] In spite of numerous studies, only a few of them addressed the presence of surfactant molecules in water systems.[10,30,33–35] The interaction of AgNPs with surfactants is very well-known and widely applied in the development of nano-based microelectronics and catalysts, where surfactants serve as capping agents.[35,36] The adsorption of surfactants on the nanosurface may significantly change the behavior and reactivity of AgNPs in wastewaters.[30] The presence of surfactants may even transform AgNPs into more toxic forms.[30] There are different possibilities for the types of structures that will form upon the interaction of AgNPs with surfactants depending on the particular water environment.[30,37] Detailed knowledge about the transformation processes of AgNPs in a particular environment is the prerequisite for any risk and safety assessment of AgNPs in aquatic environments. Numerous studies have highlighted the importance of in-depth investigations on the transformation processes of nanomaterials released into the environment.[38,39] To the best of our knowledge, there has been no comprehensive study reporting the combined effects of surfactants and electrolytes on the stability and mobility of AgNPs in aqueous media.

Therefore, the objective of this study was to systematically investigate the behavior, *i.e.* aggregation and dissolution, of AgNPs (i) over a range of different pH values; (ii) in different electrolytes; (iii) in the presence of non-ionic, anionic and cationic surfactants used in commercial detergents; (iv) in mixed systems containing different surfactants and different electrolytes dissolved in ultrapure water. Citrate-coated AgNPs were used as a model nanomaterial system as recommended by the Organization for Economic Cooperation and Development (OECD) and due to their popularity for general and specific applications.[40,41] Two concentration levels of AgNPs were tested; the lower level (1 mg L^{-1}) was comparable with the highest Ag level found in a leakage experiment of commercially available sock fabrics[10] and the higher was 10 times higher. The selection of surfactants was based on the components of commercial laundry detergents[42] including negatively charged, positively charged and nonionic surfactants. The overall aim of this investigation was to refine the predictive parameters for the interpretation and analysis of the environmental behavior of metal-based NPs.

Materials and methods

Chemicals

Crystalline silver nitrate, sodium citrate, sodium borohydride, sodium hydroxide, and "Suprapur" nitric acid were purchased from Merck (Darmstadt, Germany). The plastic and glassware used for chemical analysis and cell culturing were from Sarstedt (Belgium). Osmium tetroxide was purchased from Agar Scientific (Stansted, UK) and TAAB epoxy resin (medium hard) was from Aldermaston (Berkshire, UK). All other chemicals were purchased from Sigma Chemical Co. (Taufkirchen, Germany). All dilutions were made with high purity deionised water (18.2 MΩ cm), which was obtained from a GenPure ultrapure water system (TKA Wasseraufbereitungssysteme GmbH, Niederelbert, Germany) and is referred throughout the text as ultrapure water (UW).

Synthesis of silver nanoparticles

Citrate-coated AgNPs were synthesized following a method described by Munro and co-workers.[43] Briefly, 0.045 g of silver nitrate was dissolved in 245 mL of ultrapure water and heated to boiling under rapid stirring. Immediately after boiling commenced, 5 mL of 1% (w/v) sodium citrate dihydrate was added rapidly. The final molar ratio $AgNO_3/Na_3C_6H_5O_7{\cdot}2H_2O$ was 1/5. The solution was kept at 80 °C for 90 minutes with continuous stirring. The color of the reaction solution changed from colorless to yellow. The transparent and yellow reaction solution was further boiled for 1 h under stirring to warrant formation of uniform quasi-spherical AgNPs. In order to obtain purified and stable AgNPs, the freshly prepared NP suspension was washed twice with ultrapure water immediately after synthesis using centrifugation at 15 790 × *g* for 30 min. The washed AgNPs were resuspended in ultrapure water using ultrasound and stored in the dark at 4 °C until use.

Characterization of silver nanoparticles

The formation of nanosized silver particles was verified by the presence of a surface plasmon resonance (SPR) peak by measuring the absorbance of the aqueous AgNP suspension using a UV-vis spectrophotometer (CARY 300, Varian Inc., Australia).

The size and charge of the AgNPs were measured at 25 °C by dynamic light scattering (DLS) and electrophoretic light scattering (ELS), respectively, at 173° using a Zetasizer Nano ZS (Malvern, UK) equipped with a green laser (532 nm). To avoid overestimations arising from the scattering of larger particles, the hydrodynamic diameters (d_H) were obtained at the peak maximum of the size volume distribution function. Size values are reported as the average of 10 measurements. The charge of the NPs was characterized by ζ potential values,

which were calculated from the measured electrophoretic mobility by means of the Henry equation using the Smoluchowski approximation. The data were processed by the Zetasizer software 6.32 (Malvern Instruments).

The total silver concentrations in AgNP colloidal suspensions were determined by analysis of the total Ag content using an Agilent Technologies 7500cx inductively coupled plasma mass spectrometer (Agilent, Waldbronn, Germany). Samples were prepared by simple dilution in 10% (v/v) HNO_3. A silver standard solution (1000 mg dm^{-3} in 5% HNO_3) from Merck (Darmstadt, Germany) was used for calibration.

The dissolved silver fraction in the AgNPs was quantified by diluting the AgNP stock suspensions with ultrapure water or Tris buffer to a desired starting concentration (*i.e.* 10, 100 and 300 mg dm^{-3}) and then tracking the appearance of dissolved silver ions using an Orion 9616BNWP Sure-Flow™ Combination Silver/Sulfide Electrode (Ag-ISE, Thermo Scientific, USA) connected to a SevenEasy ISE meter (Mettler Toledo, Switzerland) during a 24 h period. The electrode was preconditioned before each experiment by immersion in a solution containing 0.01 M Ag^+ for 3 h. The detection limit of the electrode was 10^{-7} M Ag^+. Silver stock solutions (2.8 mM Ag) were prepared in ultrapure water from reagent grade $AgNO_3$ and used for calibration standards that bracket the expected sample concentration. A linear calibration curve was obtained over the whole range with a slope of 59.3 mV/log [Ag^+]. For measurements in AgNP dispersions, dilutions of the original suspension were prepared in the range 1 : 10 to 1 : 100. Concentrations of Ag^+ were calculated from the obtained potential using the linear calibration line.

In addition, dissolved Ag ions were separated from AgNPs by ultrafiltration using Amicon-4 Ultra centrifugal filter units with a 3 KDa cut-off (Merck Millipore, Darmstadt, Germany) and were quantified by graphite furnace atomic absorption spectrometry (GFAAS) (PerkinElmer AAnalyst 600, PerkinElmer, Shelton, USA) with Zeeman background correction. Standard Reference Material® (SRM) 1643e Trace Elements in Water (NIST, USA) was used to confirm the reliability of the analytical methods. However, adsorption of silver onto the filters was observed. Results for SRM 1643e were within ±20% of the certified values, while recovery of the standard Ag solution diluted to 100 μg L^{-1} in neutral media (ultrapure water) was in the range of 70–85%. Thus, only dissolution results obtained using Ag-ISE are presented.

All results were expressed as the average values of data obtained by performing measurements 5 times using freshly prepared samples.

Visualization of silver nanoparticles

Visualization of AgNPs by TEM was performed with a TEM (Zeiss 902A) operated in bright field mode at an acceleration voltage of 80 kV. Images were recorded with a Canon PowerShot S50 camera attached to the microscope. TEM samples were prepared by depositing a drop of the particle suspension on a Formvar® coated copper grid and air-drying at room temperature.

AFM imaging was performed using a Multimode AFM with a Nanoscope IIIa controller (Veeco Instruments, Santa Barbara, CA) with a vertical engagement (JV) 125 μm scanner, using contact mode. Contact mode imaging was performed using sharpened silicon nitride (NPS, Bruker, nom. freq. 23 kHz, nom. spring constant of 0.06 N m^{-1}) and silicon tips (MSNL, Bruker, nom. freq. 7 kHz, nom. spring constant of 0.01 N m^{-1}). The force was kept at the lowest possible value in order to minimize the forces of interaction between the tip and the surface. The linear scanning rate was optimized between 1.5 and 2 Hz with a scan resolution of 512 samples per line. Processing and analysis of images was carried out using NanoscopeTM software (Digital Instruments, version V614r1). All of the presented images are raw data except for the first order two-dimensional flattening. Measurements were performed in air at room temperature and 50–60% relative humidity, which leaves the samples with a small hydration layer, helping to maintain the structure[44] using freshly cleaved mica as a substrate. For AFM imaging, 5 μL of 10 μg mL^{-1} AgNP suspension in 0.1 M NaCl (after 1 hour, 4 hours and 24 hours in contact) was pipetted directly onto freshly cleaved mica. Mica sheets were left to dry in enclosed Petri dishes for approximately 30–45 minutes. Samples were then rinsed three times for 30 s in ultrapure water and placed in enclosed Petri dishes at a relative humidity of 60% to evaporate the excess water on the mica.

Magnetic properties of silver nanoparticles

The magnetization M of silver nanoparticles in powder form was measured with an MPMS5 commercial magnetometer operating with a superconducting quantum interferometer device (SQUID). The measured magnetic moment of the sample was corrected against the contribution of the ampoule. It was completely filled with powder in order to minimize the magnetic signal of the oxygen. The temperature dependence of magnetization for all compounds, $M(T)$, was measured in the temperature range 2–300 K in different constant magnetic fields. The field dependences of magnetization, $M(H)$, were measured at several stable temperatures ranging from 2 K to 300 K.

Stability evaluation of AgNPs under different test conditions

To investigate the effect of different test conditions on the stability and aggregation behavior of the AgNPs, measurement of the size distribution by means of volume, zeta potential values, SPR peaks, and % of dissolved Ag fraction was performed in each test medium. All of the parameters were monitored 1 h, 4 h and 24 h after dispersion of AgNPs in a particular test system. Measurements were repeated 5 times for each parameter and the results are expressed as average values.

The following test conditions were evaluated: (i) different pH values ranging from 3–9; (ii) different ionic strengths

encompassing both monovalent and divalent cations and anions (NaCl, $MgCl_2$, Na_2SO_4 and $MgSO_4$) at two different molar concentrations, *i.e.* 0.01 and 0.1 M; (iii) test media with non-ionic surfactant Triton-X100, cationic surfactant dodecylammonium chloride (DDACl) and anionic surfactant sodium dodecyl sulphate (SDS); (iv) mixed media that combine each surfactant with 0.1 M NaCl.

Ultrapure water (UW), characterized by pH 6.8, was used as a reference test medium and the results obtained for all test systems were compared with the values obtained in UW. To evaluate the impact of different pH values on AgNP stability, the pH values of the test solutions were adjusted with 1 M HNO_3 and/or with 1 M NaOH to pH 3 and 9, respectively. Test media of different ionic strengths were prepared by dissolving the appropriate amount of each salt, *i.e.* NaCl, $MgCl_2$, Na_2SO_4 or $MgSO_4$, in UW and by adjusting their molar concentrations to 0.01 and 0.1 M. Sodium and magnesium were chosen as representatives of the most abundant monovalent and divalent cations in natural freshwaters, respectively.[45] Surfactant solutions were prepared either in UW or in 0.1 M NaCl at the following concentrations: 5 and 30 mM for DDACl, 0.5, 5 and 15 mM for SDS, and 0.1 and 1 mM for Triton X-100.

Dispersion experiments were performed by adding 0.1 mL of AgNP stock suspension (1000 mg dm^{-3}) to 10 mL of the test media. Thus, the approximate final AgNP concentration was 10 mg dm^{-3}. AgNPs were added immediately before measurements, vortexed, and typically less than 1 min elapsed between the mixing of samples and the start of a measurement. For salt media, including NaCl, $MgCl_2$, Na_2SO_4 or $MgSO_4$, an appropriate aliquot of 100 mM stock salt solution was added to a volume of UW such that the salt medium volume was 9.9 mL before the addition of the AgNPs and the desired concentration of salt (*e.g.*, 0.01 M) was correct in the final 10 mL dispersion.

Results and discussion

This study was designed to evaluate the aggregation and dissolution behavior of citrate-coated AgNPs under different environmentally relevant conditions including a pH range from 3 to 9, different electrolyte concentrations and the presence of surfactants used in commercial detergents.

Physicochemical characteristics of citrate-coated AgNPs

The characteristics of AgNPs prepared by reduction of $AgNO_3$ with sodium citrate have already been documented in our recent publications.[46,47] For the purpose of this study, freshly prepared citrate-coated AgNPs were characterized in UW by means of visualization by TEM and AFM (Fig. 1), paramagnetic properties (Fig. 2), size distribution and surface charge (Fig. 3), dissolution properties (Table 1), and SPR peak evaluation (Table S1 in the ESI†). DLS measurements showed a bimodal size distribution of AgNPs with the dominant population (82.9% of the mean volume) having a d_H value of 9.33 ± 2.03 nm and a smaller population (17.1% of the mean volume) characterized by a d_H value of 27.96 ± 3.26 nm. Freshly prepared citrate-coated AgNPs were stable not only during a 24 h period, as can be seen from the results presented in Table 1 and Fig. 3, but also for a much longer time (more than 3 months), as expected from the large negative ζ potential value, *i.e.* −45.5 ± 0.7 mV. As the ζ potential is related to the electrical potential at the interface between the diffuse ion layer surrounding the NPs and the bulk solution,[48] the high absolute ζ potential value provides a repulsive force keeping the NPs away from each other. Thus, a ζ potential value close to zero means that the repulsion between NPs decreases as does the stability of the NP dispersion.

The UV-vis absorption spectrum of the suspension showed a SPR peak at a wavelength of 433 nm, which is consistent with the classical Mie theory.[49,50] The position and width of the plasmon band in the UV-vis absorption spectrum of the NP suspension depend on the size and polydispersity of the NPs as well as the presence of adsorbed substances or an oxidation layer on the surface of the NPs.[51–53] The oxidized surface layer on the NP surface will broaden and shift the SPR peak to increased wavelengths.[53–55] Due to the very high stability of the prepared AgNPs, the position and height of the SPR peak did not change during 24 h (Table S1 of ESI†).

Visualization of AgNPs by TEM showed particles of different shapes, *i.e.* spherical, rod-like and triangular (Fig. 1a). This observation may explain why DLS measurements showed a bimodal size distribution. In addition to TEM, AgNPs were visualized by AFM, which is an excellent characterization tool. At the same time, the AFM technique offers

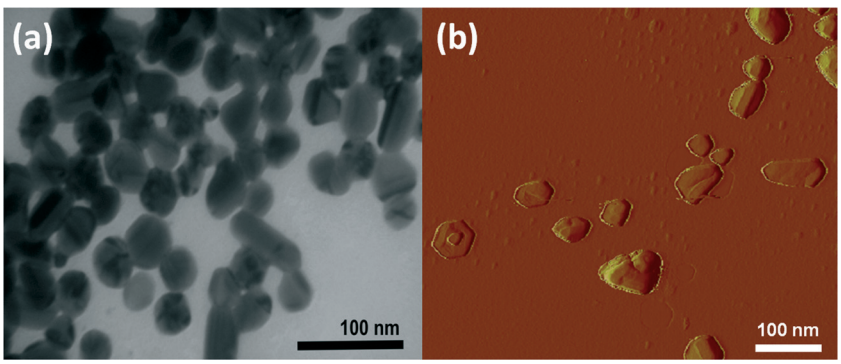

Fig. 1 Images of citrate-coated AgNPs in ultrapure water obtained by (a) transmission electron microscopy and (b) atomic force microscopy.

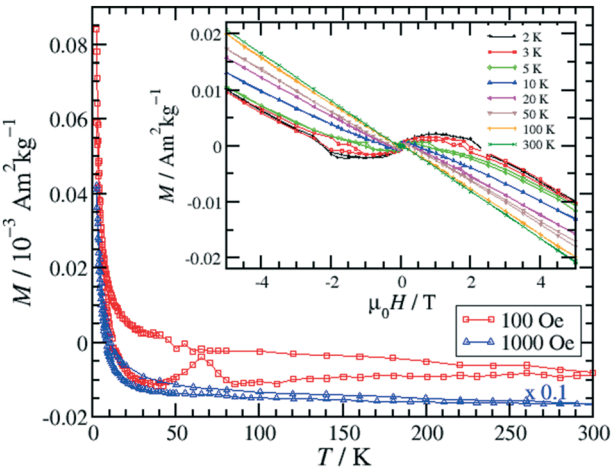

Fig. 2 The temperature dependence of the magnetization $M(T)$ of AgNPs in ultrapure water measured in different applied magnetic fields H and the isothermal field dependence of magnetization $M(H)$ measured at different temperatures T.

the capability of 3D visualization and both the qualitative and quantitative evaluation of many physical properties including size, morphology, surface texture and roughness.[56] AFM imaging confirmed AgNPs of various shapes including spherical, oval, triangular, hexagonal and rod-like NPs, with triangular NPs being the most frequent (Fig. 1b). AFM experiments provided information on the average height and height distribution of AgNPs on a larger scale. They showed that individual AgNPs had an average height between 20–50 nm (Fig. S2, given in the ESI†).

The release of Ag^+ from the AgNP surface in UPW was determined to be >0.7% of the total Ag (Table 1). There was no change in the Ag-ISE potential of the AgNP suspension during 24 hours, which provided additional evidence for their long-term stability.

In addition, the magnetic properties of citrate-coated AgNPs were evaluated. The temperature-dependent magnetization $M(T)$ was measured in different applied magnetic fields H and the isothermal field dependence of magnetization $M(H)$ was measured at different temperatures T (Fig. 2). For all the temperatures, a clear linear decrease in $M(H)$ dependence at higher fields was observed with the same slope for all curves (−0.003 $Am^2\ kg^{-1}\ T^{-1}$) in agreement with the diamagnetic susceptibility of silver, reflecting the temperature independent diamagnetic contribution. Above 50 K, $M(H)$ is fully linear showing dominantly the diamagnetic contribution. However, interesting S-curved features around the central part of the $M(H)$ curves appear at 50 K and below. This is a signature of the large magnetic moments superposed onto the mentioned diamagnetic behavior. A detailed

Table 1 Effect of pH and various electrolytes on the dissolution behavior of AgNPs. The percentage of free Ag^+ was determined in 10 mg L^{-1} AgNPs suspended in ultrapure water (UW), in media with pH 3 and 9, in different electrolytes, and in the presence of different surfactants: dodecylammonium chloride (DDACl), sodium dodecyl sulphate (SDS) and Triton X-100 after 1 h, 4 h and 24 h

Medium	Ag^+ release (%)		
	1 h	4 h	24 h
UW	0.45	0.48	0.74
pH 3	0.62	0.65	0.87
pH 9	0.73	0.73	0.74
0.01 M NaCl	2.50	2.00	0.50
0.1 M NaCl	2.58	2.43	0.61
0.01 M Na_2SO_4	2.00	1.59	1.11
0.1 M Na_2SO_4	0.87	1.00	1.14
0.01 M $MgCl_2$	1.77	2.67	0.75
0.1 M $MgCl_2$	0.25	4.38	9.05
0.01 M $MgSO_4$	1.03	0.80	1.23
0.1 M $MgSO_4$	1.44	0.80	0.96
5 mM DDACl	0.43	0.08	0.38
5 mM DDACl + 0.1 M NaCl	8.75	9.40	17.77
5 mM SDS	0.14	0.22	0.49
15 mM SDS	0.48	0.42	0.53
15 mM SDS + 0.1 M NaCl	3.75	5.57	13.46
0.1 mM Triton X-100	0.63	0.70	0.53
1 mM Triton X-100	0.86	0.86	1.04
0.1 mM Triton X-100 + 0.1 M NaCl	1.24	1.24	1.36
1 mM Triton X-100 + 0.1 M NaCl	1.48	1.69	2.27

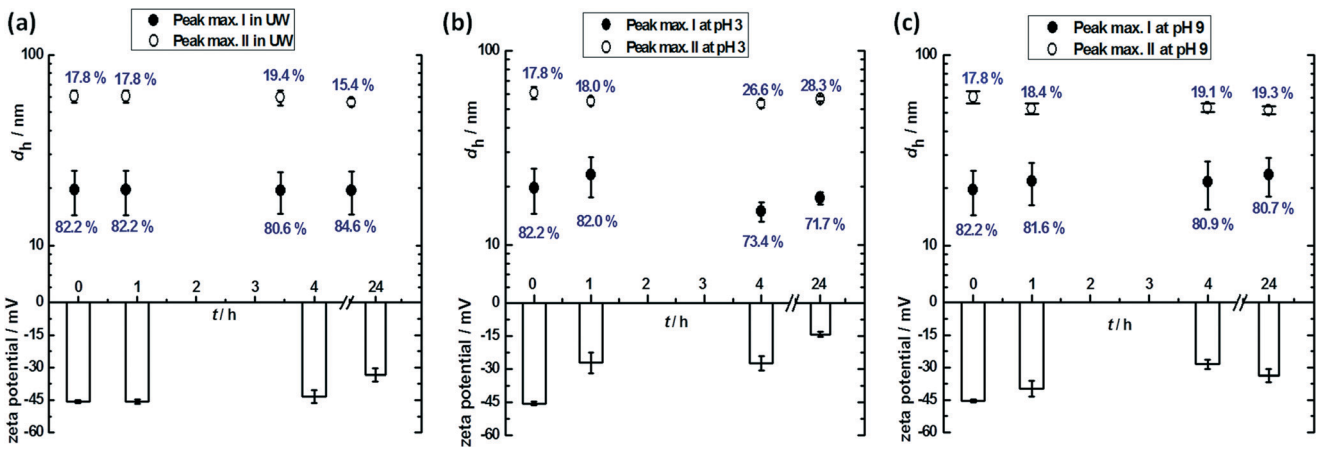

Fig. 3 Change in hydrodynamic diameter (d_H) and zeta potential of AgNPs in a) ultrapure water (UW), b) a medium with pH 3 and c) a medium with pH 9 during 24 hours at 25 °C. The mean volume % of particle populations with different sizes are indicated.

description of the modeling of the magnetic properties of citrate-coated AgNPs is given in the ESI.† The formation of the magnetic moments could be connected to the nanoparticulated structure of the AgNP powder. More specifically, atoms at the surface of AgNPs could develop magnetic moments because of the boundary effects and unsaturated chemical bonds. The number of such unpaired electrons is considerable as the NPs become smaller and smaller, due to a bigger relative amount of surface atoms in the measured sample. The coating of the NPs makes the moments isolated, as confirmed by the performed modeling of magnetically independent particles. The temperature dependence of magnetization points to the paramagnetic behavior of the system, which considerably increases the magnetization below a temperature of 20 K. The pure silver in bulk form could not develop such paramagnetism at low temperatures. Therefore, we concluded that the increase in magnetization comes from the superparamagnetic contribution of AgNPs, which have magnetic moments much larger than the single electronic one. This paramagnetism has its origin in the AgNPs as a whole but not the single silver atoms or bulk piece of silver. It is termed *superparamagnetism* because of the large magnetic moment sitting on the isolated magnetic units. The surface coating of the AgNPs is crucial for their independence, but it is also reasonable to expect the tuning of a magnetic moment with the chemistry happening between the functionalized surface and the silver core. It is expected that the magnetic moment of the nanoparticles becomes bigger for smaller particles because of the considerably increased relative amount of surface atoms. Magnetic results give insight into one important functionality of the studied AgNPs, which is useful in the treatment of water contaminated with NPs. More precisely, the magnetic moment that appears due to the nanosized dimensions of the AgNPs can be used to produce the force on the NPs when they are exposed to the inhomogeneous magnetic field and drag the AgNPs in the direction of the magnetic field gradient. This effect is already used in some drug-delivery systems. In its simple form, this effect could be used to separate the studied NPs using the magnetic field of permanent Nd–Fe–B magnets, which are strong enough and have a very pronounced field gradient. Separation would be even more efficient and important for smaller AgNPs, which are not suitable for separation with usual filtering processes.

Effect of pH on AgNP stability

A significant increase or decrease in the pH value of the dispersion media decreased the absolute ζ potential value of AgNPs. After 24 h, the measured ζ potential (Fig. 3) changed from initial values of −45.5 ± 0.7 mV at pH 6.8 in UW to −14.3 ± 1.1 mV and −33.8 ± 3.1 mV after dispersion in media with pH 3 and 9, respectively. pH 9 had a minimal effect on the surface charge and aggregation behavior of electrostatically stabilized AgNPs (Fig. 3c). As citrate-coated AgNPs are electrostatically stabilized by negatively charged citrate ions, an increase in the pH of the dispersion media should lead to more negative AgNP surfaces and increase repulsion forces. In contrast, a lower pH would protonate the citrate ion and cause decreased repulsion.[7,24] Thus, the results obtained at pH 3 are in good agreement with this explanation, already demonstrated for the same and similar AgNPs.[30,57,58] This observation is in accordance with the observed aggregation behavior of AgNPs. The dispersion of AgNPs in the medium with pH 3 led to an increase in the percentage of the bigger NP population indicating their aggregation (Fig. 3b). Despite the observed change in ζ potential value by more than 15 mV in pH 9, citrate-coated AgNPs showed an almost identical size distribution at pH 9 to that in UW. In general, it is considered that NPs characterized by ζ potential in the range between +20 mV and −20 mV are unstable.[24] Thus, our AgNPs were sufficiently charged to avoid aggregation either in UW or at pH 9 (Fig. 3a–c).

Furthermore, pH 9 had a moderate effect on the dissolution of AgNPs, while pH 3 significantly increased the rate of Ag^+ release from the AgNP surface as expected (Table 1). These findings were corroborated with the UV-vis data (Table S1 in the ESI†). No changes in the SPR peak were observed going from UW to pH 9, while the decrease in the SPR peak height at pH 3 compared to that in UW indicated the disappearance of single AgNPs as a result of their dissolution. Thus, an increase in the ζ potential value of citrate-coated AgNPs obviously resulted not only in the protonation of the AgNP surface but also in the dissolution and release of silver cations. The dissolution of AgNPs in nitric acid has been documented well as a mechanism corresponding to the chemical reaction controlled process affected by the acid concentration, the temperature of the reaction and the particle size.[59]

Effect of electrolyte concentration on AgNP stability

The effect of increasing electrolyte concentration on the stability of AgNPs was evaluated using two different concentrations (0.01 and 0.1 M) of four different electrolytes. The most prevalent electrolyte components of natural freshwaters[45] were selected, namely, NaCl, $MgCl_2$, Na_2SO_4, and $MgSO_4$. Thus, the experimental set-up covered both mono- and divalent cations, as well as mono- and divalent anions. We have previously investigated the behavior of AgNPs in natural freshwater (*i.e.* well water)[46] as well as in a model freshwater (*i.e.* reconstituted hard freshwater),[21] while this study was focused on a simpler test system to be able to monitor the behavior of AgNPs for assessing the influence of the tested factors in more detail. DLS and ELS methods were used for the investigation of the time-dependent aggregation behavior of AgNPs. Representative aggregation profiles of AgNPs in different electrolyte solutions are presented in Fig. 4 and 5. The aggregation behavior of AgNPs was consistent with the DLVO theory.[26] It was clearly controlled by electrostatic interactions. At higher electrolyte concentrations, the charge of citrate-coated AgNPs became screened, which eliminated the energy barrier between the AgNPs. Interestingly, no changes in the

aggregation behavior of AgNPs were observed in the 0.01 M media containing sodium chloride (Fig. 4a), indicating the importance of cationic electrolyte components for the stability of citrate-coated AgNPs. The increase in cation charge (Mg^{2+} *vs.* Na^{+}) at the same electrolyte concentration significantly affected electrostatically stabilized AgNPs (Fig. 4). Since cations can neutralize the surface charge of citrate-coated AgNPs through specific interactions with the carboxyl groups of the adsorbed citrate coatings, replacement of Na^{+} by Mg^{2+} induced aggregation even at an electrolyte concentration of 0.01 M. These observations are fully in accordance with the results published by Li *et al.*,[26] who tested the stability of citrate-coated AgNPs in different concentrations of NaCl, $NaNO_3$ and $CaCl_2$. In the case of the medium with monovalent cations at 0.01 M, the absolute values of the ζ potential either did not change significantly or increased by *ca.* 10 mV. For the media with $MgCl_2$ or $MgSO_4$, a significant decrease in the absolute values of the ζ potential was observed (Fig. 4b *vs.* Fig. 5b). This indicates that the presence of divalent cations had a much larger effect on the surface charge of AgNPs than the anionic components of the background electrolyte (Cl^{-} and SO_4^{2-}). Introduction of divalent cations (Mg^{2+}) into the media instead of monovalent cations (Na^{+}) significantly destabilized AgNPs due to the decrease of the ζ potential absolute values even at a lower electrolyte concentration of 0.01 M (Fig. 4 and 5). At a higher electrolyte concentration, the presence of SO_4^{2-} anions increased the ζ potential in media with Na^{+} (Fig. 5a), but insufficiently for maintaining colloidal stability. It is interesting to note that ζ potentials were more negative in the presence of Cl^{-} anions compared to the media containing SO_4^{2-}, which may be explained by the formation of colloidal $AgCl_x^{(x-1)}$ particles. The change in ζ potential also explains the pronounced aggregation behavior of AgNPs in the media with electrolytes. Thus, the AgNP suspension was destabilized due to the increase in ionic strength, when the complexation of Na^{+} with the citrate carboxyl groups on the AgNP surface led to particle aggregation.

After AgNP dispersion in electrolyte solutions, UV-vis analysis showed a significant red shift observed only for the media containing Mg salts, while no significant changes in the SPR peak position were observed in media containing NaCl or Na_2SO_4 (Table S1 in the ESI†). However, the typical SPR peak of the AgNP aggregates that can be found in the range between 600–800 nm was not found in all of the tested samples. In the case of 0.1 M Na_2SO_4, $MgSO_4$ and $MgCl_2$, the appearance of double SPR peaks was observed (Fig. S3†). The aggregation behavior of AgNPs may be evidenced either by the presence of additional SPR peaks or by the decrease of the height of the SPR peak.[26] Indeed, the peak height slightly decreased in 0.01 M NaCl or Na_2SO_4 and almost disappeared in the media with Mg salts, or at higher NaCl and Na_2SO_4 (Table S1 in the ESI†) concentrations. However, the absence of SPR peaks at red-shifted wavelengths is not straightforward evidence that AgNPs did not aggregate, as aggregates may precipitate below the spectrometer beam path, which was actually evidenced. These results correspond well with the DLS data (Fig. 4 and 5). However, the observed decrease in absorbance values cannot be ascribed only to the aggregation but also to the dissolution of AgNPs and the appearance of free Ag^{+} ions. Thus, a significant increase in the percentage of free Ag^{+} was observed in all electrolyte solutions (Table 1). AgNPs are extremely sensitive to oxygen and the chemisorbed Ag^{+} can be released once it comes into contact with water.[13,14,41] Oxidation and subsequent dissolution of AgNPs have been demonstrated to determine not just the fate but also the observed toxicity of AgNPs to different organisms under aerobic environmental conditions.[14] Due to the reactivity of AgNPs, different environmental transformations should be taken into account including agglomeration, oxidation, precipitation, sorption, but also the interaction with various inorganic and organic ligands.[14] Transformation of AgNPs to Ag_2S has been demonstrated to be a rapid reaction under anaerobic

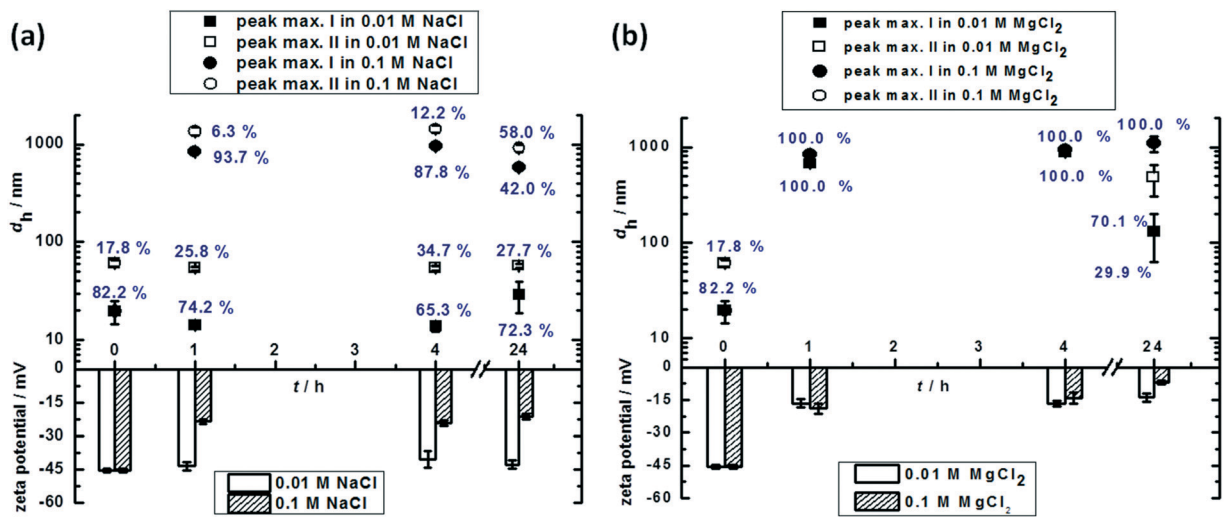

Fig. 4 Change in the hydrodynamic diameter (d_H) and zeta potential of AgNPs in the presence of different concentrations of a) NaCl and b) $MgCl_2$ during 24 hours at 25 °C. The mean volume % of particle populations with different sizes are indicated.

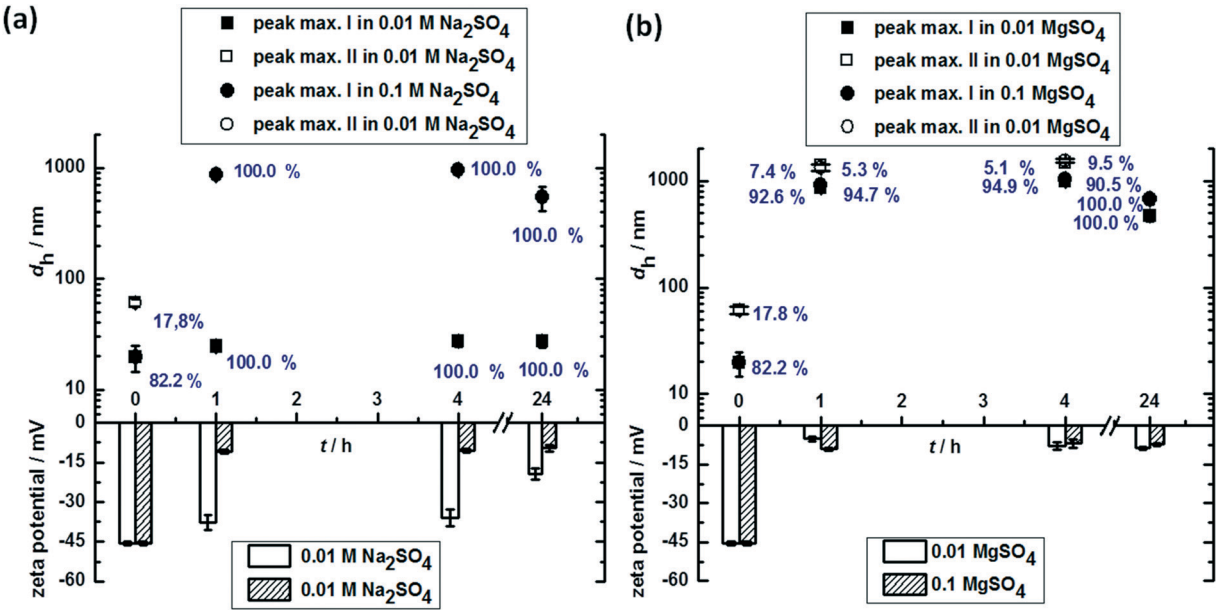

Fig. 5 Change in the hydrodynamic diameter (d_H) and zeta potential of AgNPs in the presence of different concentrations of a) Na_2SO_4 and b) $MgSO_4$ during 24 hours at 25 °C. The mean volume % of particle populations with different sizes are indicated.

conditions in the wastewater treatment process.[60] Another relevant topic concerning AgNPs in the WWTP is effects of natural organic matter, *i.e.* humic acids, which may affect not just the stability of AgNPs but also silver chlorides and sulfides.[14,60] These interactions may increase AgNP stability due to the formation of a biomolecular corona that protects the AgNP surface from corrosion but also decrease the solubility of formed Ag_2S particles in biosolids or sewage sludge.[14,61]

In the simple test system used in this study, the most pronounced AgNP dissolution occurred in the medium containing 0.1 M $MgCl_2$ after 4 h. It is interesting to note that the percentage of free Ag^+ ions in all electrolyte solutions decreased after 24 h as compared to the results obtained after 4 h. The reason may be the attachment of free Ag^+ on the surface of AgNP aggregates that formed sediments at the bottom of the testing flask. The prediction of AgNP dissolution behavior in the presence of oxygen and Cl^- ions is very complicated due to the possibility of formation of AgCl shells on the AgNP surface and/or dissolution and formation of different complex $AgCl_x^{(x-1)-}$ ions.[13,31,32] The results presented in Table 1 show that AgNPs dissolved to a much higher extent in all electrolyte solutions than in UW, while the formation of soluble silver chloride complexes may have accelerated their dissolution. In the presence of Cl^-, the dissolution and aggregation of AgNPs are simultaneous with the formation of a silver chloride precipitate.[31] Our results are consistent with the observation recently published by Odzak *et al.*, who found faster AgNPs dissolution in media with low ionic strength and low pH. They also discussed that adsorption of Cl^- and formation of AgCl on the surface of AgNPs were more feasible than precipitation of AgCl in the presence of Cl^-.[32]

We further performed AFM imaging of AgNPs from a 10 mg L^{-1} suspension in 0.1 M NaCl after 1, 4 and 24 h. The typical AgNP aggregates are shown in Fig. 6. The AFM images clearly showed the co-existence of single dispersed AgNPs and aggregates of several hundred nm after 1 h (Fig. 6a and b). After 4 h, no single AgNP can be found, while the height of aggregates ranged from 50 to 100 nm (Fig. 6c and d). Further aggregation resulted in deformed structures where some surfaces obviously underwent dissolution and oxidation processes that resulted in agglomerates with both d_H and height of several hundred nanometers (Fig. 6e and f). The presence of Cl^- ions in the electrolyte solutions obviously led to the formation of soluble silver chloride complexes, such as $AgCl_2^-$ and $AgCl_3^{2-}$, which accelerated the dissolution of AgNPs. Dissolution affected the mechanism of AgNP aggregation due to the precipitation of AgCl that enhanced interparticle bridging between AgNPs and subsequently also the aggregation kinetics. Due to the difference in size, corrosion of the AgNP surface is predicted to be faster than for the bulk Ag and extremely complicated in media such as sewage sludge, wastewaters, or soil, due to the presence of many possible agents that may interact with AgNPs and affect their surface properties and stability.[14,60] Even the results obtained for the simple test system encompassing two different concentrations of four different electrolytes (Fig. 4–6) demonstrated the complexity of AgNP behavior, whereas prediction of transformations, transport, reactivity, and toxicity of AgNPs under real environmental conditions should take into account a plethora of possible pathways.[60]

Stability of AgNPs in the presence of surfactants

AgNPs released from consumer products into the environment may undergo different transformation routes depending on the condition of each environmental

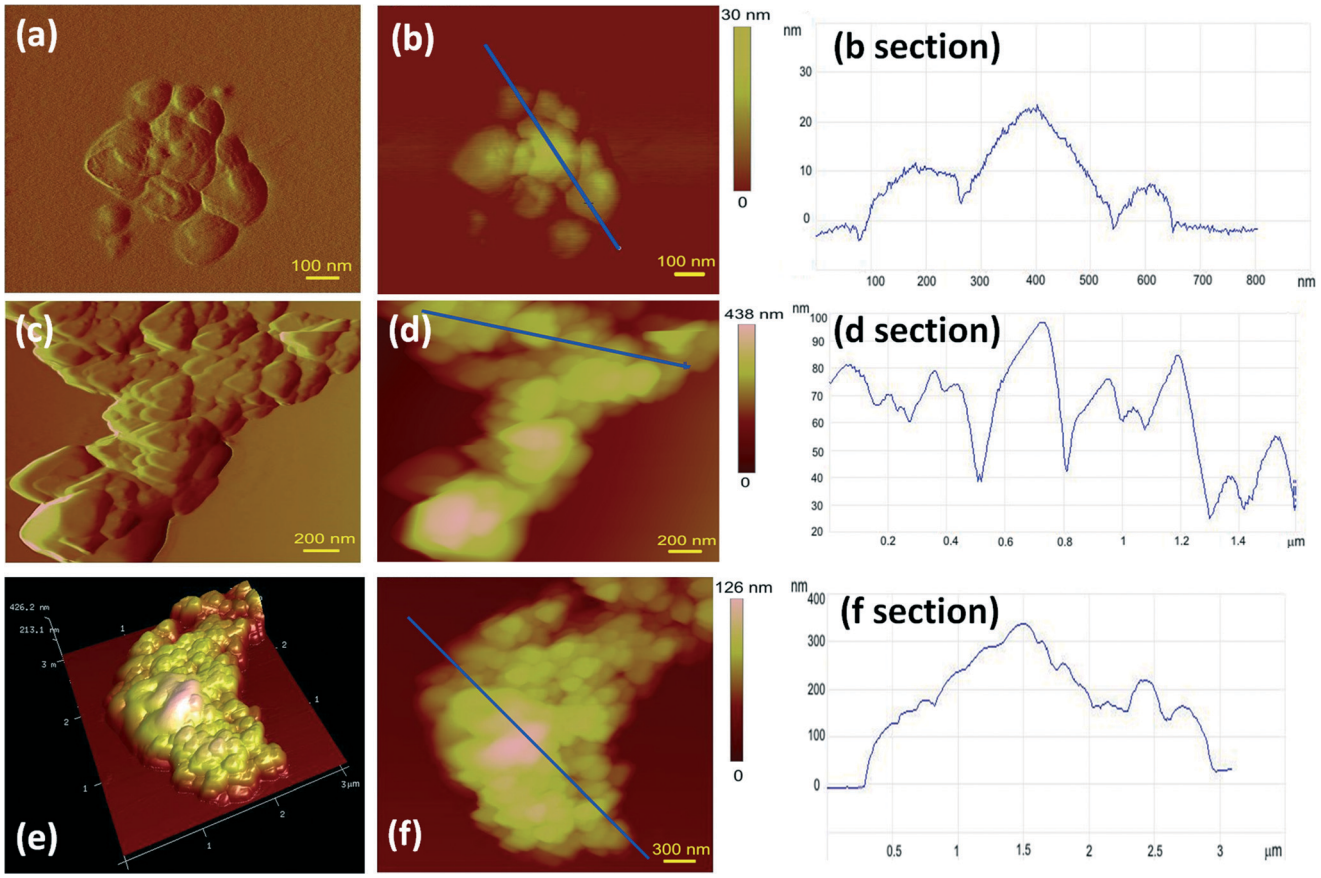

Fig. 6 Atomic force microscopy images of AgNP aggregates in 0.1 M NaCl: (a) after 1 h, deflection data, scan size 1 mm × 1 mm; (b) after 1 h, top view of height data, scan size 1 mm × 1 mm, vertical scale 30 nm, with section analysis along the indicated line; (c) after 4 h, deflection data, scan size 2 mm × 2 mm; (d) after 4 h, top view of height data, scan size 2 mm × 2 mm, vertical scale 438 nm, with section analysis along the indicated line; (e) after 24 h, deflection data, scan size 3 mm × 3 mm; (f) after 24 h, top view of height data, scan size 3 mm × 3 mm, vertical scale 426 nm, with section analysis along the indicated line.

compartment.[62] In wastewater systems, the presence of laundry surfactants may also affect their speciation. The stability of a nanosystem is determined by different forces including hydrodynamic, electrostatic, electrodynamic, solvent and steric interactions between the surfactant and the NP surface.[63] To increase the knowledge needed for environmental risk assessment, the stability evaluation of AgNPs was undertaken in the presence of surfactants relevant to the laundry cycle. Interactions between AgNPs and three differently charged surfactants were investigated using two different surfactant concentrations, based on being below and above the critical micellar constant (CMC). The CMC is defined as the concentration of surfactants above which micelles are formed. Essentially, a micellar solution is a colloidal dispersion of self-assembled surfactant molecules. Below the CMC, the surfactant exists mainly as a solvated monomeric species.[64] Thus, non-ionic Triton X-100 was used at 0.1 and 1 mM, positively charged DDACl was used at 0.05 mM, 5 mM and 30 mM, and negatively charged SDS was used at 0.1 and 15 mM. In addition, mixed systems consisting of a high ionic strength medium (0.1 M NaCl) with the addition of a surfactant at the concentration above the CMC were also tested.

None of the surfactants affected the aggregation behavior of the AgNPs, either at the concentration below or above the CMC values (Fig. 7–9 and Table S2 in the ESI†). As expected, Triton X-100 did not give rise to any significant changes in the aggregation behavior of citrate-coated AgNPs (Fig. 7). Although it has already been described that only minor or no reduction can be expected for the surface charge of charged AgNPs in nonionic surfactants,[30] we observed a decrease in the absolute value of the ζ potential of citrate-coated AgNPs below and above the CMC values of Triton X-100 (*i.e.*, at 0.1 and 1 mM, respectively). The ζ potential value changed by ~20 mV even upon immersion of AgNPs in the Triton X-100 solutions and remained unchanged during 24 h (Table S3 in the ESI†). The reason for this may be the screening of the negative citrate ions at the AgNP surface by molecules and/or micelles of Triton X-100. As expected, the negative surface charge of AgNPs became more negative upon suspension in the media containing the negatively charged surfactant SDS above its CMC value, while no changes in ζ potential were observed in the solution containing SDS below the CMC value (Table S3 in the ESI†). Due to the large negative value of the ζ potential, citrate-coated AgNPs were very stable in the presence of SDS (Fig. 8). This goes hand

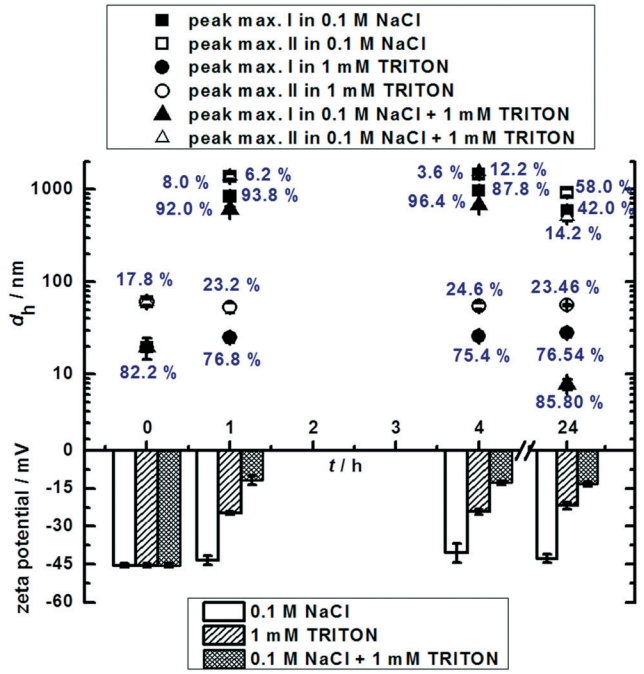

Fig. 7 Change in the hydrodynamic diameter (d_H) and zeta potential of AgNPs in the presence of 0.1 M NaCl, a micellar concentration of Triton (1 mm) and a mixture of NaCl and Triton during 24 hours at 25 °C. The mean volume % of particle populations with different sizes are indicated.

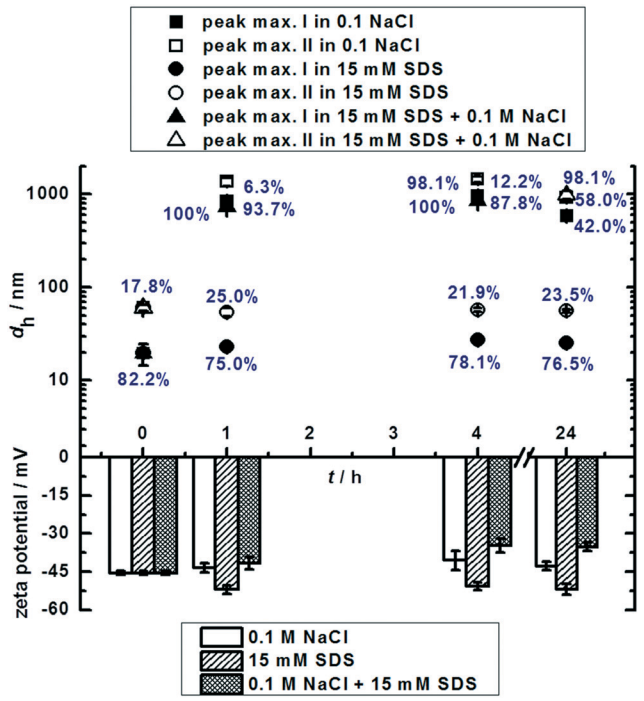

Fig. 8 Change in the hydrodynamic diameter (d_H) and zeta potential of AgNPs in the presence of 0.1 M NaCl, a micellar concentration of SDS (15 mm) and a mixture of NaCl and SDS during 24 hours at 25 °C. The mean volume % of particle populations with different sizes are indicated.

in hand also with the unchanged SPR peak position (Table S1 in the ESI†) and dissolution behavior of AgNPs (Table 1) in the

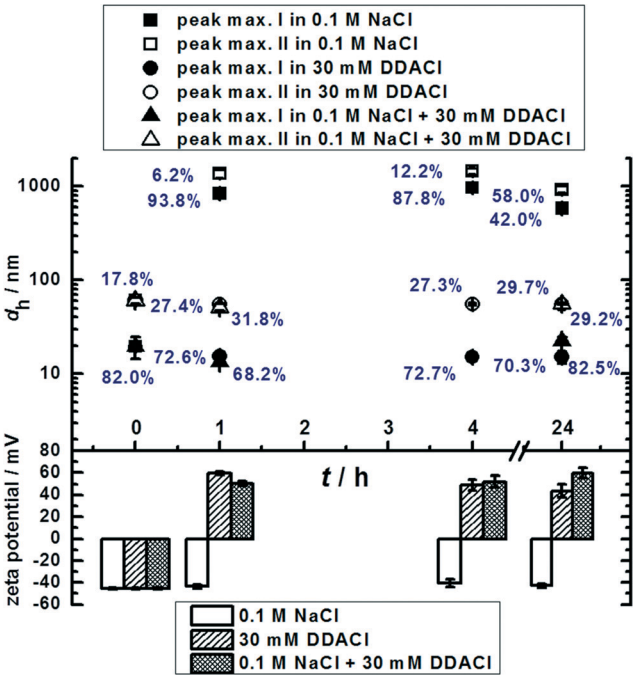

Fig. 9 Change in the hydrodynamic diameter (d_H) and zeta potential of AgNPs in the presence of 0.1 M NaCl, a micellar concentration of DDACl (30 mm) and a mixture of NaCl and DDACl during 24 hours at 25 °C. The mean volume % of particle populations with different sizes are indicated.

presence of SDS as compared to UW. Negatively charged surfactants are widely used in laundry detergents to solubilize dirt by preventing their adsorption on the negatively charged textile fibers.[42] Hence, the higher stability of AgNPs due to the increased negative value of their surface charge in the presence of SDS also increases the potential release of AgNPs from the laundry washing cycle into wastewater streams. As compared to UW, the presence of DDACl did not result in any observable effects on the size distribution of AgNPs either at the concentration below or above its CMC value (Fig. 9 and Table S2 in the ESI†). It is evident from the ζ potential results (Table S3 in the ESI†) that the addition of DDACl moved the ζ potentials of AgNPs in the positive direction. At the same time, DDACl did not affect dissolution, but it shifted the SPR peak to higher wavelengths. Positively charged surfactants are not used as a normal component of laundry detergents but in laundry softeners.[42] Thus, their use may also increase the environmental release of AgNPs. As in the case of SDS, the charge reversal of AgNPs in the presence of DDACl was probably caused by the surface adsorption of surfactants due to a combination of electrostatic attractions between the negatively charged AgNPs and DDACl. A similar behavior was described for the cationic surfactants CTAB and DTAC.[30,33] The observed behavior of AgNPs in the presence of SDS and DDACl was expected since the ζ potentials were large enough ($\leq$20 mV or $>$20 mV, respectively) to prevent NP aggregation. The same behavior was already described for similar surfactants.[33] Our results clearly indicate that the presence of surfactants in any environmental compartment where AgNPs may be released will prevent their

aggregation, sedimentation, and dissolution at neutral pH and low ionic strength. This emphasizes the higher potential of AgNP release from any system where surfactants are used. However, different environmental compartments are complex and usually characterized with higher ionic strength. Therefore, the combined effects of surfactants (Triton X-100, SDS and DDACl) and higher electrolyte concentrations (0.1 M NaCl) on AgNP behavior were examined. As already described in the previous section, a suspension in 0.1 M NaCl led to severe aggregation of citrate-coated AgNPs (Fig. 4). Interestingly, only DDACl significantly inhibited the aggregation behavior of AgNPs in the solution containing 0.1 M NaCl (Fig. 9). Neither Triton X-100 nor SDS was able to prevent the aggregation of AgNPs caused by the high concentration of NaCl (Fig. 7 and 8). It was quite surprising that SDS did not prevent the aggregation behavior in the mixed system, *i.e.* surfactant +0.1 M NaCl (Fig. 8), although the surface charge of AgNPs stayed highly negative. The measured ζ potential value in such a mixed system was probably not just a result of the surface charge of AgNPs. Indeed, the observed ζ potential value for pure 15 mM SDS in 0.1 M NaCl was -23.9 ± 2.6 mV. In the case of DDACl, negatively charged AgNPs interacted strongly by electrostatic interactions with the positively charged surfactant DDACl, resulting in stabilized nanoparticles. The observed reversal in net charge might have been due to the hydrophobic interactions between DDACl tails, which may form a bilayer through cooperative adsorption. The cooperative adsorption of DDACl on silver is similar to previous findings of adsorption of nonionic and cationic surfactants at hydrophilic silica.[65] Unfortunately, a detailed mechanistic description of the effect of such a mixed system on the electrostatic or steric repulsion forces between ligand-coated NPs is not straightforward due to the hybrid nature of ion *vs.* surfactant *vs.* NP interactions.[7] After inflowing a water system, the stability and fate of AgNPs will primarily be controlled by the presence or absence of a capping layer that depends on the pH, ionic strength, and organic contents of water. As already demonstrated, AgNPs are highly mobile in environmental porous media, implying the need for further work on their stability, mobility and transformation behavior in different environmental compartments.[22] Our results emphasize the attraction between different types of AgNPs and laundry surfactants, as well as the fact that AgNPs may not just exit the laundry cycle but also be present wastewater effluents when laundry surfactants are adsorbed onto their surfaces. Another important implication of this study is that the interaction of AgNPs with surfactants present in wastewater effluents could potentially become more environmentally hazardous due to the increased dissolution of AgNPs or due to the already proven increased toxicity of surfactant-coated AgNPs to natural microbiomes.[66] Additional difficulties may arise from the (in)stability of surfactants in the water effluents. For example, SDS can be easily degraded by the bacteria present in the wastewaters.[67] Thus, not only detergent components by themselves but also degradation products will affect AgNPs in wastewaters.

Concerning the evidence that WWTPs have proven to be very efficient at removing Ag from treated water, modelling and predicting the fate of AgNPs in WWTP systems is of utmost importance for risk assessment of AgNP-enabled products.[14,60] Here, we provided results on the behavior of citrate-coated AgNPs in very simple and artificial test systems. The obtained results could only serve as a starting point for the design of more complex and realistic studies. In addition to agglomeration and dissolution behavior of AgNPs under different experimental conditions as presented here, future studies should include oxidation, sulfidation and biomolecular corona formation as additional scenarios for AgNP transformational pathways.[14,60] These are of particular importance for the evaluation of the toxicity of AgNPs and their transformed products in water effluents. Recent studies already showed that AgNP toxicity can be significantly reduced after transformation of AgNPs in the WWTP.[68] Sulfidation is one of the possible processes that has been already demonstrated to decrease AgNP toxicity to different eukaryotes including zebrafish, killfish, nematode worm and least duckweed.[69] However, transformed AgNPs, like sulfidized or oxidized forms, may still be bioavailable,[70] which encourages the evaluation of risk on bioaccumulation, biomagnification, and long-term and chronic effects of AgNPs and their by-products.

Conclusion

This study highlighted the importance of pH, ionic strength and interaction with surfactants relevant to the laundry cycle to the stability and environmental fate of citrate-coated AgNPs. Measurements of agglomeration and dissolution *in situ* made by DLS and UV-vis agreed well with AFM observations, enabling a rapid pre-screening for colloidal stability by colorimetry. The magnetic study of AgNPs pointed to the appearance of superparamagnetic moments sitting on independent NPs due to their nanometre size. This large magnetic moment of each particle is useful in the treatment of water contaminated with AgNPs since the magnetic field gradient of a strong permanent magnet would produce a large force on every particle and generally help in their separation/extraction from water. Separation would be even more efficient and important for smaller AgNPs, which cannot be filtered out simply with usual techniques. AgNPs readily and reversibly interacted with laundry surfactants depending on the surfactant concentration, which indicates very complex and unpredictable changes in the speciation of AgNPs during washing and upon dilution when leaving the laundry cycle but also their behavior in wastewater effluents. However, it should be highlighted that this study employed a simple and artificial test system to provide information on the role of some important parameters on the behavior of AgNPs. In every transient stage, the life cycle assessment of AgNPs in the environment will depend on their speciation, which is affected by a myriad of different processes such as agglomeration, dissolution, degradation, corrosion, oxidation, and sulfidation. Hence, there is a substantial knowledge gap in the role of different environmental components (surfactants,

thiols, inorganic agents, organic matter, *etc.*) in the environmental fate and toxicity of AgNPs. There is an immediate need for information on specific exposure scenarios and temporal speciation measurements to fully assess the potential environmental risk of using AgNPs in consumer products.

Conflicts of interest

There are no conflicts to declare.

Acknowledgements

This work was supported by the Croatian Science Foundation [grant number HRZZ-IP-2016-06-2436]. We are grateful to Tea Mišić Radić for her help in AFM figure analysis and preparation.

References

1 S. F. Hansen, L. R. Heggelund, P. R. Besora, A. Mackevica, A. Boldrin and A. Baun, Nanoproducts–what is actually available to European consumers?, *Environ. Sci.: Nano*, 2016, **3**(1), 169–180.

2 S. Hansen and A. Mackevica, Chapter 11: Methods and Tools for Assessing Nanomaterials and Uses and Regulation of Nanosilver in Europe, Silver Nanoparticles for Antibacterial Devices, in Book: *Silver Nanoparticles for Antibacterial Devices: Biocompatibility and Toxicity*, 2018, pp. 281–300, DOI: 10.1201/9781315370569-12, CRC Press. ISBN: 9781498725323.

3 PEN, *The Project on Emerging Nanotechnologies: Consumer Products Inventory [WWW Document]*, URL http://www.nanotechproject.org/cpi (accessed 7.4.16), 2016.

4 D. He, M. W. Bligh and T. D. Waite, Effects of Aggregate Structure on the Dissolution Kinetics of Citrate-Stabilized Silver Nanoparticles, *Environ. Sci. Technol.*, 2013, **47**, 9148–9156.

5 M. E. Vance, T. Kuiken, E. P. Vejerano, S. P. McGinnis, M. F. Hochella, D. Rejeski and M. S. Hull, Nanotechnology in the real world: Redeveloping the nanomaterial consumer products inventory, *Beilstein J. Nanotechnol.*, 2015, **6**, 1769–1780.

6 Q. Li, S. Mahendra, D. Y. Lyon, L. Brunet, M. V. Liga, D. Li and P. J. J. Alvarez, Antimicrobial nanomaterials for water disinfection and microbial control: potential applications and implications, *Water Res.*, 2008, **42**, 4591–4602.

7 C. Pfeiffer, C. Rehbock, D. Huhn, C. Carrillo-Carrion, D. J. de Aberasturi, V. Merk, S. Barcikowski and W. J. Parak, Interaction of colloidal nanoparticles with their local environment: the (ionic) nanoenvironment around nanoparticles is different from bulk and determines the physico-chemical properties of the nanoparticles, *J. R. Soc., Interface*, 2014, **11**, 20130931.

8 N. S. Tulve, A. B. Stefaniak, M. E. Vance, K. Rogers, S. Mwilu, R. F. LeBouf, D. Schwegler-Berry, R. Willis, T. A. Thomas and L. C. Marr, Characterization of silver nanoparticles in selected consumer products and its relevance for predicting children's potential exposures, *Int. J. Hyg. Environ. Health*, 2015, **218**(3), 345–357.

9 G. Brunetti, E. Donner, G. Laera, R. Sekine, K. G. Scheckel, M. Khaksar, K. Vasilev, G. De Mastro and E. Lombi, Fate of zinc and silver engineered nanoparticles in sewerage networks, *Water Res.*, 2015, **77**, 72–84.

10 T. M. Benn and P. Westerhoff, Nanoparticle silver released into water from commercially available sock fabrics, *Environ. Sci. Technol.*, 2008, **42**, 4133–4139.

11 R. K. Cross, C. Tyler and T. S. Galloway, Transformations that affect fate, form and bioavailability of inorganic nanoparticles in aquatic sediments, *Environ. Chem.*, 2015, **12**, 627–642.

12 L. M. Furtado, A. Md, E. Hoque, D. M. Mitrano, J. F. Ranville, B. Cheever, P. C. Frost, M. A. Xenopoulos, H. Hintelmann and C. D. Metcalfe, The persistence and transformation of silver nanoparticles in littoral lake mesocosms monitored using various analytical techniques, *Environ. Chem.*, 2014, **11**, 419–430.

13 B. J. Plowman, K. Tschulik, E. Walport, N. P. Young and R. G. Compton, The fate of nano-silver in aqueous media, *Nanoscale*, 2015, **7**, 12361–12364.

14 S. Kampe, R. Kaegi, K. Schlich, C. Wasmuth, H. Hollert and C. Schlechtriem, Silver Nanoparticles in Sewage Sludge: Bioavailability of Sulfidized Silver to the Terrestrial Isopod Porcellio scaber, *Environ. Toxicol. Chem.*, 2018, **37**(6), 1606–1613.

15 F. Gottschalk and B. Nowack, The release of engineered nanomaterials to the environment, *J. Environ. Monit.*, 2011, **13**, 1145–1155.

16 R. Kaegi, A. Voegelin, B. Sinnet, H. Hagendorfer and M. Burkhardt, Behavior of metallic silver nanoparticles in a pilot wastewater treatment plant, *Environ. Sci. Technol.*, 2011, **45**, 3902–3908.

17 K. Schlich, T. Klawonn, K. Terytze and K. Hund-Rinke, Hazard assessment of a silver nanoparticle in soil applied via sewage sludge, *Environ. Sci. Eur.*, 2013, **25**, 1–14.

18 F. Gottschalk, T. Sondere, R. Schols and B. Nowack, Modeled environmental concentrations of engineered nanomaterials for different regions, *Environ. Sci. Technol.*, 2009, **43**, 9216–9222.

19 F. Gottschalk and B. Nowack, The release of engineered nanomaterials to the environment, *J. Environ. Monit.*, 2011, **13**, 1145.

20 O. Bondarenko, K. Juganson, A. Ivask, K. Kasemets, M. Mortimer and A. Kahru, Toxicity of Ag, CuO and ZnO nanoparticles to selected environmentally relevant test organisms and mammalian cells in vitro: a critical review, *Arch. Toxicol.*, 2013, **87**, 1181–1200.

21 L. Ulm, A. Krivohlavek, D. Jurašin, M. Ljubojević, G. Šinko, T. Crnković, I. Žuntar, S. Šikić and I. Vinković Vrček, Response of biochemical biomarkers in the aquatic crustacean Daphnia magna exposed to silver nanoparticles, *Environ. Sci. Pollut. Res.*, 2015, **22**, 19990–19999.

22 C. M. Park, J. Heo, N. Her, K. H. Chu, M. Jang and Y. Yoon, Modeling the effects of surfactant, hardness, and natural

organic matter on deposition and mobility of silver nanoparticles in saturated porous media, *Water Res.*, 2016, **103**, 38–47.

23 J. S. Gebauer and L. Treuel, Influence of individual ionic components on the agglomeration kinetics of silver nanoparticles, *J. Colloid Interface Sci.*, 2011, **354**, 546–554.

24 A. M. El Badawy, T. P. Luxton, R. G. Silva, K. G. Scheckel, M. T. Suidan and T. M. Tolaymat, Impact of environmental conditions (pH, ionic strength, and electrolyte type) on the surface charge and aggregation of silver nanoparticles suspensions, *Environ. Sci. Technol.*, 2010, **44**, 1260–1266.

25 B. J. R. Thio, M. O. Montes, M. A. Mahmoud, D.-W. Lee, D. Zhou and A. A. Keller, Mobility of capped silver nanoparticles under environmentally relevant conditions, *Environ. Sci. Technol.*, 2012, **46**, 6985–6991.

26 X. Li, J. J. Lenhart and H. W. Walker, Aggregation kinetics and dissolution of coated silver nanoparticles, *Langmuir*, 2012, **28**, 1095–1104.

27 X. Jin, M. Li, J. Wang, C. Marambio-Jones, F. Peng, X. Huang, R. Damoiseaux and E. M. V. Hoek, High-throughput screening of silver nanoparticle stability and bacterial inactivation in aquatic media: influence of specific ions, *Environ. Sci. Technol.*, 2010, **44**, 7321–7328.

28 R. I. MacCuspie, K. Rogers, M. Patra, Z. Suo, A. J. Allen, M. N. Martin and V. A. Hackley, Challenges for physical characterization of silver nanoparticles under pristine and environmentally relevant conditions, *J. Environ. Monit.*, 2011, **13**, 1212.

29 R. Ma, C. Levard, S. M. Marinakos, Y. Cheng, J. Liu, F. M. Michel, G. E. Brown and G. V. Lowry, Size-controlled dissolution of organic-coated silver nanoparticles, *Environ. Sci. Technol.*, 2012, **46**, 752–759.

30 J. Hedberg, M. Lundin, T. Lowe, E. Blomberg, S. Wold and I. O. Wallinder, Interactions between surfactants and silver nanoparticles of varying charge, *J. Colloid Interface Sci.*, 2012, **369**, 193–201.

31 X. Li, J. J. Lenhart and H. W. Walker, Dissolution-accompanied aggregation kinetics of silver nanoparticles, *Langmuir*, 2010, **26**, 16690–16698.

32 N. Odzak, D. Kistler, R. Behra and L. Sigg, Dissolution of metal and metal oxide nanoparticles under natural freshwater conditions, *Environ. Chem.*, 2015, **12**, 138–148.

33 S. Skoglund, T. A. Lowe, J. Hedberg, E. Blomberg, I. O. Wallinder, S. Wold and M. Lundin, Effect of laundry surfactants on surface charge and colloidal stability of silver nanoparticles, *Langmuir*, 2013, **29**, 8882–8891.

34 J. Soukupová, L. Kvítek, A. Panáček, T. Nevěčná and R. Zbořil, Comprehensive study on surfactant role on silver nanoparticles (NPs) prepared via modified Tollens process, *Mater. Chem. Phys.*, 2008, **111**, 77–81.

35 L. Fan and R. Guo, Growth of Dendritic Silver Crystals in CTAB/SDBS Mixed-Surfactant Solutions, *Cryst. Growth Des.*, 2008, **8**, 2150–2156.

36 Y.-H. Chen and C.-S. Yeh, Laser ablation method: Use of surfactants to form the dispersed Ag nanoparticles, *Colloids Surf., A*, 2002, **197**, 133–139.

37 L. Kvítek, A. Panáček, J. Soukupová, M. Kolář, R. Večeřová, R. Prucek, M. Holecova and R. Zbořil, Effect of Surfactants and Polymers on Stability and Antibacterial Activity of Silver Nanoparticles (NPs), *J. Phys. Chem. C*, 2008, **112**, 5825–5834.

38 G. Oberdörster, A. Maynard, K. Donaldson, V. Castranova, J. Fitzpatrick, K. Ausman, J. Carter, B. Karn, W. Kreyling, D. Lai, S. Olin, N. Monteiro-Riviere, D. Warheit, H. Yang and ILSI Research Foundation/Risk Science Institute Nanomaterial Toxicity Screening Working Group, Principles for characterizing the potential human health effects from exposure to nanomaterials: elements of a screening strategy, *Part. Fibre Toxicol.*, 2005, **2**, 8.

39 K. W. Powers, S. C. Brown, V. B. Krishna, S. C. Wasdo, B. M. Moudgil and S. M. Roberts, Research strategies for safety evaluation of nanomaterials. Part VI. Characterization of nanoscale particles for toxicological evaluation, *Toxicol. Sci.*, 2006, **90**, 296–303.

40 J. Liu and R. H. Hurt, Ion Release Kinetics and Particle Persistence in Aqueous Nano-Silver Colloids, *Environ. Sci. Technol.*, 2010, **44**, 2169–2175.

41 C. Damm and H. Münstedt, Kinetic aspects of the silver ion release from antimicrobial polyamide/silver nanocomposites, *Appl. Phys. A: Mater. Sci. Process.*, 2008, **91**, 479–486.

42 E. Smulders, W. Rybinski, E. Sung, W. Rähse, J. Steber and A. Nordskog, Laundry Detergents, *Ullmann's Encyclopedia of Industrial Chemistry*, Wiley-VCH, 2007.

43 C. H. Munro, W. E. Smith, M. Garner, J. Clarkson and P. C. White, Characterization of the Surface of a Citrate-Reduced Colloid Optimized for Use as a Substrate for Surface-Enhanced Resonance Raman Scattering, *Langmuir*, 1995, **11**, 3712–3720.

44 E. Balnois and K. J. Wilkinson, Wilkinson, Sample preparation techniques for the observation of environmental biopolymers by atomic force microscopy, *Colloids Surf., A*, 2002, **207**, 229–242.

45 S. D. Faust, D. Samuel and O. M. Aly, *Chemistry of natural waters*, Ann Arbor Science Publishers, 1981, p. 400.

46 T. Vinković, O. Novák, M. Strnad, W. Goessler, D. Domazet Jurašin, N. Parađiković and I. Vinković Vrček, Cytokinin response in pepper plants (Capsicum annuum L.) exposed to silver nanoparticles, *Environ. Res.*, 2017, **156**, 10–18.

47 L. Ulm, A. Krivohlavek, D. Jurašin, M. Ljubojević, G. Šinko, T. Crnković, I. Žuntar, S. Šikić and I. Vinković Vrček, Response of biochemical biomarkers in the aquatic crustacean *Daphnia magna* exposed to silver nanoparticles, *Environ. Sci. Pollut. Res.*, 2015, **22**, 19990–19999.

48 B. F. Leo, S. Chen, Y. Kyo, K.-L. Herpoldt, N. J. Terrill, I. E. Dunlop, D. S. McPhail, M. S. Shaffer, S. Schwander, A. Gow, J. Zhang, K. F. Chung, T. D. Tetley, A. E. Porter and M. P. Ryan, The Stability of Silver Nanoparticles in a Model of Pulmonary Surfactant, *Environ. Sci. Technol.*, 2013, **47**, 11232–11240.

49 G. Mie, Beiträge zur Optik trüber Medien, speziell kolloidaler Metallösungen, *Ann. Phys.*, 1908, **330**, 377–445.

50 H. C. van de Hulst, *Light scattering by small particles*, John Wiley & Sons, New York, 1957.

51 T. Linnert, P. Mulvaney and A. Henglein, Surface chemistry of colloidal silver: surface plasmon damping by chemisorbed iodide, hydrosulfide (SH-), and phenylthiolate, *J. Phys. Chem.*, 1993, **97**, 679–682.
52 N. L. Sukhov, N. B. Ershov, V. K. Mikhalko and A. V. Gordeev, Absorption spectra of large colloidal silver particles in aqueous solution, *Russ. Chem. Bull.*, 1997, **46**, 197–199.
53 Y. Yin, Z.-Y. Li, Z. Zhong, B. Gates, Y. Xia and S. Venkateswaran, Synthesis and characterization of stable aqueous dispersions of silver nanoparticles through the Tollens process, *J. Mater. Chem.*, 2002, **12**, 522–527.
54 A. Henglein, Colloidal Silver Nanoparticles: Photochemical Preparation and Interaction with O2, CCl4, and Some Metal Ions, *Chem. Mater.*, 1998, **10**, 444–540.
55 M. Chen, L.-Y. Wang, J.-T. Han, J.-Y. Zhang, Z.-Y. Li and D.-J. Qian, Preparation and Study of Polyacryamide-Stabilized Silver Nanoparticles through a One-Pot Process, *J. Phys. Chem. B*, 2006, **110**, 11224–11231.
56 J. Scalf and P. West, *Part I: Introduction to Nanoparticle Characterization with AFM*, Pacific Nanotechnology, 2006, available from: http://www.nanoparticles.org/pdf/Scalf-West.pdf.
57 S. Elzey and V. H. Grassian, Agglomeration, isolation and dissolution of commercially manufactured silver nanoparticles in aqueous environments, *J. Nanopart. Res.*, 2010, **12**, 1945–1958.
58 R. A. Alvarez-Puebla, E. Arceo, P. J. G. Goulet, J. J. Garrido and R. F. Aroca, Role of Nanoparticle Surface Charge in Surface-Enhanced Raman Scattering, *J. Phys. Chem. B*, 2005, **109**, 3787–3792.
59 C. Özmetin, M. Çopur, A. Yartasi and M. M. Kocakerim, Kinetic Investigation of Reaction Between Metallic Silver and Nitric Acid Solutions, *Chem. Eng. Technol.*, 2000, **23**, 707–711.
60 C. Levard, E. M. Hotze, G. V. Lowry and G. E. Brown, Environmental transformations of silver nanoparticles: impact on stability and toxicity, *Environ. Sci. Technol.*, 2012, **46**, 6900–6914.
61 T. Cedervall, I. Lynch, S. Lindmann, T. Berggard, E. Thulin, H. Nilsson, K. A. Dawson and S. Linse, Understadning the nanoparticle protein corona using methods to quantify exchange rates and affinities of proteins for nanoparticles, *Proc. Natl. Acad. Sci. U. S. A.*, 2007, **104**, 2050–2055.
62 J. Fabrega, S. N. Luoma, C. R. Tyler, T. S. Galloway and J. R. Lead, Silver nanoparticles: behaviour and effects in the aquatic environment, *Environ. Int.*, 2011, **37**, 517–531.
63 D. F. Evans and H. Wennerström, *The Colloidal Domain: Where Physics, Chemistry, Biology, and Technology Meet*, John Wiley and Sons, New York, Wiley-VCH, 2nd edn, 1999.
64 D. Jurašin and M. Dutour Sikirić, Higher Oligomeric Surfactants — From Fundamentals to Applications, in *Oligomerization of Chemical and Biological Compounds*, InTech, 2014.
65 G. H. Bolt, Determination of the Charge Density of Silica Sols, *J. Phys. Chem.*, 1957, **61**, 1166–1169.
66 E. J. Bae, H. J. Park, J. S. Park, J. Y. Yoon, Y. H. Kim, K. H. Choi and J.-H. Yi, Effect of Chemical Stabilizers in Silver Nanoparticle Suspensions on Nanotoxicity, *Bull. Korean Chem. Soc.*, 2011, **32**, 613–619.
67 R. Shahbazi, R. Kasra-Kermanshahi, S. Gharavi, Z. Moosavi-Nejad and F. Borzooee, Screening of SDS-degrading bacteria from car wash wastewater and study of the alkylsulfatase enzyme activity, *Iran. J. Microbiol.*, 2013, **5**, 153.
68 S. Kühr, S. Schneider, B. Meisterjahn, K. Schlich, K. Hund-Rinke and C. Schlechtriem, Silver nanoparticles in sewage treatment plant effluents: chronic effect and accumulation of silver in the freshwater amphipod Hyalella azteca, *Environ. Sci. Eur.*, 2018, **30**, 7.
69 C. Levard, E. M. Hotze, B. P. Colman, A. L. Dale, L. Truong, X. Y. Yang, A. J. Bone, G. E. Brown, R. L. Tanguay, R. T. Di Giulio, E. S. Bernhardt, J. N. Meyer, M. R. Wiesner and G. V. Lowry, Sulfidation of silver nanoparticles: natural antidote to their toxicity, *Environ. Sci. Technol.*, 2013, **47**, 13440–13448.
70 M. Kraas, K. Schlich, B. Knopf, F. Wege, R. Kägi, K. Terytze and K. Hund-Rinke, Long-term effects of sulfidized silver nanoparticles in sewage sludge on soil microflora, *Environ. Toxicol. Chem.*, 2017, **36**, 3305–3313.

9. ŽIVOTOPIS

Ivona Capjak rođena 06.06.1986. godine u Livnu, BIH. Osnovnu školu i II Opću Križanićevu gimnaziju završila je u Zagrebu, a 2005. godine upisala je studij farmacije na Farmaceutsko-biokemijskom fakultetu Sveučilišta u Zagrebu te je 2010. godine diplomirala. Diplomski rad pod nazivom „Utjecaj sirovinskog sastava na makronutritivnu kakvoću dijetnog čajnog peciva“ izradila je na Zavodu za biokemiju prehrane pod mentorstvom prof.dr.sc. Irene Vedrine Dragojević. Nakon studija, zapošljava se u ljekarni najprije kao farmaceut pripravnik, a nakon položenog stručnog ispita kao magistar farmacije. Godine 2013. upisuje posljediplomski doktorski studij na Farmaceutsko-biokemijskom fakultetu, smjer farmaceutske znanosti. Iste godine, zapošljava se na pozicij stručnog suradnika u Odjelu za osiguranje kvalitete u proizvodnji infuzijskih otopina, u Hrvatskom zavodu za transfuzijsku medicinu. U 2015. godini upisuje jednogodišnje stručno usavršavanje na poslovnom učilištu „Supera“, smjer „Menadžer upravljanja kvalitetom“ koje završava u lipnju 2016. obranom zvaršnog rada pod nazivom „Quality by design“ izrađenog pod mentorstvom dr.sc. Miljenko Košiček. U siječnju 2017. godine preuzima funkciju voditelja odjela za Osiguranje kvalitete u Hrvatskom zavodu za transfuzijsku medicinu. Sudjelovala je na više međunarodnih i domaćih kongresa sa sveukupno 6 posterskih izlaganja.

Popis znanstvenih radova:

1. Domazet Jurašin, Darija; Ćurlin, Marija; Capjak, Ivona; Crnković, Tea; Lovrić, Marija; Babič, Michal; Horák, Daniel; Vinković Vrček, Ivana; Gajović, Srećko. Surface coating affects behavior of metallic nanoparticles in a biological environment. *Beilstein Journal of Nanotechnology*. (2016) , 7; 246-262.
2. Capjak, Ivona; Šupraha Goreta, Sandra; Domazet Jurašin, Darija; Vinković Vrček, Ivana. How protein coronas determine the fate of engineered nanoparticles in biological environment. *Arhiv za higijenu rada i toksikologiju*. 68 (2017) , 4; 245-253.
3. Kubo, Anna-Liisa; Capjak, Ivona; Vinković Vrček, Ivana; Bondarenko, Olesja M.; Kurvet, Imbi; Vija, Heiki; Ivask, Angela; Kasemets, Kaja; Kahru, Anne. Antimicrobial potency of differently coated 10 and 50 nm silver nanoparticles against clinically relevant bacteria Escherichia coli and Staphylococcus aureus. *Colloids and surfaces. B, Biointerfaces*. 170 (2018) , 1 October; 401-410.

4. Capjak, Ivona; Zebić Avdičević, Maja; Dutour Sikirić, Maja; Domazet Jurašin, Darija; Amela Hozić, Amela; Pajić, Damir; Dobrović, Slaven; Goessler, Walter; Vinković Vrček, Ivana. Behavior of silver nanoparticles in wastewater: systematic investigation on the combined effects of surfactants and electrolytes in the model systems. *Environmental Science: Water Research and Technology*. 4 (2018); 2146-2159.

10. TEMELJNA DOKUMENTACIJSKA KARTICA

TEMELJNA DOKUMENTACIJSKA KARTICA

Sveučilište u Zagrebu
Farmaceutsko-biokemijski fakultet
Ante Kovačića 1, 10000 Zagreb

Doktorski rad

UTJECAJ VELIČINE, OBLIKA I POVRŠINSKE STRUKTURE NANOČESTICA SREBRA NA NJIHOVU INTERAKCIJU S MODELNIM PROTEINIMA

Ivona Capjak

SAŽETAK

Zbog svojstava na nano razini, primjena nanosrebra (AgNP) u potrošačkim i medicinskim proizvodima je u stalnom porastu što nužno zahtijeva stalnu procjenu njihovih učinaka na ljudsko zdravlje.
Cilj ovog doktorskog rada bio je utvrditi kako različita fizikalno-kemijska svojstva AgNP određuju njihovo ponašanje, stabilnost i interakcije u različitim biološkim medijima. U tu svrhu je sintetizirano šesnaest vrsta AgNP različitih oblika i površinske stabilizacije u veličinama od 10 nm i 50 nm. Sve AgNP vrste su pažljivo karakterizirane obzirom na raspodjelu veličina, površinski naboj, topljivost i ponašanje u vodi, u ultra čistoj vodi, pri različitim pH i ionskim jakostima, uz dodatak površinski aktivnih tvari, u fiziološkoj otopini, fosfatnom puferu i fosfatnom puferu uz dodataka 0.9% NaCl. AgNP vrstama određen je antibakterijski učinak na sojevima *E. coli* i *S. aureus*. Nano-bio interakcije istraživane su koristeći dva modelna proteina: albumin i α-1-kiseli glikoprotein. U tu je svrhu određeno kako različita fizikalno-kemijska svojstva AgNP utječu na konstante vezanja ta dva proteina na površinu nanočestica, te što se događa sa sekundarnom strukturom proteina uslijed vezanja na AgNP.

Utvrđeno je da osim naboja površinskog stabilizatora, značajnu ulogu u nano-bio interakcijama ima nominalni promjer AgNP. S porastom ionske jakosti ili značajnom promjenom pH medija mijenja se površinski naboj, a AgNP se destabiliziraju. Ukoliko u mediju nema biomolekula kao što su proteini, AgNP su nestabilne i podložne aglomeraciji i otapanju. Proteini se vežu na AgNP površinu čim se AgNP izlože mediju koji sadrže proteine, a konstante vezanja proteina na površinu AgNP slične su vezanju tih proteina s nekim lijekovima. Promjena sastava medija ne uzrokuje značajne promjene u tim nano-bio interakcijama. Vezanje albumina s AgNP rezultira većom i raznolikijom promjene sekundarne/tercijarne strukture proteina u odnosu na onu koja se događa s α-1-kiselim glikoproteinom.

Rad je pohranjen u Središnjoj knjižnici Sveučilišta u Zagrebu Farmaceutsko-biokemijskog fakulteta.

Rad sadrži: 137 stranica, 62 slike, 24 tablice i 327 literaturna navoda. Izvornik je na hrvatskom jeziku.
Ključne riječi: nanosrebro, proteini, interakcije, albumin, α-1-kiseli glikoprotein, stabilnost, antibakterijska aktivnost, nano-bio međuprostor
Mentori: **dr.sc. Ivana Vinković Vrček**
doc.dr.sc. Sandra Šupraha Goreta
Ocjenjivači: **dr.sc. Tin Weitner**
dr.sc. Jasna Jablan
dr.sc. Maja Dotour Sikirić
Rad prihvaćen: 17.04.2019.

BASIC DOCUMENTATION CARD

Univesrity of Zagreb
Faculty of Pharmacy and Biochemistry
A. Kovačića 1, 10000 Zagreb

Doctoral dissertation

EFFECT OF SIZE, SHAPE AND SURFACE STRUCTURE OF SILVER NANOPARTICLES ON THEIR INTERACTION WITH MODEL PROTEINS

Ivona Capjak

ABSTRACT

Due to properties of silver at a nano level, silver nanoparticles (AgNP) are currently being used in an increasing number of consumer and medical products, which necessitate their safety assessment for human health.

The aim of this doctoral work is to determine how different physico-chemical properties of AgNP affect their behaviour and interaction in different biological media. For this purpose, sixteen types of AgNP of different shape, size (10 and 50 nm) and surface stabilization were prepared. Careful characterization of their size distribution, surface charge, dissolution, and behaviour in water, at different pH and ionic strength, in the presence of surface active agents, in phosphate buffer, in 0.9 % NaCl solution, and in phosphate buffer with addition of 0.9 % NaCl was carried out. Antimicrobial efficacy of AgNP were tested using two bacterial strains, *E. coli* i *S. aureus*. Nano-bio interactions were investigated using two model proteins: albumin and α-1-acid glycoprotein. For this purpose, effect of various physical-chemical properties of AgNP on the binding constants of these two proteins on the AgNPs surface was evaluated, as well as the changes in the secondary protein structure due to binding to AgNP.

Obtained results demonstrated that the surface charge and nominal diameter of AgNP both have a significant role in nano-bio interactions. The surface charge and AgNP changes upon increase in ionic strength or significant changes in pH of the inclusion media, which lead to AgNP destabilization. In media without biomolecules like proteins, AgNP are unstable and susceptible to agglomeration and dissolution. Proteins present in the media bind to the AgNP surface as soon as AgNP are suspended in these media. Binding constants of proteins to AgNP surface are similar to binding between these proteins and some drugs. Changing the media composition does not cause significant changes in these nano-bio interactions. Binding of albumin to AgNP results in a greater and more varied alteration of the secondary / tertiary protein structure compared to α-1-acid glycoprotein.

The dissertation is deposite in the Central Library of the University of Zagreb, Faculty of Pharmacy and Biochemistry.

Dissertation includes: 137 pages, 62 figures, 24 tables and 327 references. Original is in Croatian language.
Key words: nanosilver, stability, ionic strength, electrolytes, antibacterial efficacy, coating, logKa, BSA, AGP
Supervisors: **dr.sc. Ivana Vinković Vrček**
doc.dr.sc. Sandra Šupraha Goreta
Reviewers: **dr.sc. Tin Weitner**
dr.sc. Jasna Jablan
dr.sc. Maja Dotour Sikirić
The thesis was accepted: 17.04.2019.